PHD

Actions of chloronicotinyl insecticides

Lind, Robert

Award date:
1999

Awarding institution:
University of Bath

Actions of chloronicotinyl insecticides

Submitted by **Robert Lind**

for the degree of Ph.D. of the

University of Bath, 1999

ProQuest LLC
789 East Eisenhower Parkway
P.O. Box 1346
Ann Arbor, MI 48106-1346

Acknowledgements

My deepest thanks go to my supervisor at Bath University, Stuart Reynolds, and those at Zeneca Agrochemicals, Martin Clough and Fergus Earley, for their constant support and encouragement. Thanks also to Sue Wonnacott and her lab for putting up with my grinding and binding, and Bridget Baker and her lab for my dicing and slicing work. I would also like to acknowledge my friends and colleagues at Zeneca, particularly Mark Birchmore, Phil Wege, Andy Bywater, Dave Foster, Stuart Dunbar, Ian Hayhurst and John Windass. Lastly I wish to thank Helen Eastham and Chris Sharples for collaboration on the α-bungarotoxin and vertebrate binding work at the Univeristy of Bath. Funding for this thesis was provided by the BBSRC and Zeneca Agrochemicals.

Abstract

The naturally occurring neurotoxins α-bungarotoxin (α-BgTx), epibatidine and methyllycaconitine (MLA), all known to interact specifically with vertebrate nicotinic acetylcholine receptors (nAChR) were used to investigate nAChR of insects, principally the aphid *Myzus persicae*. Additionally studied was the synthetic chloronicotinyl insecticide imidacloprid (IMI) which is particularly effective against sucking insect pests such as aphids.

Saturation, displacement and dissociation binding studies utilised membranes prepared from a mixed population of whole aphids and bound ligand was isolated either using vacuum filtration or centrifugation. Saturable binding demonstrated that [^{125}I]-α-BgTx, [^{3}H]-epibatidine and [^{3}H]-IMI each labelled two sites distinguished by differing affinities in a ratio of 1:3 of high to low affinity sites. Of particular interest, was the finding that the affinity for binding of IMI to its high affinity binding site (K_d=0.14nM) was an order of magnitude higher in *M. persicae* and another hemiptera, *N. cincticeps*, than in a number of non-hemipterous insects which may explain why IMI is particularly useful in controlling sucking pests. The novel nicotinic ligand [^{3}H]-MLA labelled a single binding site with a K_d of 0.95nM and a B_{max} of 1290fmol/mg which is equal to that of the sum of the high and low affinity sites labelled by the other ligands. Furthermore MLA displaced α-BgTx, epibatidine and IMI with high potency. The rate of α-BgTx dissociation from its high affinity binding site was markedly increased by the presence of MLA, but not by the other ligands. These data are consistent with a model in which at least the majority of aphid nAChR have 2 different nicotinic binding sites per receptor which can interact allosterically with each other.

The larvae of the tobacco hornworm *Manduca sexta* are specialist tobacco feeders. The tolerance of this insect to nicotine has been postulated to be due to an altered nAChR which could provide cross resistance to the chloronicotinyl insecticides. Binding studies with [^{125}I]-α-BgTx revealed no differences in affinity or pharmacology between *M. sexta* larvae or adults (which feed on nectar) compared to other nicotine sensitive insects. Similarly no pharmacological differences of [^{3}H]-IMI

binding between the nicotine susceptible *M. persicae* and the tobacco aphid *Myzus nicotianae* could be resolved. Therefore tobacco feeding insects do not appear to possess an altered nicotine insensitive nAChR and thus must rely on physical and/or metabolic barriers to prevent nicotine reaching the CNS.

Systemic feeding experiments with [^{3}H]-IMI of 0.1, 0.01 and 0.001ppm were investigated to quantify internal aphid concentrations needed to bring about lethal and sublethal symptoms. Subsequent TLC analysis of treated leaf and aphid material revealed that substantial [^{3}H]-IMI metabolism occurs in the leaf and to a lesser degree in the aphid. IMI concentrations within the insect of ~0.5nM brought about paralysis and death, whereas a dose 10-fold less was required to bring about sublethal effects which include a drastic decrease in nymph production. These very low concentrations suggest that the high affinity binding sites may be important in IMI toxicology.

List of Abbreviations

ACh	Acetylcholine
AChE	Acetylcholinesterase
AChR	Acetylcholine receptor
α-BgTx	α-bungarotoxin
B_{max}	Maximal binding capacity
BSA	Bovine serum albumin
BW284c51	(1,5 bis(4 allyl dimethylammoniumphenyl)pentan3one)
EPI	Epibatidine
EPSP	Excitatory post synaptic potential
GABA	γ-amino butyric acid
5HT	5-Hydroxytripamine
IC_{50}	Inhibitor concentration to reduce binding to 50%
IMI	Imidacloprid
K_d	Dissociation constant
K_i	Inhibition constant
MAb	Monoclonal antibody
mAChR	Muscarinic acetylcholine receptors
MLA	Methyllycaconitine
nAChR	Nicotinic acetylcholine receptors
n-BgTx	Neuronal bungarotoxin
NCB	Non-competitive blocker
OP	Organophosphate
PMFS	Phenylmethylsulfonylfluoride
PNS	Peripheral nervous system
THA	(9 amino 1,2,3,4 tetrahydroacridine hydrochloride)

Table of contents

List of Figures and Plates

List of Tables

Chapter 1
Introduction

1.1. Insect wars: insecticides and insecticide resistance

An arms race between farmers and herbivorous insects has existed from times of antiquity. Insecticides, substances which are toxic to insects, have long been used by man to protect his crops and insects have countered this offensive through microevolution yielding resistance mechanisms which circumvent these weapons. This is not a new battle but has been also raging between insects and plants with botanic toxins to prevent herbivory. In response man's use of insecticides has become more sophisticated, evolving from crude organic mixes, which were both toxic to invertebrates and vertebrates, to highly tuned molecules with favourable physiochemical properties displaying considerable insecticidal specificity.

The first insecticides were organic in nature and botanical in origin. Their utilisation for insect control goes back at least 2000 years, when extracts of *Chrysanthemum* flowers were used (Evans, 1984; Casida and Quistad, 1998). The insecticidal properties of these extracts are due to pyrethrins whose synthetic analogues, the pyrethroids, are widely used today. It was not until the 1800's that the first synthetic insecticides appeared in the form of inorganic arsenicals. These included Paris green (copper arsenide) successfully used against Colorado potato beetle (*Leptinotarsa decemlineata*) in 1865. It is only since the 1900's that insecticides have been widely employed, a development catalysed by the discovery of synthetic organic insecticides (Evans, 1984).

Insecticide resistance has long been recognised as one of the major challenges facing applied entomologists (Devonshire and Field, 1991). Resistance is now visualised as a complex biochemical, physiological, genetic, and ecological dynamic phenomenon (Brattsten, 1986). It results from the selection of pre-existing, rare resistant individuals

within a population that survive following insecticide exposure. The spread of resistance is greatest when selection pressure is high, this occurs when the insecticide is applied at a rate giving a high percentage kill and is persistent. *R* genes are those involved in resistance and are maintained in populations at high levels by conferring a selective advantage over susceptible individuals when insecticidally challenged. Although some *R* genes are mutations that result in an altered gene product that is less susceptible to insecticidal action, most *R* gene mechanisms are believed to involve a change in the expression level of a gene product, rather than an alteration of the product itself. This can be achieved by either a change in gene copy numbers or a mutation of the regulatory sequence (Devonshire and Field, 1991). Through these genetic alterations mechanisms of resistance can manifest themselves as changes in behaviour, pesticide penetration, excretion, sequestration, target site or metabolism.

The problems of insecticide resistance are amplified when cross or multiple resistance occurs. Cross resistance occurs when following exposure to an insecticide, an insect population gains resistance to a chemical class to which it has never been exposed. This commonly occurs when different classes of insecticide act on the same target site or share a common detoxification pathway (Metcalf, 1989). Multiple resistance occurs following exposure to many differently acting insecticides to which resistance occurs through different mechanisms. Multiple resistance is wide-spread and by 1989 had been recorded in several hundred arthropod species from 10 Orders and 44 families (Metcalf, 1989), among these were 46 hopper and aphid species (Georghiou, 1990).

Once resistance genes have become established they have a very lengthy persistence in wild insect populations. Although *R* gene frequency in a population may decrease after insecticidal selection pressure is lifted, resistance will quickly build up again on re-application of the insecticide. For example, pyrethroid resistance in the diamond back moth *Plutella xylostella* remained for 10-16 generations with no selection pressure imposed (Metcalf, 1989).

To help understand the nature of a resistance mechanism the mode of action of the insecticide need to be known. The predominant organic insecticide classes interfere with nervous transmission and are therefore fast acting (Casida and Quistad, 1998). A smaller minority interfere with other vital life functions such as mimicking insect hormones to interfere with growth at critical times such as ecdysis (Casida and Quistad, 1998). Central and peripheral neuronal signalling pathways provide many different target proteins for the neurotoxic insecticides to exert their biological activity (Figure 1.1).

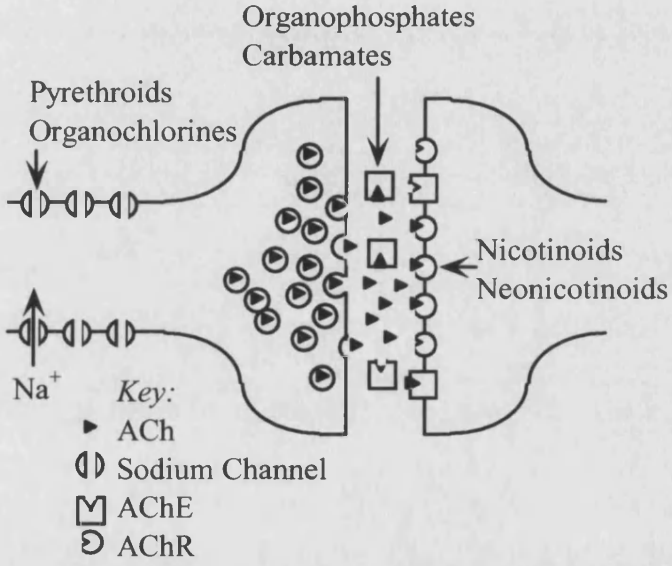

Figure 1.1. Stylised diagram of the cholinergic synapse showing the target sites of the major classes of insecticide.

The wave of depolarisation that travels down the axon is controlled by the opening and closing of sodium channels which are the targets of pyrethroid and organochlorine insecticides (Narahashi, 1992; Zlotkin, 1999). Nature has long exploited this target site with natural neurotoxins such as tetrodotoxin isolated from puffer fish (Narahashi, 1988). Indeed, many insecticides have their origins from natural sources; the pyrethroids, which also affect sodium channel functioning through stabilising the open

conformation are a good example based on the pyrethrins isolated from *Chrysanthemum.*

Once the electrical signal has reached the axon terminal end it is converted to a slow chemical one that must travel across the synaptic cleft. This is another target for insecticidal action. Neurotransmitters can take many forms but acetylcholine (ACh), γ-amino butyric acid (GABA) and L-glutamate perhaps play the most important signalling roles in insects (Burrows, 1996) (See appendix 1). After exocytosis from the pre-synaptic membrane, these transmitters have a transient role, diffusing across the synaptic gap and binding to their specific receptors located on the post-synaptic membranes. The receptors may cause direct action themselves or activate a second messenger system. After the transmitters have completed their signal transduction task they need to be removed to avoid re-activation of the receptors. Transmitters are removed actively by membrane transport and passively by diffusion. Still others are broken down by hydrolytic enzymes, and it is these that are the target site for two important insecticide classes, the organophosphates (OP's) and carbamates which are specific inhibitors of acetylcholinesterase (AChE). Inhibition of this enzyme prolongs the synaptic life of ACh and therefore results in an inappropriate prolongation of the activation of nicotinic acetylcholine receptors (nAChR). The nicotinoids and neonicotinoids mimic the actions of ACh and are the topic of discussion in section 1.5.

However the three main insecticide classes in use, namely pyrethroids, carbamates and OP's suffer from cross resistance due to an Achilles' heel which is that all these molecules contain an ester bond (figure 1.2).

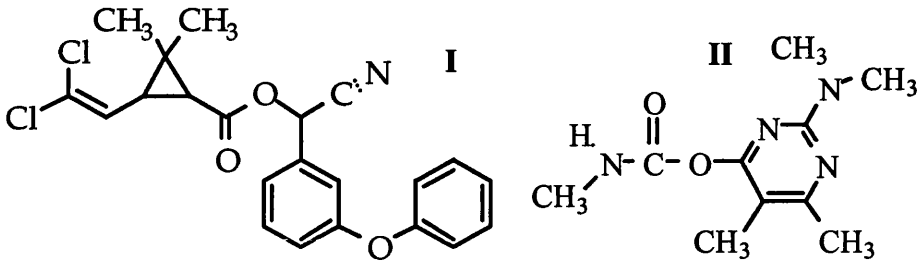

Figure 1.2. Examples of pyrethroid and carbamate insecticides demonstrating the presence of an ester bond. **I** (Cypermethrin), **II** (Pirimicarb).

Insects can become resistant by over expressing esterase genes through gene multiplication, enabling the rapid metabolism of these insecticides. Levels of these esterases may be up to 1% of the total protein in very resistant aphid strains (Devonshire, 1989). Furthermore, target site alterations have also been well documented for AChE, sodium channels and GABA receptors synergising the resistance problem (Devonshire and Moores, 1984; Martinez-Torres *et al.,* 1998; ffrench-Constant *et al.*, 1993; Hosie *et al.,* 1997).

1.1.1 Nicotine as an insecticide and its mode of action

The tobacco alkaloid nicotine, readily isolated from *Nicotiana tabacum* leaf, has a long history of use as an insecticide and is still in use today. However its high mammalian toxicity, relatively narrow range of biological targets (confined mainly to hemipteran pests) and short persistence have led to a decline in its use. Its redeeming feature as an insecticide is that it does not suffer from cross resistance problems associated with a structural ester bond or from target site resistance associated with pyrethroid, cyclodiene, carbamate and OP insecticides underlining its distinctive mode of action at the ACh receptor (Eldefrawi, 1985).

1.2 The acetylcholine receptor

1.2.1 The ligand gated ion channel superfamily

Chemo-electrical signalling in the nervous system demands both neurotransmitters and receptors. Those receptors that mediate fast ionic synaptic currents all belong to the ligand gated ion channel (LGIC) super family of membrane spanning proteins (Ortells and Lunt, 1995). In vertebrates, neurotransmitters and their corresponding receptors may be either excitatory or inhibitory. Excitatory receptor types gate transmembrane fluxes of cations and known types are sensitive to ACh, 5-hydroxytryptamine ($5HT_3$) or glutamate, and conversely inhibitory receptors gate movement of anions using glycine or GABA as neurotransmitters (See appendix 1). These receptor types can be divided into two families based on their amino acid sequence homologies with those gated by glutamate forming one family unique amongst themselves while the others can be grouped into the second family. A further family recently characterised by Brake *et al.* (1994) is made of receptors that are gated by ATP, but the predicted structure of these receptor differs from that of either of the other LGIC families.

Of interest in this thesis are the AChRs which can be further divided into those that are sensitive to the fungal toxin muscarine (readily isolated from the fly agaric *Amanita muscaria*) and those sensitive to the tobacco alkaloid nicotine. The muscarinic AChRs (mAChR) differ markedly in their manner of eliciting signals compared to the nicotinic AChR (nAChR). In the latter, binding of ACh leads directly to a conformational change in the receptor protein allowing the opening of the central cation channel (ionotropic). By contrast, when ACh binds to the mAChR the signal is elicited through the activation of an intracellular second messenger system involving G proteins which modulate further cellular signalling systems such as ion channels and enzymes (metabotropic).

1.3 The Nicotinic acetylcholine receptor

1.3.1 Historical elucidation

Vertebrates have provided the vast majority of the structural and functional knowledge of nAChR. In particular the electric organs, which are modified muscles, from the electric fish *Torpedo marmorata* contain very high receptor densities present in the electrocyte cells and provided the material for initial investigation (reviewed by Changeux, 1993). In order to distinguish the receptor from the rest of the material earlier investigators needed a substance which could be radiolabelled and would bind with high affinity to the AChR. Venom from the banded krait snake (*Bungarus multicinctus*) had previously been shown to irreversibly block the action of ACh in vertebrate muscle tissue and the active venom component α-bungarotoxin (α-BgTx) thus provided a suitable candidate ligand to study the *Torpedo* AChR (Changeux *et al.,* 1970). The task of purifying the *Torpedo* AChR was undertaken using an affinity chromatography approach whereby AChR proteins were purified from the crude membrane preparation using an affinity ligand attached to a sepharose column, in this case the neurotoxins from snakes *Naja naja siamensis* (Thailand cobra) and *B. multicinctus* (Ong and Brady, 1974). AChR were then removed from the beads to provide a pure supply of receptor for study. Further analysis of the protein sequence revealed the AChR was composed of 5 protein chains, or subunits, which collectively formed the pentameric structure observed later in electron micrographs (Lindstrom *et al.,* 1979; Raftery *et al.,* 1980; reviewed in Unwin, 1998).

The individual subunits that made up the ~270 kDa receptor were separated using polyacrylamide gel electrophoresis revealing 4 bands of differing molecular weights designated α, β, γ and δ, the relative quantities of which gave a stoichiometry of $(\alpha)_2\beta\gamma\delta$ (Lindstrom *et al.,* 1979). Furthermore, amino acid sequence homologies among muscle subunits from different species were high indicating the pivotal importance and high degree of conservation of these proteins. Specific regions of the

subunits share conserved structural features. The α subunit contains peptides that would provide a putative binding site for agonists and competitive antagonists which is located in the extracellular N-terminal domain.

Later studies by Unwin (1993) on the three-dimensional structure at 9 Å resolution of the *Torpedo* nAChR, using cryo-electron microscopy confirmed that the nAChR was an apparently pentameric structure surrounding a central ion pore (Figure 1.3).

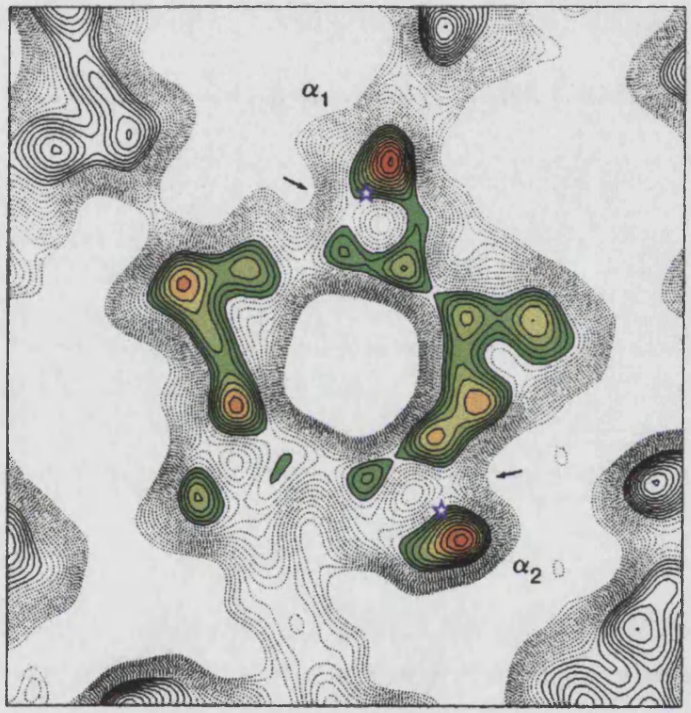

Figure 1.3. The nAChR viewed at 30 Å above the bilayer surface. Each subunit shows three density peaks (coloured); subunits arranged in pseudo-5-fold symmetry. The two α subunits are marked and the blue star represent the putative α-BgTx binding site while the arrow represents clefts which are distinctive features of α subunits. Colour enhanced and redrawn from Unwin (1993).

A further favourable property of electric fish electrocytes for the investigation of nAChR, is that when electroplax is homogenised into membrane preparations, the cell membranes spontaneously form microsacs that can be loaded with radioactive isotopes

of sodium and potassium ions (West and Huang, 1982). Evidence that the receptor harboured a central ion channel was obtained by adding ACh to such microsac preparations, from which an efflux of radioactive ions was detected (Hess and Andrews, 1977).

1.3.2 Neuronal nAChR

Pioneering work on nAChR was confined to receptor types from the electrocytes of electric fish and subsequently mammalian muscle, but it was evident that ACh was also used in the CNS of vertebrates at neuronal nAChR (Norman *et al.,* 1982). Within the last decade new techniques using complementary DNA (cDNA) have been used to isolate and characterise neuronal nAChR chiefly from chick and rat neuronal tissue. To date 8 different α subunit types (α2-α9) and 3 non-α, termed β (β2-β4), have been isolated from neuronal tissues (reviewed by Sargent, 1993; Elgoyhen *et al.,* 1994). Interpretations of the evolutionary relationships between subunits are conflicting and unclear (Ortells and Lunt, 1995; Changeux, 1995), although evolution from a common ancestor gene is probable (Devillers-Thiéry *et al.,* 1993). However neuronal α subunits can be classed into 2 or 3 different categories not on their protein sequences, but rather on their pharmacological properties using the snake toxin α-BgTx. This toxin demonstrates high affinity binding to nAChR containing α1 subunits, found in muscle, and to α7- and α8-containing neuronal nAChR (which are very similar in sequence) and also to α9, whose sequence differs markedly from the former subunits (Schoepfer *et al.,* 1990; Elgoyhen *et al.,* 1994). The other α subunits are insensitive to α-BgTx.

1.3.3 Native function neuronal nAChR

Following the isolation of cDNA clones of α and β subunits, the next challenge was to determine which subunits combine to provide functional ion channels *in vivo*. First, pure samples of neuronal nAChR were required and these were isolated from chick brain using affinity chromatography with monoclonal antibodies (MAb) produced

against muscle nAChR from electric fish. A mixture of receptor subunits were isolated containing either 49 and 59, or 49 and 75 kDa peptides (Whiting and Lindstrom, 1986; Whiting *et al.,* 1987; Whiting and Lindstrom, 1987a). Subsequent comparison of the isolated subunit sequences identified that the 49, 59 and 75 kDa corresponded respectively to the β2 (Schoepfer *et al.,* 1988), α2 (with possible trace amounts of α3) (Sargent, 1993) and α4 subunits (Whiting *et al.,* 1991). This was construed as evidence that in chick brain the majority of nAChR subtypes are composed of α2/β2, α4/β2 and to a lesser degree α3/β2. Further investigation of native chick brain nAChR by Conroy *et al.* (1992) suggested that the α5 subunit could also be involved. Using MAb's raised against the chick 49 kDa peptide Whiting and Lindstrom (1987b) immunopurified putative nAChR from rat brain, and found 2 protein bands on electrophoretic separation of 51 and 79 kDa corresponding to β2 and α4 subunits (Whiting *et al.,* 1987; Schoepfer *et al.,* 1988).

Subunit heterogeneity in native neuronal nAChR was investigated by Vernallis *et al.* (1993) in chick ciliary ganglion neurons and demonstrated that receptors from this location contain three receptor subtypes. The first subtype was identified using subunit specific MAbs and comprised α5 co-assembling with α3 and β4 to form a functional neuronal nAChR. The second receptor subtype was found in ~20% of these α5, α3 and β4 containing receptor subtypes which in addition harboured the β2 subunit indicating that neuronal nAChR may be as complex in subunit composition as their muscle counterparts. The third subtype apparently contained only the α7 subunit (Conroy and Berg, 1995).

Native nAChR subtypes that were responsible for the high affinity binding of α-BgTx were investigated by several groups using α-BgTx affinity columns (Norman *et al.,* 1982; Conti-Tronconi *et al.,* 1985; Kemp *et al.,* 1985; Whiting and Lindstrom, 1987b; Gotti *et al.,* 1991). The number of subunits identified on denaturing electrophoresis gels ranged from 1 to 5, which is consistent with either homo or heteromeric nAChR, with molecular weights between 45 and 72 kDa.

1.3.4 Functional expression of neuronal nAChR genes

Once the complementary co-existence of α and β subunits in neuronal nAChR was established the next step was to achieve *in vitro* expression to investigate the functioning of nAChR with known subunit composition. The expression system used was that of *Xenopus laevis* oocytes into which mRNAs can be co-injected in any desired combination and expressed nAChR appraised electrophysiologically. Using this approach Boulter *et al.* (1987), Wada *et al.* (1988) and Deneris *et al.* (1989) demonstrated that when rat α2, α3 or α4 mRNA was co-injected with β2 mRNA, functional heteromeric receptors resulted that were sensitive to ACh and nicotine but not blocked by α-BgTx. A further toxin isolated from *Bungarus* venom called neuronal BgTx (n-BgTx) differs significantly in pharmacology from α-BgTx and the chimeric α3/β2 and α4/β2 receptors were both blocked by n-BgTx. When expressed alone none of these subunits gave convincing functional receptors; although ionotropic responses could be elicited from α4 homomers, these were found only in the presence of non-physiologically high concentrations of ACh.

No functional nAChR were found when the α5 subunit was co-expressed with any of β2, β3 or β4 (Boulter *et al.,* 1990). Further investigation indicated that actually α5 was behaving as a structural component of nAChR and when co-injected with α4 and β2 produced different responses to the α4/β2 functional receptors (Ramirez-Latorre *et al.,* 1996). The rationale of this finding is that although α5 is classified as an α subunit because of its possession of cysteines at positions 192 and 193, it does not appear to act as an ACh binding subunit (see section 1.3.11).

1.3.5 Subunit heterogeneity in neuronal nAChR

The α7 subunit is able to form *in vitro* functional channels in the absence of β subunits (Couturier *et al.,* 1990a). However pharmacological comparisons of artificial homomeric and native α7-containing nAChR suggests that *in vivo* α7 subunits may exist within heteromeric receptors (Anand *et al.,* 1993). A further α-BgTx sensitive subunit, α8, can also form homomeric receptors *in vitro* in *Xenopus* oocytes (Gotti *et al.,* 1994). Interestingly, when α7 and α8 mRNAs are co-injected in varying ratios into oocytes the resulting receptors always have the pharmacological properties belonging to α7 (Schoepfer *et al.,* 1990; Gotti *et al.,* 1994). The last α-BgTx sensitive subunit, α9, can also form functional homomeric receptors *in vitro* (Elgoyhen *et al.,* 1994) which are characterised by sensitivity not only to nicotinic agents such as α-BgTx and *d*-tubocurarine, but also the muscarinic agent atropine, giving it a mixed nicotinic/muscarinic pharmacology.

1.3.6 Subunit composition and functional diversity of nAChR

The agonist binding properties of expressed nAChR were investigated by Luetje and Patrick (1991) with rat α2, α3, and α4 with β2 and β4. Two important points emerged from this study. First, receptor sensitivity to the agonist cytisine was determined by the β subunit, those containing β4 showing a high sensitivity. Therefore the β subunit has an input into the binding of agonists. Second, although combinations containing β4 showed a high affinity for cytisine, this did not correlate with an efficacious opening of the ion channel. Thus high affinity binding of agonist does not necessarily imply that it will lead to a conformational change in the receptor.

The stoichiometry and arrangement of subunits forming the receptor can affect single channel conductance. Subunit assembly in *Xenopus* oocytes was investigated by Papke *et al.* (1989) using single cloned α and β subunits. Two different conductance states could be evoked indicating the presence of two different receptors. Receptors could

differ either due to post translational modifications, a faulty stoichiometry (e.g. 2α2β, 3α2β or 3α3β) or due to different arrangements of the subunits within the pentamer (e.g. ααβββ or αβαββ). However an investigation of stoichiometry by Amand *et al.* (1991) using [^{35}S]-methionine labelling of mRNAs encoding α4 and β2 subunits found a ratio of 1:1.46, suggesting the presence of pentamers comprising two α and three β subunits, as expected. Moreover, Cooper *et al.* (1991) investigated channel conductance of putative ion channels and reached the same conclusion that a stoichiometry of 2α:3β was favoured, consistent with a molecular weight of ~300 kDa. Electron microscopy using α-BgTx or anti α subunit antibodies in electric fish or skeletal muscle demonstrates that the α subunits are not adjacent to each other (Kubalek *et al.,* 1987). The formation of *Torpedo* muscle nAChR was investigated by Green and Wanamaker (1998) and contrary to earlier investigations, it was found that the ACh binding sites form at different times during subunit assembly. A trimer of α, β and γ forms first, a δ is then added to make a tetramer and finally a second α is added to form the complete pentamer.

1.3.7 Subunit composition in native nAChR

Despite our increasing wealth of knowledge of neuronal nAChR there is still only very sparse evidence to correlate the properties and subunit composition of native receptors with those subunit combinations expressed and investigated in *Xenopus* oocytes. Apparently conflicting affinity values for ACh between different nAChR from different species sharing a high sequence homology only confuses matters. For example α3/β4 and α3/β2 receptors have been reported to have ACh affinities of 158 and 5.6μM respectively for chick and 30 and 350μM for rat (Couturier *et al.,* 1990a; Cachelin and Jaggi, 1991). This variability could be due to faulty stoichiometry of the expressed receptors or to differences in experimental procedure. Only one study of the rat interpeduncular nucleus (IPN) has yielded *in vivo* conductance characteristics of native nAChR that can be correlated with those observed *in vitro* (Mulle *et al.,* 1991; Papke *et al.,* 1989). The IPN is known to express genes encoding the α2, α3, α4, α5

and β2 subunits; conductance studies indicate that a composition of α2/β2 may form the main class of nAChR. However, the agonist efficacy of cytisine and ACh are not in agreement between the native and artificial receptors (Mulle *et al.,* 1991; Luetje and Patrick, 1991).

1.3.8 Presynaptic nAChR

The physiological roles played by nAChR to mediate fast excitatory transmission at neuromuscular junctions and in autonomic ganglia in the peripheral nervous system (PNS) are well known. Although the physiological roles of nAChR in the vertebrate brain are less well understood, presynaptic nAChR may offer an insight into how they might be involved in the modulation of transmitter release from presynaptic terminals. Presynaptic receptors can be defined as 'receptors at or near the nerve terminal that can positively or negatively modulate transmitter release directly, or influence the probability of an action potential resulting in exocytosis' (Wonnacott, 1997). Examples of the function of presynaptic nAChR are to be found in dopamine release at striatal dopamine terminals (Clarke and Reuben, 1996), and the ability of nicotine to enhance synaptic transmission of glutamate in the medial habenula (McGehee *et al.,* 1995).

1.3.9 Agonist and antagonist binding sites

A full understanding of the receptor-ligand interaction is vital to understand potential target site alterations that could give rise to a decrease in affinity for a particular drug. Again the major contribution to understanding of the ACh binding site has been provided by studies of vertebrate nAChR, particularly muscle types from electric fish. The functioning of vertebrate nAChR are presumed to reflect those of invertebrates since they share considerable homology.

Three classes of ligand have been used pharmacologically to distinguish discrete receptor populations. First are the agonists such as ACh, nicotine and epibatidine (EPI)

which elicit opening of the ion channel. Second are the competitive antagonists such as α-BgTx, *d*-tubocurarine and methyllycaconitine (MLA) that bind to the cholinergic binding site but do not elicit a response. Third are the non-competitive antagonists such as histrionicotoxin (Rapier *et al.,* 1987) which exhibit their actions by preventing the normal functioning of the ion channel opening by either directly blocking the channel or acting allosterically at a site other than the ACh binding site.

1.3.10 Structural features of the nAChR

All nAChR share conserved sequence homologies that give rise to characteristic structural features. These include an extracellular N-terminal domain which in α subunits contains the ACh binding site. All subunit types also possess four conserved putative transmembrane spanning regions (named M1-M4), of which M2 is proposed to line the ion channel. The large cytoplasmic loop connecting M3 and M4 contains phosphorylation sites and the protein ends with a short extracellular C-terminal domain. These features are depicted in figure 1.4 and reviewed by Hucho *et al.* (1996).

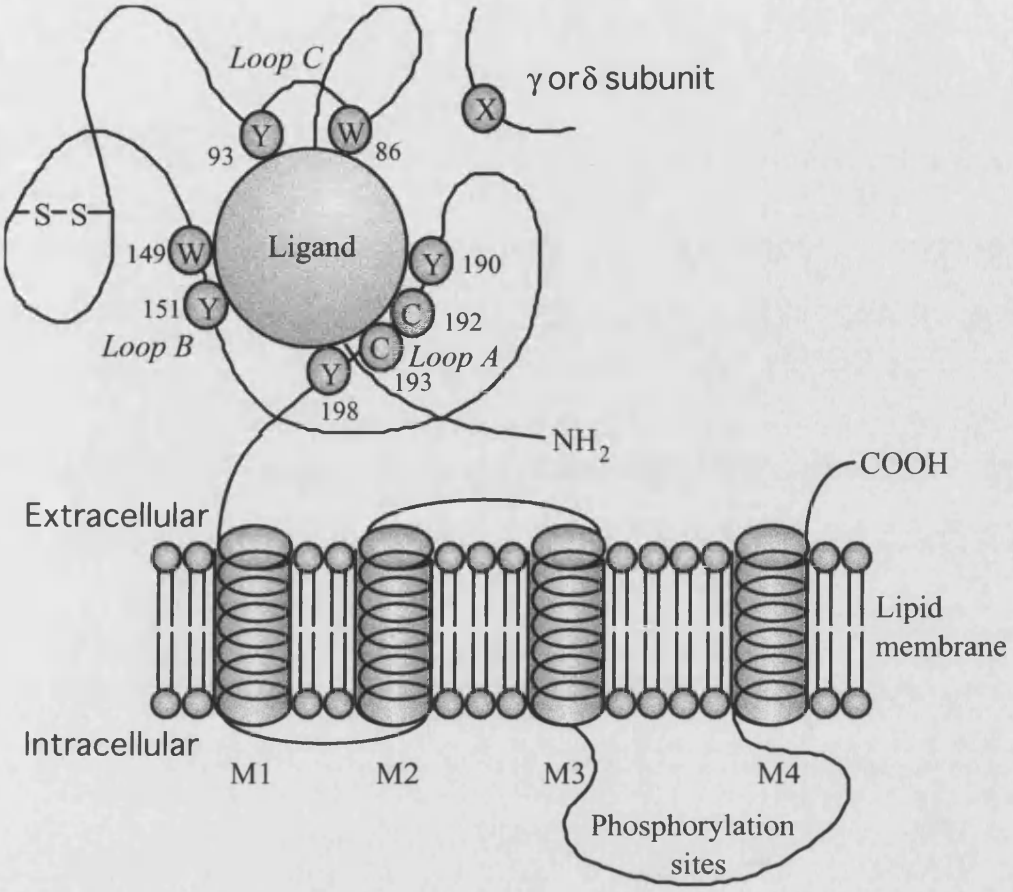

Figure 1.4. Conserved features of the nAChR α subunit depicting the 3 loop model. Redrawn and enhanced from Devillers-Thiéry *et al.* (1993)

The interaction of ACh at ligand binding sites elicits conformational changes in the nAChR protein in the topographically distinct ion channel which can be open or closed. In order for this to occur the ACh binding site must be mechanically linked to the ion channel. The conformations taken by the nAChR are not restricted to only an open or closed state; in reality, the situation is rather more elaborate involving a resting, active, intermediate and desensitised states and all the respective intermediate states (Changeux *et al.,* 1984; McCarthy and Stroud, 1989) depicted in Figure 1.5.

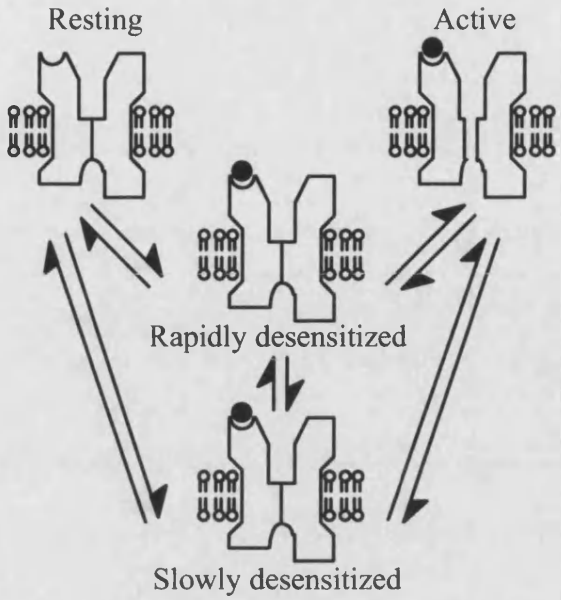

Figure 1.5. Minimal four-state model for the allosteric transitions of the nAChR (Redrawn from Changeux *et al.,* 1984)

The phenomenon of desensitisation is thought to be rare *in vivo* since AChE rapidly hydrolyses ACh once the receptor has been activated. Thus the physiological purpose of desensitisation remains obscure (Stroud *et al.,* 1990). However phosphorylation sites on the receptor may regulate its extent. Mutational studies removing phosphorylation sites from nAChR give rise to receptors that desensitise slower than the wild type (Hoffman *et al.,* 1994). Furthermore phosphorylation of purified *Torpedo* nAChR in the presence of cAMP-dependent protein kinase could be correlated with the rate of agonist induced desensitisation (Huganir *et al.,* 1986). Similarly Hopfield *et al.* (1988) demonstrated that increasing the extent of phosphorylation by incorporating exogenous protein tyrosine kinase together with nAChR in reconstituted lipid bilayers leads to increasingly rapid desensitisation. It has been postulated that the degree of nAChR phosphorylation could be regulated *in vivo* by a protein kinase, regulated itself by calcium concentrations (Swope *et al.,* 1992; Miles *et al.,* 1994).

1.3.11 The ACh binding site

The topology of the ACh binding site was investigated in *Torpedo* nAChR with photoaffinity labelling probes and subsequently a three loop model of agonist and competitive antagonist binding site was proposed (reviewed by Galzi *et al.,* 1991) depicted in figure 1.4. The photoaffinity label predominantly used was DDF (p(N, N)-dimethyl-aminobenzenediazonium fluoroborate). The first loop (A) contains Trp 86 and Tyr 93, loop B contains Trp 149 and Tyr 151 and in loop C Tyr 190, the Cys doublet 192-193 and Tyr 198 appear to be important in ligand binding (Cohen *et al.,* 1991; Kao *et al.,* 1984). Interestingly these amino acids are predominantly aromatic residues which are also present in other choline binding proteins including mAChR and AChE (Satow *et al.,* 1986; Sussman *et al.,* 1991; Wess *et al.,* 1991). The DDF-labelled amino acids are conserved at homologous positions in all known α subunits from both neuronal and muscle type nAChR with the exception of α5 and the non-α subunits. The neuronal α5 subunit has been previously discussed and appears unable to bind ACh and instead appears to fulfil a structural role and furthermore determined to lack Tyr 93 and 190 (Boulter *et al.,* 1990; Couturier *et al.,* 1990b). A further binding site different from that of ACh able to activate the ion channel is located in the vicinity of loops A and B and is sensitive to physostigmine and benzoquinonium (Albuquerque *et al.,* 1991; Schrattenholz *et al.,* 1993). Photoaffinity labelling revealed that Lys 125 was pivotal at this binding site (Tano *et al.,* 1992).

The functional significance of amino acids in the molecular interaction between ACh and binding site residues was investigated by mutagenesis. Changes in the Cys 192 or 193 abolished the ACh-induced response demonstrating its pivotal importance (Mishina *et al.,* 1985). Mutation of Tyr 190 into another aromatic residue, Phe, decreases the sensitivity of the binding site for ACh by 50-fold but this did not interfere with the binding kinetics of α-BgTx. In general, further mutations of the other critical amino acids resulted in an affinity decrease for the agonists ACh and nicotine

and to a lesser extent for the competitive antagonists dihydro-β-erythroidine and α-BgTx.

The cysteine residues at positions 128 and 142 are proposed to form a disulphide bridge to form the cysteine loop which is highly conserved between the α and non-α subunits (Kao and Karlin, 1986). Modelling of this region suggests that it forms a amphiphilic β-hairpin which contributes to the conformation of the ACh binding site (Cockcroft *et al.,* 1990).

The two α subunits present in the *Torpedo* muscle nAChR are encoded by a single gene yet the binding sites are not strictly equivalent indicating that the non-α subunits contribute to ACh binding. They differ in the kinetics of binding and dissociation of α-BgTx and in affinity for certain ligands such as *d*-tubocurarine (Conti-Tronconi *et al.,* 1990; Pedersen and Papineni, 1995). Further analysis of this enigma concluded that the most probable cause was that the ligand binding sites were at the interface between α and non-α subunits, and thus the latter were contributing to the binding site. In the case of *d*-tubocurarine evidence suggested that the γ subunit is involved with the high affinity site and that the δ subunit contributes to the low affinity one (Pederson and Cohen, 1990). However, contradictory evidence that the binding site is not at the interface of subunits comes from direct visual determination using electron microscopy by Unwin (1993).

As has been mentioned previously, the nAChR is capable of multiple conformational states whose affinities for ACh differ markedly; the underlying mechanisms were investigated by Galzi *et al.* (1991). The structural modifications of residue conformation were investigated using DDF photoaffinity labelling. The three loops on the α subunit were differentially affected upon desensitisation with loop C undergoing no change while binding at loops A and B increased up to 6-fold. This observation is consistent with a tighter binding of the ligand and therefore an increase in affinity of

the desensitised state. During the transition from the resting to the desensitised state the affinity for ACh increases 10,000-fold from μM to nM concentrations.

1.3.12 The ion channel

Affinity labelling using non-competitive blockers (NCB) has been used to investigate the role of amino acids that delineate the ion channel (Reviewed in Devillers-Thiéry *et al.,* 1993). The NCB [^{3}H]-chlorpromazine was used in association with carbamylcholine to induce a desensitised state. The amino acids labelled under equilibrium conditions were: α-Ser 248, β-Ser 254, β-Leu 257, γ-Thr 253, γ-Ser 257, γ-Leu 260 and δ-Ser 262. All these residues belong to the M2 transmembrane region of each subunit with each Ser residue occupying equivalent positions. The functional role of the M2 regions was confirmed in mutation studies and the importance of the threonine ring, serine ring, equatorial leucine ring, valine ring and outer leucine rings was established (Figure 1.6).

Further affinity labelling by the NCB trimethylphosphonium indicates that additional residues become available when the nAChR is in a desensitised conformation. From these studies it was concluded first that the M2 segments of each subunit are symmetrically packed and line the ion channel, and second that the affinity labelling is consistent with an alpha helical organisation. The profile of the channel was determined by Unwin (1993) through cryo-electron microscopy and a proposed mechanism of channel gating by the M2 regions was put forward. In this model, the helical M2 regions are not straight but kinked in the middle and thus rotation can gate the open and closed state of the channel (Figure 1.7).

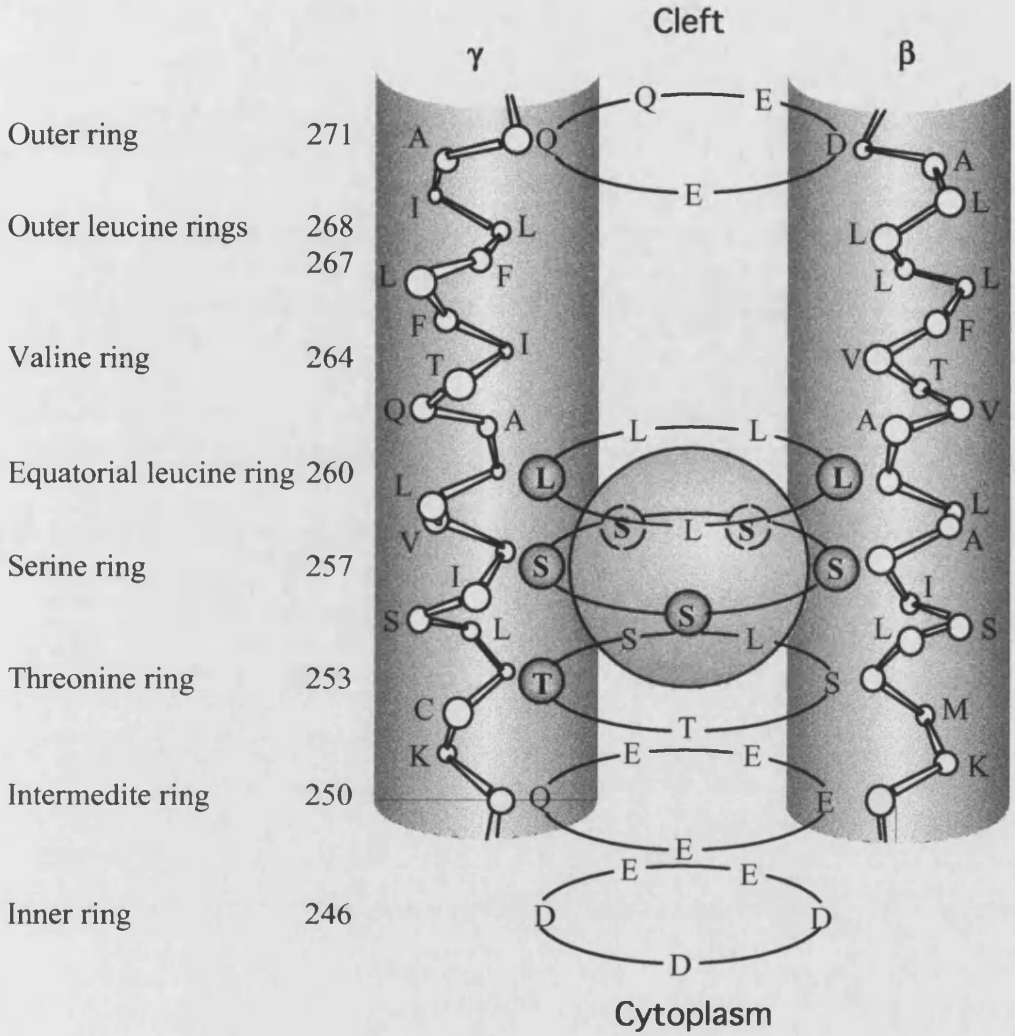

Figure 1.6. The ion channel of *Torpedo* nAChR showing the binding site for chlorpromazine (shown as a sphere) showing the important amino acids that line the ion channel lumen. Redrawn from Devillers-Thiéry *et al.* (1993).

Figure 1.7. The nAChR in profile showing the M2 regions (in red) and the extent of the lipid bilayer (blue dots). The large protein at the base of the receptor is thought to act as an anchor to the cytoskeleton. Colour enhanced and redrawn from Unwin (1993).

1.3.13 Summary of vertebrate nAChR

In summary, nAChR are membrane-spanning proteins assembled from a pentamer of subunits which collectively form a cation-selective central ion channel. Opening of the channel is mediated by binding of ACh which controls ion passage. Subunits which contain an ACh binding site are referred to as α subunits and others as non-α subunits, although these also contribute to the selectivity of the ACh binding site. Muscle nAChR possess 2α and 3 non-α (γ, δ and β) subunits while neuronal nAChR are assembled from a portfolio of 8 different types of α (α2-α9) and 3 non-α (β2-β4) subunits, although the composition of native receptors is believed not to be random, and only particular combinations are functional. Subunit combinations may be either homomeric or heteromeric in terms of the receptor's α and non-α subunit content. Vertebrate nAChR can be classified by their pharmacology because particular ligands, most of which are naturally occurring neurotoxins, can selectivity label specific subunit combinations. The nAChR is a protein capable of multiple conformational states, and allosteric interactions between ACh binding sites on the same nAChR are known to occur.

1.4 Nicotine resistant insects

Specialist tobacco feeders have evolved to subsist on tobacco plants despite high dietary concentrations of nicotine and related allochemicals in this plant. Larvae of the tobacco hornworm *Manduca sexta* (Lepidoptera: Sphingidae) can cope with high levels of alkaloids associated with a diet comprising the leaves of solanaceous plants which include tobacco, potato and tomato, all of which are of commercial importance. *M. sexta* is not the only tobacco feeder to cause economic damage; of particular importance the tobacco budworm *Heliothis virescens* (Lepidoptera: Noctuidae) also eats tobacco, as well as lesser pests which include stem borers, leaf miners, flea beetles, aphids, whitefly, thrips, stink bugs, grasshoppers and of course the aptly named cigarette beetle! However of these insects *M. sexta* has received the most attention due partly to its ease of rearing in the laboratory and ease of handling due to its large size.

1.4.1 Nicotine tolerance in the tobacco hornworm

M. sexta larvae are notably tolerant to nicotine in their diet. Fifth (final) instar larvae of *M. sexta* eat about 6g of tobacco per day (Reynolds *et al.,* 1986). Of course, enough nicotine can still be toxic. Parr *et al.* (1972) demonstrated that *M. sexta* does have a threshold of nicotine concentration above which its neurotoxicity is fatal. Green tobacco leaves typically contain 0.1-0.5% nicotine and concentrations of >2% in an artificial diet lead to the insects' demise.

The intrinsic nicotine resistance mechanisms harboured by *M. sexta* have been the intrigue of numerous investigations. The supposition that *M. sexta* would require protection from nicotine at synaptic junctions derives from the knowledge that ACh is a major neurotransmitter in the insect CNS. Trimmer and Weeks (1989) showed that in *M. sexta* ACh is the likely neurotransmitter used at synapses controlling activation of the prolegs via the PPR motorneuron. Evidence for this was that transmission at these synapses could be reversibly inhibited by the cholinergic drugs *d*-tubocurarine,

atropine, mecamylamine and α-BgTx. An interesting point issued from the study by Trimmer and Weeks (1989) was that the sensitivity of the nAChR to nicotine was reduced. Furthermore, the receptors for ACh were apparently of both nicotinic or muscarinic types.

Protectant mechanisms to prevent nicotine reactivation of nAChR in *M. sexta* were first investigated by Self *et al.* (1964), who demonstrated that 5th instar larvae could tolerate a high haemolymph nicotine concentration of 100μM and that a high ratio of excretion and egestion of nicotine gave a partial explanation to the puzzle. However no metabolism of nicotine *in vivo* was resolvable after topical, injection or ingested doses were given. A potential ally for the breakdown of ingested alkaloids are nicotinophilic bacteria present in the gut but these were not thought to contribute significantly.

Maddrell *et al.* (1976) further investigated the rapid excretion of nicotine by the Malpighian tubule system in *M. sexta* larvae which was not inducible but rather constituent in its nature. By contrast, the adult moth lacks the ability to excrete nicotine via the Malpighian tubules reflecting the adult's exclusive nectar diet (Maddrell *et al.*, 1976). Snyder *et al.* (1994) studied the properties of nicotine metabolism in *M. sexta* using the techniques of mass spectrometry and [^{1}H]NMR. These sensitive approaches were not available to previous investigators and by contrast led to the discovery that *M. sexta* does in fact metabolise ingested nicotine to less polar molecules. This aids their excretion, the major product being cotinine-N-oxide. Moreover, the rapid metabolism of nicotine in the gut of *M. sexta* was demonstrated to be inducible upon the dietary inclusion of tobacco alkaloids.

Physiological barriers to prevent nicotine interacting at its target synaptic site in *M. sexta* were the subject of an extensive study by Catherine Morris (Morris, 1983a, 1983b, 1983c, 1984; Morris and Harrison, 1984). Penetration of the insect CNS by nicotine was equally fast in a comparison between nicotine insensitive (*M. sexta*) and sensitive (*P. americana*) insects. Both insect types rapidly metabolised nicotine to

water soluble conjugates in the CNS which is analogous to the functioning of mammalian liver. Metabolism of nicotine by perineurial cells is intracellular, constitutive and initiated by the cytochrome P450 system associated with the smooth endoplasmic reticulum which performs oxidative and conjugative roles.

Critical comparison shows that nicotine efflux differs in *M. sexta* from that in *P. americana* in that the latter has simpler kinetics and is slower. This difference was peculiar to nicotinoids while other molecules such as atropine were handled identically by *M. sexta* and *P. americana*. This suggests that nicotinoids are dealt with differently by nicotine sensitive and insensitive insects. The tracheal system provides a potential axial diffusion pathway for nicotinoids leading into the core of the CNS. However, cells lining this passive aeration system are adapted to this problem and are capable of rapid nicotine metabolism.

A further barrier to nicotine reaching the nAChR is the spatial pattern of the perineurium basal cells which form the blood brain barrier. In order for nicotine to interact with the nAChR it has to be in its protonated state but in order to breach the cuticle and ion barrier it needs to be in its unprotonated lipophilic state (Yamamoto *et al.*, 1995) (Figure 1.8).

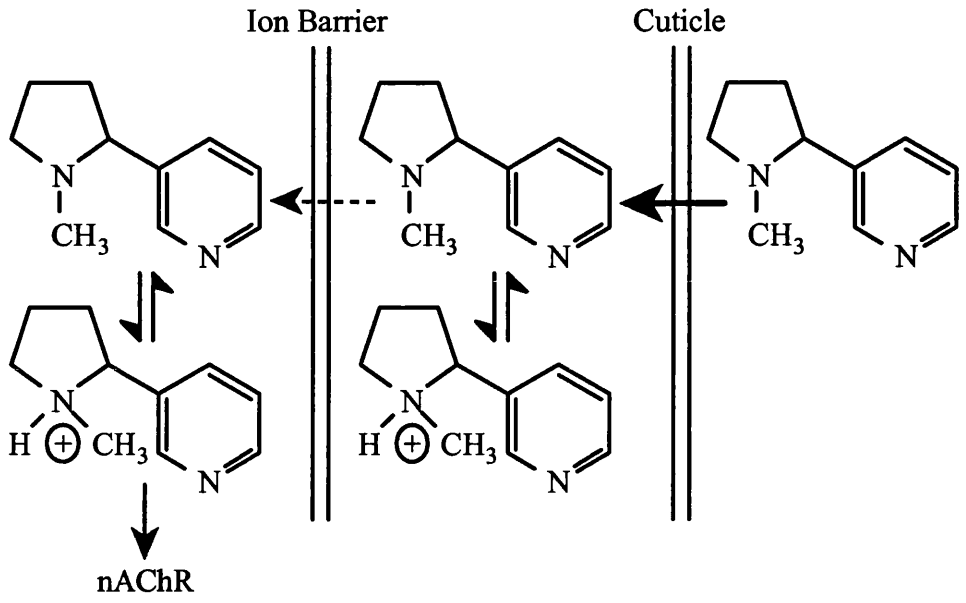

Figure 1.8. Movement of nicotine through the insect cuticle and ion barrier in its protonated and unprotonated states. Redrawn from Yamamoto *et al.* (1995).

Electron micrographs demonstrate that perineural cells are fewer in number and have less contact with one another in *M. sexta* (Morris and Harrison, 1984) compared to those in *P. americana* (Lane *et al.*, 1977). This structuring of the basal cells in *M. sexta* was postulated to be an adaptation to reduce the intracellular diffusion of protonated nicotine. Further protective mechanisms in the CNS are putative alkaloid pumps in the *M. sexta* nerve cord. However when these were inhibited by N-methylnicotinamide the PPR response to nicotine was only weakly potentiated suggesting that the pumps do not markedly contribute to nicotine resistance (Trimmer and Weeks, 1989). The same authors went on to suggest that the intrinsic nicotine insensitivity apparently possessed by the *M. sexta* CNS could be the result of a modified nAChR.

1.4.2 Receptor modification

Receptor modification must certainly be considered as a possible explanation of nicotine insensitivity in *M. sexta* given that the receptors themselves appeared to have a

reduced sensitivity to nicotine (Trimmer and Weeks, 1989). This is in fact the underlying resistance mechanism to another class of chemicals that target the insect $GABA_A$ receptor (Hosie *et al.,* 1997). These include dieldrin, a cyclodiene insecticide, and picrotoxinin a natural plant toxin. The pharmacological properties of a resistant mutant of *Drosophila melanogaster* conferred by the *Rdl* (resistance to dieldrin) gene were shown to be due to this gene's encoding of an ionotropic GABA receptor subunit. *Rdl* gene products were studied electrophysiologically in cultured neurones and also expressed in *Xenopus* oocytes (ffrench-Constant *et al.,* 1993; Zhang *et al.,* 1994; Shirai *et al.,* 1995). The resistance is conferred by a single point mutation of alanine to serine at residue 302 within the second membrane-spanning domain (M2), thought to line the anion channel. These drugs bind preferentially to the desensitised state of the $GABA_A$ receptor and the mutation causes a weakened drug binding interaction with this conformation. The mutation also further destabilises the desensitised state making it more transitory (Zhang *et al.,* 1994).

A final twist to the tale of nicotine insensitive insects is that certain species of *Nicotiana*, notably *N. stockii*, possess a novel, and as yet unidentified, nicotinoid in its leaf exudates which confers antifeedant properties against *M. sexta* (Huesing and Jones, 1987).

1.5 Neonicotinoids - the new generation insecticides

The terms 'nicotinoid' and 'neonicotinoid' were proposed by Tomizawa and Yamamoto (1993). Nicotinoids include nicotine and its analogues; their essential feature is a basic nitrogen which becomes positive by protonation within the insect so that they mimic the neurotransmitter ACh. The neonicotinoids, which include the nitromethylene and nitroguanidine compounds, are distinguished by a nitrogen having a partial positive charge due to the electron-withdrawing effect of the substituents on the 2-position (Yamamoto *et al.,* 1998).

Nitromethylenes were the first neonicotinoids and their insecticidal chemistry was presented at the 1978 IUPAC Conference in Zurich by Soloway *et al.* (1979) who put forward nithiazin as the most active compound within the series. Nitromethylenes did not prove to be useful practical insecticides, however, partly due to poor persistence in the field due to photoinstability. Subsequently in 1984 chemists at Nihon Tokushu Noyaku Seizo K.K. put forward the nitroguanidine 1-(6-chloro-3-pyridylmethyl)-N-nitroimidazolidin-2-ylideneamine (NTN 33893), with the common name of imidacloprid (IMI).

1.5.1 Biological effects of neonicotinoids

IMI exhibits good contact, translaminar and systemic activity against hemipteran pests such as aphids, whitefly and planthoppers as well as activity towards coleopteran, isopteran and lepidopteran pests (Elbert *et al,* 1991; Boucias *et al.,* 1996; Leicht, 1996) with low mammalian toxicity (Zwart *et al.,* 1992, 1994). However the spectrum of activity delivered by IMI does not include nematodes or spider mite (Acari). IMI is also used in a veterinary context against fleas (Siphonaptera) (Jacobs *et al.,* 1997), although it is not effective against ticks (Acari).

The lethal symptoms brought about by IMI are typical of a nerve-acting agent and include tremoring and uncoordinated movement (Leicht, 1993). The sublethal effects of IMI on the peach potato aphid *Myzus persicae* (Sulzer) were investigated by Nauen (1995) demonstrating that at low systemic doses IMI induces antifeedant behaviour. This was associated with a decrease in honey dew, nymph production and weight and an increase in probing. The behaviour modifying effects of low systemic doses were seen to be reversible when aphids were allowed to feed on untreated leaves. A sibling species of *M. persicae* the tobacco aphid *Myzus nicotianae* (Blackman) was the subject of investigation of Nauen *et al.* (1996) and Devine *et al.* (1996) since this aphid feeds on tobacco and was therefore likely to be exposed to its alkaloids. The tobacco feeding form is differentiated by the mobility of glutamate oxaloacetate transaminase by electrophoretic separation (Blackman and Spence, 1992). Earlier studies by Guthrie *et al.* (1962) proposed that *M. nicotianae* avoids exposure to the nicotine containing xylem and instead is a phloem feeder. However it seems likely that exposure to nicotine is unavoidable and this insect may harbour a nicotine tolerance which could provide cross resistance to the chloronicotinyl insecticides. In comparison to a susceptible strain of *M. persicae* (US1L originating from Rothamsted experimental station), *M. nicotianae* (isolated from Greek peach) showed a 5-fold resistance factor to both nicotine (fumigation bioassay) and IMI (dip bioassay). Furthermore, sublethal effects of IMI were significantly less prevalent in *M. nicotianae* compared to *M. persicae* (Devine *et al.,* 1996). A Japanese strain of *M. persicae* was further shown to exhibit a 4 to 7-fold resistance to IMI depending on the bioassay employed (Nauen *et al.,* 1996). However these resistance factors are relatively small compared to those encountered with carbamate insecticides which in the case of the Japanese *M. persicae* clone were >385-fold compared to the susceptible strain US1L.

The choice of bioassay becomes an important factor when a behavioural IMI resistance mechanism occurs. Nauen and Elbert (1997) investigated a French field collected strain of *M. nicotianae* which exhibited an apparent resistance of over 50-fold in oral ingestion bioassays. However dip bioassays demonstrated that the true tolerance was

under 10-fold and the explanation for the increased hardiness of the French strain related to its ability to survive a longer starvation period than the susceptible strain. Potential biochemical mechanisms of increased IMI tolerance in *M. nicotianae* were investigated by Nauen *et al.* (1998a) and these studies concluded that oxidative detoxification, hydrolytic metabolism and the involvement of endosymbiotic bacteria were not involved.

Cross resistance to IMI was also apparent in strains of the German cockroach *Blattella germanica* and the house fly *M. domestica* (Zhimou and Scott, 1997). All the strains tested demonstrated significant resistance to pyrethroids, OPs, carbamates and cyclodiene insecticides. However in all cases the tolerance shown to IMI was less than 10-fold compared to that of the susceptible strains. Treatment with piperonyl butoxide (PBO), which inhibits mixed function oxidases (cytochrome P450), failed to suppress the cross resistance in all the tested strains of cockroach or fly indicating that other mechanisms yet to be elucidated were involved.

Base line levels of susceptibility have been measured in insects controlled by IMI, such as the small brown planthopper *Laodelphax striatellus*, to evaluate any future resistance (Sone *et al.,* 1995). Mechanisms of low susceptibility to IMI were investigated by Sone *et al.* (1997) in a malathion and propoxur pressured strain of *L. striatellus*. This strain demonstrated a 20-fold resistance to IMI which was reduced by 50% when the metabolic inhibitors PBO, tributylphosphorotrithioate, and trichlorobenzene ester were used in conjunction with IMI. None of the synergists alone was shown to be insecticidal at the dose used. Therefore a portion of the IMI resistance in *L. striatellus* seems likely to be due to metabolic activity. The cuticular penetration of insecticide was investigated with [^{14}C]-IMI but demonstrated no difference between susceptible and resistant insects. Artificial pressuring maintains a sublethal persistence of insecticide which provides ripe conditions for the appearance of a resistant clone. This approach has been used for over 90 generations with IMI on *M. persicae* but resulted in no significant tolerance appearing (Elbert *et al.,* 1996).

Zhao *et al.* (1995) investigated cross resistance in the western flower thrip *Franklinella occidentalis* between susceptible (UMC) and resistant (KCM) strains in which strong resistance (>100-fold) was shown against pyrethroids and OPs. Despite no previous exposure to IMI the KCM strain demonstrated a 14-fold tolerance compared to UMC. The authors account for the IMI tolerance due to differences in pharmacokinetics or speculate that diazinon has selected for a modified ACh receptor in addition to an altered AChE.

The Colorado potato beetle *L. decemlineata* is a major pest of potatoes and has developed considerable multiple resistance to many insecticide classes leading to control problems. Thus, the advent of IMI with its novel mode of action led to its extensive use in Michigan in 1995 on 80% of the potato crop increasing to 90% in 1996 (Grafius and Bishop, 1996). Widespread use increases the risk of resistance and surviving beetles isolated from the field in 1995 were pressured with IMI and studied in topical application bioassays comparing to susceptible insects. However, the resistance factor was less than 10-fold between IMI resistant and susceptible strains (Grafius and Bishop, 1996).

In summary, insects highly resistant to insecticides already in use demonstrate only a very low level of cross resistance to IMI, typically with a resistance factor less than 10-fold compared to a susceptible strain. The metabolic actions of cytochrome P450 have been shown to provide part of this tolerance in *L. striatellus*.

1.5.2 Resistance management of neonicotinoid insecticides

The neonicotinoids represent a new class of insecticide which circumvent existing resistance mechanisms and thus provide an opportunity to control a range of pests effectively. In order to achieve this their continued use must be closely managed to prevent the occurrence and spread of resistance (Elbert *et al.,* 1996). Resistance to IMI in *L. decemlineata* is of particular concern and a management strategy of inter-

cropping IMI treated and untreated plants was investigated by Dively *et al.* (1998). Good control of *L. decemlineata* was achieved by a mixture of treated and untreated rows with a combined protective perimeter to provide an effective toxic barrier to colonising beetles. This strategy reduces both the economic and environmental cost and creates refuges to minimise resistance developing.

Another resistance strategy is to incorporate IMI into an integrated pest management (IPM) approach which harmonises biological and chemical control. Koppenhofer and Kaya (1998) demonstrated that the entomopathogenic nematode *Heterorhabditis bacteriophora* (Poinar) could synergise with IMI for the control of white grubs in turf belonging to the genus *Cyclocephala.* Another successful synergism between IMI and an entomopathogenic fungus *Beauveria bassiana* was investigated for the control of the termite *Reticulitermes flavipes* (Boucias *et al.,* 1996). Termites are highly resistant to fungal infection, not through endogenous antifungal substances but rather due to social behaviour such as grooming. Sublethal doses of IMI appear to disrupt the social interactions leading to a fungal epidemic providing an effective control of termites.

1.5.3 Mode of action of the neonicotinoid insecticides

The molecular target of the neonicotinoids was first reported to be the nAChR by Schröder and Flattum (1984) who used electrophysiological methods. Later, it was shown that chloronicotinyl insecticides could displace specifically bound [^{3}H]-α-BgTx in homogenates of the stable fly, *Stomoxys calcitrans* (Abbink, 1991). Conclusive evidence was provided by Bai *et al.* (1991) using IMI in both displacement-studies involving [^{125}I]-α-BgTx binding to cockroach nerve cord preparations and electrophysiological evidence from cockroach motor neurone D_f where it caused depolarisation thus acting as an agonist at nAChR.

The pharmacological profile of the nAChR differs both quantitatively and qualitatively depending on the assay system employed. In the binding studies of Bai *et al.* (1991),

IMI was shown to be 50 times more potent than nicotine in displacing α-BgTx. By contrast, Abbink (1991) using *S. calcitrans*, found that nicotine displaced labelled α-BgTx at 100-fold lower concentrations than IMI, and further Tomizawa and Yamamoto (1992) utilising honey bee homogenates ascribed similar binding affinities to nicotine and IMI. It may be concluded that for applied purposes, for example determination of bioefficacy and appraising the potential for cross resistance, binding studies should be directed towards target pests otherwise misinformation may result.

Further evidence that IMI binds to the nicotinic receptor comes from the work of Liu and Casida (1993). These workers utilised [^{3}H]-IMI which was found to specifically bind in *Musca domestica* heads as well as other insect nerve tissue, with a dissociation constant of 1.2nM; this binding was displaceable by nicotinic ligands. There is some evidence that IMI may also act at mAChR since its actions are sensitive to muscarinic agents in electrophysiological (Schröder and Flattum, 1984) and radioligand binding studies (Lui *et al.,* 1993; Liu and Casida, 1993). However evidence suggesting that the primary target of IMI is the nAChR comes from radioligand binding (Tomizawa and Yamamoto, 1992, 1993), patch-clamp (Leech *et al.,* 1991; Cheung *et al.,* 1992; Zwart *et al.,* 1992, 1994; Nagata *et al.,* 1997; Buckingham *et al.,* 1997) and two-electrode voltage-clamp (Benson, 1989, 1992; Sattelle *et al.,* 1989a; Buckingham *et al.,* 1995; Matsuda *et al.,* 1998) electrophysiological studies.

Kagabu and Medei (1994) demonstrated that IMI and nicotine share similar affinities as measured by α-BgTx displacement, but differ drastically in their biological activity towards green leafhopper (*Nephotettix cincticeps*), IMI exhibiting some 3000 times the activity of nicotine. The difference in activity has been attributed by Yamamoto *et al.* (1995) to the basicity of nicotine which limits its penetration through the lipophilic barriers needed to gain access to the CNS.

In order to resolve which region of the molecule conferred insecticidal activity the structure-activity relationship of IMI and 19 related compounds was investigated by

Tomizawa and Yamamoto (1993) using bioassays with green leafhoppers and binding studies with honey bee heads. It was concluded that biological activity of IMI depends on the chloronicotinyl moiety; close analogues of IMI lacking this essential structure show no biological activity. It is not surprising then that the potent alkaloid frog toxin epibatidine which shares this chloropyridyl moiety is also known to be a potent nicotinic agonist (Badio and Daly, 1994). This active moiety is shared by three other commercially important neonicotinoids nitenpyram (TI-304), acetamiprid (NI-25) and, introduced most recently, thiamethoxam (CGA 293'343) (Senn *et al.,* 1998). The prediction of binding of IMI and related compounds to housefly nAChR was attempted using comparative molecular field analysis by Okazawa *et al.* (1998). Results suggested that of the four stable conformations of IMI only one is active at the nAChR binding site.

1.5.4 Novel nicotinic receptor target sites for insecticides

Spinosad is an insecticide recently introduced by Dow AgroSciences for the control of lepidopteran pests in cotton (Salgado, 1998a, 1998b). Spinosyn is a natural product isolated from the soil actinomycete *Saccharopolyspora spinosa* and two isomers (A and D) exist of which spinosyn A is the major active component of spinosad. The initial symptoms displayed are involuntary muscle contractions and tremors eventually resulting in paralysis. Spinosyn's mode of action was investigated in electrophysiology experiments using *P. americana*, *M. sexta* and *M. domestica* in which spinosyn A was most active in *M. sexta* with an ED_{50} of 5nM. Spinosyn is believed to act by a novel mechanism that is independent of the conventional nAChR agonist site (Salgado *et al.,* 1997; Nauen *et al.,* 1999).

1.6 Nicotinic AChR in insects

ACh is understood to be the predominant excitatory neurotransmitter in the insect CNS (Sattelle, 1980). Evidence for its use is provided by the presence of the ACh synthesising enzyme cholineacetyltransferase, the ACh hydrolysing enzyme AChE, and binding sites for ACh characterised mostly by α-BgTx. Interestingly, insects use glutamate at neuromuscular synapses and not ACh as in vertebrate systems (Usherwood, 1980) so that insect nAChR are believed to be exclusively neuronal. New insecticides which mimic ACh have provided an impetus to study insect nAChR at both the pharmacological and molecular level.

1.6.1 Pharmacological characterisation

Early work on the characterisation of insect nAChR using binding studies made exclusive use of α-BgTx. The insects studied were fruitflies *Drosophila melanogaster*, locusts *Schistocerca gregaria* and *Locusta migratoria*, cockroach *Periplaneta americana* and the moth *M. sexta*. The pharmacological properties of α-BgTx in membranes of *D. melanogaster* have been investigated several times using radioligand binding experiments. In most studies, binding was well described by a single component; dissociation constants (K_d) of 0.1-1.2nM were found, and maximal binding values (B_{max}) of 0.2-1.4 pmol/mg were determined (Dudai, 1977, 1978; Dudai and Amsterdam, 1977; Schmidt-Nielsen *et al.,* 1977; Rudloff, 1978). Moreover the pharmacological profile demonstrated with ACh, nicotine, α-BgTx and *d*-tubocurarine was typically nicotinic while displacement by the muscarinic agents atropine and quinuclidinyl benzilate (QNB) demonstrated only low potency. However, Schloß *et al.* (1988) were able to distinguish at least 2 saturable α-BgTx binding components in head membranes of *D. melanogaster* with K_d values of ~0.1 and 4.0nM with B_{max} values of ~0.24 and ~1.1 pmol/mg respectively. These conflicting results are discussed in more detail in Chapter 2 but in brief could be due to differences in the methods of membrane preparation. The α-BgTx binding site has been further characterised in *S.*

gregaria (Filbin *et al.,* 1983; MacAllan *et al.,* 1988), *L. migratoria* (Breer, 1981), *Musca domestica* (Harris *et al.,* 1979; Mansour *et al.,* 1980; Jones *et al.,* 1981), *Apis mellifera* (Tomizawa *et al.,* 1995a), *P. americana* (Lummis and Sattelle, 1985) and *M. sexta* (Sanes *et al.,* 1977). It is only since 1995 that novel radioligands have been used to investigate putative insect nAChR in radioligand binding assays due to the development of insecticides having a nicotinic mode of action. These include studies with tritiated IMI (Liu and Casida, 1993), nitromethyleneimidazolidine (NMI) (Liu *et al.,* 1994), epibatidine (Orr *et al.,* 1997), and the NCB phencyclidine (Tomizawa *et al.,* 1995a).

1.6.2 Isolation of insect nAChR

Purification by affinity chromatography of putative nAChR from several insects has been achieved. Hall (1980) used a cobratoxin affinity column and eluted with carbamylcholine to remove the nAChR providing a 1200-fold purification. Using similar approaches other workers have isolated insect nAChR with molecular weights of 460-500 kDa determined by gel filtration chromatography (Hall, 1980; Rudloff *et al.,* 1980; Schmidt-Glenewinkel *et al.,* 1981) and weights determined by sucrose density gradients of 250-300kDa (Hall, 1980; Jimenez and Rudloff, 1980). Whole nAChR could then be denatured into individual subunits and their sizes identified on an SDS polyacrylamide gel. Two subunits were identified from *Musca* heads having weights of ~40 and ~20 kDa (Osborne *et al.,* 1982) and, by contrast, 3 subunits were isolated from *S. gregaria* supraoesophageal ganglion having weights of 25, 41 and 60 kDa (Filbin *et al.,* 1983). Breer *et al.* (1985) identified a 250-300 kDa complex from *L. migratoria* which under denaturing conditions split into a single 65 kDa component suggesting a homomeric nAChR. Functional analysis of the isolated subunit in a planar lipid bilayer resulted in ion channels with nicotinic characteristics (Hanke and Breer, 1986). More recently Tomizawa *et al.* (1996) isolated at least 3 subunits from *M. domestica* of molecular weights 61, 66 and 69 kDa using an affinity column with an open heterocycle analogue of IMI. In a duplicate experiment using α-BgTx at least

three subunits were isolated having the same molecular weights as those isolated with the IMI analogue. However the identity or non-identity of those subunits isolated with IMI or α-BgTx affinity columns has not been determined.

1.6.3 Autoradiographical localisation

Studies to date have all used [^{125}I]-α-BgTx to autoradiographically localise putative nAChR containing regions of the insect CNS. α-BgTx as an iodinated radioligand affords favourable binding kinetics for these studies having a slow off rate and labelling with I^{125} ensures a rapid exposure of silver grains typically within 10 days. Workers have focused principally on frozen sections of *D. melanogaster* (Dudai and Amsterdam, 1977; Schmidt-Nielsen *et al.,* 1977; Rudloff, 1978). Binding of [^{125}I]-α-BgTx was shown to be specifically restricted to the CNS and its binding could be blocked by the cholinergic agents nicotine, *d*-tubocurarine and α-BgTx. The reduced silver grain patterning in the brain region was confined to highly localised areas which corresponded to areas of neuropil, namely the medulla and lobula plate of the optic lobes, although specific binding could not be detected in the lamina region.

Putative nAChR binding sites at synapses in *P. americana* were investigated in the sixth abdominal ganglion by Sattelle *et al.* (1983) and mapped in the brain by Orr *et al.* (1990). Those in the abdominal ganglion were located either side of the midline and could be blocked by pre-incubation with nicotine or *d*-tubocurarine. Moreover they were consistent with nAChR at synaptic connections between cercal afferent fibres and giant interneurons. However, specific binding was also observed at the ganglion periphery, a non-synaptic region, implying that some of specific binding observed was artifactual. [^{125}I]-α-BgTx binding in the cockroach brain demonstrated that the majority of specific binding was restricted to neuropil areas, principally the central body, mushroom bodies as well as the glomeruli of the antennal lobes. Binding could be blocked by 1μM carbamylcholine, 100μM lobeline, 1μM MLA, and 0.1μM α-BgTx. In the same study, radioligand binding of [^{125}I]-α-BgTx in a displacement assay

with n-BgTx demonstrated the presence of at least two distinct binding sites not differentiated by [^{125}I]-α-BgTx. This result was confirmed by autoradiographic studies using either 0.1 or 10μM n-BgTx to block [^{125}I]-α-BgTx binding. High concentrations of n-BgTx displaced [^{125}I]-α-BgTx throughout the neuropil areas while lower concentrations displaced mainly from the α and β lobes of the mushroom bodies. Thus the population of labelled [^{125}I]-α-BgTx sites is heterogeneous in nature and can be differentiated by n-BgTx.

The localisation of [^{125}I]-α-BgTx in cricket *Acheta domesticus* terminal ganglion was investigated by Meyer and Reddy (1985) who demonstrated that specific binding was restricted to neuropil areas, notably the cercal glomerulus. Binding detected in the glial elements of the cortical rind and dorsal pit were not displacable by nicotine thus representing non-specific toxin binding. A similar observation was made in *P. americana* by Sattelle *et al.* (1983).

The large brain of adult *M. sexta* moths was studied by Hildebrand *et al.* (1979) allowing a better distinction between brain regions. [^{125}I]-α-BgTx localisation was consistent with synaptic regions in the neuropil, notably concentrated in the glomeruli of the mushroom bodies. Of particular interest the effects of deafferentation on the distribution of putative nAChR was investigated in the antennal lobes. Despite a lack of normal afferent inputs the distribution and production of nAChR appeared normal.

1.6.4 Electrophysiological characterisation of native nAChR

Putative native insect nAChR have been investigated using electrophysiology to characterise their functionality and drug interactions. Their study has been facilitated by the ability to identify specific neurones. *P. americana* has been the subject of the majority of work with the synapses connecting the cercal sensory neurones to the giant interneuron 2 (GI2) located in the terminal ganglion and the fast coxal depressor motorneurone D_f receiving the most attention. Single excitatory post synaptic potentials

(EPSPs) can be generated when the preparation is challenged either mechanically or with drug application.

Sattelle *et al.* (1983) demonstrated that synaptic transmission between the cercal sensory neurons and the giant interneuron 2 in *P. americana* could be irreversibly blocked by 50nM α-BgTx. Circumstantial evidence that transmission was cholinergic was provided by conditions either favouring increased levels of presynaptic ACh release or decreased AChE hydrolysis which both delayed the time taken to block the EPSP. By contrast the muscarinic agent QNB was ineffective at blocking inhibition by α-BgTx up to concentrations of 1μM. QNB is known to have a high affinity binding site in *P. americana* with a K_d of 8nM (Lummis and Sattelle, 1985). The putative nAChR located on the motorneurone D_f were further shown to be affected by nicotine, ACh, carbamylcholine and TMA in a dose-dependent manner and blocked by α-BgTx and *d*-tubocurarine, whilst they were insensitive to micromolar concentrations of QNB.

Identification of both α-BgTx sensitive and insensitive nAChR has been observed in cultured neurones from embryonic *P. americana*, the majority of which were α-BgTx sensitive (Lees *et al.,* 1983). The α-BgTx insensitive nAChR can be detected in electrophysiological preparations involving the dorsal unpaired median (DUM) neurones which are sensitive to ACh but blocked by *d*-tubocurarine in the orthopterans *Schistocerca nitens* and *P. americana* (Goodman and Spitzer, 1979; Harrow *et al.,* 1982). Further, voltage clamp experiments on isolated thoracic ganglion somata from *L. migratoria* demonstrate rapid depolarisation when challenged by ACh, nicotine, anabasine and TMA whilst they are inhibited by α-BgTx (Benson, 1992) (See appendix 1). Single channel recordings from *Drosophila* cultured neurones indicate that they are responsive to ACh and nicotine suggesting a nicotinic character (Albert and Lingle, 1993). Finally functional putative nAChR have been identified in *M. sexta* located at synapses connecting planta hair afferents to motorneurons (Trimmer and Weeks, 1989).

1.6.5 Cloning of insect nAChR genes

Our knowledge of the nucleotide sequence of vertebrate nAChR genes has led to the identification of invertebrate genes coding for nAChR. Invertebrate gene sequences can be correlated to their vertebrate counterpart α and non-α (β) subunits. They share similar topology containing the membrane spanning regions, a cysteine loop and the α subunits identified by their vicinal cysteines. The starting point in the identification of invertebrate genes coding for nAChR was to use a fragment of the chick α2 gene and hybridise it with a *D. melanogaster* genomic library; this resulted in the identification of the first α-like subunit, ALS (Bossy *et al.,* 1988). Using probes based on ALS two further α-like subunits from *D. melanogaster* were identified, namely Dα2 which is also known as SAD (Jonas *et al.,* 1990) and Dα3 (Schulz *et al.*, 1998). Dα2 has been isolated using similar techniques by Baumann *et al.* (1990) using synthetic probes modelled on highly conserved amino acids coding for a region preceding the M4 transmembrane domain (Sawruk *et al.,* 1990a). A fourth partially sequenced α subunit, Dα4, has recently been reported in *D. melanogaster* (Schulz *et al.,* 1998).

The identification of non-α subunits from *D. melanogaster* followed a similar approach to that of the α subunits utilising a vertebrate probe, in this case the cDNA encoding the *Torpedo* γ subunit. This yielded the cDNA leading to the identification of the gene encoding a non-α subunit called ARD (Hermans-Borgmeyer *et al.,* 1986; Sawruk *et al.,* 1988). Working in parallel using the same approach Wadsworth *et al.* (1988) identified the same gene and named it AChR64B. A further non-α subunit, denoted SBD, was isolated by Sawruk *et al.* (1990b) employing similar tactics as for the α subunit using synthetic probes of highly conserved amino acid sequences.

Orthopteran insects have revealed considerable heterogeneity at the gene level for nAChR subunits. α and non-α subunits, named αL1 and ARL1 respectively, have been identified from *S. gregaria* with a starting probe of the chick β2 (Marshall *et al.,* 1988; Marshall *et al.,* 1990). Further multiplicity of locust nAChR has been demonstrated in

L. migratoria from which 4 α and 2 non-α subunit cDNAs were isolated (Hermsen *et al.,* 1991; Hermsen *et al.,* 1998). Further α subunit encoding cDNAs have been isolated from the lepidopterans *H. virescens* (Hermsen *et al.,* 1998) and an α and non-α cDNA from *M. sexta* (Eastlake *et al.,* 1997; Eastham *et al.,* 1998).

The greatest number of insect nAChR cDNAs have been isolated to date comes from the aphid *M. persicae* having at least 6 α and 2 non-α subunit genes. The cotton whitefly *Bemisia tabaci* also demonstrates considerable heterogeneity with at least 5 α and 1 non-α subunit genes (Huang *et al.,* 1998; Huang *et al.,* 1999).

The predicted structure of insect subunits includes features found in their vertebrate counterparts which include sites for 1-3 N-glycosylation, putative protein phosphorylation and kinase A and C interaction. Of particular interest the phosphorylation sites may be implicated in a regulatory role as in vertebrates (reviewed in Gundelfinger and Hess, 1992).

The current rate of the isolation of insect nAChR cDNAs is increasing and figure 1.9 displays a family tree of relatedness. Included are genes encoding vertebrate receptor subunits from rat and nematode subunits from *C. elegans* for comparative purposes.

Figure 1.9. (Overleaf) Evolutionary relationships of the nAChR family. Phylogenetic relationships were calculated with DISTANCES (Kimura protein distance algorithm) based on multiple alignments of amino acid sequences from PileUp and the tree was made with GROWTREE (UPGMA algorithm) of the GCG package (redrawn from Huang *et al.,* 1999). Database accession numbers for vertebrate muscle subunits are: rα1 (X74832), rβ1 (X74833), rδ (X74835), rγ (X74834), rε (X13252); for vertebrate neuronal subunits are: rα2 (L10077), rα3 (L31621), rα4 (L31621), rα5 (J05231), rα6 (L08227), cα7 (X68586), cα8 (X52296), rα9 (U12336), rβ2 (L31622), rβ3 (J04636), rβ4 (U42976), for nematode subunits are: ce21 (X83887), unc38 (X98600), tar1 (U56903), acr2 (X86403), acr3 (Y08637), cel3 (X83888), lev1 (X98601); and for insect subunits are: ALS (X07194), SAD (X53583), Dα3 (Y15593), ARD (X04016), SBD (X55676 and Y14678), αL1 (X55439), Locα1 (AJ000390), Locα2 (AJ000391), Locα3 (AJ000392), Locβ1 (AJ000393), MARA1 (Y09795), Hvα1 (AJ000399), Mpα1 (X81887), Mpα2 (X81888).

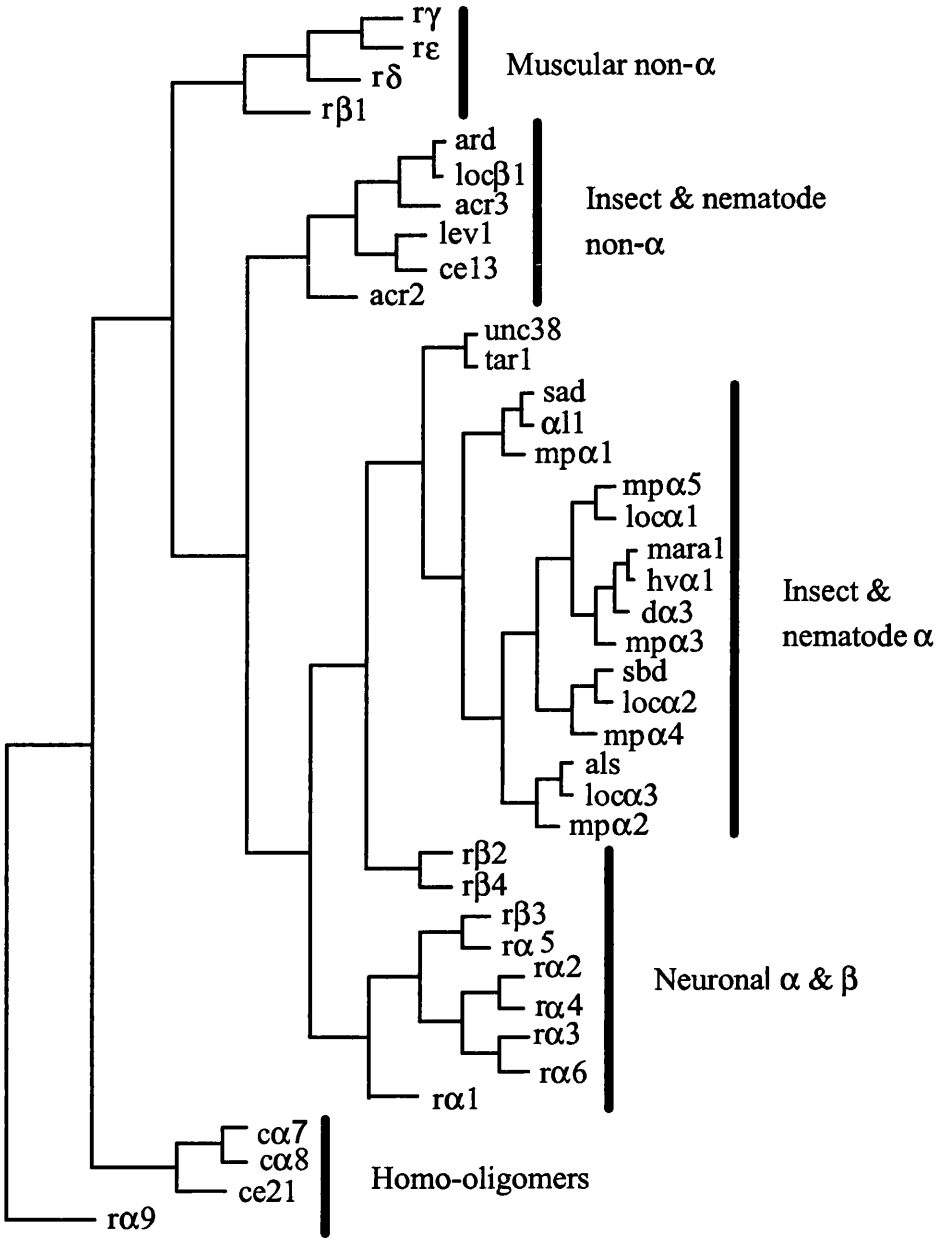
rγ
rε
rδ
rβ1
Muscular non-α
ard
locβ1
acr3
lev1
ce13
acr2
Insect & nematode non-α
unc38
tar1
sad
αl1
mpα1
mpα5
locα1
mara1
hvα1
dα3
mpα3
sbd
locα2
mpα4
als
locα3
mpα2
Insect & nematode α
rβ2
rβ4
rβ3
rα5
rα2
rα4
rα3
rα6
rα1
Neuronal α & β
cα7
cα8
ce21
Homo-oligomers
rα9

These genes can be grouped on their sequence similarity, for example the *M. sexta* and *H. virescens* α subunit share a 93% identity similarity. This suggests that they have arisen from a common ancestral gene (le Novere and Changeux, 1995). However homology between α subunits is not always greater than that to non-α. For example, SBD shares a higher homology with the ALS and Dα2 than with the other non-α subunit ARD. From an evolutionary aspect it is interesting to note that the sequences of insect subunits are closer to those of vertebrate neuronal than muscle types. It is unfortunately very clear from figure 1.9 that the nomenclature of insect nAChR subunits is very unsatisfactory, with names clearly out of alignment with relationships. For example Mara1 and Hvα1 are closely related to Dα3, names to date have reflected the historical discovery process rather than sequence homology relationships as is used for the nomenclature of the vertebrate nAChR subunits.

The intron and exon organisation within the DNA sequences coding for nAChR genes have been compared by Gundelfinger (1992). The vertebrate neuronal α2-α5 and β4 genes contain only 4 splicing sites but the genes for the subunits contained in vertebrate muscle (α1, β1, γ, δ, ε) have between 8-11 splicing sites. There are 4-7 intron/exon splicing sites in the *D. melanogaster* genes ALS, SAD and ARD and these are positioned in both similar and different sites from their vertebrate counterparts. Chromosomal localisation of the genes encoding the *D. melanogaster* subunit genes map ALS, Dα2 and SBD to the same band in the 96A region of the 3R chromosome. This suggests that these subunits have arisen by gene duplication giving rise to this cluster (Bossy *et al.,* 1988; Jonas *et al.,* 1990; Sawruk *et al.,* 1990b). By contrast, the *D. melanogaster* ARD gene maps to the 64B region of the 3L chromosome and interestingly shows the lowest homology of the subunits to any other (Sawruk *et al.,* 1988; Wadsworth *et al.,* 1988). This observation of gene clustering is not restricted to insects and has been noted for the rat and chick α3, α5 and β4 genes (Boulter *et al.,* 1990; Couturier *et al.,* 1990b). Dα3 maps to position 7E on the X chromosome (Schulz *et al.,* 1998). Coincidentally the mutant *D. melanogaster* strain *Hikon R* demonstrated a phenotype of nicotine resistance and in addition an altered isoelectric

point of an α-BgTx binding protein which can be linked to the X chromosome (Hall *et al.,* 1978; Hall, 1980; Restifo and White, 1990). However the relationship between the mutation associated with the *Hikon R* strain and the nicotine insensitive phenotype observed is unclear.

The study by Sgard *et al.* (1993) investigated the homology between α subunits cloned from *D. melanogaster* to those isolated from a panel of insect species. The approach taken was PCR using degenerate primers coding for a conserved region near the vicinal cysteines based on the sequence encoding the ALS, Dα2 and Lα1 subunits. The insects investigated were the aphid *M. persicae* and the lepidopterans *H. virescens*, *Spodoptera frugiperda* and *Chilo suppressalis*. The isolated sequence fragments could be categorised as either ALS- or Dα2-like. Those amplified from the lepidopterans were all of the Dα2 type while *M. persicae* harboured both ALS and Dα2 types.

1.7 Functional expression of insect nAChR genes

The investigation of functional receptors arising from cloned genes for insect nAChR subunits has involved the use of [^{125}I]-α-BgTx, immunoprecipitation and expression in *Xenopus* oocytes. Schloß *et al.* (1988) produced antisera against the *D. melanogaster* ALS and ARD subunits to correlate high affinity binding of [^{125}I]-α-BgTx to those subunits involved. The ARD antiserum precipitated 20-30% of the [^{125}I]-α-BgTx binding proteins and further Scatchard analysis of the isolated proteins was consistent with a single binding component. The ARD antisera appeared not to interfere with the binding of [^{125}I]-α-BgTx suggesting that this subunit has a structural role within the receptor complex. A similar approach using ALS again isolated 20-30% of the [^{125}I]-α-BgTx binding proteins, although with lower affinity than for ARD (Ohana and Gershoni, 1990; Schloß *et al.,* 1991). When both ARD and ALS antisera were used in conjunction no additivity was observed, with still only 20-30% of the α-BgTx binding protein isolated. This suggests that ARD and ALS associate within the same nAChR protein and the heteromeric state could involve additional subunit types.

Further investigation of ALS expression in *Xenopus* oocytes gave rise to a functional homomeric receptor but which only responded to artifactually very high concentrations of nicotine (10-15mM) and was unresponsive to 1μM α-BgTx and 100μM *d*-tubocurarine (Sawruk *et al.,* 1990a). This suggests that although ALS can form homomeric receptors they appear to be unlike native types in their physiological sensitivity to cholingeric drugs. Co-expression with ARD had no effect on drug sensitivities. This suggests either that problems exist with the *Xenopus* cellular machinery to assemble insect nAChR correctly or that further subunits are necessary for the native receptor. These potential problems were investigated by Lansdell *et al.* (1997). Heterologous expression of *D. melanogaster* subunit genes in mammalian cell lines at 37°C appeared to produce misfolded nAChR proteins. To overcome this problem either mammalian cell lines could be grown at lower temperatures or a *D. melanogaster* cell line used (also at lower temperature). Despite expression in a low

temperature environment functional channels could only be achieved by the co-expression of a vertebrate β2 subunit. It was suggested that to produce functional channels a further, and as yet unidentified, insect subunit is required for co-assembly.

A functional homomeric insect nAChR was reported by Marshall *et al.* (1990) using the αL1 subunit isolated from *L. migratoria.* Electrophysiological responses with nicotine were in the micromolar range and blocked by α-BgTx, n-BgTx, bicuculline and strychnine. Amar *et al.* (1995) further characterised the functional receptors formed by αL1 but found it less sensitive to nicotine, possibly due to different experimental methods. These results were consistent with those of native nAChR studied electrophysically *in situ* (Sattelle *et al.,* 1983). The gene sequence of αL1 incorporates the necessary residues for α-BgTx binding and this taken with the electrophyiological data suggests that αL1 contributes to a high affinity α-BgTx binding site. It is possible that further structural subunits occur *in vivo* to evoke responses at physiological concentrations of ACh (Amar *et al.,* 1995).

The cloning of nAChR genes from the locust *L. migratoria* resulted in the identification of 4 α and 2 non-α subunits (Hermsen *et al.,* 1998). However the expression of combinations of these α and non-α genes in *Xenopus* oocytes failed to produce any electrophysiologically functional channels.

1.7.1 Chimeric expression of insect and vertebrate subunits

In most cases in which insect nAChR subunits have been expressed within functional receptors, chimeric combinations of invertebrate and vertebrate subunits have been used. Although the physiological responses of these receptors cannot be correlated to native nAChR at least the ability of individual subunits to participate in functional receptors can be investigated.

Co-expression of the *D. melanogaster* ALS with the chick β2 resulted in functional ion channels which gave large ACh evoked currents which could be blocked by α-BgTx (Bertrand *et al.,* 1994). Similarly when Dα2 was co-expressed with the chick β2 subunit, a functional receptor resulted but this chimeric nAChR was not blocked by α-BgTx and had a faster rate of desensitisation than ALS/β2. Co-expression of Dα3 and chick β2 formed functional receptors that were sensitive to ACh, reversibly blocked by α-BgTx, and characterised by very slow desensitisation (Schulz *et al.,* 1998). The different physiology of the ALS/β2, Dα2/β2 and Dα3/β2 receptors indicates that the α subunit contributes to the ligand binding and desensitising properties since the β subunit was the same in all cases. Since receptors demonstrating native properties containing ALS, Dα2 or Dα3 can only be achieved with the inclusion of further subunits it seems likely that *in vivo* these subunits are parts of heteromeric nAChR complexes. However earlier experiments indicated that ALS and ARD associate in native nAChR, but are not functional when co-expressed, suggesting that further subunits are required for functional receptors. Co-expression of α subunits isolated from *L. migratoria* when combined with the vertebrate β2 subunit was unsuccessful in that functional receptors did not result (Hermsen *et al.,* 1998).

In summary, perhaps apart from αL1, no other complete insect nAChR has been artificially expressed to produce functional channels with the pharmacology of physiological preparations and systems. This could reflect an incomplete repertoire of subunit genes which need to be co-expressed and that the heterogeneity of insect nAChR is rather more complex than first thought. Alternatively most studies have used vertebrate cell lines which could harbour inadequate cellular machinery and conditions for the formation of functional insect nAChR.

1.7.2 Correlating subunit composition to native insect nAChR

To correlate the pharmacology of native insect nAChR to that observed in artificial expression systems is exceptionally difficult at present. Artificial expression to form physiologically functional insect receptors has required the intervention of vertebrate β subunits and thus these chimeras are not representative of insect nAChR. However, some insights can be drawn from experiments with *D. melanogaster* in which 2 binding components for α-BgTx were observed *in situ* in adult brain (Schloß *et al.,* 1991). High affinity α-BgTx binding has previously been discussed and ALS and ARD, co-assembling in the same nAChR, are thought to be involved. Dα3 may be involved in the second class of lower affinity α-BgTx binding (Schulz *et al.,* 1998). Fusion protein produced by *E. coli* of the Locα3 isolated by Hermsen *et al.* (1998) from *L. migratoria* was demonstrated to bind [^{125}I]-α-BgtX *in vitro*, and probably co-assembles into the native nAChR responsible for the binding of this toxin. Recently, functional studies of two cDNAs encoding α subunits from *M. persicae* demonstrated differential sensitivities to α-BgTx (Sgard *et al.,* 1998).

1.8 Localisation by immunohistochemical and *in situ* hybridisation studies

The spatial and temporal distribution of ALS and ARD in life stages of *D. melanogaster* was investigated by Schuster *et al.* (1993) using specific antibodies. Co-localisation was seen in adults extensively in areas of brain neuropil, although ARD was detected to occur alone in the lamina of the optic lobes. ARD is first detected ~10 hours after embryogenesis is initiated and both subunits are present in all larval, pupal and imago stages. Detection of ALS and ARD in the cortical cell bodies during embryonic and pupal development stages suggests an accumulation of newly synthesised subunits awaiting transport to newly formed synaptic connections. It is not clear if the receptor has already assembled by this stage.

Further investigation of the regulation of transcription of Dα2, ARD and SBD genes suggests that they are tightly regulated with transient expression particularly during late embryogenesis and pupal stages (Hermans-Borgmeyer *et al.,* 1986; Wadsworth *et al.,* 1988; Sawruk *et al.,* 1990a,b). Furthermore expression of ARD, Dα2 and SBD was confined to the CNS. By contrast ALS gene transcripts remained high during larval stages (Bossy *et al.,* 1988). Compared to the other *D. melanogaster* subunits Dα3 is expressed at a lower level and is restricted to the dorsal part of the embryonic ventral nerve cord and the gut (Schulz *et al.,* 1998). In the adult fly Dα3 has a much higher transcription level and its localisation in the adult CNS awaits further investigation.

Further investigation using a polyclonal antibody against the α-BgTx binding protein in *L. migratoria* demonstrated immunoreactivity in neuropil areas of the *S. gregaria* CNS (Breer *et al.,* 1985; Leitch *et al.,* 1993). The pattern of antigenic sites was traced throughout embryonesis and indicated that although initially sites were evenly distributed, by the late embryo sites were concentrated into synaptic regions (Hermsen *et al.,* 1991; Watkins *et al.,* 1995). Transcription of α subunits isolated from *L. migratoria* were mapped in adult brain and in embryos (Hermsen *et al.,* 1998). Expression begins in the embryo after 3 days and continues to adult-hood. In the adult brain, expression was differential for the 4 α and 1 β subunits in both synaptic and non-synaptic brain regions. Participation of nAChR in roles other than neurotransmission have been proposed in vertebrates (Grando *et al.,* 1995).

1.9 Summary of insect nAChR

A large body of evidence exists that ACh is the major neurotransmitter in the insect CNS. Knowledge of insect nAChR at the molecular level is revealing considerable heterogeneity in both the subunits and their co-assembly within the nAChR.

The present study investigates this heterogeneity at the pharmacological level with different radioligands, principally in the aphid *M. persicae* as well as in a comparative

panel of insects taken from diverse Orders. The intrinsic nicotine resistance observed in *M. sexta* and the tobacco aphid *M. nicotianae* were investigated to ascertain if a receptor with modified pharmacology is involved. Also included is a small pharmacological investigation of other invertebrate nAChR from crayfish and squid to examine similarities and differences compared to the insects. Suitable methodology for investigating these problems resides with radioligand binding experiments to ascertain the affinities, maximal binding capacities and pharmacologies of insect nAChR. Radioligands were used to record any pharmacological differences either between insect species, or between nicotine sensitive and insensitive insects to investigate the potential for target site cross resistance between nicotine and the neonicotinoid insecticides. Of crucial importance in this study was the choice of radioligands employed. Radiolabelled nicotine was not used in this study since this ligand has previously been demonstrated to have low affinity to insect nAChR which generates problems of noise leading to variable data (see section 4.4).

α-BgTx was the first obvious candidate radioligand (Chapter 2) since it is readily available and has been used extensively to investigate insect nAChR which would allow a comparison with previous studies to be drawn. The second radioligand of choice was IMI (Chapter 3) since questions around the potential for cross resistance between neonicotinoid insectides and nicotine could be answered using both nicotine sensitive and insensitive insect membrane preparations. Epibatine (Chapter 4) was a novel radioligand with which to investigate insect nAChR and shares some structural similarities with IMI. MLA (Chapter 5) was a further novel radioligand with which to study insect nAChR and has previously been demonstrated to be potent in competition radioligand binding and electrophysiological studies when used as an unlabelled ligand, furthermore its insecticidal properties are well known. Lastly an investigation to quantify the systemic uptake and biological effects of imidacloprid on *M. persicae* was undertaken (Chapter 6).

Chapter 2

α-BgTx radioligand binding

This chapter is based on a composite of two published papers referenced Eastham, H. M., Lind, R. J., Clarke, B. S., Towner, P., Reynolds, S. E., Wolstenholme, A. J., and Wonnacott, S. (1998) Characterisation of a nicotinic acetylcholine receptor from the insect *Manduca sexta*. *Eur J. Neurosci.* **10,** 879-889. The second is referenced as Robert J. Lind, Martin S. Clough, Fergus G. P. Earley, Susan Wonnacott and Stuart E. Reynolds (1999) Characterisation of multiple α-bungarotoxin binding sites in the aphid *Myzus persicae* (Hemiptera: Aphididae). *J. Insect. Biochem. Mol. Biol.* **29,** 979-988.

2.1 Introduction

The snake toxin α-bungarotoxin (α-BgTx) has been extensively used to characterise vertebrate and invertebrate nicotinic acetylcholine receptors in binding experiments and functional assays. In vertebrates the toxin demonstrates strong selectivity towards neuronal type nAChR containing α7-α 9 subunits and also towards the muscle receptor containing the α1 subunit (McGehee and Role, 1995). There has been a number of studies of the interaction between α-BgTx and insect nAChR. Neurophysiological evidence shows that α-BgTx inhibits responses to ACh in some, but not all, insect neurones, and specific binding of radiolabelled α-BgTx to insect nerve membranes has been demonstrated (Breer and Satelle, 1987).

Schmidt-Neilson *et al.* (1977), Rudoff (1978), Hildebrand *et al.* (1979), Sattelle *et al.* (1983), Meyer and Reddy (1985) and Orr *et al.* (1990) further demonstrated in autoradiographic studies that [^{125}I]-α-BgTx bound specifically to regions of *D. melanogaster*, *Manduca sexta*, *Acheta domesticus* and *Periplaneta americana* brain and thoracic CNS. These results are consistent with the α-BgTx protein binding to nAChR located in the neuropil areas of the CNS.

cDNAs coding for invertebrate nAChR subunits and their respective toxin sensitivities are now beginning to be isolated from a range of insects, most notably from *D. melanogaster* and the locusts *Schistocerca gregaria* and *Locusta migratoria* (reviewed by Gundelfinger, 1992; Hermsen *et al.,* 1998; Schulz *et al.,* 1998). Expression studies have shown that the *D. melanogaster* genes ALS and ARD can contribute to an α-BgTx sensitive nAChR (Schloß *et al.,* 1991) as can αL1 from *S. gregaria* (Marshall *et al*, 1990; Amar *et al*, 1995) and Locα3 isolated from *L. migratoria* (Hermsen *et al.,* 1998). A further α subunit identified in *D. melanogaster,* Dα3, may contribute to the class of low affinity α-BgTx sites identified by Schloß *et al.* (1988) (Schulz *et al.,* 1998). Recently, functional studies of two cDNAs encoding α subunits from the peach potato aphid *Myzus persicae* demonstrated differential sensitivities to α-BgTx (Sgard *et al.,* 1998).

Previously published studies of radiolabelled α-BgTx binding in *Drosophila melanogaster* have reported results which differ significantly. In saturation experiments, using head membranes, Schmidt-Nielson *et al.* (1977) found a single class of binding site whereas Schloß *et al.* (1988) reported the presence of multiple binding sites. The differences may be the consequence of the methodologies employed, especially the use of detergents in the preparation of the membranes (Hjelmeland and Chrambach, 1984). Binding properties of α-BgTx have also been further investigated in the hymenopteran *Apis mellifera* (Tomizawa *et al*, 1995a).

The present study was undertaken to examine radiolabelled α-BgTx binding in adult brain and whole larva of the tobacco hornworm *Manduca sexta* and in a mixed population of the peach potato aphid *Myzus persicae.* This was used to determine whether pharmacological differences exist between α-BgTx binding sites in the nicotine resistant insect *M. sexta* and insects from other Orders, in addition squid optic lobe was also investigated for comparative purposes. Binding studies involving *M. sexta* were carried out in collaboration with Helen Eastham (University of Bath).

2.2 Materials and Methods

2.2.1 Chemicals

Both iodinated and tritiated α-BgTx were used in the experiments, for operational reasons. [^{125}I]-Na was obtained from Amersham International, Cardiff, UK and was used to iodinate α-BgTx to a specific activity of 750 Ci/mmol. [^{3}H]-α-BgTx was purchased from Amersham International at a specific activity between 50-70 Ci/mmol. Sources for other compounds were as follows: α-BgTx, ACh, (±)anabasine, (+)anatoxin a, BSA, cytisine, *d*-turbocurarine, carbachol, (±)EPI, lobeline, leupeptin, MLA, (+)nicotine, (-)nicotine, pepstatin A, and PMSF (phenylmethylsulphonylfluoride) and PEI (polyethylenimine) from Sigma-Aldrich Ltd (Fancy Road, Poole, Dorset, UK). GF/C filters were obtained from Whatman International Ltd., Maidstone, UK. The Bio-Rad protein assay reagent was supplied by Bio-Rad Laboratories Ltd., Hemel Hempstead, UK. All other buffer reagents were purchased either from Sigma-Aldrich or Fisons Scientific Equipment, Loughborough, UK. The muscarinic ligands, atropine, (±)muscarine and oxotremorine and acetylcholinesterase inhibitors BW284c51 (1,5 bis(4 allyl dimethylammoniumphenyl)pentan3one), neostigmine bromide, physostigmine and THA (9 amino 1,2,3,4 tetrahydroacridine hydrochloride) were also purchased from Sigma-Aldrich Ltd. IMI, nitenpyram and cartap of technical purity were synthesised by Zeneca Agrochemicals. Compound structures are shown in appendix 1. All drugs were made into 10mM stock solutions. Where a drug was insoluble in water a small volume (~100µl-500µl) of either ethanol or acetone was used to dissolve the drug prior to dilution in incubation buffer. The maximum concentration of ethanol in the final incubation was 1%.

2.2.2 Invertebrate rearing and collecting

Experiments used apterous *Myzus persicae* (strain USIL, originating from Rothamsted Experimental Station) of mixed ages. These were mass reared on 30-40 day old chinese cabbage plants (*Brassica pekinensis)* at 20±2°C on a 16 hr light:8 hr dark photocycle and collected by brushing the leaves with a 1 inch paint brush. Insects were killed by freezing in liquid nitrogen and stored at -80°C until required. This strain has an FE4 esterase level corresponding to resistance level R1 and is moderately resistant to organophosphate, carbamate and pyrethroid insecticides. It is referred to in this thesis as 'R1'. Tobacco hornworms *Manduca sexta* (Lepidoptera: Sphingidae) were reared according to Bell and Joachim (1976). Whole brains were dissected from pharate adults and stored at -80 until required. First instar larvae <24 hours after hatching were frozen whole at -80 until required. Nervous tissue from the squid *Loligo vulgaris* were supplied by the Plymouth Marine Association, further details in section 5.2.2.

2.2.3 Membrane preparation

M. persicae, M. sexta and *L. vulgaris* were made into membrane preparations using methods based on those described by Schmidt-Nielsen *et al.* (1977) and wherever possible preparation was carried out at 4°C. Aphids (25g) comprising some 100,000 individuals, *M. sexta* brains (50-200) or 1st instar larvae (10g) and squid optic lobes (4g) were homogenised with a motor driven Ultra Turrax® for 30 seconds at 5000rpm in 0.32M sucrose, 100µM EDTA, 1µM leupeptin, 1µM pepstatin, and 200µM PMSF (pH 7.2). The homogenate was centrifuged at 1,000g for 30 min. The resulting supernatant fraction from *M. persicae* and *L. vulgaris* was strained through 4 layers of fine nylon mesh and re-centrifuged at 30,000g for 60 min. In the case of *M. sexta* only, larvae were strained through 2 layers of muslin and the supernatants of both adults and larvae further centrifuged at 30,000g for 30 min. The pellet was reconstituted in incubation buffer containing 0.05M Tris, 0.12M NaCl, and 100µM EDTA (pH 7.4). The protein concentration was determined using the method of Bradford (1976) with

bovine serum albumin (BSA) as a standard. Detergents were not employed in any case. Unless otherwise stated, the binding assay consisted of incubation of 100µg, 25µg, 23µg and 93µg of aphid, squid and adult and larval *M. sexta* membrane preparation respectively in a final volume of 200µl incubation buffer containing, additionally, 0.25% BSA.

2.2.4 Filtration assay

Bound and free ligand were separated employing either a Millipore vacuum manifold for iodinated α-BgTx or a Tomtech Mach 2 cell harvester where tritiated α-BgTx was used. In saturation and displacement studies, membranes were incubated with the labelled ligand for 60 minutes at room temperature (22°C) which proved adequate in previous [^{125}I]-α-BgTx binding studies (Lummis and Sattelle, 1985). Non-specific binding was determined using a final concentration of either 1µM α-BgTx or 1µM MLA. There were no demonstrable differences in the levels of specific binding determined with these 2 displacing ligands. In the case of the Millipore manifold, incubation was performed in LP4 tubes and was terminated by rapid filtration (<30 seconds) through GF/C filters (presoaked in 0.3% polyethyleneimine) using five 3ml washes of ice cold incubation buffer (+0.25% BSA) to separate the bound [^{125}I]-BgTx from free. Filters were counted in a Packard Cobra II gamma counter at 100% efficiency. Incubation of [^{3}H]-α-BgTx was performed in 96 well microtitre plates compatible with the cell harvester and quantification of bound [^{3}H]-α-BgTx employed Wallac thin filter mats (A grade) pre-soaked in 0.3% polyethyleneimine, using a 5 wash cycle of ice cold incubation buffer (+0.25% BSA). Solid scintillant (Meltalex A, Wallac) was melted onto filter mats, which were counted at 34% efficiency in a Wallac beta plate counter. Unless otherwise stated all experiments were performed 3 times, each with duplicate or triplicate determinations for [^{125}I]-α-BgTx and [^{3}H]-α-BgTx respectively.

2.2.5 Centrifugation assay

Binding of 1nM [^{3}H]-α-BgTx to *M. persicae* membranes was also determined in centrifugation assays to determine whether significant losses of specifically bound [^{3}H]-α-BgTx occurred during filtration experiments. In centrifugation assays, incubation was performed in 1.5ml microcentrifuge tubes which were centrifuged at 30,000g for 5 min in a Beckman bench top ultrafuge in order to terminate incubation. The supernatant fraction was removed, and the pellet washed three times with 1ml distilled water. Pellets were then dissolved overnight in 10% sodium deoxycholic acid and the redissolved pellet (0.5ml) was transferred into 4.5ml of liquid scintillant (Optiphase safe) and counted at 43% efficiency. A single experiment was performed with triplicate determinations of each data point.

2.2.6 Kinetic analysis

A concentration of 1nM [^{3}H]-α-BgTx was used to investigate association and dissociation rate kinetics in *M. persicae* membranes at room temperature (22°C). Association rates were determined for time periods from 0.5 to 180 min and terminated by filtration. To investigate the kinetics of dissociation, membranes were allowed to associate with [^{3}H]-α-BgTx for 3 hours before isotopic dissociation was initiated by the addition of either 1μM α-BgTx, IMI, EPI or MLA. Residual bound radioligand was determined between 0.5 and 60 min, in the presence and absence of 1μM MLA for non-specific and total binding respectively.

The temperature dependence of the kinetics of [^{125}I]-α-BgTx binding was investigated in *M. sexta* membranes by the association of 10nM [^{125}I]-α-BgTx at 25°C or 37°C with time points up to 180 min. In this case, approximate values for kinetic constants ($t_{½}$) were estimated by fitting a simple rectangular hyperbola.

2.2.7 Metabolic breakdown of (-)nicotine

To investigate any metabolic breakdown of (-)nicotine in adult *M. sexta* membranes during competition assays this ligand was preincubated for either 0 minutes followed by a 60 min incubation at 4°C with [^{125}I]-α-BgTx or preincubation for 10 and 60 min with (-)nicotine followed by a 60 min incubation with [^{125}I]-α-BgTx at 25°C.

2.2.8 Displacement Studies

Ligands employed for displacement studies were added to aphid membranes 30 minutes prior to the addition of 1nM [^{125}I]-α-BgTx. Competing ligands were assayed in a dilution series of 1, 3, 10, 30, 100, 300, etc. with at least 6 concentrations in triplicate focused around the IC_{50} point (at which 50% of bound [^{125}I]-α-BgTx is displaced). In the case of acetylcholine (ACh), it was necessary to inhibit acetylcholinesterase (AChE). A range of AChE inhibitors were investigated (BW284c51, neostigmine bromide, physostigmine and THA). Of these, neostigmine bromide was selected at an inhibitory concentration of 10μM which did not interfere [^{125}I]-α-BgTx binding (see Table 2.4). The inhibitor was added to aphid membranes 10 minutes before the addition of ACh.

2.2.9 Data Calculation

Specific binding cannot be measured directly, but rather is determined by the difference between total and non-specific binding. Total binding of radioligand is that to both the receptor and non-receptor entities. Non-specific (strictly, non-saturable) binding is measured in the presence of an excess (e.g. 1,000-fold) of unlabelled ligand known to occupy the same receptor as the radioligand. It is assumed that the number of specific (strictly, saturable) receptors is finite and that they have high affinity for both the radioligand and unlabelled ligand used to determine non-specific binding. Those non-receptor sites are assumed to be infinite in number and to display low affinity for

the radioligand. Thus, non-specific binding can be visualised as binding of the radioligand to all non-receptor entities but its binding to the receptor is effectively completely blocked by the large excess of unlabelled ligand.

Non-linear regression analysis with Microsoft Excel's solver macro (Bowen and Jerman, 1995) was used to determine the dissociation constant (K_d) and maximal binding capacity (B_{max}) from a rectangular hyperbola plot using equation (**1**) for saturation data (Hulme and Birdsall, 1992). Saturation data could be transformed to a linear representation in the form of a Scatchard plot, equation (**2**) and a Hill plot (**3**). Where data better fitted a two site model then a double hyperbola plot was used additively to calculate K_d and B_{max} values for high and low affinity components, equation (**4**). The pitfalls of interpretation of Scatchard plots with multiple components are discussed by Nørby *et al.* (1980). Non-linear regression was also used to determine the IC_{50} and Hill coefficient for displacement data using the Hill plot, equation (**5**). In order to compare IC_{50} values the K_d and ligand concentration need to be taken into consideration to generate a inhibition constant (K_i) value (**6**) from the method of Cheng and Prusoff (1973). In kinetic experiments the initial dissociation and association rate constants were determined using non-linear regression from pseudo-first-order kinetics using equations (**7** and **8**) and (**9** and **10**) respectively. Where kinetics were demonstrated to be biphasic the fast and slow components were summed. The dissociation constant, K_d, can be determined from the dissociation and association constants (**11**).

$B = (B_{max}*x)/(K_d+x)$ (Hyperbola Plot) **(1)**

where B is the amount of radioligand bound, typically expressed in fmol/mg, and x is the free concentration of radioligand. The B_{max} and K_d value are determined by non-linear regression analysis.

$B/F=(-1/K_d)*B+B_{max}/K_d$ (Scatchard Plot) **(2)**

where B/F is the ratio of bound and free ligand. In the Scatchard plot the K_d is derived from the slope of line and the B_{max} is the point of intersection with the X-axis. Where 2 binding sites are determined by a plot clearly not described well by a straight line determination of K_d and B_{max} values of the high and low affinity sites is complex and often inaccurate, particularly for the low affinity site (Hulme and Birdsall, 1992). Thus, the Scatchard plot is used in this thesis only to illustrate the presence of multiple affinity sites and not in the determination of K_d and B_{max} values.

$y=(c+(\log_{10}[ligand]* n_H)$ (Hill plot; saturation) **(3)**

where c is the intercept, [ligand] is the ligand concentration added and n_H is the Hill number.

$B = (B_{max}^1*x)/(K_d^1+x)+ (B_{max}^2*x)/(K_d^2+x)$ (double additive Hyperbola Plot) **(4)**

where B is the amount of radioligand bound, typically expressed in fmol/mg, and x is the free concentration of radioligand. The binding properties of the high affinity (B_{max}^1 and K_d^1) and low affinity site (B_{max}^2 and K_d^2) are determined by non-linear regression analysis.

$B=100\%/(1+([ligand]/IC_{50})^{nH})$ (Hill plot; displacement) **(5)**

where B= % bound radiolabel, [ligand] = concentration of displacing ligand and n_H is the Hill number.

$K_i=IC_{50}/(1+([radioligand]/K_d))$ (Cheng Prusoff equation) **(6)**

where [radioligand] is the concentration of radioligand employed, K_d is the dissociation constant determined either by saturation or kinetics and IC_{50} is the concentration of unlabelled ligand required to displace half the bound labelled ligand.

$B_t=B_0e^{-koff*t}$ (Dissociation kinetics) **(7)**

$\log_e(B_t)$ vs t (Dissociation kinetics; linearising plot) **(8)**

where B_t is the amount of bound radioligand at any point in time, B_0 is the amount of radioligand bound at time 0, k_{off} is the dissociation rate and t is time.

$B_t=B_{eq}*(1-e^{-(Kon*L+Koff)t})$ (Association kinetics; non-linear) **(9)**

$-\log_e(1-B_t/B_{eq})$ vs t (Association kinetics; linearising plot) **(10)**

where B_t is the amount of bound radioligand at any point in time, B_{eq} is the amount of radioligand bound at equilibrium, K_{on} is the association rate, k_{off} is the dissociation rate, L is the free ligand concentration and t is time.

$K_d=K_{off}/K_{on}$ (determination of K_d by association and dissociation kinetics **(11)**

where K_{off} is the dissociation constant and K_{on} is the association constant.

2.3 Results

Specific binding of radiolabelled α-BgTx to *M. persicae* (whole organism) and *M. sexta* (brains) membranes was readily demonstrable. There was a linear relationship between specific binding of [^{125}I]-α-BgTx and increasing amounts of *M. persicae* and *M. sexta* (adult and larval) membranes with protein content (Figures 2.1, 2.2 and 2.3). A comparison of 1nM specific [^{3}H]-α-BgTx binding in *M. persicae* membranes using either filtration or centrifugation to separate bound from free ligand demonstrated no differences and thus B_{max} values determined in saturation experiments using filtration are accurate in terms of separation of bound and free ligand.

2.3.1 Saturation binding experiments

At all concentrations of [^{125}I]-α-BgTx ligand depletion was under 10% for all experiments. Saturable binding of [^{125}I]-α-BgTx in *M. sexta* membranes was well described by a single binding site with K_d and B_{max} values of 5.3±1.0nM and 188±50 fmol/mg and 8.32±1.91nM and 87±12 fmol/mg for adults and larvae respectively (Table 2.1, Figures 2.4-2.9). Hill values of ~1 for adult and larval *M. sexta* membranes were consistent with a single binding site (Table 2.1).

By contrast, saturation data for the binding of [^{125}I]-α-BgTx to *M. persicae* membranes were consistent with 2 binding components, one of high affinity (K_d=1.2±0.2nM, B_{max}=167±6fmol/mg) and one of low affinity (K_d=33.7±1.5nM, B_{max}=640±18fmol/mg), (Table 2.1, Figures 2.10-2.12). A Hill value (n_H) of 0.71±0.03 was determined (Table 2.1).

Insect	High affinity K_d (nM)	B_{max} (fmol/mg)	Low affinity K_d (nM)	B_{max} (fmol/mg)	Hill values (n_H)
M. persicae	1.18±0.12	167±7	33.7±1.5	640±18	0.71±0.03
M. sexta adult	5.34±1.01	188±50	-	-	1.05±0.06
M. sexta larva	8.32±1.91	87±12	-	-	0.97±0.02
A. mellifera	7.45	451	-	-	
S. gregaria	0.8	1200	-	-	
P. americana	1.09	8926	-	-	
[1]*D. melanogaster*	1.8	190	-	-	
[2]*D. melanogaster*	0.15	240	4.3	1080	

Table 2.1. Comparison of [^{125}I]-α-BgTx saturable binding in *M. persicae* and *M. sexta* showing K_d (nM), B_{max} (fmol/mg) and Hill (n_H) values. Tabulated results for *M. persicae* and *M. sexta* larvae represent the mean ±SEM of three separate experiments and n=4 for *M. sexta* adults. Saturation constants for *A. mellifera* (Tomizawa *et al.*, 1995a), *S. gregaria* (MacAllan *et al.*, 1988), *P. americana* (Orr *et al.*, 1990) and *D. melanogaster* ([1]Rudloff, 1978; [2]Schloß *et al.*, 1988) are provided for comparison.

Specific [^{3}H]-α-BgTx binding was detected in membranes of the cephalopod *L. vulgaris*. A single concentration of 1nM was used giving 19 fmol/mg of specific binding. The affinity or density of this [^{3}H]-α-BgTx binding site was not determined.

2.3.2 Kinetic analysis of high affinity [^{3}H]-BgTx binding

A concentration of 1nM [^{3}H]-α-BgTx was used to investigate the kinetics of the high affinity binding site only present in *M. persicae* membranes. [^{3}H]-α-BgTx associates with and dissociates from the high affinity binding site in a monophasic manner at 22°C (Figures 2.13-2.16). When α-BgTx was bound at a concentration of 1nM the association and dissociation rate constants, k_{+1} and k_{-1}, had values of $1.4x10^{-2}$ ($T_{½}$=37±2.4mins) and $3.5x10^{-3}$ min^{-1} ($T_{½}$=225±53 min) respectively, resulting in a k_{-1}/k_{+1} (K_d) of 0.25nM. The isotopic dissociation of [^{3}H]-α-BgTx from aphid membranes using an excess of either EPI or IMI was not markedly different from that produced by addition of α-BgTx, and was characterised by a slow monophasic dissociation (Table

2.2). In contrast, MLA evoked a biphasic dissociation of [^{3}H]-α-BgTx which had fast and slow dissociation rate constants of $2.4x10^{-1}$ and $8.2x10^{-3}$ min^{-1} respectively (Table 2.2, Figures 2.17-2.18). Such biphasic data suggest either a two-stage sequential reaction or parallel reactions with different kinetic properties (Galper *et al.,* 1977).

Ligand	Slow Rate (K_{-1} $mins^{-1}$) $x10^{-3}$	Fast Rate (K_{-1} $mins^{-1}$)
BgTx	3.5±0. 8	-
EPI	3.1±0.8	-
IMI	2.6±0.4	-
MLA	8.2±0.7	$2.4±0.4x10^{-1}$

Table 2.2. Isotopic dissociation of [^{125}I]-α-BgTx from *M. persicae* membranes initiated by either 1μM α-BgTx, EPI, IMI or MLA. Tabulated results represent the mean ±SEM of three separate experiments.

2.3.3 Temperature dependence of [^{125}I]-α-BgTx binding

There was no detectable effect of temperature on [^{125}I]-α-BgTx binding to *M. sexta* membranes at 25°C or 37°C with approximate $T_{½}$ values of 11 and 13 min respectively (Figure 2.17).

2.3.4 Metabolic breakdown of (-)nicotine

An attempt was made to assess the possible contribution of (-)nicotine metabolism by *M. sexta* membranes to the apparent ability of this ligand to displace [^{125}I]-α-BgTx (Figure 2.18). There was no marked difference between IC_{50} values of 0.75, 1.05 and 2.80μM determined from preincubation at 4°C for 0 min and at 25°C for 10 and 60 min respectively. It was concluded that there was no evidence that breakdown of (-)nicotine was a factor in limiting the effectiveness of this ligand as a displacing ligand.

2.3.5 Displacement studies

A wide range of cholinergic ligands was tested for their ability to displace [^{125}I]-α-BgTx binding to *M. sexta* and *M. persicae* membranes, in order to compare the pharmacology of [^{125}I]-α-BgTx high affinity binding with that of other invertebrates (Table 2.3). [^{125}I]-α-BgTx was used at a concentration of 1nM in these experiments in order to examine competition at its high affinity site only.

Table 2.4 shows the interaction between a number of AChE inhibitors and [^{125}I]-α-BgTx binding. The AChE inhibitor neostigmine bromide exhibited the least interference with [^{125}I]-α-BgTx binding and so was subsequently used in assays involving ACh.

AChE inhibitor (10μM)	Inhibition of [^{125}I]-α-BgTx binding (1nM)
Neostigmine	2%
BW284C51	16%
THA	48%
Physostigmine	64%

Table 2.4. Inhibition of [^{125}I]-α-BgTx binding in adult brain *M. sexta* membranes by AChE inhibitors.

The pharmacological profiles of [^{125}I]-α-BgTx displacement (Table 2.3, Figures 2.19-2.29) for *M. sexta* and *M. persicae* each demonstrate a typically nicotinic character and are similar to the profile determined previously for *Apis mellifera* by Tomizawa *et al.* (1995a). For *M. persicae*, the most potent displacing ligand after α-BgTx itself was MLA, which was also the case in *M. sexta* (Figures 2.19 and 2.20). EPI was over an order of magnitude more potent in displacing [^{125}I]-α-BgTx from *M. persicae* membranes (K_i=25nM) than it was in adult (K_i=840nM) and larval (K_i=670nM) *M. sexta* (Figure 2.21). The natural neurotoxin anatoxin-a shares structural similarities to EPI by way of the nitrogen bridge but was an order of magnitude less potent as a

	M. persicae		*M. sexta* (Adult)		*M. sexta* (Larva)		*A. mellifera*	*D. Melanogaster*	*M. domestica*	*P. americana*	*S. gregaria*	*L. migratoria*
Ligand	K_i±SEM (M)	Hill (n_H)	K_i±SEM (M)	Hill (n_H)	K_i±SEM (M)	Hill (n_H)						
α-BgTx	$7.6\pm3.0\times10^{-10}$	0.72±0.07	$1.3\pm0.9\times10^{-9}$ (3)	0.92±0.08	$9.7\pm3.8\times10^{-9}$ (3)	0.68±0.11	5.5×10^{-9}	1.5×10^{-9}	10^{-9}	8.5×10^{-10}	8.9×10^{-9}	1.8×10^{-10}
MLA	$1.7\pm0.3\times10^{-9}$	0.93±0.11	$1.0\pm0.9\times10^{-9}$ (2)	0.33	$3.1\pm1.8\times10^{-9}$ (3)	0.24±0.02	ND	ND	[1]2.5×10^{-5}	[3]1.4×10^{-9} [5]1.8×10^{-9}	1.8×10^{-8}	ND
(±)EPI	$2.5\pm0.4\times10^{-8}$	0.60±0.04	$8.4\pm2.9\times10^{-7}$ (3)	0.46±0.09	$6.7\pm3.5\times10^{-7}$ (2)	0.26±0.04	ND	ND	ND	ND	ND	ND
(+)Anatoxin a	$2.2\pm0.2\times10^{-7}$	0.63±0.05	ND	ND	ND	ND	ND	ND	ND	ND	1.6×10^{-8}	ND
(-)Nicotine	$6.7\pm2.5\times10^{-7}$	0.91±0.07	$2.0\pm0.4\times10^{-6}$ (4)	0.39±0.03	$1.6\pm0.8\times10^{-6}$ (4)	0.28±0.03	1.2×10^{-6}	1.4×10^{-7}	9.0×10^{-7}	3.5×10^{-6} [4]9.8×10^{-6} [5]1.1×10^{-6}	5.1×10^{-7}	1.1×10^{-8}
(-)Cytisine	$6.9\pm3.1\times10^{-7}$	0.60±0.02	ND	ND	ND	ND	2.1×10^{-7}	ND	[2]1.2×10^{-6}	ND	ND	ND
IMI	$8.0\pm2.8\times10^{-7}$	0.62±0.01	$1.7\pm0.5\times10^{-6}$ (3)	0.44±0.02	$2.1\pm1.4\times10^{-6}$ (2)	0.13±0.08	1.5×10^{-6}	ND	ND	[4]2×10^{-7}	ND	ND
Lobeline	$8.6\pm5.2\times10^{-7}$	0.68±0.08	ND	ND	ND	ND	3.6×10^{-6}	ND	[2]1.3×10^{-5}	[5]7.7×10^{-6}	ND	ND
d-Tubocurarine	$1.4\pm0.8\times10^{-6}$	0.55±0.04	ND	ND	ND	ND	2.6×10^{-6}	1.4×10^{-6}	[2]1.9×10^{-6}	[5]3.6×10^{-7}	ND	2.6×10^{-6}
*Anabasine	$1.5\pm0.9\times10^{-6}$	0.63±0.08	$3.6\pm0.3\times10^{-5}$ (3)	0.52±0.05	$1.6\pm0.9\times10^{-4}$ (3)	0.13±0.06	1.6×10^{-6}	ND	ND	ND	ND	ND
ACh	$2.0\pm0.8\times10^{-6}$	0.59±0.07	$5.6\pm1.2\times10^{-5}$ (3)	0.43±0.03	$8.0\pm3.2\times10^{-6}$ (3)	0.23±0.05	ND	1.2×10^{-6}	1.8×10^{-5}	1.8×10^{-5}	[6]2.7×10^{-6}	1.1×10^{-4}
(+)Nicotine	$7.6\pm3.2\times10^{-6}$	0.92±0.06	ND	ND	ND	ND	1.7×10^{-5}	ND	ND	ND	1.5×10^{-5}	ND
Nitenpyram	$8.2\pm3.9\times10^{-6}$	0.47±0.08	ND	ND	ND	ND	4.8×10^{-5}	ND	ND	ND	ND	ND
Carbachol	$4.3\pm2.7\times10^{-5}$	0.46±0.11	ND	ND	ND	ND	7.1×10^{-5}	ND	ND	ND	ND	ND
Cartap	$1.7\pm0.4\times10^{-4}$	0.81±0.08	ND	ND	ND	ND	ND	ND	ND	ND	ND	ND
Nereistoxin	ND	ND	ND	ND	ND	ND	1.8×10^{-4}	ND	[2]1.9×10^{-4}	ND	ND	ND

Table 2.3. Displacement of [^{125}I]-α-BgTx from *M. persicae* and *M. sexta* membranes using nicotinic ligands. K_i (M) and Hill values are derived as described in Methods and Materials. Experiments performed in triplicate (Mean±SEM) for *M. persicae* and mean ± SEM where n=3 or 4 and mean ± range where n=2 for adult and larval *M. sexta*, n numbers are given in parentheses. K_i values for *M. persicae*, *M. sexta* adult and larva assume K_d values of 1.2, 5.3 and 8.3nM and [^{125}I]-α-BgTx concentrations of 1nM, 1nM and 5nM respectively. In addition previously published K_i and IC_{50} values from similar studies of [^{125}I]-α-BgTx displacement are given for comparison. K_i values for ***Apis mellifera*** from Tomizawa *et al.*, 1995a. K_i values for ***Drosophila melanogaster*** from Schmidt-Nielsen *et al.*, 1977. IC_{50} values for ***Musca domestica*** from Cattell *et al.*, 1980; [1]K_i values from Jennings *et al.*, 1985; [2]K_i values from Tomizawa and Yamamoto, 1992. K_i values for ***Periplaneta americana*** from Lummis and Sattelle, 1985; [3]IC_{50} values from Sattelle *et al.*, 1989b; [4]IC_{50} values from Bai *et al.*, 1991. [5]K_i values from Orr *et al.*, 1990. K_i values for ***Schistocerca gregaria*** from MacAllan *et al.*, 1988; [6]Filbin *et al.*, 1983. K_i values for ***Locusta migratoria*** from Breer, 1981.

displacer of [^{125}I]-α-BgTx (K_i=220nM) in the aphid. (-)Nicotine was only a moderately potent displacer of [^{125}I]-α-BgTx, and the K_i value (0.7μM) found with *M persicae* was similar to the K_i values seen in adult (K_i=2.0μM) and larval (K_i=1.6μM) *M. sexta* and *A. mellifera* (K_i=1.2μM) (Tomizawa *et al.,* 1995a) (Figure 2.23). Another tobacco alkaloid, anabasine, was most potent in aphid membranes compared to *M. sexta* in which larval membranes were less sensitive than those of the adult (Figure 2.24). (+)Nicotine was an order of magnitude less potent in displacing [^{125}I]-α-BgTx in *M. persicae* membranes than the naturally occurring (-) enantiomer, as has been observed previously in *A. mellifera* (Tomizawa *et al.,* 1995a) and *S. gregaria* (MacAllan *et al.,* 1988) (Figure 2.28). Cytisine shares the bridged nitrogen harboured by anatoxin-a and EPI and had a similar potency (K_i=690nM) to anatoxin-a in the aphid (Figures 2.27 and 2.29).

Lobeline was slightly more potent as a displacer of [^{125}I]-α-BgTx in *M. persicae* than in *A. mellifera* with K_i values of 0.86μM and 3.6μM respectively (Figure 2.26). *d*-Tubocurarine was moderately potent (K_i =1.4μM) in displacing [^{125}I]-α-BgTx in aphid membranes and gave a similar value to that previously determined in *A. mellifera* (Tomizawa *et al*, 1995a) (Figure 2.29). ACh was more than an order of magnitude more potent in *M. persicae* membranes compared to those of *M. sexta* (Figure 2.25).

Interestingly, the high affinity [^{125}I]-α-BgTx binding site in *M. persicae* was relatively insensitive to the neonicotinoid insecticides IMI and nitenpyram. The inferred K_i value for displacement of [^{125}I]-α-BgTx in *M. persicae* by IMI was 0.8μM. Nevertheless, this value implies a slightly higher affinity for IMI at the aphid [^{125}I]-α-BgTx binding site than was seen in adult (K_i=1.7μM) and larval (K_i=2.1μM) *M. sexta* and *A. mellifera* (K_i=1.2μM) (Tomizawa *et al.,* 1995a) (Figure 2.22). Similarly, nitenpyram was half an order of magnitude more potent in *M. persicae* membranes (K_i=8.2μM) compared to *A. mellifera* (K_i=48μM) (Figure 2.28). By contrast, carbachol gave similar K_i values in *M. persicae* (K_i =43μM) and *A. mellifera* (K_i =71μM) (Figure 2.26). The long used synthetic chemical insecticide cartap is structurally similar to the natural

neurotoxin nereistoxin (See Appendix 1). Both of these compounds were very weak displacers of α-BgTx at insect nAChR (Figure 2.27).

Data for inhibition of [^{125}I]-α-BgTx binding by the muscarinic ligands muscarine, oxotremorine and atropine in *M. sexta* and *M. persicae* are shown in table 2.5. The muscarinic antagonist atropine was in general the most potent inhibitor of [^{125}I]-α-BgTx in *M. persicae* and *M. sexta* membranes. Interestingly, the definitive muscarinic inhibitor muscarine was the least potent. There is a general trend of these muscarinic agents to be more inhibitory against larval *M. sexta* [^{125}I]-α-BgTx binding compared to that of adults.

Ligand (concentration)	*M. persicae*	Adult *M. sexta*	Larval *M. sexta*
Muscarine (10μM)	100	ND	89
Oxotremorine (10μM)	80	ND	61
Atropine (10μM)	82	ND	52
Muscarine (100μM)	41	75	33
Oxotremorine (100μM)	43	59	28
Atropine (100μM)	27	39	37

Table 2.5. Inhibition of [^{125}I]-α-BgTx binding by muscarinic ligands in *M. persicae* and *M. sexta* adult brain and whole larva. Figures are specific binding (% of control) where 100% is specific binding in the absence of any competing ligand. ND = not determined.

2.4 Discussion

Membranes prepared from discrete *M. sexta* life stages and from a mixed population of *M. persicae* each demonstrated a high density of specific binding sites for [^{125}I]-α-BgTx. Saturation studies in *M. sexta* were compatible with the presence of a single binding site, whilst, by contrast, data from *M. persicae* membranes were consistent with 2 binding components having different affinities with a corresponding Hill value (n_H=0.71) markedly less than 1. When determined at a single concentration of 1nM, the squid *L. vulgaris* demonstrated specific binding of [^{3}H]-α-BgTx, but at a level an order of magnitude lower compared to *M. persicae* and *M. sexta.*

In the case of binding to the insect membranes, loss of bound ligand through wash off during filtration was minimal since a comparison using either filtration or centrifugation revealed that there was no difference between these two separation methods. This result is consistent with the slow dissociation kinetics observed when dissociation was initiated by an excess of unlabelled toxin (Figure 2.13-2.16). However, although B_{max} values are unlikely to have been limited by ligand wash off, it is likely that B_{max} values determined were underestimates owing to the slow association kinetics of α-BgTx since only a one hour incubation was used.

A comparison of saturable binding between the present study and previous investigations in insects is shown in table 2.1. With the exception of *M. persicae* (present study) and *D. melanogaster* (Schloß *et al.,* 1988), the saturation data from all insects investigated to date are consistent with a single [^{125}I]-α-BgTx binding component. There have been numerous investigations into [^{125}I]-α-BgTx binding in membranes of *D. melanogaster*, with those of Schmidt-Neilsen *et al.* (1977), Rudloff (1978), Jiminez and Rudloff (1980) and Dudai (1977) consistent with a single binding site while that of Schloß *et al.* (1988) clearly demonstrates the presence of multiple binding sites. The discrepancies may relate to differences in the method of membrane preparation. The K_d values of *S. gregaria*, *P. americana*, and *D. melanogaster* and the

high affinity site in *M. persicae* are ~1nM while the toxin binding sites of *A. mellifera* and *M. sexta* are less avid (5-10nM). The density of binding sites found in the various insects varies considerably; typically B_{max} values range from 100 to 1000 fmol/mg. The cockroach *P. americana* was the highest value reported so far. In comparing different insects and different studies, however, it should be borne in mind that different tissues and different membrane preparation methods were used.

The pharmacological profile of *M. sexta* (adult and larval) and *M. persicae* are typically nicotinic and are similar to that found previously for *A. mellifera* (Tomizawa *et al.,* 1995a) and other insects (Table 2.3). In *M. persicae* membranes with the exceptions of MLA, (-)nicotine and (+)nicotine, all the displacing ligands including α-BgTx itself, demonstrated Hill values markedly less than 1 (between 0.46 and 0.81). Similarly, with the exception of α-BgTx in adult *M. sexta*, all tested ligands in adult and larval *M. sexta* membranes gave low Hill values (between 0.13-0.68). In *M. persicae* the most potent displacer of [^{125}I]-α-BgTx was unlabelled α-BgTx itself, but the *Delphinium* toxin MLA was also able to displace [^{125}I]-α-BgTx with high potency. Likewise, MLA had a similar potency to α-BgTx in adult and larval *M. sexta*. Vertebrate neuronal α7-type nAChR are sensitive to both α-BgTx and MLA, and this result may reflect structural similarity, and perhaps an evolutionary relationship, between the α-BgTx high affinity binding sites in insects and α7-type nAChR in vertebrates (Ortells and Lunt, 1995).

A low Hill value for α-BgTx displacement in *M. persicae* indicates the possibility of allosteric interactions between α-BgTx binding sites within the aphid nervous system. This differs from adult *M. sexta* in which displacement of [^{125}I]-α-BgTx by unlabelled α-BgTx gave a Hill value of ~1. In the case of *M. persicae*, the higher affinity toxin binding site may be subject to cooperativity effects of a lower affinity α-BgTx binding site which is absent in *M. sexta*.

EPI, cytisine and anatoxin-a molecules have structural features in common, but differ markedly in their abilities to displace α-BgTx in aphid membranes, with anatoxin-a and cytisine being over an order of magnitude less potent than EPI in *M. persicae*. Anatoxin-a has previously been shown to be a better displacer of [^{125}I]-α-BgTx in *S. gregaria* ganglia (MacAllan *et al.,* 1988) (Table 2.3). The frog neurotoxin EPI was also a relatively poor displacer of [^{125}I]-α-BgTx in adult *M. sexta* (K_i=840nM) and furthermore no specific binding of [^{3}H]-EPI could be detected in this insect (See Chapter 4). In contrast, a high affinity [^{3}H]-EPI binding site that is sensitive to α-BgTx is detectable in *M. persicae* (See Chapter 4), suggesting that the difference between these two insects in K_i values for displacement of [^{125}I]-α-BgTx by EPI could reflect the presence or absence of a high affinity binding site for EPI.

In the aphid (-)nicotine demonstrated a 10-fold higher potency than the (+) isomer reflecting the stereoselectivity of insect nAChR (Tomizawa *et al.*, 1995a). The displacement of [^{125}I]-α-BgTx by nicotine in adult and larval *M. sexta* membranes was of particular interest in relation to this insect's intrinsic nicotine insensitivity. There is no marked difference in nicotine sensitivity between the high affinity [^{125}I]-α-BgTx binding site of *M. sexta* and those of other insects (Table 2.2). Thus, the population of binding sites labelled by [^{125}I]-α-BgTx in adult and larval *M. sexta* appear to be as sensitive to nicotine as are those of other insects. Moreover, only the larval stage of *M. sexta* encounters dietary nicotine, since the adult is a nectar feeder, but no developmental change in nicotine sensitivity was detected with [^{125}I]-α-BgTx. The tentative conclusion to be drawn here, is that the nicotine tolerance of *M. sexta* probably does not depend on nicotine-insensitive nAChR. However, other possibilities remain. Another possible strategy *M. sexta* could employ would be to have different pharmacological populations of nAChR, a subset of which are insensitive to nicotine, and which are deployed only in CNS regions likely to come into contact with nicotine. Taking this hypothesis further, the hypothetical nicotine-insensitive nAChR may not necessarily be sensitive to [^{125}I]-α-BgTx, and so would not necessarily be detected in this study. Conversely, the nicotine sensitivity displayed by the population of nAChR

labelled by [^{125}I]-α-BgTx is not high (K_i~1μM) when compared to the high affinity [^{3}H]-nicotine binding that is observed in vertebrate brain (Marks *et al.,* 1986; Lippiello *et al.,* 1987; Martino-Barrows and Keller, 1987). The question then arises of whether [^{125}I]-α-BgTx is a suitable ligand with which to investigate the nicotine sensitivity of *M. sexta* nAChR. This is a topic of discussion in Chapter 4.

However a further tobacco alkaloid, anabasine, did demonstrate a lower potency in *M. sexta* compared to *M. persicae* (present study) and *A. mellifera* (Tomizawa *et al.,* 1995a). The relative potencies of nicotine and anabasine were equal in membranes of *M. persicae* and *A. mellifera* (Table 2.3), which is consistent with observations in vertebrate studies (Marks *et al.,* 1986). However the interpretation of the decreased sensitivity of *M. sexta* membranes to anabasine compared to other insects is complicated by the availability of anabasine at the time of experimentation. The only sample of technical purity available for the *M. sexta* investigation from Sigma-Aldrich was several years old. Therefore degradation of the anabasine sample could have accounted for the unexpectedly low potencies observed with this compound.

IMI and its open chain heterocycle analogue nitenpyram demonstrated low potencies as displacers of [^{125}I]-α-BgTx having K_i values of 0.8 and 8.2μM respectively. IMI is also a relatively poor displacer of [^{125}I]-α-BgTx in adult and larval *M. sexta* (K_i>1μM) and in *A. mellifera* (Tomizawa *et al.,* 1995a) and *Musca domestica* (Liu *et al.,* 1994). It has been previously been suggested (Tietjen *et al.,* 1998) that the high affinity binding sites for IMI and α-BgTx may be different, in terms of either physio-chemically distinct binding sites, or conformational states of the same receptor (Prince and Sine, 1998). Evidence for subunit heterogeneity sufficient to generate distinct binding sites for α-BgTx and IMI comes from the cloning of nAChR subunit genes from *M. persicae* in which 6 α and 1 non-α subunit genes have been identified to date (Huang *et al.,* 1998; Huang *et al.,* 1999). Likewise subunit heterogeneity is becoming apparent in *M. sexta* (Eastham *et al.,* 1998; Eastlake *et al.,* 1997). Additional evidence for heterogeneity in nAChR subunits has been provided by affinity chromatography with either α-BgTx or

a IMI analogue which revealed the presence of at least 3 protein bands in *D. melanogaster* and *M. domestica* membranes having molecular weights consistent with nAChR subunits (Tomizawa *et al.,* 1996). The latter approach of purification and sequencing could reveal which of those nAChR subunit genes identified in *M. sexta* and *M. persicae* are responsible for α-BgTx and IMI binding.

The antagonistic *Lobelia* alkaloid lobeline has been previously suggested to be able to distinguish between nicotinic receptor sub-types in insects (Battersby and Hall, 1985). *Periplaneta americana* nAChR were reported to be more sensitive (K_i=0.014μM) than those of *M. domestica* (K_i=4.4μM). The present study suggests that the sensitivity of high affinity α-BgTx binding site in *M. persicae* to lobeline is intermediate between that of *P. americana* and *M. domestica.* By contrast, a previous investigation by Tomizawa *et al.* (1995a) demonstrated that the α-BgTx binding site of *A. mellifera* is similar in lobeline sensitivity to that of *M. domestica.* Therefore insect nAChR have differential sensitivities to particular ligands which could reflect differences in receptor subtypes.

Cartap and nereistoxin share structural homology and both operate at the nAChR as open channel blockers (Sattelle *et al.,* 1985; Nagata *et al.*, 1997); in *M. persicae* and *A. mellifera* both these compounds have very low potency in displacing [^{125}I]-α-BgTx from its binding site, presumably because the displacing ligands act at different topographic sites from the toxin binding site.

The muscarinic agents, atropine, muscarine, oxotremorine, displaced [^{125}I]-α-BgTx in *M. sexta* and *M. persicae* membranes but only at very high concentrations (10-100μM). It has been previously suggested that insects possess AChR of mixed muscarinic and nicotinic pharmacology (Cattell *et al.,* 1980; Mansour *et al.,* 1980). The physiological role of receptors demonstrating mixed pharmacology remains unclear, however.

In order to investigate the ability of ACh to displace labelled α-BgTx, it was necessary to inhibit AChE during experiments. Since some AChE inhibitors are known to have additional agonist activity, a range of AChE inhibitors was appraised for the ability to displace [^{125}I]-α-BgTx. Neostigmine was found to have no detectable agonist activity, and was therefore used to prevent ACh breakdown. Other AChE inhibitors did have agonist activity, however. Of the AChE inhibitors tested, physostigmine was demonstrated to be the most potent displacer of [^{125}I]-α-BgTx. Physostigmine has previously been demonstrated to be able to interact with both vertebrate and invertebrate nAChR (Shaw *et al.,* 1985; Liu *et al.,* 1995). It belongs to the carbamate class of compounds, many of which are used as commercial insecticides. This result therefore begs the question of whether these insecticides are exerting their biological activity purely through the inhibition of AChE, or whether their activity is supplemented by interference as an agonist at the nAChR.

Kinetic analysis of α-BgTx binding at room temperature (22°C) demonstrates that [^{3}H]-α-BgTx associates slowly in a monophasic manner over 3 hours. Even after 3 hours association, binding of [^{3}H]-α-BgTx was incomplete. These slow association kinetics are a serious impediment to the use of α-BgTx as a ligand for the investigation of nAChR because they make it very difficult to estimate B_{max} accurately. It is likely that the B_{max} values reported here are significant underestimated, as is probably the case in most other published studies of insect AChR.

Isotopic dissociation of [^{3}H]-α-BgTx was initiated by addition of BgTx, EPI or IMI, all of which induced dissociation in a slow, apparently monophasic manner over 60 minutes. Dissociation of α-BgTx from both vertebrate and invertebrate membranes has been shown previously to be very slow (Schmidt-Nielsen *et al.*, 1977; Lukas *et al.,* 1981). In contrast to the [^{3}H]-α-BgTx kinetics in *M. persicae* membranes, biphasic association and dissociation has been reported for [^{125}I]-α-BgTx in *D. melanogaster* (Schloß *et al.,* 1988); the differences could relate to the experimental conditions, especially time and temperature, and until there is full association or dissociation the

exact nature of the kinetics cannot be proven. The K_d determined for *M. persicae* from kinetic analysis was 0.25nM which is in reasonably good agreement with the value of 1.2nM determined for the *M. persicae* high affinity site by saturation experiments.

It was therefore particularly interesting that the isotopic dissociation of [^{3}H]-α-BgTx from *M. persicae* membranes was dramatically accelerated when initiated by MLA. Dissociation was biphasic, and the fast component was nearly 2 orders of magnitude faster than that initiated by α-BgTx. The slow rate of dissociation was however not markedly different from that initiated by α-BgTx. A biphasic interaction could represent either a two-stage sequential reaction or parallel reactions with different kinetic properties (Galper *et al.,* 1977). These dissociation kinetics are consistent with a model in which at least the majority of aphid high affinity [^{3}H]-α-BgTx binding sites have 2 different ligand binding sites at each nicotinic receptor which can interact allosterically with each other. A similar observation has been made in *Torpedo* nAChR (Pedersen and Papineni, 1995) and may help to explain the low Hill values that we observed with almost all ligands in displacement studies. It is therefore possible that [^{3}H]-α-BgTx labels only one of these two nicotinic sites with high affinity, and that the other site may have only a low affinity for α-BgTx. Therefore in displacement studies, carried out at low [^{125}I]-α-BgTx concentrations so as to label only the high affinity sites, the interaction of a displacing ligand with the unoccupied low affinity α-BgTx binding site may influence, through allosteric effects, the nature of [^{125}I]-α-BgTx binding at its high affinity site.

The common observation of low Hill values in the majority of displacement experiments in *M. sexta* and *M. persicae* could be explained by cooperativity between 2 or more binding sites on the same nAChR. Alternatively [^{125}I]-α-BgTx could be labelling a heterogeneous population of binding sites to which the displacing ligand has differential sensitivity resulting in a biphasic displacement which would be misinterpreted as a shallow displacement curve. A further explanation is that at least

some of the ligands tested exist in a mixture of enantiomers, such as (±)EPI and (±)anabasine, which have different [^{125}I]-α-BgTx displacing abilities.

In summary, [^{125}I]-α-BgTx labels a single high affinity binding site in *M. sexta*, and in contrast labels multiple binding sites in *M. persicae.* The high [^{125}I]-α-BgTx affinity binding site demonstrates pharmacology which is consistent with that of a nAChR. The nicotine sensitivity determined by displacement of [^{125}I]-α-BgTx in adult and larval *M. sexta* was no different from that of nicotine sensitive insects. Dissociation experiments in *M. persicae* are consistent with a model in which there are at least 2 binding sites per aphid nAChR to which [^{3}H]-α-BgTx can only bind to a subset with high affinity.

Figure 2.1. Dependence of [^{125}I]-α-BgTx binding to *M. persicae* membranes on protein concentration. Membranes were incubated for 1 hour with 1nM [^{125}I]-α-BgTx and bound and free radioligand separated using vacuum filtration with GC/C filters. Data from a single experiment. The horizontal axis indicates the amount of protein per assay tube. Symbols denote total binding(◆), specific binding (●), and non-specific binding (▲).

Figure 2.2. Protein dependence of [^{125}I]-α-BgTx binding to adult *M. sexta* membranes. Methods and symbols as described in Figure 2.1.

Figure 2.3. Protein dependence of [^{125}I]-α-BgTx binding to larval *M. sexta* membranes. Methods and symbols as described in Figure 2.1.

Figure 2.4. Saturation isotherm, **Figure 2.5.** Scatchard, and **Figure 2.6.** Hill plot of [^{125}I]-α-BgTx binding in adult *M. sexta* brain homogenates. Membranes were incubated for 1 hour with a range of [^{125}I]-α-BgTx concentrations (0.1-30nM) and bound and free radioligand separated using vacuum filtration with GC/C filters. A concentration of 1μM unlabelled α-BgTx was used to determine non-specific binding. Saturation isotherm data are fitted to a rectangular hyperbola and used to calculate values for K_d and B_{max} as described in Materials and Methods. The Hill plots gave a value of unity suggesting a single class of binding site. Symbols denote total binding(◆), specific binding (●), and non-specific binding (▲). Data are mean of 4 independent experiments ±SEM.

Figure 2.1

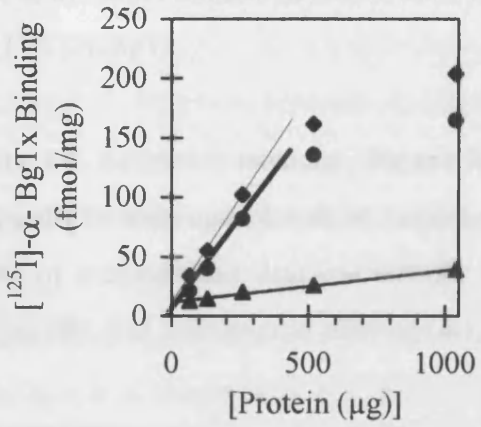

Figure 2.2

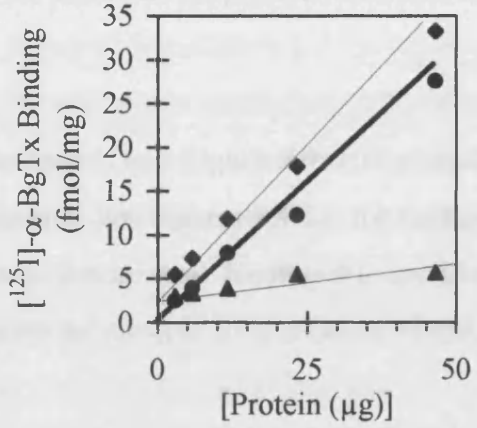

Figure 2.3

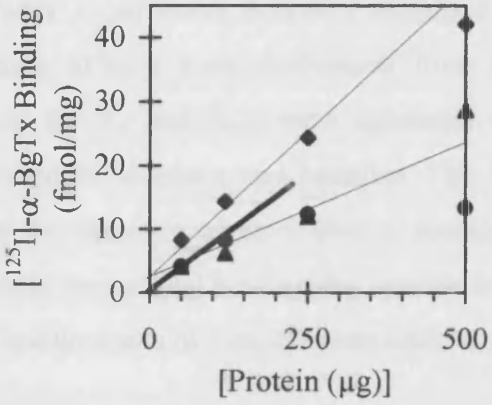

Figure 2.4

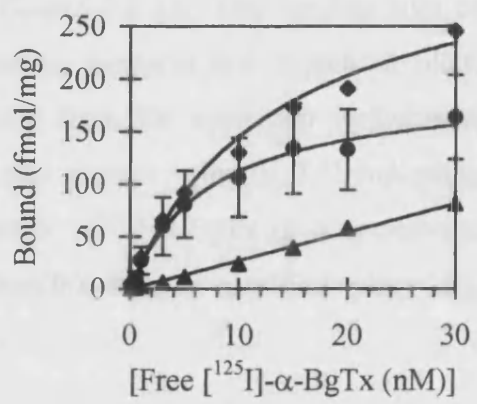

Figure 2.5

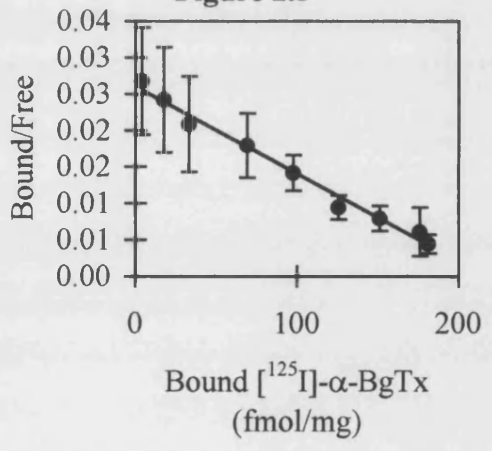

Figure 2.6

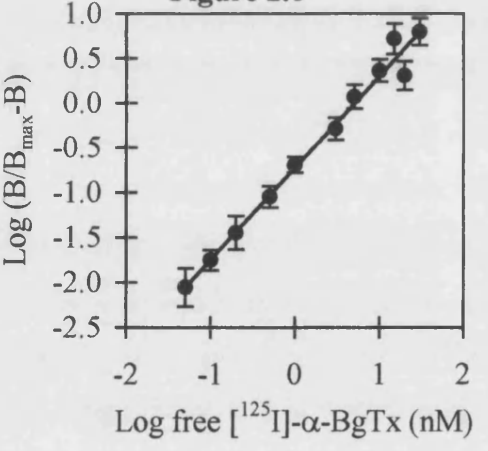

Figures 2.7-2.12. Saturation isotherm of larval *M. sexta* and *M. persicae* membranes with [^{125}I]-α-BgTx.

Figure 2.7. Saturation isotherm, **Figure 2.8.** Scatchard, and **Figure 2.9.** Hill plot of [^{125}I]-α-BgTx binding in larval *M. sexta* homogenates. See Figures 2.4-2.6 for further details of methods and data calculation. Symbols denote total binding(◆), specific binding (●), and non-specific binding (▲). Data are the mean of 3 experiments ±SEM.

Figure 2.10. Saturation isotherm, **Figure 2.11.** Scatchard, and **Figure 2.12.** Hill plot of [^{125}I]-α-BgTx binding in *M. persicae* homogenates. Method and Materials of saturation experiments is briefly described in Figures 2.4-2.6. Two binding sites of differing affinity were determined from saturation isotherm and Scatchard plots. Values for K_d and B_{max} were estimated directly from the saturation isotherm as described in Materials and Methods. The Hill plot gives a value of 0.71 indicating either the presence of more than 1 binding site for [^{125}I]-α-BgTx or cooperativity. Symbols denote total binding(◆), specific binding (●), and non-specific binding (▲). Data are the mean of 3 experiments ±SEM.

Figure 2.7

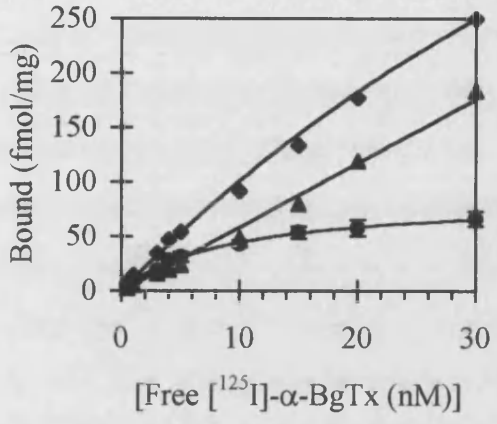

Figure 2.8

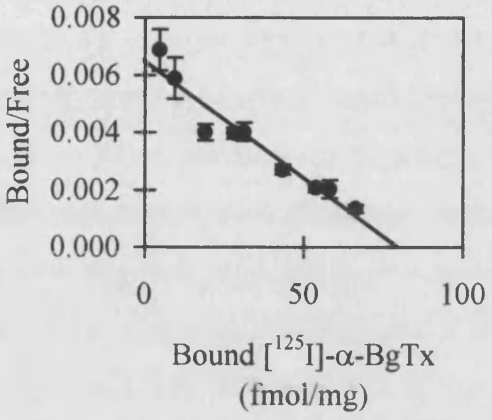

Figure 2.9

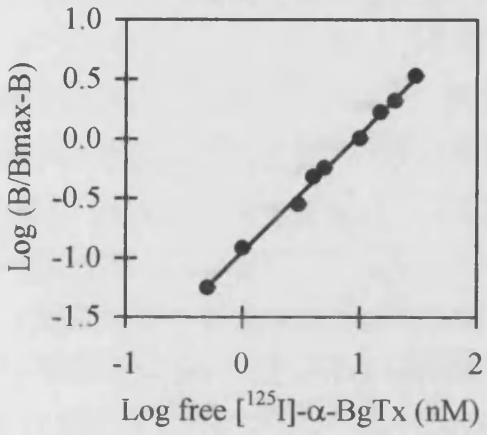

Figure 2.10

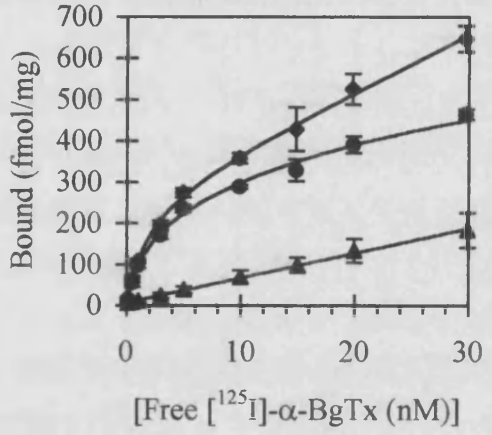

Figure 2.11

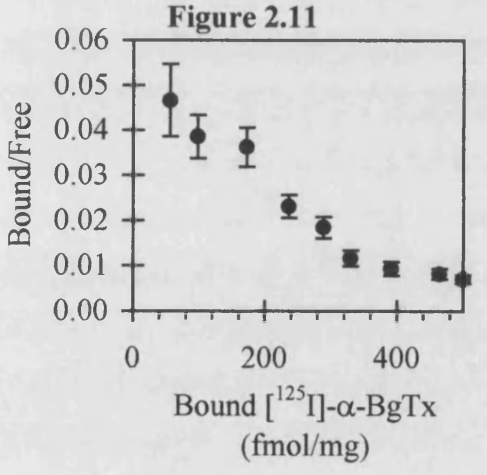

Figure 2.12

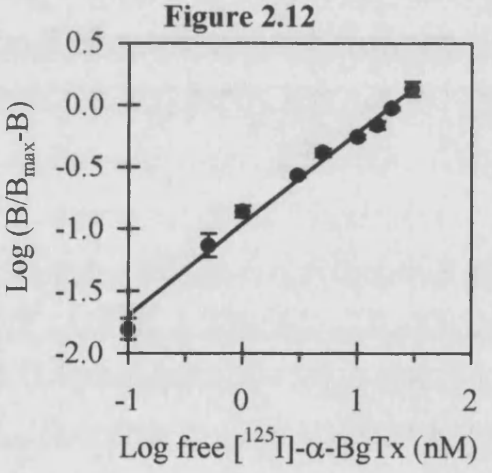

Figures 2.13-2.16. Kinetic data of [^{3}H]-α-BgTx binding in *M. persicae* membranes. **Figure 2.13**. Association of [^{3}H]-α-BgTx to *M. persicae* membranes at 22°C. Membranes were incubated with 1nM [^{3}H]-α-BgTx at room temperature before bound ligand was harvested by filtration using a cell harvester. Data are the mean ± SEM of three independent experiments and are fitted to a one-site model. **Figure 2.14.** Linear transformation of the [^{3}H]-α-BgTx binding kinetics shown in Figure 2.13. The slow association demonstrates a monophasic interaction. **Figure 2.15.** Dissociation of [^{3}H]-α-BgTx from high affinity binding sites on aphid membranes initiated by either 1μM MLA or unlabelled α-BgTx. 1nM [^{3}H]-α-BgTx was allowed to equilibrate for 3 hours before dissociation was initiated by either 1μM α-BgTx (●) or MLA (■) and reactions stopped at the specified times by rapid filtration. All experiments were carried out at 22°C. Data are the mean ± SEM of three independent experiments and are fitted to a one-site model. **Figure 2.16.** Linear transformation of the [^{3}H]-α-BgTx binding kinetics shown in Figure 2.15. The dissociation is initiated by α-BgTx is slow and monophasic, that initiated by MLA is greatly accelerated and biphasic. Data are the mean ± SEM of three independent experiments.

Figure 2.17. Temperature dependence of [^{125}I]-α-BgTx binding to adult *M. sexta* membranes. Membranes were incubated with 10nM [^{125}I]-α-BgTx for the time points 0-180 min after which bound and free ligand were separated on GF/C filters using vacuum filtration. Non-specific binding was determined in the presence of 1μM α-BgTx. Data are fitted to a rectangular hyperbola to yield approximate $T_{½}$ values.

Figure 2.18. Preincubation effects of (-)nicotine on the inhibition of [^{125}I]-α-BgTx binding. Adult *M. sexta* membranes were preincubated under 3 regimes of time and temperature denoted below the figure prior to the addition of 1nM [^{125}I]-α-BgTx for 1 hour. Non-specific binding was determined with a final concentration of 1μM α-BgTx. Bound and free radioligand were separated by vacuum filtration on GF/C filters. Data were fitted to the Hill equation.

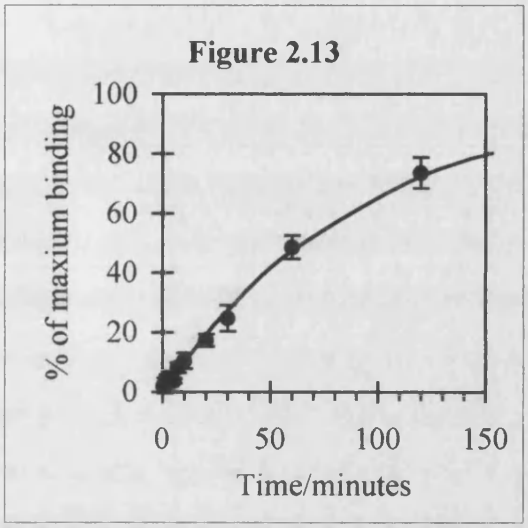
Figure 2.13
% of maxium binding
100
80
60
40
20
0
0
50
100
150
Time/minutes

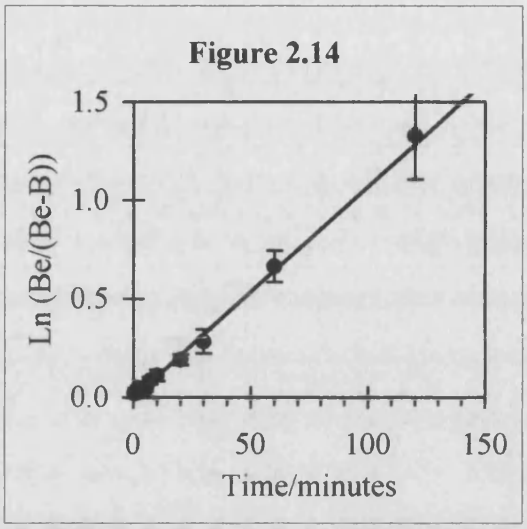
Figure 2.14
Ln (Be/(Be-B))
1.5
1.0
0.5
0.0
0
50
100
150
Time/minutes

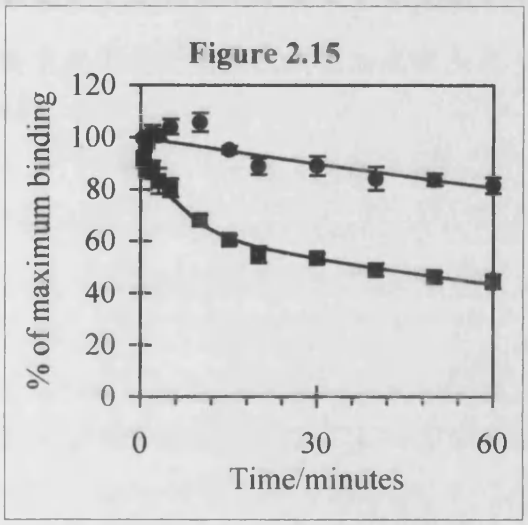
Figure 2.15
% of maximum binding
120
100
80
60
40
20
0
0
30
60
Time/minutes

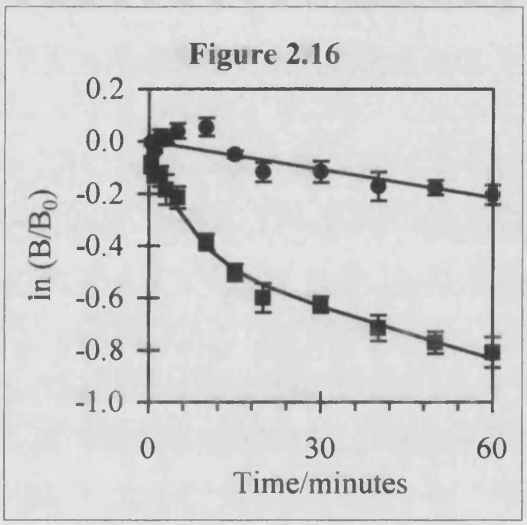
Figure 2.16
in (B/B0)
0.2
0.0
-0.2
-0.4
-0.6
-0.8
-1.0
0
30
60
Time/minutes

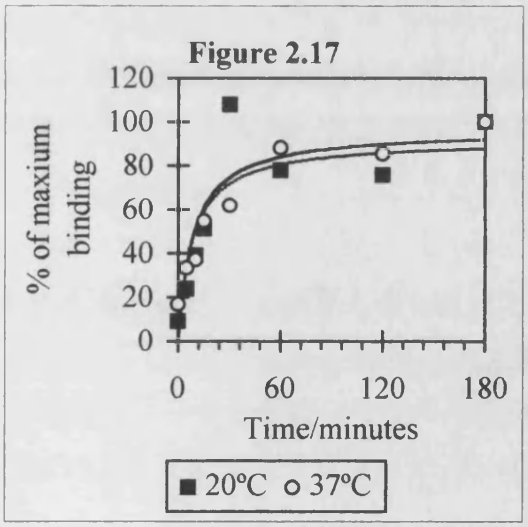
Figure 2.17
% of maxium binding
120
100
80
60
40
20
0
0
60
120
180
Time/minutes
■ 20°C o 37°C

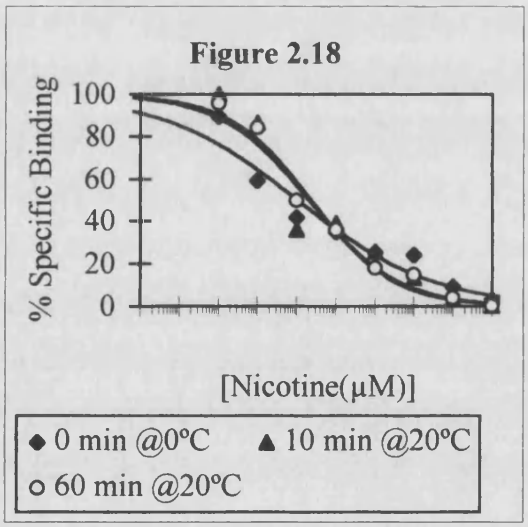
Figure 2.18
% Specific Binding
100
80
60
40
20
0
[Nicotine(μM)]
◆ 0 min @0°C ▲ 10 min @20°C
o 60 min @20°C

Figures 2.19-2.25. Competition binding assays of cholinergic ligands at the [^{125}I]-α-BgTx binding site in *M. persicae*, adult and larval *M. sexta* membranes. Increasing concentrations of α-BgTx (**figure 2.19**), MLA (**Figure 2.20**), EPI (**Figure 2.21**), IMI (**Figure 2.22**), (-)nicotine (**Figure 2.23**), (±)anabasine (**figure 2.24**) and ACh (**Figure 2.25**) were preincubated with membranes for 10 minutes before the addition of 1nM [^{125}I]-α-BgTx for 1 hour. Bound and free radioligand were separated on GF/C filters using vacuum filtration. Non-specific binding was determined with a final concentration of 1μM α-BgTx. Data points represent the mean±SEM of 3 or 4 independent experiments or mean±range where n=2. Symbols denote data from *M. persicae* (□), adult *M. sexta* (●), and larval *M. sexta* (Δ). Mean data are fitted to the Hill equation as outlined in section 2.2.9.

Figure 2.19 - α-BgTx

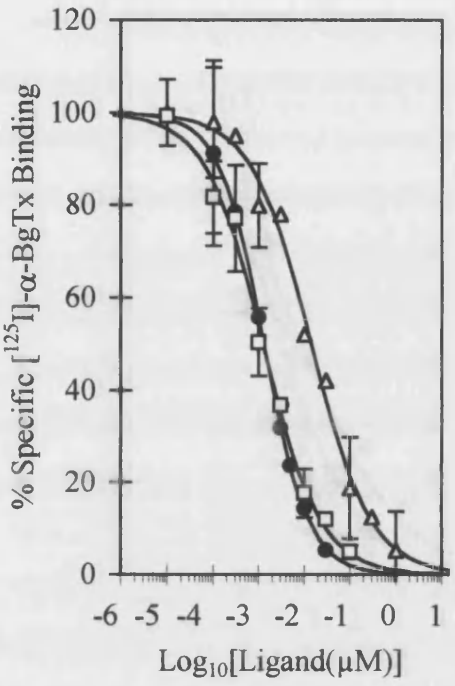

Figure 2.20 - MLA

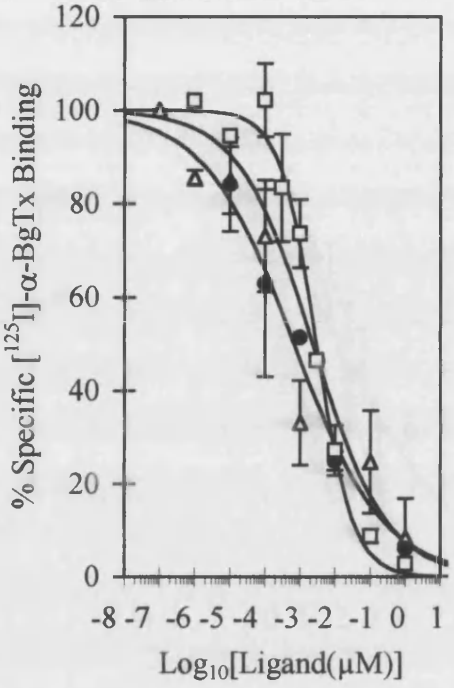

Figure 2.21 - (±)EPI

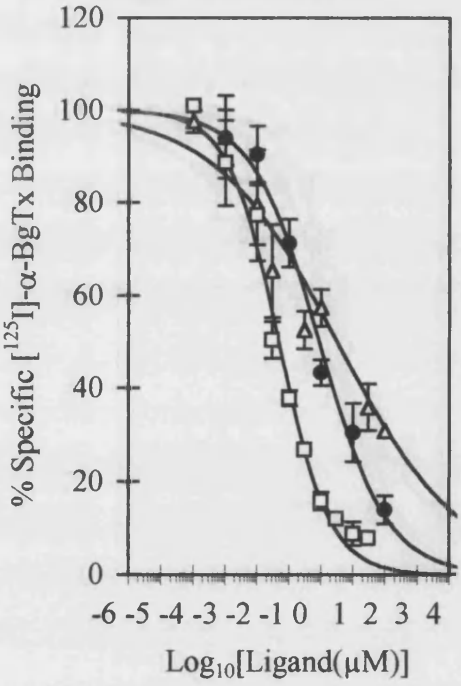

Figure 2.22 - IMI

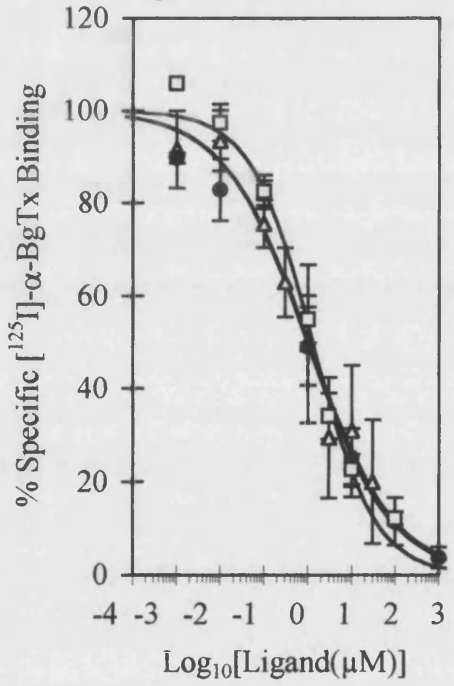

Figure 2.23 - (-)Nicotine

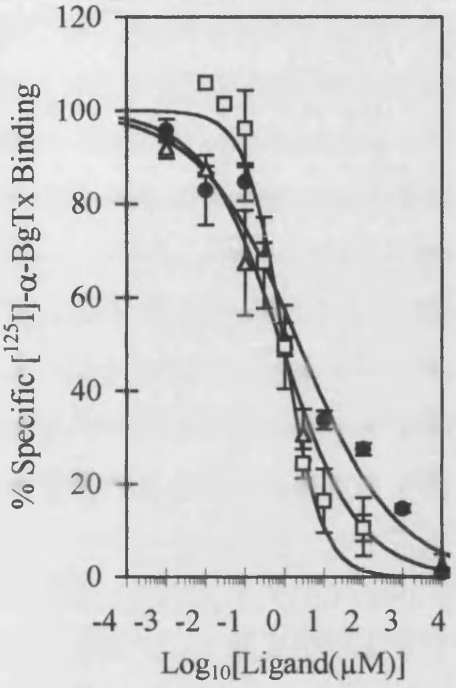

Figure 2.24 - (±)Anabasine

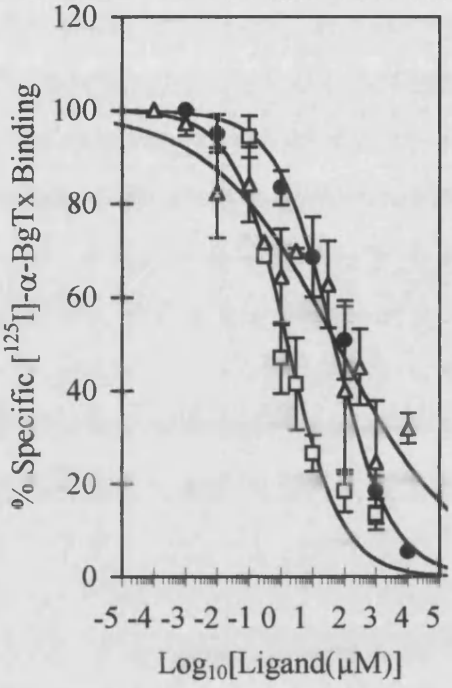

Figure 2.25 - ACh

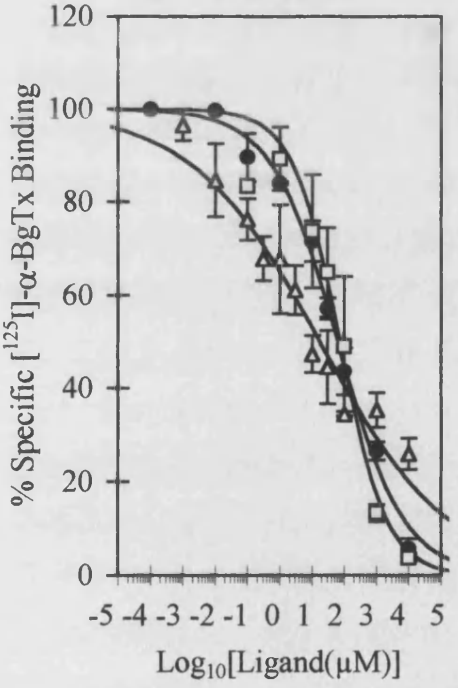

Figures 2.26.-2.29. Competition binding assays of cholinergic ligands at the [^{125}I]-α-BgTx binding site in *M. persicae* membranes. Methods and Materials as briefly described in Figures 2.19.-2.25. Data are the Mean±SEM of 3 independent experiments.

Figure 2.26

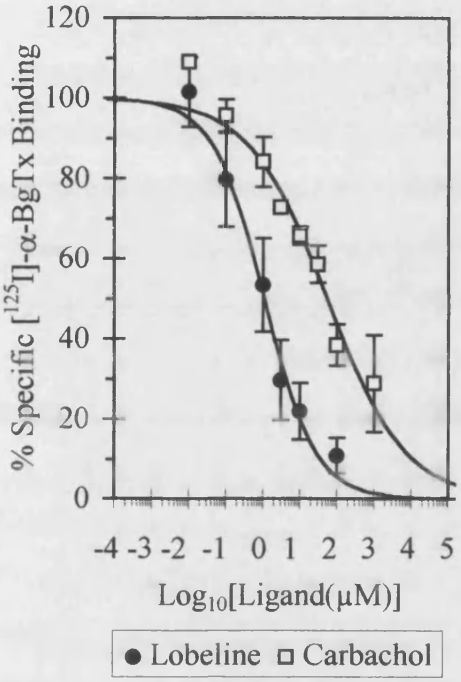

Figure 2.27

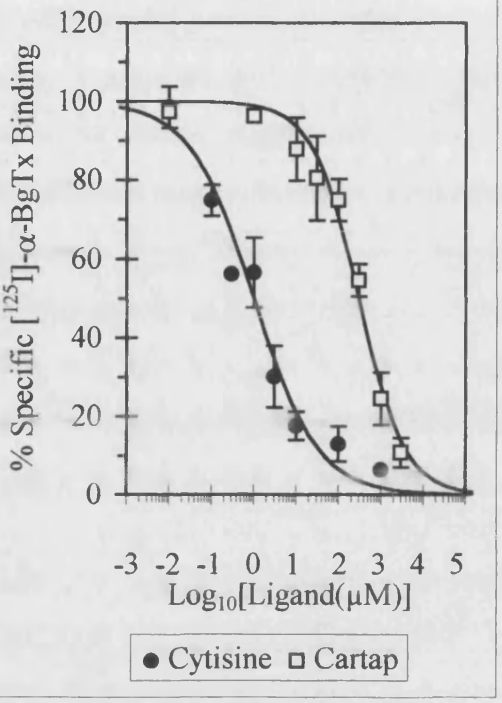

Figure 2.28

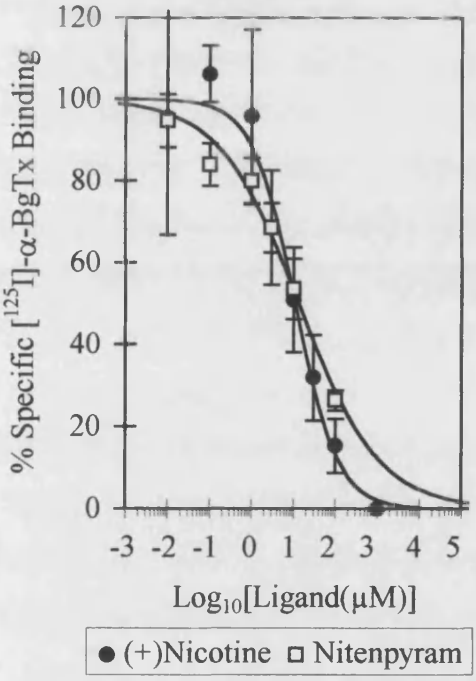

Figure 2.29

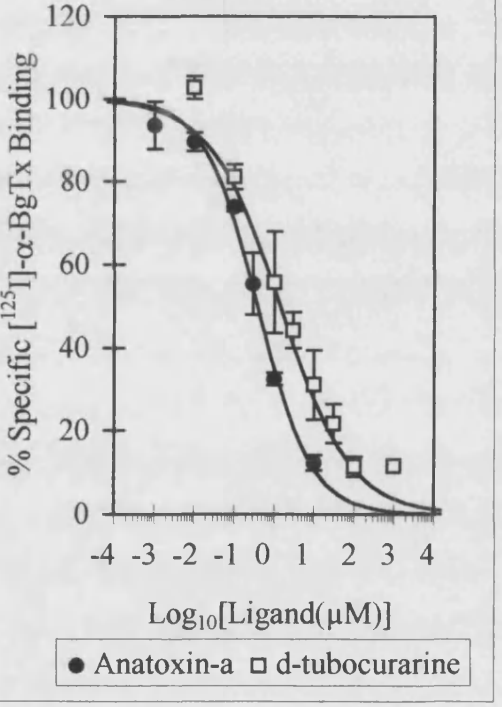

Chapter 3

[^{3}H]-Imidacloprid radioligand binding

This chapter is a slightly modified version of a published paper: Lind, R. J., Clough, M. S., Reynolds, S. E. and Earley, F. G. P. (1998) [^{3}H]-Imidacloprid labels high and low affinity nicotinic acetylcholine receptor-like binding sites in the aphid *Myzus persicae* (Hemiptera: Aphididae). *Pestic. Biochem. Physiol.*, **62,** 3-14.

3.1 Introduction

The nitroguanidine insecticide imidacloprid (IMI) (Elbert *et al.,* 1991; Leicht, 1993) has a novel mode of action and exhibits good contact and systemic activity. These properties make IMI particularly suited for the control of sucking pests such as aphids, whitefly and planthoppers, with additional activity against coleopteran and some lepidopteran pests (Elbert *et al.,* 1991). IMI is also used in a veterinary context against fleas (Jacobs *et al.,* 1997).

The molecular target of IMI and related compounds is postulated to be the nicotinic acetylcholine receptor (nAChR). The evidence for this includes a number of electrophysiological and radioligand binding studies on a variety of insect tissues (Schröder and Flattum, 1984; Abbink, 1991; Bai *et al.,* 1991; Tomizawa and Yamamoto, 1992). Most notably, Liu and Casida (1993) showed that [^{3}H]-IMI binds specifically to membranes from housefly (*Musca domestica*), as well as other insect nerve tissue, and that the binding was displaceable by nicotinic ligands.

Up until recently, rather little has been known about nAChR receptor subtypes in insects; although a number of subunit cDNAs (both α and non-α) have been cloned (reviewed by Gundelfinger, 1992) it has not so far been possible to relate this information to receptor pharmacology. However, Buckingham *et al.* (1997) have now found that the actions of IMI on cultured cockroach (*Periplaneta americana*) neurones

can be classified into 3 distinct pharmacological types. This suggests that further study of insect nAChR may be important in understanding IMI toxicology.

Further, little work has so far been done on the molecular interaction of IMI with the insects against which it is used in the field to investigate any increase in sensitivity. The present investigation set out to study [^{3}H]-IMI binding to membranes of the aphid *Myzus persicae*, and to compare this with that seen in other insects. The nicotinic ligands epibatidine (Badio and Daly, 1994) and methyllycaconitine (MLA) (Drasdo *et al.,* 1992) were used to investigate the pharmacology of IMI binding through displacement studies since they are able to discriminate nAChR subunit types in vertebrates.

3.2 Materials and Methods

3.2.1 Chemicals

[^{3}H]-IMI (30Ci/mmol, radiochemical purity > 95%) was synthesised by Amersham International according to Latli and Casida (1992). Sources for other compounds were as follows: acetylcholine chloride (ACh), neostigmine bromide, and (-)nicotine from Sigma chemicals. α-Bungarotoxin (α-BgTx), (±)epibatidine, and methyllycaconitine (MLA) from RBI (now Sigma-Aldrich Ltd). Imidacloprid of technical purity was synthesised by Zeneca Agrochemicals. Further reagents were purchased as indicated in Chapter 2.

3.2.2 Invertebrate and vertebrate rearing and collecting

Unless otherwise stated, insects were killed by freezing in liquid nitrogen and stored at -80°C until required.

Experiments used apterous *Myzus persicae* (strain 405D, originating from Rothamsted Experimental Station) of mixed ages. These were mass reared on 30-40 day old chinese cabbage plants (*Brassica pekinensis)* at 20±2°C on a 16 hr light:8 hr dark photocycle and collected by brushing the leaves. This strain has an FE4 esterase level corresponding to resistance level R1 and is moderately resistant to organophosphate, carbamate and pyrethroid insecticides (Devonshire, 1989; Devonshire and Field, 1991).

For comparative purposes, further *Myzus* sp. clones were collected from the field having previous exposure to chemical insecticides. Two clones were collected from Holland by the author. The *Myzus* sp. clone H3 was collected from a glasshouse growing sweet pepper in Lange broekweg, Honselersdijk having a spray history of 2 applications of IMI and a single application of pirimicarb. The second *Myzus* clone

from Holland, H7, was collected from field grown potatoes in Middenmeer having previous exposure to mevinfos, heptenofos, priricarb and lambda-cyhalothrin. It is uncertain if the clones from Holland were *M. persicae* or *M. nicotianae.* A further *Myzus* sp. was collected from the USA by M. S. Clough (Zeneca Agrochemicals). The USA *Myzus* clone U1 was isolated in North Carolina and was a tobacco feeding form likely to be *M. nicotianae*, the spray history was unknown. Levels of esterase were determined for each of the aphid clones with H7 and U1 corresponding to R3 and H3 to R2.

A mixed population of green leaf hopper *Nephotettix cincticeps* (Hemiptera: Cicadellidae) was reared on young (3 week old) rice (*Oryza sativa*) plants at 20±2°C on a 16 hr light:8 hr dark photocycle. *N. cincticeps* was collected by vigorously shaking infested plants in a large polyethylene bag. *Bemisia tabaci* (IMI susceptible strain) were supplied by Martin Williamson of Rothamsted Experimental Station. Adult male American cockroaches *P. americana* (Dictyoptera: Blattidae) were obtained from Blades Biological Products (Edenbridge, Kent, UK). They were decapitated and the heads used immediately for preparation. Blowflies *Lucilia sericata* (Diptera: Calliphoridae) were obtained from Blades Biological Products as pupae; upon emergence they were confined in a muslin cage which could be immersed in liquid nitrogen. Bodies were shaken and the heads separated by sieving out wings and legs as described by Liu and Casida (1993). Adult fruitflies *Drosophila melanogaster* (Canton S) (Diptera: Drosophiloidea) were reared using standard methods. Flies were anaesthetised with carbon dioxide, collected in a muslin bag, allowed to revive and the bag immersed in liquid nitrogen. Tobacco hornworms *Manduca sexta* (Lepidoptera: Sphingidae) were reared according to Bell and Joachim (1978); brains were dissected from pharate adults and frozen. Tobacco budworms *Heliothis virescens* (Lepidoptera: Noctuidae) were also reared on artificial diet. Whole heads from adult moths were separated using a series of sieves as described for *L. sericata.* Cat fleas *Ctenocephalides felis* (Siphonaptera: Pulicidae) were reared on an artificial feeding system and whole bodies used for membrane preparation. All insects used are shown

on plate 1. Optic lobes of the squid *Loligo vulgaris* were supplied by the Plymouth Marine Association, further details in section 5.2.2. Fresh water crayfish, *Austropotamobius* sp, were obtained from Jealott's Hill Research Station restaurant and the nerve cord and associated ganglia dissected from the abdomen from 7 adults (2 male and 5 female) and used immediately for membrane preparation. Vertebrate brains (minus cerebellum) were harvested from adult male Wistar rats and rapidly frozen until required (work in collaboration with Chris Sharples, University of Bath).

3.2.3 Membrane preparation and [^{3}H]-IMI binding

Aphids (25g) comprising some 100,000 individuals were homogenised with a motor driven Ultra Turrax® for 30 seconds at 5000rpm in 0.32M sucrose, 100µM EDTA, 1µM leupeptin, 1µM pepstatin, and 200µM PMSF (pH 7.2). The homogenate was centrifuged at 1000g for 30 minutes and the resulting supernatant fraction strained through 4 layers of fine nylon mesh and re-centrifuged at 30,000g for 60 minutes. The pellet was reconstituted in incubation buffer containing 0.05M Tris, 0.12M NaCl, and 100µM EDTA (pH 7.4). The protein concentration was determined using the method of Bradford (1976) with bovine serum albumin (BSA) as a standard. Membrane preparations for the other invertebrates were produced in a similar fashion to aphids. Membranes from rat brain were obtained from Chris Sharples (University of Bath), produced as described by MacAllen *et al.* (1988). Detergents were not employed in any case. Unless otherwise stated the aphid binding assay consisted of incubation of 100µg of membrane preparation in a final volume of 200µl incubation buffer containing, additionally, 0.25% BSA in a 96 well microtitre plate. Protein levels for the other membrane preparations were between 25 and 100µg per incubation. Incubation was for either 120 minutes for displacement or 180 minutes for saturation studies at room temperature (22°C) on a plate shaker. Green leaf hopper membrane preparation (80µg) was incubated in a total volume of 1ml to avoid severe ligand depletion at very low concentrations (<0.05nM) of [^{3}H]-IMI. Bound [^{3}H]-IMI was quantified by filtration using a Tomtec Mach 2 cell harvester employing Wallac thin filter mats pre-soaked in

0.3% polyethyleneimine (Bruns *et al.,* 1983), using a 2 wash cycle of ice cold incubation buffer (+0.25% BSA). Solid scintillant (Meltalex A, Wallac) was melted onto filter mats, which were counted at 34% efficiency in a Wallac beta plate counter. Non-specific binding was determined using a final concentration of 1µM MLA, which gave values that were no different from non-specific binding determined with 1µM IMI.

3.2.4 Centrifugation assay

The amount of binding at low (500pM) and saturating (30nM) concentrations of [^{3}H]-IMI was determined in centrifugation assays to investigate if bound [^{3}H]-IMI was washed off during filtration experiments. In centrifugation assays incubation was performed in 1.5ml microcentrifuge tubes which were centrifuged at 30,000g for 5 min in a Beckman bench top ultrafuge in order to terminate incubation. The supernatant fraction was removed, and the pellet washed three times with 1ml distilled water. Pellets were then dissolved overnight in 10% sodium deoxycholic acid and the redissolved pellet (0.5ml) was transferred into 4.5ml of liquid scintillant (Optiphase safe) and counted at 43% efficiency.

3.2.5 Kinetic analysis

A concentration of 500pM [^{3}H]-IMI was used to study only the high affinity binding site for both association and dissociation rate kinetics in *M. persicae* membranes. Dissociation was initiated by the addition of 1µM MLA which gave results that were no different from using 1µM IMI.

3.2.6 Displacement Studies

Ligands employed for displacement studies were added to aphid membranes 30 minutes prior to the addition of 500pM [^{3}H]-IMI. Competing ligands were assayed in a dilution series of 1, 3, 10, 30, 100, 300, etc. with at least 6 concentrations in triplicate focused around the IC_{50} point (at which 50% of bound [^{3}H]-IMI is displaced). In the case of acetylcholine (ACh), it was necessary to inhibit acetylcholinesterase. To do this, a final concentration of 10μM neostigmine bromide was added to aphid membranes 10 minutes before the addition of ACh (Neostigmine was separately determined not to affect IMI binding in *M. persicae* - data not shown). All data presented are the mean±SEM of 3 independent experiments.

3.2.7 Data Calculation

Non-linear regression analysis with Microsoft Excel's solver macro (Bowen and Jerman, 1995) was used to determine the dissociation constant (K_d) and maximal binding capacity (B_{max}) from double hyperbola plots for saturation data (Hulme and Birdsall, 1992). Non-linear regression was also used to determine the IC_{50} and Hill coefficient for displacement data. K_i values were determined using the Cheng and Prusoff relationship assuming a K_d value of 0.14nM for [^{3}H]-IMI (see section 2.2.9). In kinetic experiments the initial association and dissociation rate constants were determined using non-linear regression from pseudo-first-order kinetics (Bylund and Yamamura, 1990).

3.3 Results

[^{3}H]-IMI bound specifically to membranes from previously frozen whole R1 *M. persicae*, allowing the collection of highly reproducible binding data. At concentrations up to 10nM ligand, specifically bound [^{3}H]-IMI accounted for >90% of total binding for all insects investigated. Specific binding of [^{3}H]-IMI (determined at 500pM) demonstrated a linear relationship to increasing amounts of aphid membranes with protein content up to 500µg (data not shown). Aphid membranes remained stable at -80°C for at least 6 months and when thawed showed unchanged binding capacity for at least 4 hours at 22°C.

3.3.1 Saturation binding experiments

At low concentrations up to 1nM [^{3}H]-IMI significant ligand depletion of up to 50% occurred. This was corrected for in the analysis by assuming that the free [^{3}H]-IMI concentration was equal to the total minus bound concentration. Interpretation of the data for [^{3}H]-IMI saturable binding in R1 *M. persicae* membranes by filtration is shown in figures 1a and 1b. This is consistent with 2 binding components, one of high (K_d=0.14±0.01nM, B_{max}=284±16fmol/mg) and one of low affinity (K_d=12.6±1.8nM, B_{max}=486±78fmol/mg). A Hill value (n_H) of 0.61±0.02 was determined (Figures 3.1, 3.2).

3.3.2 Kinetic analysis of high affinity [^{3}H]-IMI binding to R1 M. persicae *membranes*

[^{3}H]-IMI associates with and dissociates from the high affinity binding site in a biphasic manner at 22°C (Figures 3.3-3.6). The fast association and dissociation constants, k_{+1} and k_{-1}, have values of 3.917 ($T_{½}$=18 sec) and 0.419 min^{-1} ($T_{½}$=99 sec) respectively. This results in a k_{-1}/ k_{+1} (K_d) of 0.11nM which is consistent with the K_d of 0.14nM determined in saturation experiments. The biphasic association and dissociation of IMI with R1 *M. persicae* membranes is in accord with the data of Liu

and Casida (1993) for housefly. The data suggest either a two-stage sequential reaction or parallel reactions with different kinetic properties (Galper *et al.,* 1977).

3.3.3 Centrifugation assay

A comparison of [^{3}H]-IMI specific binding to R1 *M. persicae* membranes using either filtration or centrifugation revealed that when [^{3}H]-IMI was used at 500pM, only insignificant amounts of specifically bound ligand were lost during filtration, but that at 30nM, 45% of the bound [^{3}H]-IMI was washed off during filtration. Thus, although the B_{max} value determined for high affinity [^{3}H]-IMI binding from filtration experiments is accurate, the B_{max} value determined for the low affinity [^{3}H]-IMI binding sites is an underestimate. The corrected value is 883±142 fmol/mg.

3.3.4 Displacement studies

A number of cholinergic ligands were tested for their ability to displace [^{3}H]-IMI binding to R1 *M. persicae* membranes. [^{3}H]-IMI was used at a concentration of 500pM in these experiments in order to examine competition at the high affinity [^{3}H]-IMI site only. The pharmacological profile (Table 3.1, Figure 3.7) demonstrates a nicotinic character, and is similar to that determined previously for [^{3}H]-IMI binding in housefly (Liu and Casida, 1993) and whitefly (Chao *et al.,* 1997). ACh and (-)-nicotine were only poor displacers of [^{3}H]-IMI with IC_{50} values respectively more than 3 and 2 orders of magnitude higher than that for IMI itself. α-BgTx, epibatidine and MLA were found to be more effective displacers of [^{3}H]-IMI, with IC_{50} values of approximately 60, 20 and 14-fold greater than for IMI. Epibatidine, imidacloprid and (-)-nicotine all gave Hill values of approximately 1, whereas MLA, α-BgTx and ACh all exhibited Hill values markedly less than 1.

	R1 *M. persicae*			House fly[a]	Whitefly[b]
Ligand	IC_{50} (nM)	K_i (nM)	Hill (n_H)	IC_{50} (nM)	IC_{50} (nM)
Imidacloprid	1.1±0.4	0.24±0.08	1.15±0.1	9.5±0.9	1.6±0.1
MLA	15.1±3.1	3.3±0.7	0.58±0.1	ND	ND
(±)Epibatidine	21.9±2.9	4.8±0.6	1.03±0.03	350±70	ND
α-BgTx	62.4±26.8	13.7±5.9	0.56±0.1	4500±260	1310±50
(-)nicotine	643±197	141±43	0.87±0.19	21000±940	402000±16000
ACh	2390±1610	522±352	0.48±0.04	48000±2690	37000±740

Table 3.1. Displacement of 500pM [^{3}H]-IMI from R1 *M. persicae* membranes using nicotinic ligands giving IC_{50}, K_i and Hill values with ±SEM. Tabulated results are n=3. [a]Comparable data (IC_{50}, nM) for house fly (Liu and Casida, 1993; Liu *et al.,* 1995). [b]Comparable data (IC_{50}, nM) for whitefly (Chao *et al.,* 1997). ND = Not determined.

3.3.5 [^{3}H]-IMI saturation experiments in a panel of organisms

Membrane preparations from *P. americana*, *L. sericata*, *D. melanogaster*, *H. virescens*, *M. sexta* and *C. felis* all displayed saturable binding of [^{3}H]-IMI, with saturation data indicating the presence of only a single population of sites. K_d values ranged between 1.30 and 4.82nM, and B_{max} values varied greatly, from 126.0 to 2140.3 fmol/mg (Table 3.2, Figures 3.8-3.19). Because these were filtration experiments, it is possible that B_{max} values may be underestimates (see above). Binding of [^{3}H]-IMI in each of these insects gave a Hill value between 0.92 to 1.04. By contrast, saturation experiments in *N. cincticeps* were consistent with the presence of two [^{3}H]-IMI binding sites of high and low affinity, having apparent K_d values of 0.0043 and 1.23nM and B_{max} values of 32.5 and 179.1 fmol/mg respectively and a Hill value of 0.67 (Table 3.2, Figure 3.20, 3.21). The value of K_d for the high affinity [^{3}H]-IMI binding site in *N. cincticeps* must be regarded as only approximate using [^{3}H]-IMI at a specific activity of 30Ci/mmol, because the lowest concentration used was 5pM. It would have been difficult to obtain useful data from lower concentrations than this. It is clear, however, that the high affinity [^{3}H]-IMI binding site in *N. cincticeps* is at least an order of magnitude higher than that of *M. persicae.*

A further hemipteran insect, *B. tabaci*, also demonstrated the presence of two [^{3}H]-IMI binding components with K_d values of 0.10 and 2.14nM and corresponding B_{max} values of 33 and 112 fmol/mg for the high and low affinity sites respectively (Table 3.2, Figure 3.22, 3.23). The three field collected clones of *Myzus* also gave [^{3}H]-IMI binding data consistent with two binding sites with similar K_d values as found in R1 *M. persicae* (Table 3.2, Figures 3.24-3.29). The B_{max} values of the *Myzus* clones also demonstrated higher densities of low affinity [^{3}H]-IMI binding sites compared to high affinity sites as exhibited in R1 *M. persicae* membranes.

Insect	High affinity		Low affinity		Hill value
	K_d (nM)	B_{max} (fmol/mg)	K_d (nM)	B_{max} (fmol/mg)	(n_H)
R1 *M. persicae*	0.14±0.01	284±16	12.58±1.83	486±78	0.61±0.02
Myzus sp. H3	0.09±0.02	252±74	9.19±1.65	608±146	0.54±0.01
Myzus sp. H7	0.08±0.03	170±66	7.49±2.52	642±38	0.68±0.07
Myzus sp. U1	0.18±0.07	140±35	11.48±2.22	438±120	0.64±0.06
N. cincticeps	0.0043	33	1.23	179	0.67
B. tabaci	0.10	19	2.14	112	0.50
*M. sexta**	1.30	150			0.99
*H. virescens**	1.51	134			0.92
D. melanogaster	1.42	126			1.04
*L. sericata**	1.75	539			1.02
*P. americana**	3.14	2140			1.01
C. felis	4.82	369			0.95

Table 3.2. Comparison of [^{3}H]-IMI saturable binding in a panel of insects showing K_d (nM), B_{max} (fmol/mg) and Hill (n_H) values. Tabulated results for R1 *M. persicae* represent the mean ±S.E. of five separate experiments and n=3±SEM for the *Myzus* sp. from Holland and the USA, but are n=2 for *N. cincticeps* and n=1 for other insects. *heads only.

Specific [^{3}H]-IMI binding was readily demonstrated in membranes from the abdominal nerve cord of fresh water crayfish, although there was insufficient material to complete a full saturation isotherm so the affinity of the binding site could not be ascertained. At a concentration of 1nM non-specific binding was ~1% of the total binding and specific

binding was 1179 fmol/mg. There was no detectable specific binding of 10nM [^{3}H]-IMI to rat brain with total and non-specific cpm of 290 and 283 respectively. Likewise no high affinity [^{3}H]-IMI binding was detected in squid optic lobe membranes at a concentration of 1nM, with total and non-specific cpm of 17 and 12 respectively.

3.4 Discussion

Specific saturable [^{3}H]-IMI binding in membranes prepared from homogenates of whole R1 *M. persicae* represented >90% of the total binding at concentrations up to 10nM providing good quality data. Saturation experiments with aphid membranes revealed the existence of two [^{3}H]-IMI binding components ("sites") differentiated by their affinities with K_d values of 0.14nM and 12.6nM, consistent with a Hill value of 0.61. Corrected B_{max} values determined with centrifugation assays indicate a ratio of approximately one high affinity (284 fmol/mg) to three low affinity binding sites (883 fmol/mg). Likewise the three field collected *Myzus* clones exhibited two [^{3}H]-IMI binding components of differing affinity which were in good agreement with those of R1 *M. persicae*. The B_{max} values determined were also consistent with those of R1 *M. persicae* in having more low than high affinity sites. Of particular interest, clone U1 was collected from tobacco and is likely to be the related species *M. nicotianae* (positive identification of *M. nicotianae* requires confirmation using biochemical tests (Blackman and Spence, 1992) which were not obtained for this study). This sibling species of *M. persicae* has been demonstrated to exhibit a 5-fold resistance factor to both nicotine and IMI in dip bioassays (Nauen *et al.,* 1996). However the affinities and density of [^{3}H]-IMI binding sites are not markedly different from R1 *M. persicae*, and thus these parameters cannot account for the IMI tolerance observed in the laboratory. Likewise, the clone H3 was isolated after 2 applications of IMI and displayed no marked differences in its binding properties of [^{3}H]-IMI compared to R1 *M. persicae.*

Two [^{3}H]-IMI binding sites were also observed in the green leaf hopper *N. cincticeps* and the sweet potato whitefly *B. tabaci*, whereas in the other insects studied binding to only a single site was observed. The non-hemipteran insects all showed Hill values of approximately 1. This may indicate that in these insects only a single class of binding site is present and/or that there is no cooperativity between binding sites. The hemipteran insects therefore differ from the other insect Orders examined, namely Lepidoptera, Diptera, Dictyoptera and Siphonaptera, in having two binding sites for

[^{3}H]-IMI. Moreover, the affinity of the more avid of the two hemipteran sites was much higher than that of the single sites in the other insects. *N. cincticeps* demonstrated high and low affinity [^{3}H]-IMI binding sites an order of magnitude higher than those present in aphids. The *N. cincticeps* high affinity [^{3}H]-IMI site has a much lower K_d value than the sites present in other insects. Conversely, the K_d value for the *N. cincticeps* and *B. tabaci* low affinity site is similar to the values for the single sites found in dipteran, lepidopteran, dictyopteran and siphonapteran insects. [^{3}H]-IMI binding in the whitefly *Bemisia argentifolii* was investigated by Chao *et al.* (1997). The authors concluded that this hemipteran insect had only a single binding site with a K_d of 2nM. This differs from the present study in which *B. tabaci* demonstrated two binding components for [^{3}H]-IMI. Our studies show that it is necessary to use [^{3}H]-IMI concentrations below 1nM in order to reveal the high affinity site: such low concentrations were not investigated by Chao *et al.* (1997), so that a high affinity binding site, if present, would not have been detected.

The specificity of [^{3}H]-IMI as a radioligand for insect nAChR is demonstrated by its inability to bind with high affinity to both vertebrate brain (phylum Chordata) and the optic lobes of the cephalopod (phylum Mollusca) (Liu and Casida, 1993; Chao and Casida, 1997). However a high degree of specific [^{3}H]-IMI binding was detected in membranes of the fresh water crayfish which may reflect the evolutionary relationship between the subphylum Crustacea (crayfish) and Uniramia (insects) which both belong to the phylum Arthropoda.

Previous work by Liu, Latli and Casida (Lui and Casida, 1993; Liu *et al.,* 1994) has examined [^{3}H]-IMI binding in *Musca domestica* head membranes. These authors found evidence of two binding components for IMI with high and low affinity when binding was measured in the absence of detergents, but also showed that in the presence of 0.1% Triton X-100 only a single type of IMI binding site was observed. In the present work we did not examine *M. domestica*, but we did not observe multiple [^{3}H]-IMI sites in the related dipteran insects *L. sericata* or *D. melanogaster*. [^{3}H]-IMI

binding to *D. melanogaster* head membranes has been investigated previously by Tomizawa *et al.* (1996) who obtained very similar results to our own. In the present study we used whole body membranes to investigate if low affinity sites were present elsewhere in the insect's body, but no low affinity binding component was detected. In the present case, the presence or absence of detergents does not explain the differences between insects showing either one or two [^{3}H]-IMI binding sites, since detergents were not present in any of the experiments. In general we do not favour the use of detergents in binding experiments, since (a) detergents may expose non-functional receptors from intracellular sites, and (b) detergents may disrupt intra- and intermolecular interactions that determine binding affinity and pharmacology. The effects of detergents on functional receptors has been reviewed by Hjelmeland and Chrambach (1984). Detergents may alter both the affinity (Shiu and Friesen, 1974) and relative numbers of binding sites (Gould *et al.,* 1981).

Multiple binding components for nicotinic radioligands have been detected before in studies of insect nAChR. The study of [^{125}I]-α-BgTx binding in *D. melanogaster* by Schloß *et al.* (1988) revealed the presence of both low and high affinity [^{125}I]-α-BgTx binding sites. The kinetics of [^{125}I]-α-BgTx binding were not affected by the addition of detergent. In contrast, another study of [^{125}I]-α-BgTx binding in *D. melanogaster* detected only a single binding site (Schmidt-Nielsen *et al.,* 1977). The discrepancy may be due to different methods of preparing membranes. Physiological studies of insect nAChR also indicate heterogeneity. The recent electrophysiological study of Buckingham *et al.* (1997) has shown that cultured *P. americana* neurones have at least 3 pharmacologically distinguishable types of response to IMI.

The pharmacology of the high affinity [^{3}H]-IMI site in *M. persicae* is clearly recognisable as that of a nicotinic acetylcholine receptor, being similar to that reported for house fly (Liu and Casida, 1993) and whitefly (Chao *et al.,* 1997) in displaying a relatively low sensitivity to ACh, α-BgTx and (-)nicotine, although the aphid is apparently much more sensitive than the housefly to all these agents (table 1). The

potent analgesic epibatidine was over an order of magnitude more potent at the high affinity [^{3}H]-IMI aphid binding site compared to that in *M. domestica* (Liu *et al.*, 1995). The increased sensitivity to epibatidine and a much lower K_d value determined for the [^{3}H]-IMI high affinity binding site in aphid suggests that this binding site in aphids differs markedly in its affinity and pharmacology from that present in *M. domestica*. Previous studies did not examine the interactions between MLA and the [^{3}H]-IMI binding site. However, in the aphid, it is clear that this agent is an extremely potent displacer at this site. IMI, epibatidine and (-)nicotine all displaced [^{3}H]-IMI with simple kinetics (Hill value ~1) which may indicate that interaction with only a single [^{3}H]-IMI binding site is involved. The difference between the Hill value determined using IMI displacement data (n_H=1.15) and from the saturation isotherm (n_H=0.61) arises because in the displacement studies, a low concentration of IMI was used, and therefore only the high affinity [^{3}H]-IMI binding site was investigated.

It is worth noticing that α-BgTx was not a particularly good displacer of the [^{3}H]-IMI from high affinity IMI binding sites in *M. persicae*. Others have obtained similar results using [^{3}H]-IMI in housefly (Liu and Casida, 1993) and whitefly (Chao *et al.*, 1997). It should be noted, however, that the very slow association kinetics for the interaction of α-BgTx with its specific binding sites (Schmidt-Nielsen *et al.*, 1977; see Chapter 2) means that equilibrium conditions would probably not have been achieved in displacement assays, and therefore these assays may not be valid indicators of the true potency of α-BgTx as a displacing ligand. Although we have previously found that IMI was a poor inhibitor of [^{125}I]-α-BgTx binding in *M. sexta* brain and also in *M. persicae* (See Chapter 2), and others have found this in honeybee head membranes (Tomizawa and Yamamoto, 1992), the same problems of interpretation also apply in these cases. It has been suggested previously (Liu and Casida, 1993), on the grounds that saturable binding of [^{3}H]-IMI can be inhibited by α-BgTx, that IMI and α-BgTx share the same high affinity binding site. However the experiments in question used a very high concentration of α-BgTx (2.5μM) and it is not certain that the toxin was only interacting with its own high affinity binding site. The question of whether IMI

and α-BgTx act at the same or different specific high affinity binding sites remains unresolved. If these are indeed two populations of binding site these could be present on different proteins, or could represent different conformational states of the same protein. It is known that vertebrate nicotinic receptors proteins can adopt conformational states with different binding properties (Prince and Sine, 1998).

Low Hill values were observed for [^{3}H]-IMI displacement by ACh, α-BgTx and MLA. Two possible explanations for this are as follows. First [^{3}H]-IMI may independently label more than one population of high affinity binding sites for which the displacing ligands have different affinities. Buckingham *et al.* (1997) determined the presence of at least two IMI sensitive nAChR in *P. americana* differentiated by their sensitivities to α-BgTx. Second there may be an allosteric interaction between at least two separate binding sites within a single nAChR. In this case, the binding of [^{3}H]-IMI to one of these sites could be influenced allosterically by the presence of another ligand at the other binding site. An allosteric effect of this kind has been noted in *Torpedo* nAChR (Pedersen and Papineni, 1995). Discrimination between these possibilities will require purification of a homogeneous receptor and determination of its subunit composition.

The pharmacology of the lower affinity aphid IMI binding site has not been investigated here, and it would be difficult to do so in crude membrane preparations without a selective ligand to block the higher affinity site. It therefore remains to be conclusively proven that the lower affinity IMI binding site is also nicotinic in character. However this site is totally blocked by MLA, a known nicotinic antagonist, in saturation experiments. It should be pointed out, however, that with a K_d of 12.6nM the affinity of this site for IMI is actually still quite high. The most economical hypothesis is that both high and low affinity IMI-binding sites correspond to nAChR in *M. persicae*.

It is possible that the multiple IMI binding components revealed by the present study to exist in *M. persicae* represent different subtypes of nAChR, which may reflect the existence of multiple α- and β-subunits of the nAChR protein. This receptor

heterogeneity may be encoded by multiple α- and β- nAChR subunit genes which may in addition have spatial or developmental differences in expression. Either non-hemipteran insects do not possess multiple IMI binding sites, or the heterogeneity of nAChR is not revealed in these insects by IMI. Molecular analysis of insect nAChR is as yet rudimentary, but it is already known from molecular genetics that *D. melanogaster* has genes for more than one type of α- and also β- subunits (Gundelfinger, 1992) and from IMI-affinity chromatography that the *M. domestica* nAChR has at least 3 protein subunits (Tomizawa *et al.,* 1996). Because α-BgTx affinity chromatography also identified 3 putative nAChR subunits with similar molecular weights, it was suggested that IMI and α-BgTx may bind to the same nAChR protein. Since the sequences of these subunits were not determined, it remains uncertain whether they are really identical.

From binding studies alone it is not possible to determine whether it is the high or the low affinity [^{3}H]-IMI binding sites which are the target responsible for the insecticidal actions of IMI when the insecticide is given at field rates. This is the subject of investigation in Chapter 6. At all events, it is clear that [^{3}H]-IMI binding to membranes from two species of Hemiptera differs markedly in terms of receptor affinity from that seen in non-hemipteran insects. We venture to suggest that this may explain why IMI is particularly useful in controlling sucking pests including aphids, plant hoppers and whitefly.

Plate 1. Insects used in [^{3}H]-IMI radioligand binding studies. Experiments used 1st instar and adult brains from the tobacco hornworm Manduca sexta (Lepidopteran: Sphingoidea), whole peach potato aphids *Myzus persicae* (Hemiptera: Aphididae), whole tabacco whiteflies *Bemisia tabaci* (Hemiptera: Aleyrodoidea), whole green leaf hoppers *Nephotettix cincticeps* (Hemiptera: Cicadellidae), heads of sheep blowflies *Lucilia sericata* (Diptera: Calliphoridae), heads of american cockroaches *Periplaneta americana* (Dictyoptera: Blattidae), heads of tobacco budworms *Heliothis virescens* (Lepidoptera: Noctuidae), whole fruitflies *Drosophila melanogaster* (Canton S) (Diptera: Drosophiloidea), and whole fleas *Ctenocephalides felis* (Siphonaptera: Pulicidae).

Plate 1

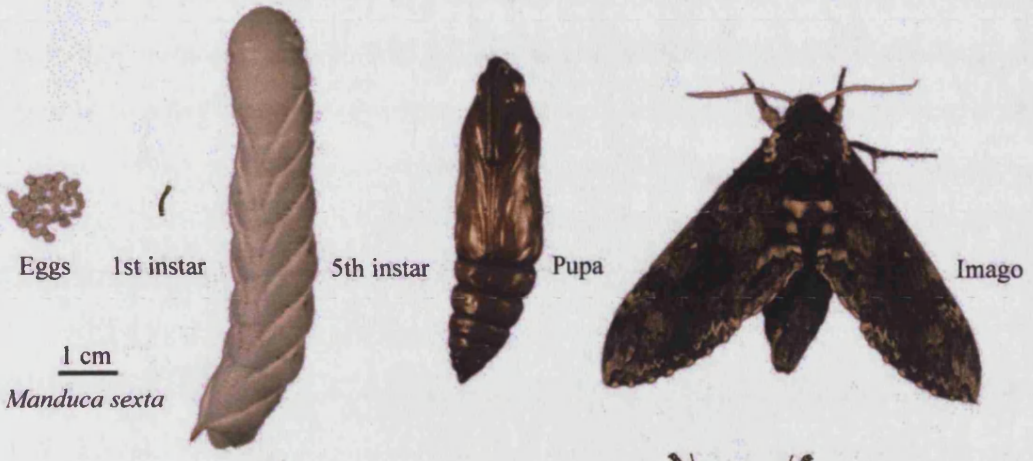

Manduca sexta

Myzus persicae

Bemisia tabaci

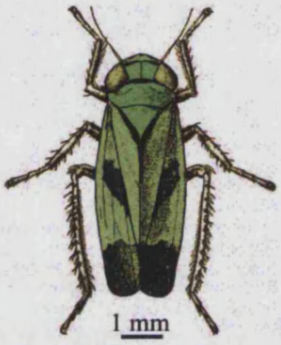

Nephotettix cincticeps

Lucilia sericata

Periplaneta americana

Heliothis virescens

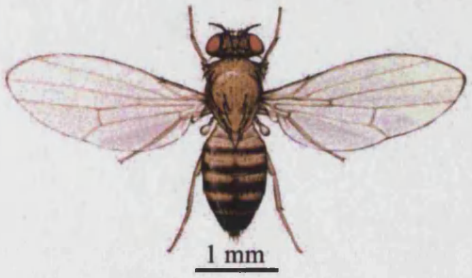

Drosophila melanogaster

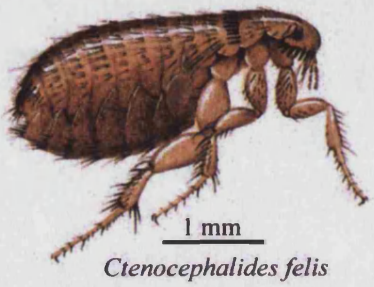

Ctenocephalides felis

Figure 3.1-3.2. [^{3}H]-IMI Saturation binding in homogenates of R1 *M. persicae.* Symbols denote total binding (◆), specific binding (●), and non-specific binding (▲). Membranes were incubated for 3 hours with a range of [^{3}H]-IMI concentrations (typically 0.05-30nM) and bound and free radioligand separated using vacuum filtration with a cell harvester. A concentration of 1μM unlabelled MLA was used to determine non-specific binding. The Hill plot is inset in the Scatchard plot and the x-axis represents Log_{10} free [^{3}H]-IMI concentration, and the y-axis portrays the Log_{10} (Bound/B_{max}-Bound). The lines fitted to the saturation data is to a two site additive fit (see section 2.2.9). The Scatchard plots clearly demonstrates the presence of multiple binding sites and is consistent with a Hill values markedly less than one indicating the presence of more than 1 binding site for [^{3}H]-IMI or cooperativity. Data are the mean of five experiments with ±SEM presented only for specifically bound [^{3}H]-IMI in the saturation isotherm.

Figure 3.1 - *M. persicae*

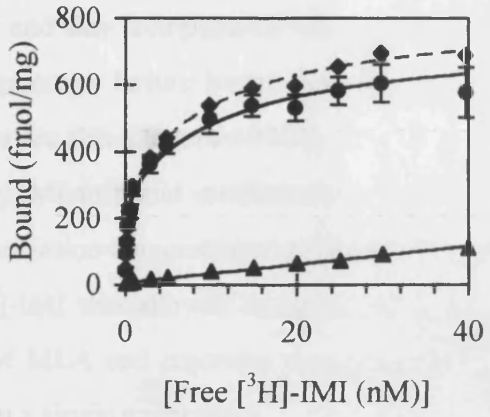

Figure 3.2

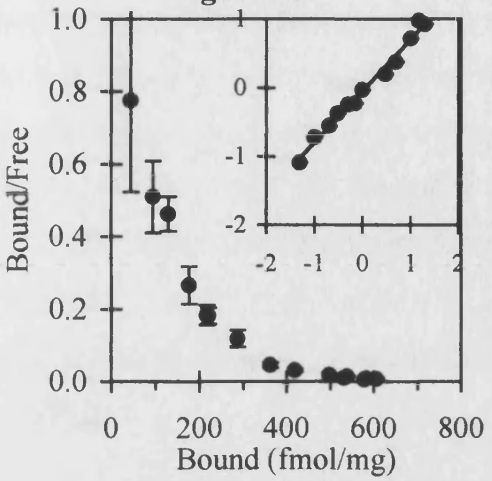

Figures 3.3-3.6. Kinetic data of [^{3}H]-IMI binding in *M. persicae* membranes. **Figure 3.3**. Association of [^{3}H]-IMI to *M. persicae* membranes at 22°C and **Figure 3.4** is the linear transform of the data. The association demonstrates a biphasic interaction with fast and slow components. Membranes were incubated with 500pM [^{3}H]-IMI at room temperature before bound ligand was harvested by filtration using a cell harvester. Data are fitted to a two-site model. **Figure 3.5**. Dissociation initiated by 1µM MLA of [^{3}H]-IMI to aphid membranes at 22°C, **Figure 3.6** shows the linear transform. The dissociation demonstrates a biphasic interaction of fast and slow components. 500pM [^{3}H]-IMI was allowed to equilibrate for 3 hours before dissociation was initiated by 1µM MLA and reactions stopped at the specified times by rapid filtration. Data are from a single experiment.

Figure 3.3

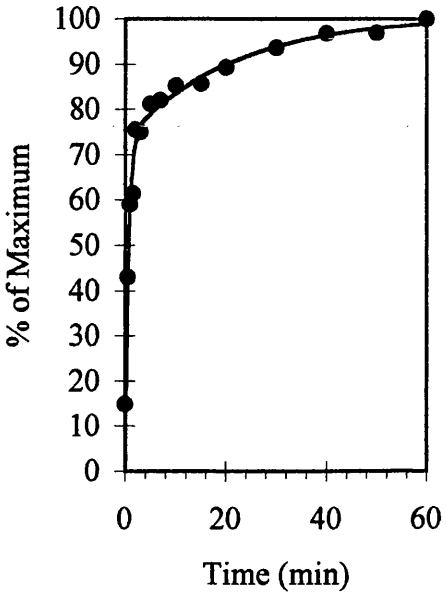

Figure 3.4

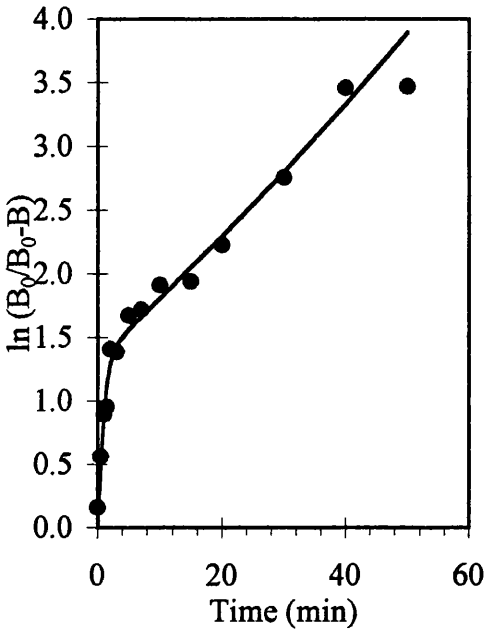

Figure 3.5

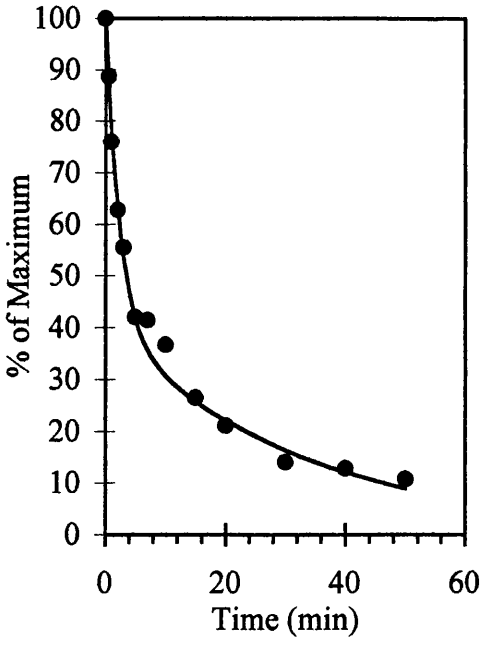

Figure 3.6

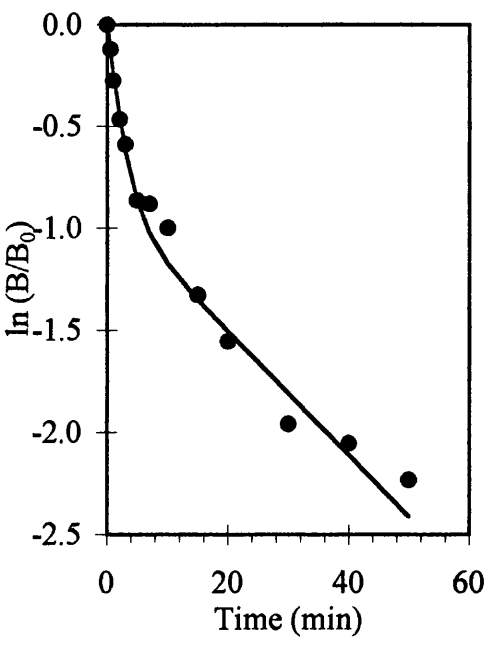

Figure 3.7. Displacement of 500pM [^{3}H]-IMI by the agonists IMI (■), (±)epibatidine (×), (-)nicotine (◆) and ACh (○) and the antagonists α-BgTx (▲) and MLA (●) in *M. persicae* membranes. Data are the mean ± SEM of three separate experiments performed in triplicate. Unlabelled ligands were preincubated with membranes for 30 minutes before the addition of 500pM [^{3}H]-IMI for 2 hours. Bound and free radioligand were separated using a cell harvester. Non-specific binding was determined with a final concentration of 1μM MLA.

Figure 3.7

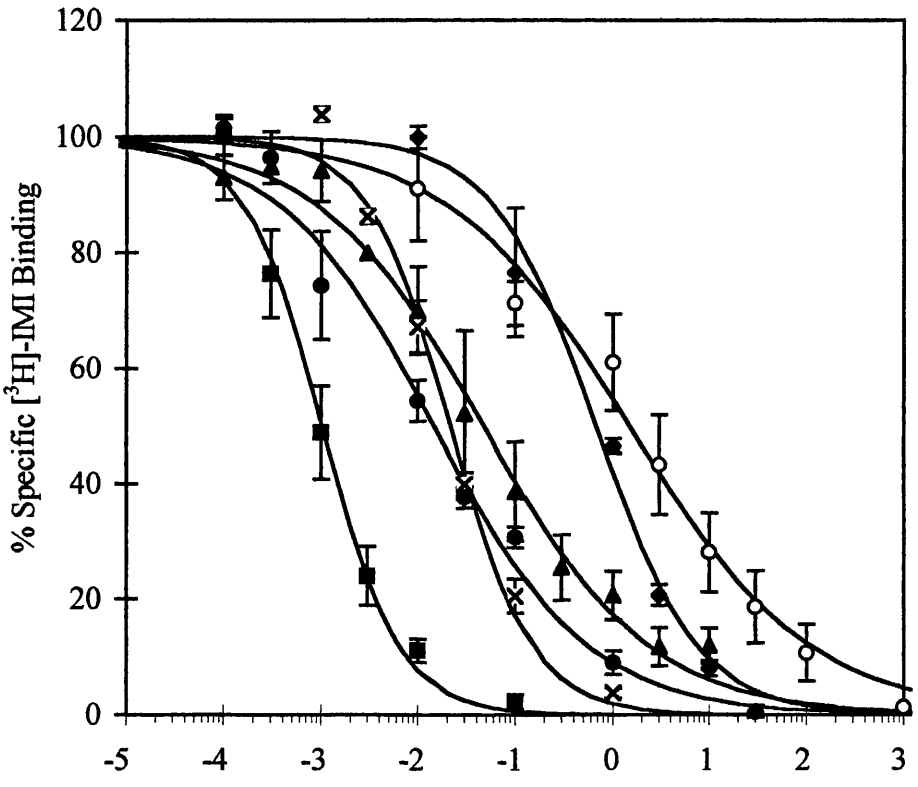
120
100
80
60
40
20
0
% Specific [3H]-IMI Binding
-5
-4
-3
-2
-1
0
1
2
3
[Ligand(μM)]

Figure 3.8-3.29. [^{3}H]-IMI Saturation binding in homogenates of *M. sexta* (Figures 3.8-3.10), *H. virescens* (Figures 3.10-3.11), *D. melanogaster* (3.12-3.13), *L. sericata* (Figures 3.14-3.15), *P. americana* (Figures 3.16-3.17), *C. felis* (Figures 3.18-3.19), *N. cincticeps* (Figures 20-21), *B. tabaci* (Figures 3.22-3.23), *Myzus* sp. clone H3 (Figures 3.24-3.25), *Myzus* sp. clone H7 (Figures 3.26-3.27) and *Myzus* sp. clone U1 (Figures 3.28-3.29). Symbols denote total binding (◆), specific binding (●), and non-specific binding (▲). See Figure 3.1-3.2 for experimental details. The lines fitted to the saturation data of non-hemipteran insects is to a single binding site while that in saturation isotherms of hemipteran insects is to a two site additive fit. The Scatchard plots of the hemipteran insects clearly demonstrates the presence of multiple binding sites and is consistent with a Hill values markedly less than one indicating the presence of more than 1 binding site for [^{3}H]-IMI or cooperativity. Data for the *Myzus* clones is the mean of three experiments, with ±SEM presented only for specifically bound [^{3}H]-IMI in the saturation isotherm. Data shown for all other insects is from a single experiment. An additional experiment for *N. cincticeps* gave similar results.

Figure 3.8 - *M. sexta*

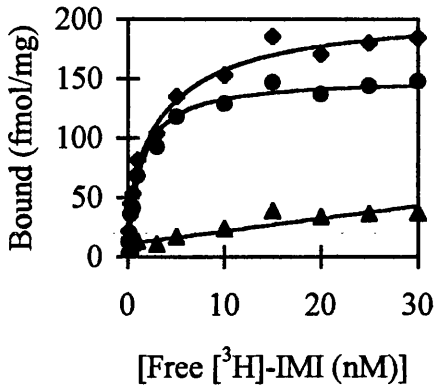

Figure 3.9

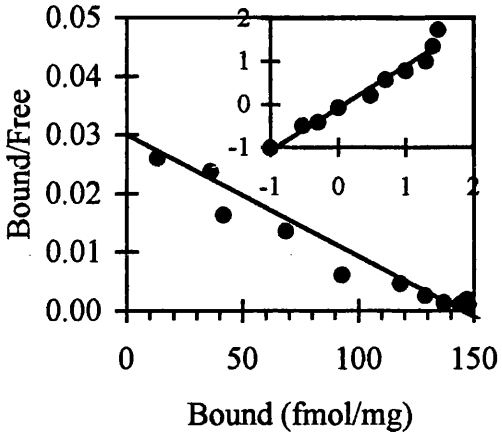

Figure 3.10 - *H. virescens*

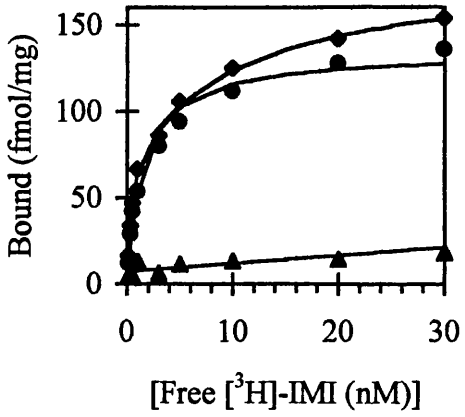

Figure 3.11

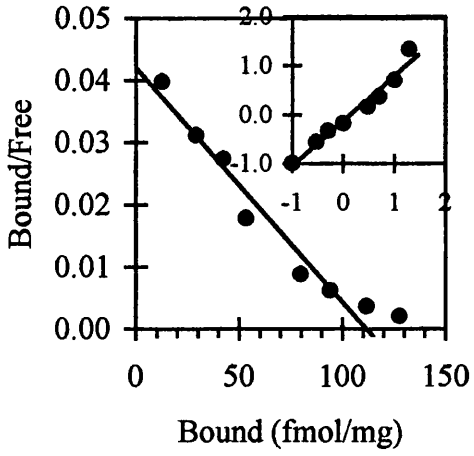

Figure 3.12
D. melanogaster

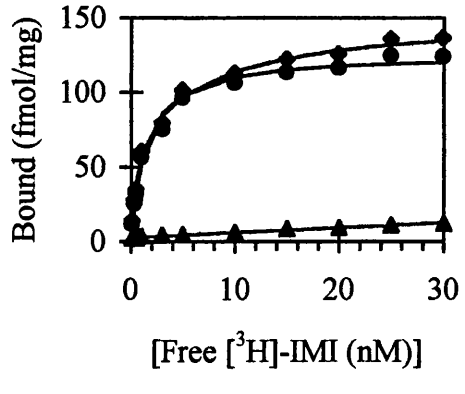

Figure 3.13

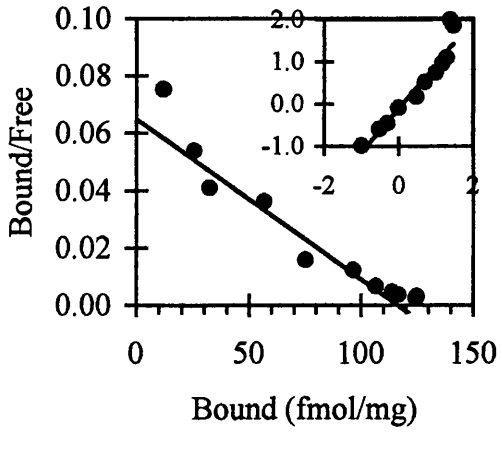

Figure 3.14 - *L. sericata*

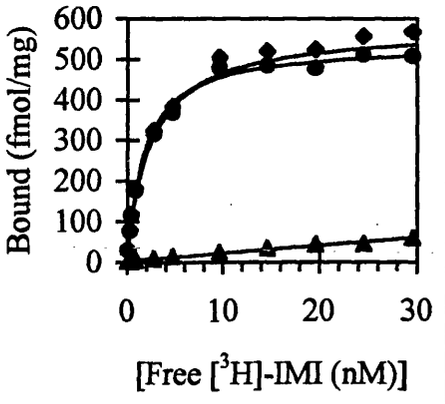

Figure 3.15

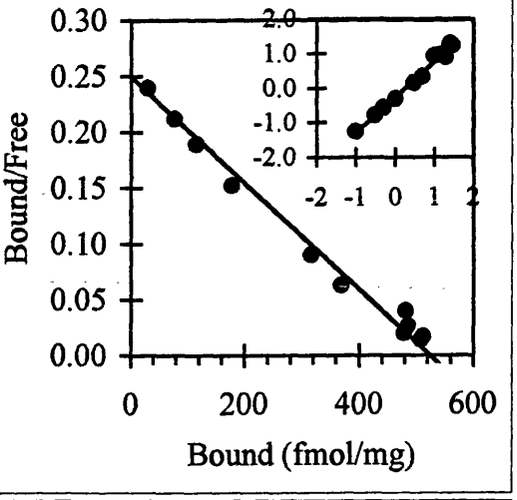

Figure 3.16 - *P. americana*

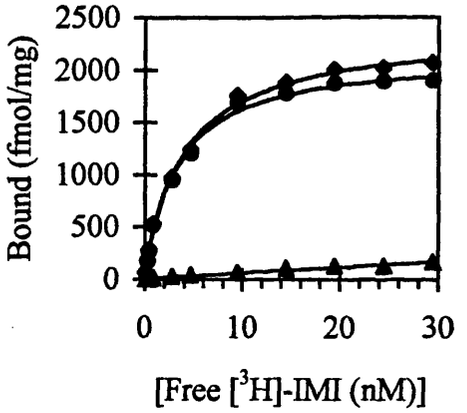

Figure 3.17

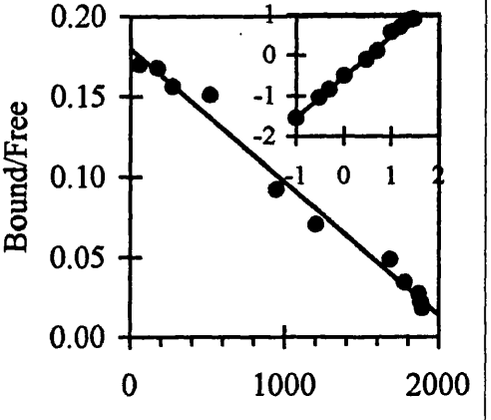

Figure 3.18 - *C. felis*

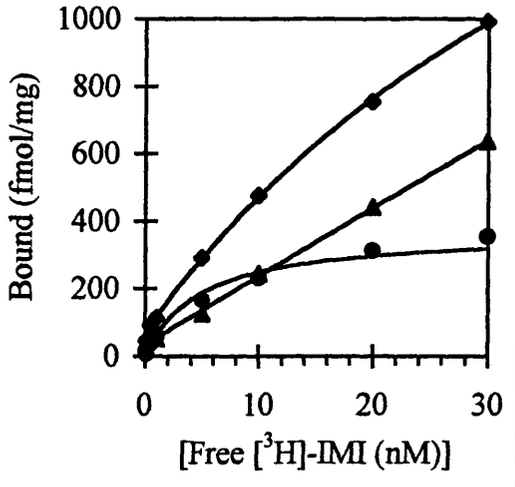

Figure 3.19

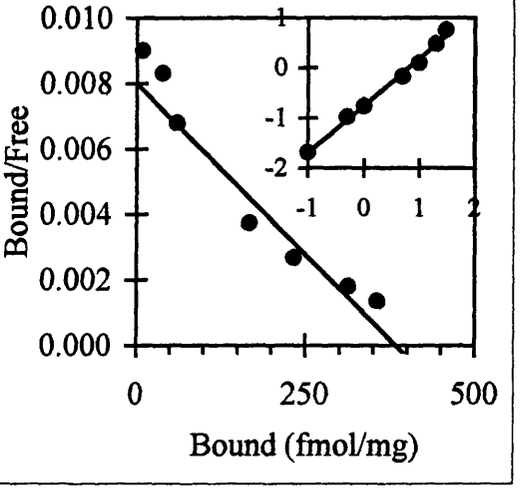

Figure 3.20 - *N. cincticeps*

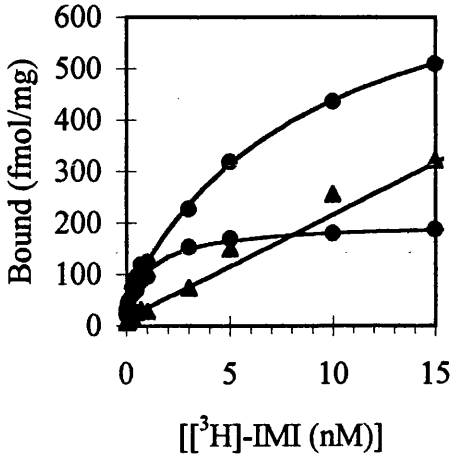

Figure 3.21

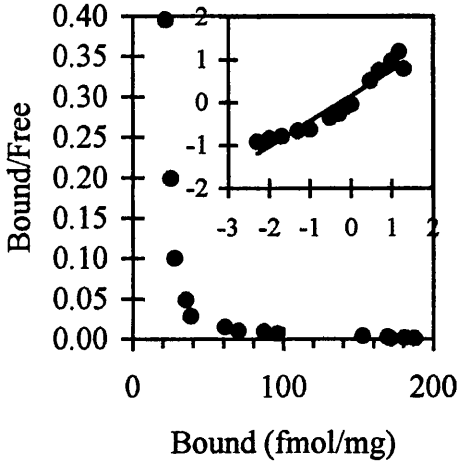

Figure 3.22 - *B. tabaci*

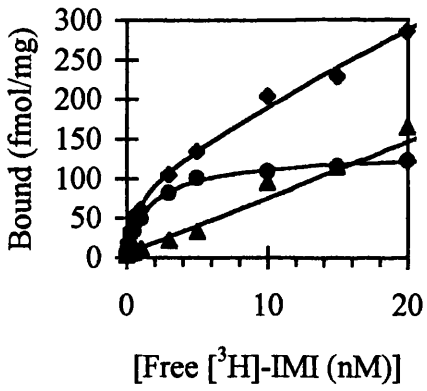

Figure 3.23

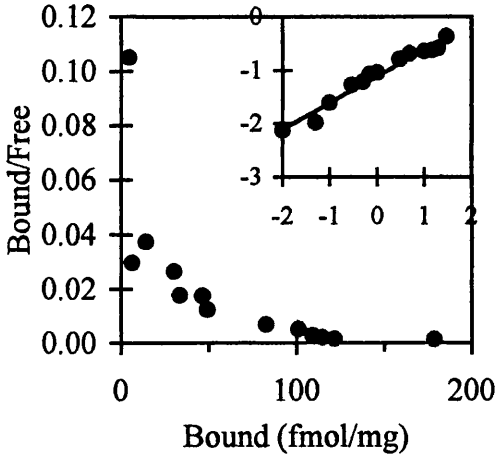

Figure 3.24 - *Myzus* H3

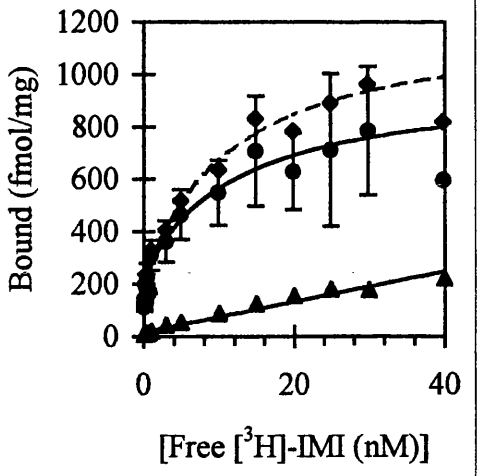

Figure 3.25

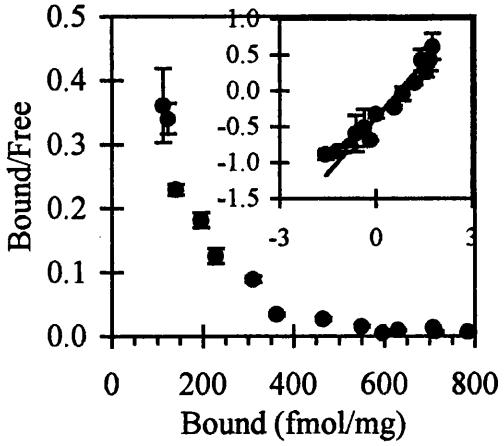

Figure 3.26 - *Myzus* H7

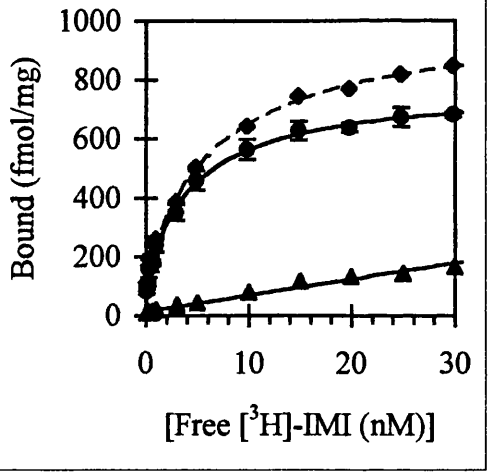

Figure 3.27

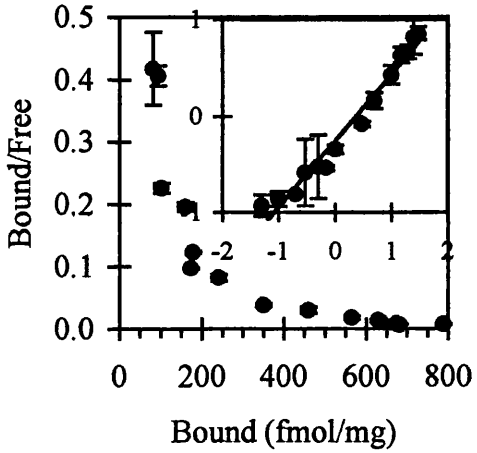

Figure 3.28 - *Myzus* U1

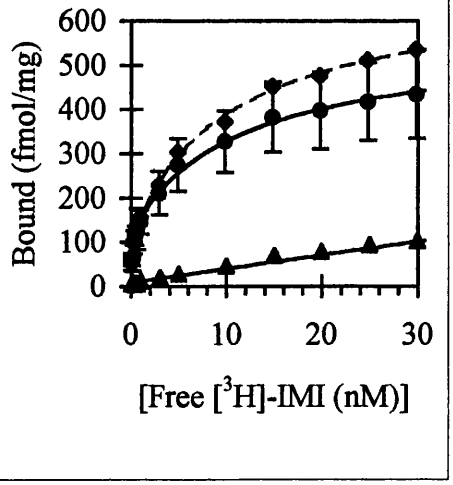

Figure 3.29

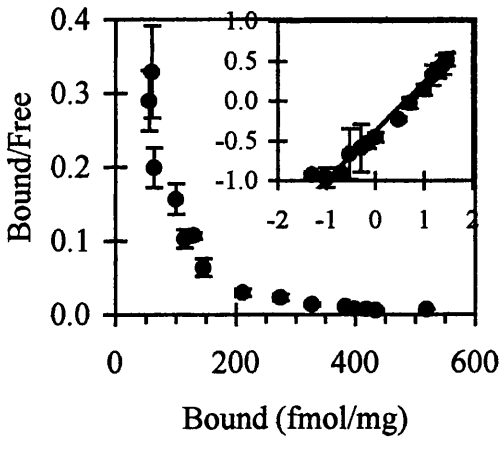

Chapter 4

[^{3}H]-Epibatidine Radioligand binding

4.1 Introduction

The neurotoxin epibatidine (EPI) is derived from the skin of the South American tree frog *Epidobates tricolor*. In mammals EPI acts as a potent analgesic as a result of its actions as an agonist at some types of nAChR (Badio and Daly, 1994). The introduction of [^{3}H]-EPI provided a new pharmacological tool with which to characterise vertebrate nAChR and was determined to selectivity label with high affinity those containing α3 and α4 subunits (Badio and Daly, 1994; Sullivan *et al.*, 1994).

Insect nAChR have been less well studied than those of vertebrates, but recent impetus has been provided by a new class of insecticides, termed neonicotinoids, which act as agonists at insect nAChR. The tobacco alkaloid nicotine has long been used as an insecticide, exploiting as a target the nAChR of the insect CNS. Synthetic neonicotinoid nAChR agonists of which the archetype is the nitroguanidine insecticide imidacloprid (IMI) share structural similarities to EPI. 'Neonicotinoids' have greater insecticidal potency, systemic activity and reduced mammalian toxicity compared to nicotine. The pharmacological properties of IMI at insect nAChR have been well characterised (Liu and Casida, 1993; Buckingham *et al.*, 1997; Chapter 3). Notably, [^{3}H]-IMI is displaced by EPI with high potency in *Myzus persicae* but not so in *Musca domestica* suggesting that pharmacological differences exist between nAChR of different insect orders.

Recently, [^{3}H]-EPI binding has been investigated in the housefly *M. domestica* and the American cockroach *P. americana* (Orr *et al*, 1997). Little specific binding of this ligand could be detected in *M. domestica* but specific binding of [^{3}H]-EPI in *P. americana* was characterised as a single binding site with a K_d of 6.4nM and a B_{max} of 3.4 pmol/mg protein. Furthermore [^{3}H]-EPI binding in *P. americana* was distinguished

by a high sensitivity to IMI and MLA and low sensitivity to α-BgTx and (-)nicotine as displacing ligands.

Here this chapter presents a study of [^{3}H]-EPI binding study in the membranes of the peach potato aphid *M. persicae* which demonstrates marked pharmacological differences between the aphid receptor and that of *P. americana* in both saturation and displacement studies.

4.2 Materials and Methods

4.2.1 Chemicals

[^{3}H]-(±)EPI (50-60Ci/mmol) was purchased from Amersham (UK). Sources for other compounds were as follows: acetylcholine chloride (ACh), α-Bungarotoxin (α-BgTx), (±)epibatidine, methyllycaconitine (MLA), neostigmine bromide and (-)nicotine from Sigma-Aldrich Ltd (Fancy Road, Poole, Dorset). Imidacloprid of technical purity was synthesised by Zeneca Agrochemicals.

4.2.2 Insect rearing and collecting

Peach potato aphids *Myzus persicae* (strain R1), fruitflies *Drosophila melanogaster*, tobacco budworms *Heliothis virescens*, tobacco hornworms *Manduca sexta*, American cockroaches *Periplaneta americana* and sheep blowflies *Lucilia sericata* were reared and harvested as previously described (see Chapter 3).

4.2.3 Membrane preparation and [^{3}H]-EPI binding

Procedures for the preparation of membranes from *M. persicae* and other insects and binding assay were identical to those described previously in Chapters 2 and 3. Briefly, insects were killed by freezing in liquid nitrogen and were homogenised with a motor driven Ultra Turrax® for 30 seconds at 5000rpm in 0.32M sucrose, 100μM EDTA, 1μM leupeptin, 1μM pepstatin, and 200μM PMSF (pH 7.2). The homogenate was centrifuged at 1000g for 30 min and the resulting supernatant re-centrifuged at 30,000g for 60 min. The pellet was reconstituted in incubation buffer containing 0.05M TRIS, 0.12M NaCl, and 100μM EDTA (pH 7.4). Unless otherwise stated the aphid binding assay consisted of incubation of 100μg of membrane preparation in a final volume of 200μl incubation buffer containing, additionally, 0.25% BSA in a 96 well microtitre plate. Incubation was for either 120 minutes for displacement or 180

minutes for saturation studies at room temperature (22°C) on a plate shaker. Bound [^{3}H]-EPI was quantified by either centrifugation or filtration.

4.2.4 Filtration assay

Separation of bound and free ligand by filtration used a Tomtec Mach 2 cell harvester employing Wallac thin filter mats pre-soaked in 0.3% polyethyleneimine (20), using a 2 wash cycle (<20 secs) of ice cold incubation buffer (+0.25% BSA). Solid scintillant (Meltalex A, Wallac) was melted onto filter mats, which were counted at 34% efficiency in a Wallac beta plate counter. Non-specific binding was determined using a final concentration of 1µM MLA, which gave values that were no different from non-specific binding determined with 1µM EPI.

4.2.5 Centrifugation assay

Incubation of [^{3}H]-EPI for centrifugation assays was performed in 1.5ml microcentrifuge tubes which were centrifuged at 30,000g for 5 min in a Beckman bench top ultrafuge in order to terminate incubation. The supernatant fraction was removed, and the pellet washed three times with 1ml distilled water. Pellets were then dissolved overnight in 10% sodium deoxycholic acid and the redissolved pellet (0.5ml) was transferred into 4.5ml of liquid scintillant (Optiphase safe) and counted at 43% efficiency.

4.2.6 Kinetic analysis

A concentration of 1nM [^{3}H]-EPI was used to study only the high affinity binding site for both association and dissociation rate kinetics in *M. persicae* membranes at room temperature (22°C). Association rates were determined for time periods from 0.5 to 60 minutes and terminated by filtration. Dissociation was isotopic and initiated by the

addition of 1μM MLA prior to a 3 hour association of [^{3}H]-EPI to *M. persicae* membranes. Dissociation points were determined between 0.5 and 60 min.

4.2.7 Displacement Studies

Ligands employed for displacement studies were added to aphid membranes 30 min prior to the addition of 1nM [^{3}H]-EPI. Competing ligands were assayed in a dilution series of 1, 3, 10, 30, 100, 300, etc. series with at least 6 concentrations in triplicate focused around the IC_{50} point (at which 50% of bound [^{3}H]-EPI is displaced). In the case of acetylcholine (ACh), it was necessary to inhibit acetylcholinesterase. To do this, a final concentration of 10μM neostigmine bromide was added to aphid membranes 10 minutes before the addition of ACh (Neostigmine was separately determined not to affect EPI binding in *M. persicae* - data not shown). All data presented are the mean±SEM of 3 independent experiments.

4.2.8 Binding of [^{3}H]-EPI to a panel of insects

Specific binding of [^{3}H]-EPI was appraised in a panel of insects, namely *D. melanogaster, L. sericata, H. virescens,* and *P. americana.*. Membranes were incubated with 1nM [^{3}H]-EPI for 2 hours in the presence and absence of 1μM to determine non-specific and total binding respectively. Bound and free radioligand were separated using a cell harvester with a 5 cycle wash of ice cold incubation buffer. Binding of [^{3}H]-EPI was investigated further in adult and larval membranes of *M. sexta* to determine the effect of the ligand used to determine non-specific binding. Membranes of *M. sexta* were incubated with 1nM [^{3}H]-EPI for 2 hours in the presence and absence of either an 1mM (-)nicotine or α-BgTx (1μM for adults, 5μM for larvae) to determine non-specific and total binding respectively. Bound and free radioligand were separated using a vacuum filtration manifold with GF/C filters as described in Chapter 2.

4.2.9 Data Calculation

Non-linear regression analysis with Microsoft Excel's solver macro (Bowen and Jerman, 1995) was used to determine the dissociation constant (K_d) and maximal binding capacity (B_{max}) from hyperbolic plots of saturation isotherm data (Hulme and Birdsall, 1992). Non-linear regression analysis was also used to determine the IC_{50} and Hill coefficient from displacement data. K_i values were determined using the Cheng and Prusoff relationship assuming a K_d value of 0.89nM for [^{3}H]-EPI (see section 2.2.9). Ligand depletion was corrected for in the analysis of saturation data by assuming that the free [^{3}H]-EPI concentration was equal to the total minus bound concentration.

4.3 Results

Binding assays using amounts of protein up to 150µg per incubation demonstrated a linear relationship for specific binding of [^{3}H]-EPI (data not shown). Routinely, 100µg protein per tube was used. Specifically bound [^{3}H]-EPI accounted for >90% of the total signal at concentrations of [^{3}H]-EPI of <15nM, although at concentrations above this non-specific binding accounted for >20%.

4.3.1 Saturation isotherm

A comparison of [^{3}H]-EPI specific binding to R1 *M. persicae* membranes using either filtration or centrifugation revealed that both separation methods gave data consistent with the presence of two binding sites with different affinities (Table 4.1, Figures 4.1-4.6).

	High affinity		Low affinity		
Separation method	K_d (nM)	B_{max} (fmol/mg)	K_d (nM)	B_{max} (fmol/mg)	*Hill value* (n_H)
Filtration	0.89±0.3	87±46	18.4±2.1	373±96	0.81±0.05
Centrifugation	1.91	344	11.3	904	0.96

Table 4.1. Comparison of [^{3}H]-EPI saturable binding in *M. persicae* homogenates determined by filtration or centrifugation giving K_d (nM), B_{max} (fmol/mg) and Hill (n_H) values. Values for filtration are mean ±S.E. of three separate experiments, but are n=1 for centrifugation.

Filtration gave K_d values of 0.9nM and 18.4nM and centrifugation gave values of 1.9 and 11.3nM for the high and low affinity site respectively. K_d values determined for the high affinity site were similar and those for the low affinity site not markedly different. The Hill values determined by filtration (0.81) and by centrifugation (0.96) were close to unity. The relative densities of high and low affinity [^{3}H]-EPI binding

sites varied considerably with the separation method used; filtration gave values of 87 and 373 fmol/mg while centrifugation gave values of 344 and 904 fmol/mg for high and low affinity sites respectively. B_{max} values are therefore seriously underestimated by filtration studies of [^{3}H]-EPI binding, due to considerable ligand wash off (75% and 59% for the high and low affinity sites respectively).

4.3.2 Kinetic analysis

[^{3}H]-EPI associates rapidly in a biphasic manner at 22°C (Figures 4.7 and 4.8) with rate constants of 5.11 and 0.14 min^{-1} for the fast and slow phases respectively. Dissociation was fast with completion in under 3 minutes (Figures 4.9 and 4.10). Determination of dissociation kinetics was not possible at room temperature and thus estimation of the k_{-1}/ k_{+1} (K_d) was not possible. The association data suggests either a two-stage sequential reaction or parallel reactions with different kinetic properties (Galper *et al.*, 1977).

4.3.3 Displacement studies

A concentration of 1nM [^{3}H]-EPI was used in displacement studies to study pharmacology at the high affinity site only. A number of cholinergic ligands were tested for their ability to displace [^{3}H]-EPI binding to R1 *M. persicae* membranes. The pharmacological profile (Table 4.2, Figure 4.11) demonstrates a nicotinic character and is broadly comparable to that determined previously with [^{3}H]-EPI in *P. americana* (Orr *et al*, 1997). In general, the [^{3}H]-EPI high affinity binding site in aphid membranes appears to be much more sensitive to all cholinergic ligands tested when compared to the binding sites of [^{3}H]-IMI, [^{125}I]-BgTx or [^{3}H]-MLA in *M. persicae* membranes (See Chapters 2, 3 and 5). IMI (K_i=0.5nM) was the most potent displacing ligand tested closely followed by (±)EPI (K_i=1.1nM), MLA (K_i=2.1nM) and α-BgTx (K_i=4.8nM). (-)Nicotine (K_i=27nM) displayed its highest potency at the [^{3}H]-EPI binding site compared to any other published K_i values in insects (Liu and Casida,

1993; Orr *et al.*, 1997). ACh (K_i=161nM) was the least potent ligand but still exhibited a high potency when compared to binding sites for the other ligands reported previously. Displacement by all ligands, including EPI, was characterised by low Hill values between 0.48 and 0.78.

Ligand	*M. persicae* K_i (nM)	Hill (n_H)	*P. americana*[a] K_i (nM)
IMI	0.5±0.8	0.68±0.07	4.7
(±)Epibatidine	1.1±1.9	0.78±0.02	N.D.
(-)Epibatidine	N.D.	N.D.	11.3
(+)Epibatidine	N.D.	N.D.	7.8
MLA	2.1±3.7	0.51±0.05	2.8
α-BgTx	4.8±8.3	0.48±0.05	N.D.
(-)Nicotine	27.3±47.2	0.64±0.07	591.7
ACh	161±280	0.51±0.09	N.D.

Table 4.2. Displacement of 1nM [^{3}H]-EPI from R1 *M. persicae* membranes using nicotinic ligands giving IC_{50} and Hill values with ±SEM Tabulated results are n=3. [a]Comparable data for *P. americana* (Orr *et al.*, 1997). ND = Not determined.

4.3.4 Binding of [^{3}H]-EPI to a panel of insects

There was only an insignificant amount of specific binding of [^{3}H]-EPI to membranes from the dipterans *D. melanogaster* and *L. sericata* (Figure 4.12). By contrast, specific binding of [^{3}H]-EPI was readily demonstrable in membranes of *M. persicae* and *P. americana*, the result for the cockroach agreeing with the study by Orr *et al.* (1997). Levels of specific binding detected in *H. virescens* were very low with total and non-specific cpm of 245±11 and 221±12 respectively. A more thorough investigation into [^{3}H]-EPI binding in both adult and larval *M. sexta* membranes revealed that there was no marked difference between total and non-specific binding determined by displacement with either α-BgTx or nicotine (Figures 4.13-4.14).

4.4 Discussion

Saturable binding of [^{3}H]-EPI was consistent with two binding components of differing affinity having K_d values of approximately 1nM for the high affinity site and between 10-20nM for the low affinity site. [^{3}H]-EPI specifically bound to aphid membranes with little evidence of ligand depletion during saturation experiments. However, [^{3}H]-EPI binding suffered from considerable wash-off during filtration assays giving inaccurate estimates of B_{max} for both low and high affinity sites, so that determination by centrifugation was necessary. This gave B_{max} values of 344 and 904 fmol/mg for high and low affinity sites respectively. Unfortunately it was not possible to perform multiple determinations of binding by centrifugation so that the values derived must be considered preliminary. Nevertheless, the estimated values provide a simple 1:3 ratio of high to low affinity sites, and furthermore when the B_{max} for low and high affinity sites are summed the total B_{max} value (1248 fmol/mg) is very similar to that determined previously in *M. persicae* membranes for [^{3}H]-IMI (Chapter 3), [^{125}I]-α-BgTx (Chapter 2) and [^{3}H]-MLA (Chapter 5).

The implications of these results are discussed in the overall conclusions in Chapter 7. The presence of multiple binding components for [^{3}H]-EPI in *M. persicae* differs from the apparent single binding site observed in *P. americana* (Orr *et al.*, 1997) which could reflect differences in the α and non-α subunit composition of the nAChR in these insects.

A kinetic analysis of [^{3}H]-EPI binding in *M. persicae* membranes revealed that this ligand has rapid association and dissociation kinetics. This may help to account for the high levels of ligand wash off experienced during filtration assays (<30 secs) owing to the rapid dissociation rate.

Hill values markedly less than 1 were determined for all displacement assays, suggesting either [^{3}H]-EPI binds with high affinity to more than one binding site at

which the displacing ligand has different affinities, or that there is allosteric interaction between at least 2 binding sites on the same nAChR. Isotopic dissociation studies with [^{3}H]-α-BgTx in aphid membranes (Chapter 2) indicate the presence of at least 2 binding sites per aphid nAChR which can interact allosterically with each other. The displacement of [^{3}H]-EPI by EPI with a Hill value of markedly less than 1 is of particular interest. A possible explanation for this phenomenon is that as concentrations of EPI increase then low affinity sites become occupied which interact allosterically with the high affinity site already occupied by [^{3}H]-EPI, leading to negative cooperativity effects between the two binding sites. A similar argument can be used to explain the behaviour of the other displacing ligands, especially α-BgTx and IMI both of which have been shown previously to occupy high and low affinity binding sites (see Chapters 2 and 3).

The displacement of [^{3}H]-EPI by α-BgTx from *P. americana* membranes (Orr *et al.*, 1997) is very different in potency from that determined in *M. persicae*, although both are characterised by a very low Hill value. There are pharmacological differences between [^{3}H]-EPI sensitive binding sites in aphids and cockroaches. In general the [^{3}H]-EPI binding site in *M. persicae* is more sensitive to α-BgTx and (-)nicotine when compared to that of *P. americana*, while IMI and MLA are equally potent in each insect homogenate.

The high potency displayed by (-)nicotine as a displacing ligand at the high affinity [^{3}H]-EPI binding site in aphid membranes (K_i=27nM) is of particular interest since in the naturally nicotine tolerant insect *M. sexta* no specific [^{3}H]-EPI binding sites could be detected. However it seems unlikely that the absence of [^{3}H]-EPI sites from *M. sexta* is related in a simple way to nicotine tolerance, since [^{3}H]-EPI binding sites were also absent from the nicotine sensitive insects *D. melanogaster* and *L. sericata*. The specific binding of [^{3}H]-(-)nicotine to membranes of the nicotine sensitive insect *Schistocerca gregaria* was investigated by MacAllan *et al.* (1988), who found that this ligand bound with a low affinity K_d of 130nM but the density of sites was high with a

B_{max} of 4055 fmol/mg. Since (-)nicotine binds specifically to sites in rat brain with very high affinity (K_d=9nM) (as reported in the same study by MacAllan *et al.,* 1988) it must be questioned whether high affinity binding sites for (-)nicotine exist in *S. gregaria* or any other insect.

It is possible that our inability to detect specific binding of [^{3}H]-EPI to membranes from dipteran or lepidopteran insects may be due not to the actual lack of a high affinity [^{3}H]-EPI binding site, but to inappropriate methodology. A likely candidate here is the washing regime which was 5 cycles on the cell harvester and a volume of 16ml incubation buffer on the vacuum manifold. As shown by the *M. persicae* saturation data, a high proportion of specially bound [^{3}H]-EPI is lost during washing. If the K_d values for the dipteran and/or lepidopteran [^{3}H]-EPI binding sites were lower than in *M. persicae,* then the extent of this wash off would have been even greater. Therefore the presence of a high affinity [^{3}H]-EPI binding site in these insects can not yet be ruled out. A further possibility is that if in the lepidopertan and dipteran insects the affinity of the [^{3}H]-EPI binding site were lower than in aphid and cockroach, the concentrations of [^{3}H]-EPI investigated may have been insufficient to reveal the specific binding. Finally there is evidence from displacement studies between [^{3}H]-IMI and EPI that the affinity of *M. domestica* membranes for EPI is reduced compared to that of aphids (Chapter 3).

In summary, saturation studies in aphid membranes indicate the presence of at least 2 binding components for [^{3}H]-EPI and displacement assays display a pharmacology demonstrating sensitivity to IMI, MLA, α-BgTx and (-)nicotine. Specific binding of [^{3}H]-EPI was detected at high levels only in aphid and cockroach of those insects investigated. This could mean that [^{3}H]-EPI binding sites are present only in some insects. Alternatively, the methods used to detect specific binding may have been inadequate. It is at least certain, however, that if specific [^{3}H]-EPI binding sites exist in lepidopteran and dipteran insects, their characteristics are different from those in aphid and cockroach.

Figures 4.1-4.6. Saturation isotherm (**Figure 4.1**), Scatchard (**Figure 4.2**) and Hill plot (**Figure 4.3**) of [^{3}H]-EPI binding in R1 *M. persicae* homogenates determined by filtration. Symbols denote total binding(◆), specific binding (●), and non-specific binding (▲). Membranes were incubated for 3 hours with a range of [^{3}H]-IMI concentrations (0.05-30m) and bound and free radioligand separated using vacuum filtration with a cell harvester. A concentration of 1μM unlabelled MLA was used to determine non-specific binding. Saturable binding determined by centrifugation is depicted in **Figures 4.4, 4.5** and **4.6** showing the saturation isotherm, Scatchard and Hill plot respectively. Filtration data underestimates specific binding, as indicated by the lower levels of bound [^{3}H]-EPI determined using this method. Both filtration and centrifugation methods clearly indicate multiple binding components, as is evident from the non-linear Scatchard plots. Lines in the figures are filled for a two-site model, as discussed in the Results section. Data shown for filtration are the mean±SEM of three separate experiments and for centrifugation data is n=1.

Figure 4.1

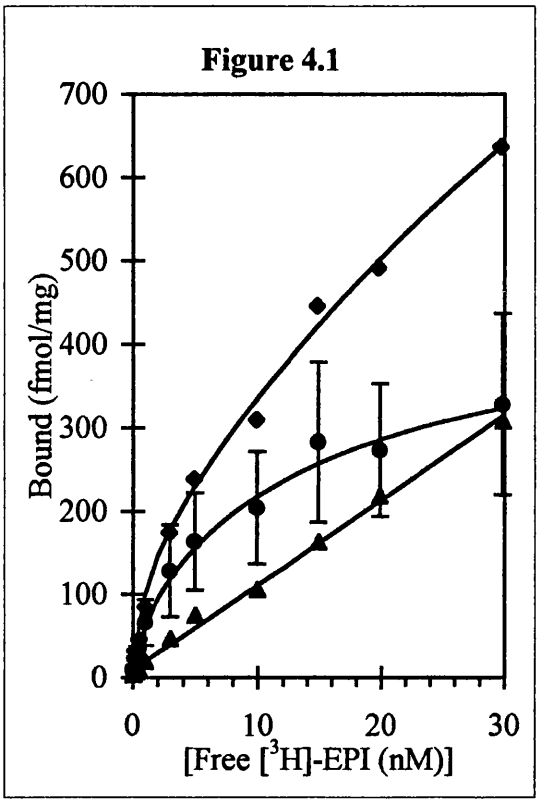

Figure 4.2

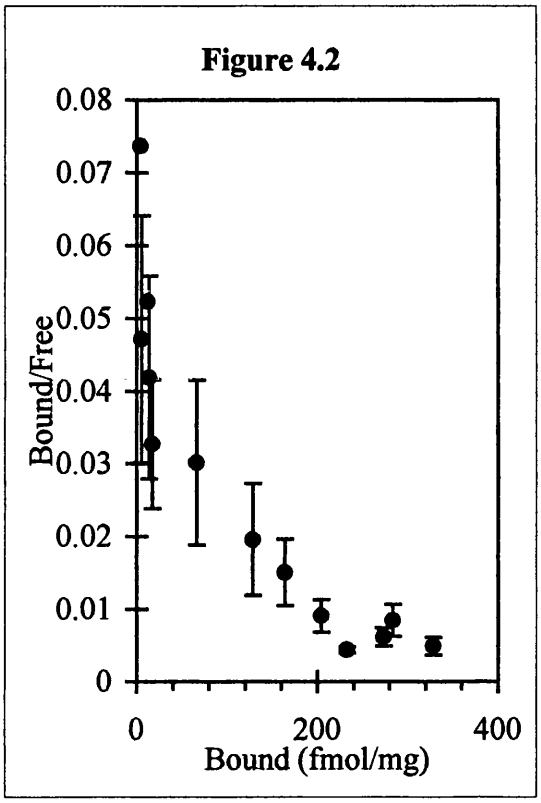

Figure 4.3

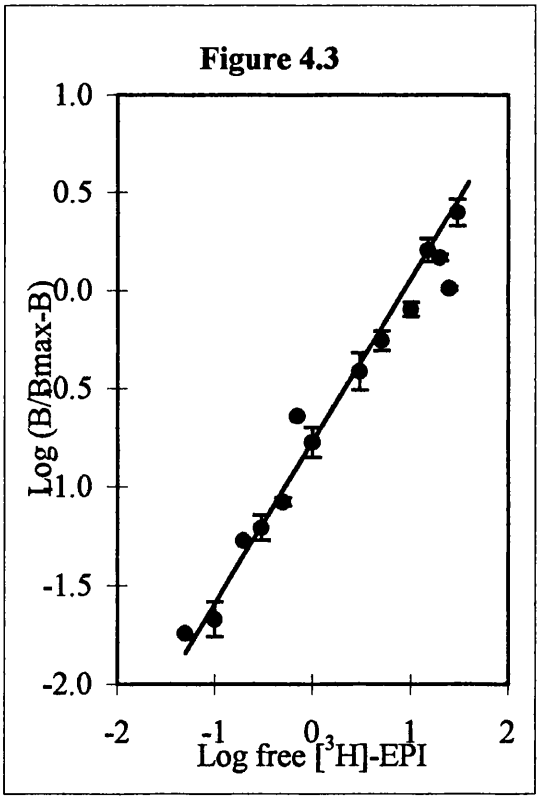

Figure 4.4

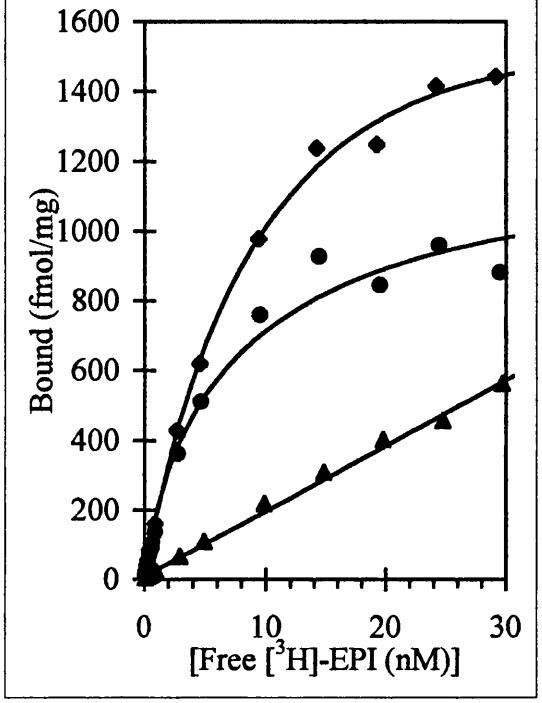

Figure 4.5

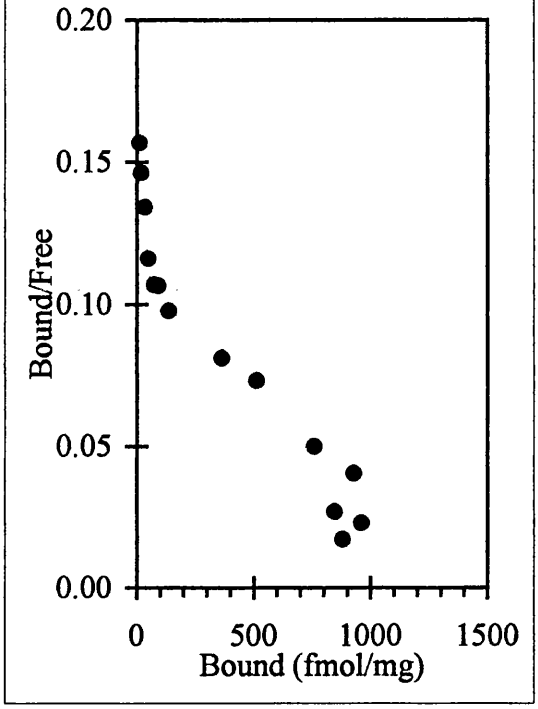

Figure 4.6

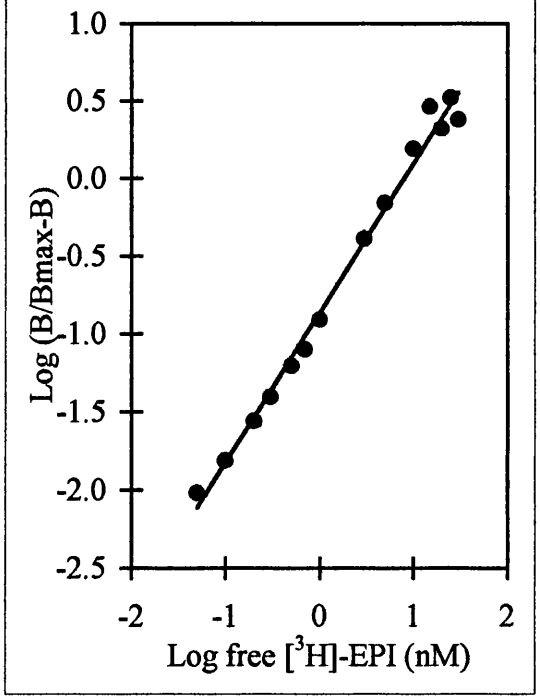

Figure 4.7-4.10. Kinetic data of [^{3}H]-EPI binding in *M. persicae* membranes. **Figure 4.7** Association of [^{3}H]-EPI to *M. persicae* membranes at 22°C demonstrates a biphasic character, **Figure 4.8** shows the linear transform. Membranes were incubated with 1nM [^{3}H]-EPI at room temperature before bound ligand was harvested by filtration using a cell harvester. Data are from a single experiment and are fitted to a two-site model. **Figure 4.9** Isotopic dissociation initiated by 1μM MLA of [^{3}H]-EPI to aphid membranes at 22°C, **Figure 4.10** shows the linear transform. The dissociation is very rapid and complete by 3 minutes. Data are from a single experiment.

Figure 4.7

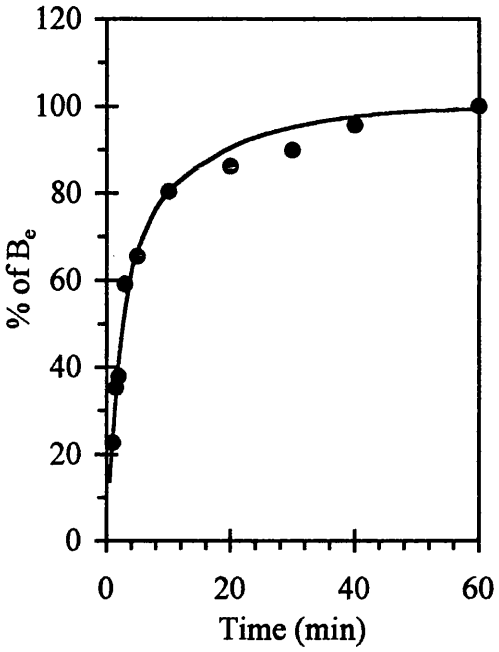

Figure 4.8

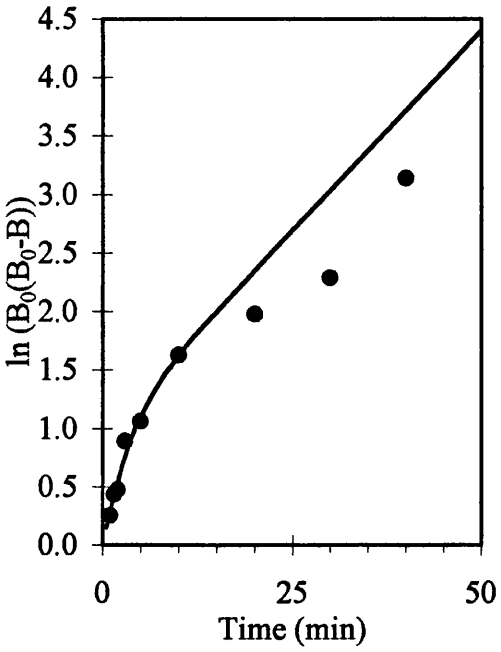

Figure 4.9

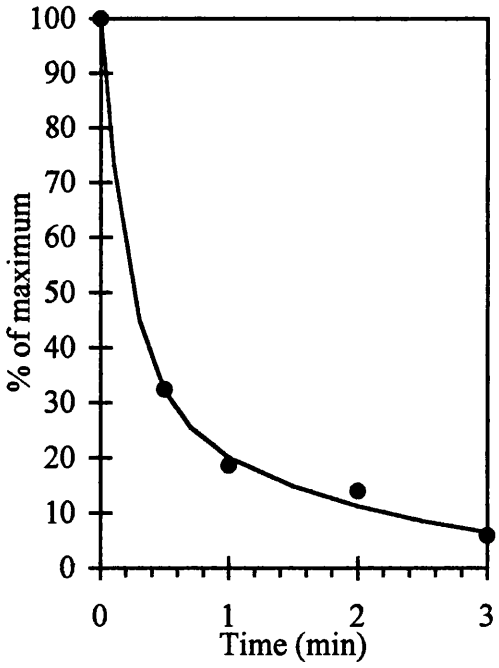

Figure 4.10

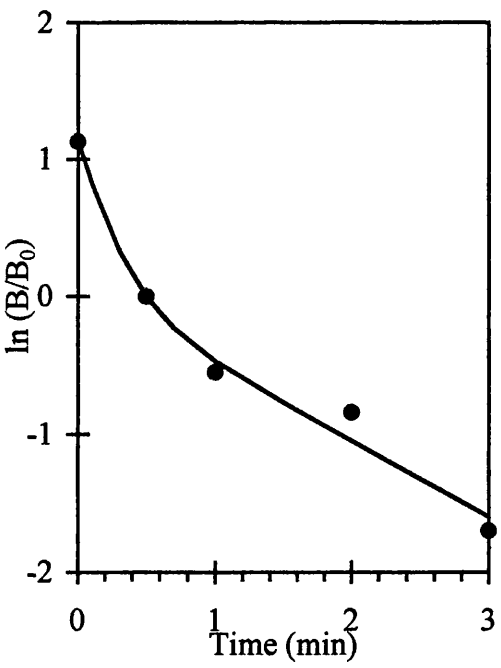

Figure 4.11. Displacement of [^{3}H]-EPI by the agonists IMI (◆), (±)epibatidine (Δ), (-)nicotine (◆) and ACh (■) and the antagoinists α-BgTx (□) and MLA (×) in *M. persicae* membranes. Data are the mean of three separate experiments performed in triplicate. Unlabelled ligands were preincubated with membranes for 30 minutes before the addition of 1nM [^{3}H]-IMI for 2 hours. Bound and free radioligand were separated using a cell harvester. Non-specific binding was determined with a final concentration of 1μM MLA.

Figure 4.11

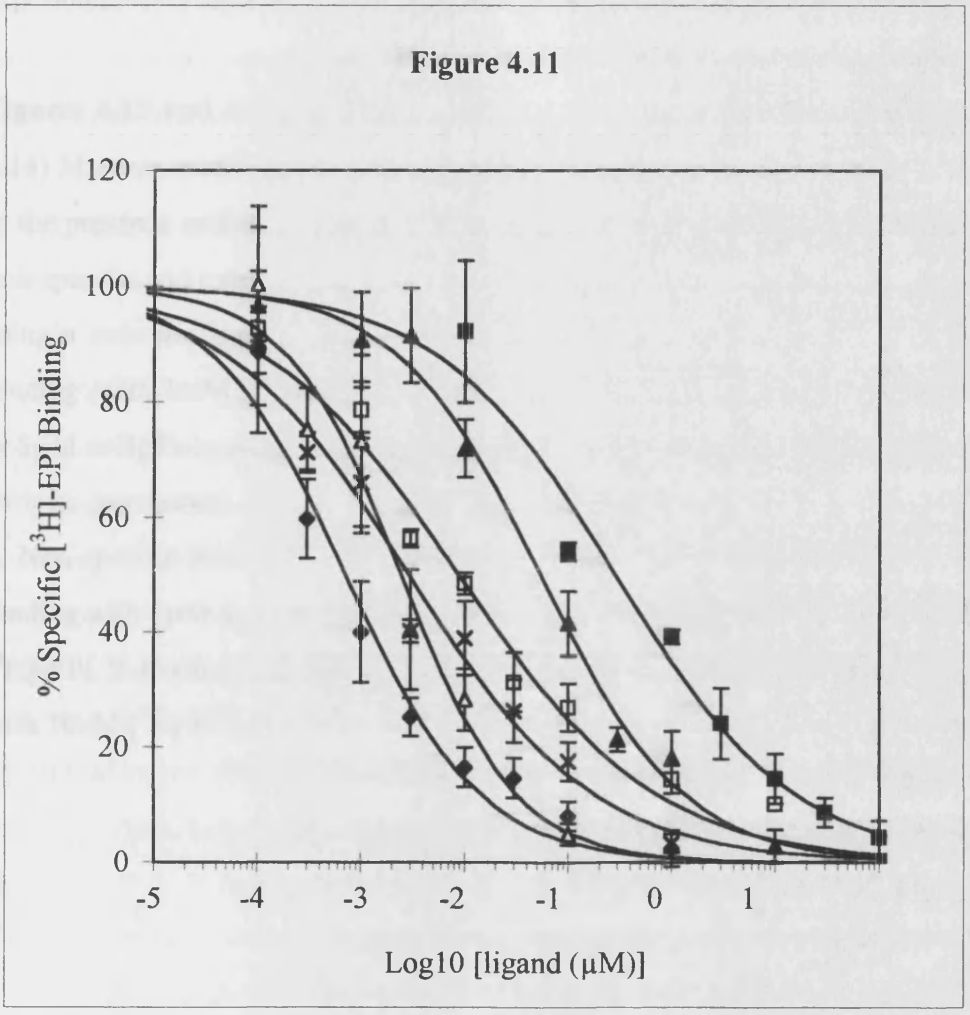
120
100
80
60
40
20
0
% Specific [3H]-EPI Binding
-5
-4
-3
-2
-1
0
1
Log10 [ligand (μM)]

Figures 4.12. Specific [^{3}H]-EPI binding to membranes from a panel of insects. Membranes were incubated with 1nM [^{3}H]-EPI for 2 hours in the presence and absence of 1µM EPI to determine non-specific and total binding respectively. Bound and free radioligand were separated using a cell harvester. Data are from a single experiment with triplicate determinations for total and non-specific binding.

Figures 4.13 and 4.14. [^{3}H]-EPI binding to adult (**Figure 4.13**) and larval (**Figure 4.14**) *M. sexta* membranes. Membranes were incubated with 1nM [^{3}H]-EPI for 2 hours in the presence and absence of either an excess of (-)nicotine or α-BgTx to determine non-specific and total binding respectively. Bound and free radioligand were separated using a vacuum filtration manifold with GF/C filters. **Treatments: 1.** Non-specific binding with 1mM (-)nicotine and 1nM [^{3}H]-EPI. **2.** Non-specific binding with 1µM or 5µM α-BgTx in adult and larval *M. sexta* respectively and 1nM [^{3}H]-EPI. **3.** Control with no membranes present with 1nM [^{3}H]-EPI. **4.** Total binding with 1nM [^{3}H]-EPI. **5.** Non-specific binding with 1mM (-)nicotine and 10nM [^{3}H]-EPI. **6.** Non-specific binding with 1µM or 5µM α-BgTx in adult and larval *M. sexta* respectively and 10nM [^{3}H]-EPI. **7.** Control with no membranes present with 10nM [^{3}H]-EPI. **8.** Total binding with 10nM [^{3}H]-EPI. Bars are the range of 2 independent experiments.

Figure 4.12

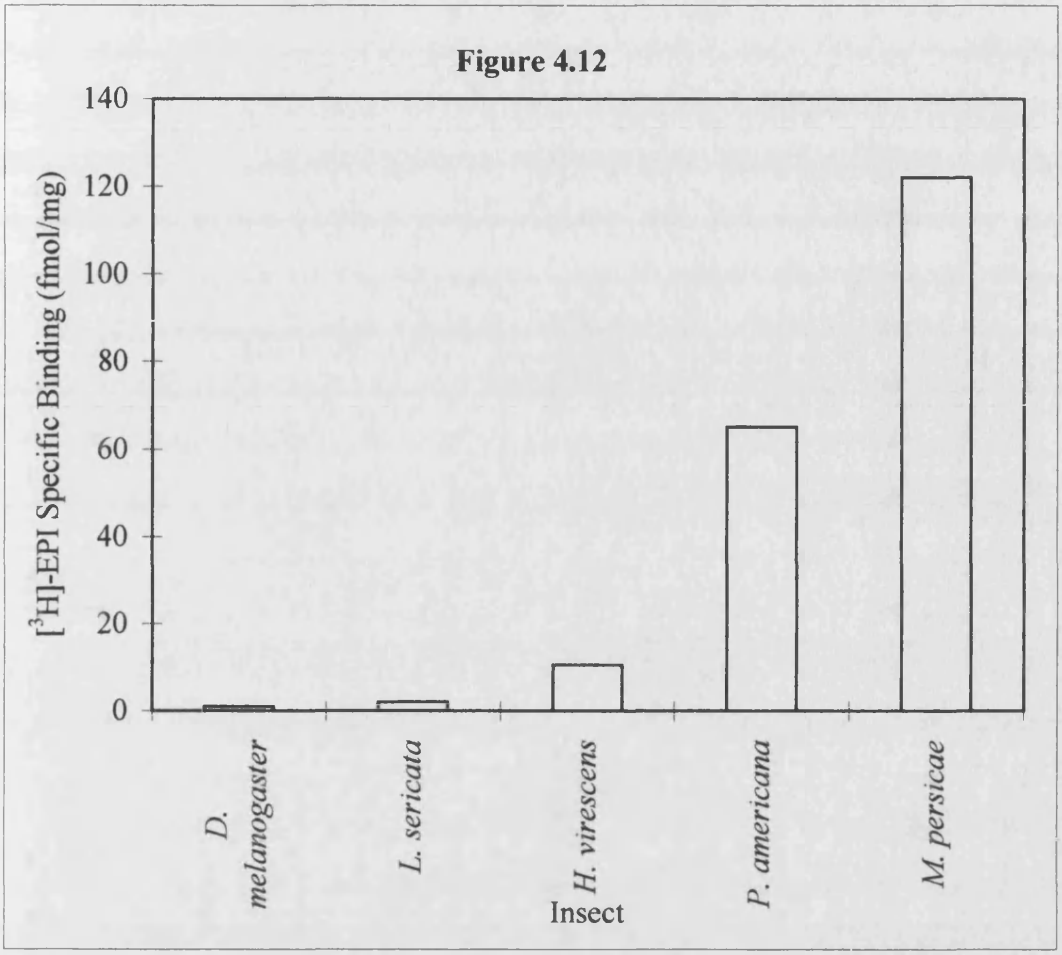

Figure 4.13

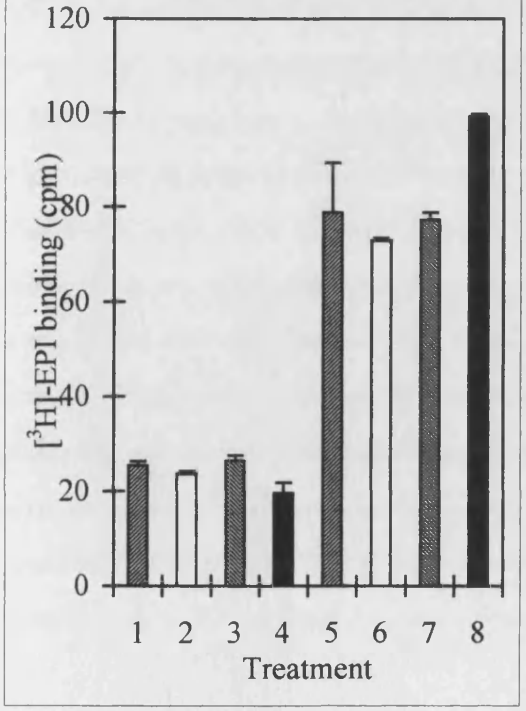

Figure 4.14

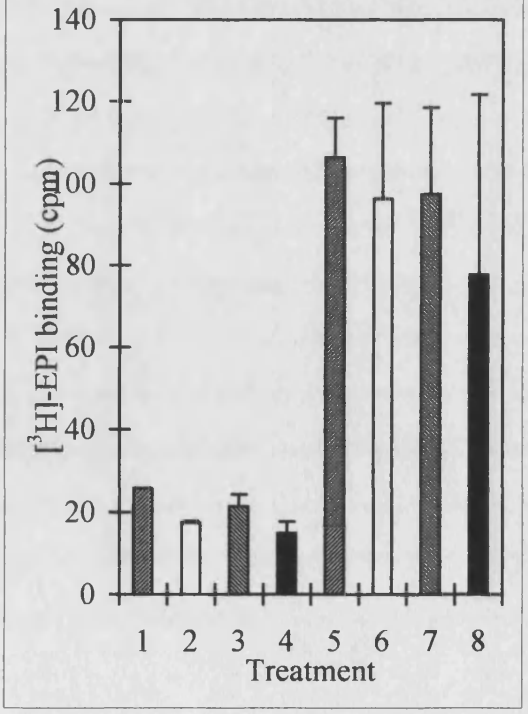

Chapter 5
[^{3}H]-Methyllycaconitine radioligand binding

This chapter is a slightly modified version of a paper submitted for publication to the Journal of Insect Biochemistry and Molecular Biology: Robert J. Lind, David J. Hardick, Ian S. Blagbrough, Barry V.L. Potter, Adrian J. Wolstenholme, Andrew R. L. Davies, Martin S. Clough, Fergus G. P. Earley, Stuart E. Reynolds and Susan Wonnacott. [^{3}H]-Methyllycaconitine: a novel high affinity ligand for invertebrate nicotinic acetylcholine receptors.

5.1 Introduction

Methyllycaconitine (MLA) is a norditerpenoid alkaloid isolated from species of *Delphinium* (larkspurs) and has neurotoxic effects in both vertebrates and invertebrates (Nambi-Aiyar *et al.,* 1979; Jennings *et al.,* 1986). MLA exerts its neurotoxic effects as a nicotinic antagonist, and displays high selectivity for vertebrate neuronal α7-type nAChR over α3- or α4-containing neuronal nAChR or muscle nAChR (Ward *et al.,* 1990; Wonnacott *et al.,* 1993; Yum *et al.,* 1996). Thus in vertebrates MLA is more discriminating than α-BgTx.

MLA is a potent competitor of [^{125}I]-α-BgTx binding to invertebrate preparations and a potent nicotinic antagonist in electrophysiology studies utilising invertebrate tissues, such as the head of the fly *Musca domestica* (Jennings *et al.*, 1986), the ganglia of the locust *Schistocerca gregaria* (MacAllan *et al.,* 1988), the nerve cord and brain of the cockroach *P. americana* (Sattelle *et al.,* 1989b; Orr *et al.,* 1990), the brain of *M. sexta* and the aphid *M. persicae* (See Chapter 2). The potency of MLA for insect nAChR recommends it as a potential radioligand and the methodology to pursue this has been recently developed (Hardick *et al.,* 1997; Davies *et al.,* 1999). The binding properties of [^{3}H]-MLA have been described in whole rat brain membrane preparations, in which

it displays a single high affinity binding site with a K_d of approximately 1nM (Davies *et al.*, 1999).

In this chapter the successful exploitation of [^{3}H]-MLA in radioligand binding assays and autoradiographic studies of the localisation of its binding sites in invertebrates is reported.

5.2 Materials and Methods

5.2.1 Chemicals

[^{3}H]-MLA (~50 Ci/mmol) was synthesised in collaboration with Tocris Cookson Ltd. (Bristol, UK). This was prepared essentially as described for the production of deuterated methylsuccinic acid by Hardick *et al.* (1996) and fully characterised (Blagbrough *et al.*, 1994; Coates *et al.*, 1995). [^{125}I]-Na was obtained from Amersham International, Cardiff, UK and was used to iodinate α-BgTx to a specific activity of 750 Ci/mmol. Sources for other compounds were as follows: acetylcholine chloride (ACh), neostigmine bromide, and (-)nicotine from Sigma-Aldrich chemicals Ltd (Poole, Dorset, UK). α-Bungarotoxin (α-BgTx), (±)EPI, and methyllycaconitine (MLA) from RBI (now Sigma-Aldrich Ltd). Imidacloprid of technical purity was synthesised by Zeneca Agrochemicals.

5.2.2 Invertebrate rearing and collecting

Peach potato aphids *Myzus persicae* (strain USIL, originating from Rothamsted Experimental Station), tobacco budworms *Heliothis virescens*, tobacco hornworms *M. sexta*, and sheep blowflies *Lucilia sericata* were reared and harvested as previously described (see Chapter 3). Optic lobes of squid *Loligo vulgaris* were obtained from the Marine Biological Association of the UK, Plymouth. The squid, approximately 2 feet in length, were caught in the English Channel during winter and optic lobes were removed and stored at -80°C in liquid nitrogen until required.

5.2.3 Membrane preparation and [^{3}H]-MLA binding

Membranes were prepared from whole *M. persicae*, heads of *H. virescens* and *L. sericata*, brains of *M. sexta* and optic lobes of *L. vulgaris*. Membrane preparation was the same for all invertebrates. Material was homogenised in an isolation buffer

containing 0.32M sucrose, 100µM EDTA, 1µM leupeptin, 1µM pepstatin, and 200µM PMSF (pH 7.2). The homogenate was centrifuged at 1,000g for 30 min and the resulting supernatant fraction re-centrifuged at 30,000g for 60 min. The pellet was reconstituted in incubation buffer containing 0.05M Tris, 0.12M NaCl, and 100µM EDTA (pH 7.4). The protein concentration was determined using the method of Bradford (1976) with bovine serum albumin (BSA) as a standard.

[^{3}H]-MLA binding was assayed by incubating membranes in a final volume of 200µl incubation buffer containing, additionally, 0.25% BSA in a 96 well microtitre plate. Amounts of membrane preparations used were 100µg, 100µg, 25µg, 200µg and 25µg for *M.* persicae, *H. virescens, M. sexta, L. sericata* and *L. vulgaris* respectively. [^{3}H]-MLA at the appropriate concentration was added and incubation at room temperature (22°C) on a plate shaker was for either 120 min for displacement or 180 min for association and saturation studies. Bound [^{3}H]-MLA was quantified by filtration using a Tomtec Mach 2 cell harvester employing Wallac thin filter mats pre-soaked in 0.3% polyethyleneimine, using a 2 wash cycle of ice cold incubation buffer (+0.25% BSA). Solid scintillant (Meltalex A, Wallac) was melted onto filter mats, which were counted at 34% efficiency in a Wallac beta plate counter. Non-specific binding was determined using a final concentration of 1µM unlabelled MLA.

Specific binding at a saturating concentration of 30nM [^{3}H]-MLA was also determined using a centrifugation assay, to ascertain if bound [^{3}H]-MLA was washed off during filtration assays. In centrifugation assays, samples were incubated in 1.5ml microcentrifuge tubes for 180 min and the tubes were then centrifuged at 30,000g for 5 min in a Beckman bench top ultrafuge in order to terminate incubation. The supernatant fraction was removed, and the pellet rinsed three times with 1ml distilled water. Pellets were then dissolved overnight in 10% sodium deoxycholic acid and the redissolved pellet (0.5ml) was transferred into 4.5ml of liquid scintillant (Optiphase safe) and counted at 43% efficiency.

5.2.4 Kinetic analysis

A concentration of 500pM [^{3}H]-MLA was used to investigate association and dissociation rate kinetics in *M. persicae* membranes at room temperature (22°C). Association rates were determined for time periods from 0.5 to 180 min and terminated by filtration. To investigate the kinetics of dissociation, membranes were allowed to associate with [^{3}H]-MLA for 3 hours before isotopic dissociation was initiated by the addition of 1μM MLA. Residual bound radioligand was determined between 0.5 and 60 min, in the presence and absence of 1μM MLA for non-specific and total binding respectively.

5.2.5 Displacement Studies

Ligands employed for displacement studies were added to *M. persicae* membranes 30 min prior to the addition of 500pM [^{3}H]-MLA. Competing ligands were assayed in a dilution series of 1, 3, 10, 30, 100, 300, etc. series with at least 6 concentrations in triplicate focused around the IC_{50} point. In the case of ACh, 10μM neostigmine bromide (final concentration) was added to aphid membranes 30 min before the addition of ACh in order to inhibit acetylcholinesterase. Neostigmine was separately determined not to affect [^{3}H]-MLA binding in *M. persicae* - data not shown.

5.2.6 Autoradiography

The localisation of [^{3}H]-MLA and [^{125}I]-α-BgTx binding sites in the brain of the tobacco hornworm *Manduca sexta* was determined. This lepidopteran offered an advantage over the other insects used for the radioligand binding study afforded by its large size.

Pharate adult *M. sexta* were decapitated and the proboscis and antennae removed from the head which was frozen in OCT compound. Serial sections (20μm) were cut with a

cryomicrotome and mounted on subbed glass slides (Boyd, 1955) and kept frozen at -80°C until required. Sections were air dried for 5 min at room temperature before the addition of either 1nM [^{3}H]-MLA or 1nM [^{125}I]-α-BgTx in incubation buffer and incubated in a humidified chamber on a plate shaker for 1 hour. Non-specific binding was determined with the addition of 1μM unlabelled MLA for both [^{3}H]-MLA and [^{125}I]-α-BgTx. Unbound toxin was removed with 3 changes of incubation buffer for 1 min each. Sections were post fixed for 30 min at 4°C in 2% glutaraldehyde in sodium 0.1 M-phosphate buffer (pH 7.4). Slides were then washed with 3 changes of distilled water and coated with Ilford K.5 nuclear research emulsion. The latter was prepared by adding the gel to 6ml distilled water and 30μl of 50% gycerol to make up a volume of 10ml at 43°C. Slides were stored at room temperature with silica gel and exposed for 10 days and 6 months for [^{125}I]-α-BgTx and [^{3}H]-MLA respectively. Slide development used standard photographic techniques with Kodak D-19 developer and fixer. Sections treated with [^{125}I]-α-BgTx were stained with 0.1% toluidine blue in distilled water for 5 min. Sections were dehydrated (2 min steps) in the ethanol series 70%, 90%, 100%, 100% and then 2 changes of xylene after which they were mounted in Permount (Guss).

5.2.7 Data Analysis

Non-linear regression analysis with Microsoft Excel's solver macro (Bowen and Jerman, 1995) was used to determine the dissociation constant (K_d) and maximal binding capacity (B_{max}) from hyperbolic plots of saturation isotherm data (Hulme and Birdsall, 1992). K_i values were determined using the Cheng and Prusoff relationship assuming a K_d value of 0.95nM for [^{3}H]-MLA. Non-linear regression analysis was also used with displacement data to determine the IC_{50} and Hill coefficient using the Hill equation. Multiple displacement was curve fitted additively. Ligand depletion was corrected for in the analysis of saturation data by assuming that the free [^{3}H]-MLA concentration was equal to the total minus bound concentration.

5.3 Results

[^{3}H]-MLA binding was examined in membrane preparations of whole *M. persicae,* heads of *H. virescens* and *L. sericata*, brains of *M. sexta* and in optic lobes of *L. vulgaris*. [^{3}H]-MLA bound specifically, with exceptionally low non-specific binding (<5% of total), to each of these invertebrate membrane preparations.

5.3.1 Saturation binding experiments

[^{3}H]-MLA binding to *M. persicae* membranes, determined by filtration is shown in Figures 5.1-5.3. At lower concentrations of [^{3}H]-MLA (<1nM) significant ligand depletion of up to 40% occurred, and this was corrected for as indicated in Materials and Methods. The results are consistent with a single binding component having a K_d=0.95±0.17nM and B_{max}=1290±131fmol/mg protein (n=3). The Hill value (n_H) was 1.06±0.03. There was no difference between specific binding of [^{3}H]-MLA (30nM) to *M. persicae* membranes determined using either filtration or centrifugation methods with counts of 20455 and 21300 dpm respectively. Therefore the B_{max} values derived from filtration assays are considered to be valid.

[^{3}H]-MLA binding to the other invertebrate preparations examined for comparison (Table 5.1, Figures 5.4-5.11) was also consistent with a single class of binding site with K_d values of 0.46nM, 0.81nM, and 2.1nM and B_{max} values of 1689, 749 and 1008 fmol/mg protein for *M. sexta*, *H. virescens* and *L. sericata* respectively. The cephalopod *L. vulgaris* also showed a single high affinity binding site (K_d=6nM), but the B_{max} value (14,111 fmol/mg protein) was over an order of magnitude higher than that determined for the insect preparations. The density of [^{3}H]-MLA binding sites in rat brain (30 fmol/mg protein) is much lower than in any of the invertebrates examined; again saturable binding conformed to a single site (Table 5.1; Davies *et al.*, 1999).

Species	K_d (nM)	n=	B_{max} (fmol/mg protein)	Hill (n_H)
M. persicae	0.95±0.17	4	1,290±131	1.06±0.03
*H. virescens**	0.81		749	0.95
M. sexta[+]	0.46		1,689	1.01
*L. sericata**	2.10		1,008	1.12
L. vulgaris[+]	5.99		14,111	1.06
Rat[+†]	0.85±0.14	3	30±4	0.99

Table 5.1. Comparison of [^{3}H]-MLA binding to a panel of organisms.

*Heads only

[+]Brain only.

[†]Data from Davies *et al.* (1999).

5.3.2 Kinetic analysis

[^{3}H]-MLA binding to *M. persicae* membranes exhibited fast, biphasic association kinetics with k_{+1} values of 0.93±0.07 ($t_{½}$=1.5±0.1 min) and 0.0257±0.0003 nM/min ($t_{½}$=36.3±0.9 min) for the fast and slow phases respectively (n=3) (Figures 5.12 and 5.13). In contrast, the dissociation of [^{3}H]-MLA (determined over 60 min) was very slow and apparently monophasic with a k_{-1} of 0.0063±0.0001 min^{-1} ($t_{½}$=110±1.7min) when using the fast association constant. This rate is comparable to the rate of dissociation of α-BgTx from *M. persicae* membranes (See Chapter 2). The K_d value estimated from the rate constants is 0.25nM, which is in good agreement with that derived from equilibrium binding experiments.

5.3.3 Displacement studies

A number of cholinergic ligands were tested for their ability to displace [^{3}H]-MLA binding to *M. persicae* membranes. The pharmacological profile (Table 5.2, Figure 5.14) demonstrates the nicotinic character of [^{3}H]-MLA binding sites. MLA itself was the most potent displacing ligand with an K_i value of 0.6nM. While displacement by unlabelled MLA was characterised by a Hill value (1.15) close to 1, the displacement curves of all the other displacing ligands were characterised by Hill values markedly

less than 1 with a single site model (0.51 to 0.74) (Table 5.2). This suggested that displacement was complex and on further analysis data fitted more closely to a two site model with high and low affinity components for α-BgTx, IMI, EPI, (-)nicotine and ACh (Table 5.2).

	Single Site Fit		Double Site Fit	
Ligand	K_i (nM)	Hill (n_H)	K_i (nM) (i)	K_i (nM) (ii)
MLA	0.6±0.1	1.15±0.11	-	-
IMI	230±103	0.51±0.05	0.31±0.08	419±188
(±)EPI	420±135	0.74±0.15	3.2±1.8	704±60
α-BgTx	599±258	0.69±0.01	5.7±3.1	1,101±472
(-)Nicotine	3,850±1484	0.72±0.15	607±432	11,351±4015
ACh	179,300±151300	0.66±0.17	131,910±130761	1057,426±997407

Table 5.2. Displacement of 500pM [^{3}H]-MLA from *M. persicae* membranes using nicotinic ligands. Data are fitted to a single site model providing K_i and Hill values but are better described by a two site fit giving K_i values for high (i) and low (ii) affinity components. Results are mean±SEM of n=3.

5.3.4 Autoradiography

The distributions of [^{3}H]-MLA and [^{125}I]-α-BgTx binding sites were compared in the brain of *M. sexta*: this lepidopteran was chosen for autoradiography because of the large size and well studied anatomy of its brain, compared with the other insects examined in the binding assays. Autoradiography of tissue slices labelled with either [^{3}H]-MLA and [^{125}I]-α-BgTx showed a highly localised pattern of reduced silver grains in the brain of *M. sexta*. The pattern of labelling with both ligands was very similar (Figure 5.15): binding is evident in neuropil areas of the brain, and is particularly concentrated in the medulla and lobula of the optic lobe, in addition to the corpora pedunculata (mushroom bodies) located in the protocerebrum. Binding of both toxins in the optic lobes was particularly striking in the medulla and lobula. If specific binding was present in the lamina of the optic lobe, then this was masked by non-specific binding for both toxins. Specific [^{125}I]-α-BgTx binding was also present in an

area located external to the lamina and adjacent to the tapetum, a reflective tracheal structure at the base of the retina; a high level of non-specific binding made it difficult to detect specific [^{3}H]-MLA binding in this brain region.

5.4 Discussion

In all the invertebrates investigated, [^{3}H]-MLA labelled a population of high affinity binding sites that is well described by a single binding component. This binding of [^{3}H]-MLA was characterised by a very low level of non-specific binding. K_d values in the range of 0.5-2nM and B_{max} values of approximately 1000 fmol/mg protein were determined for four species of insects (*M. persicae, H. virescens, M. sexta* and *L. sericata*) from three different Orders. Binding of [^{3}H]-MLA in the optic lobes of the cephalopod *L. vulgaris* was slightly less avid (K_d=6nM) but the B_{max} value (14,111 fmol/mg) was markedly higher than in the insects (Table 5.1).

The density of [^{3}H]-MLA binding sites in all of the invertebrates examined was particularly high. Because this study used a variety of starting materials for membrane preparations, ranging from whole bodies to distinct brain regions depending on the size of the organism, the B_{max} values are not directly comparable. Those determined from whole bodies (*M. persicae*) are likely to considerably underestimate the density in neural tissue. Nevertheless, it is clear that invertebrates are much richer sources of [^{3}H]-MLA binding sites than are vertebrates. In rat brain (Davies *et al.,* 1999) the K_d for [^{3}H]-MLA binding is similar to that determined in the invertebrates, but the B_{max} value is 1-2 and 3 orders of magnitude smaller compared to insects and the cephalopod respectively.

The relatively fast association kinetics coupled with very slow dissociation make [^{3}H]-MLA a particularly good radioligand for labelling invertebrate nAChR. While the slow rate of dissociation of [^{3}H]-MLA resembles that of α-BgTx (Schmidt-Neilsen *et al.*, 1977), [^{3}H]-MLA associates with the invertebrate receptor much more rapidly than α-BgTx, enabling equilibrium to be achieved in a conventional incubation period. These properties confer a significant advantage for [^{3}H]-MLA over radiolabelled α-BgTx and other radioligands for the accurate determination of B_{max} values. This was confirmed

by the excellent correspondence between values derived by filtration and centrifugation methods, and the agreement of K_d values from saturation and kinetic analyses.

The kinetics of binding also make [^{3}H]-MLA a very suitable ligand for autoradiography and studies in *M. sexta* demonstrate that [^{3}H]-MLA binds specifically to many neuropil containing regions of this insect's brain and has a similar distribution to that of [^{125}I]-α-BgTx. The distribution of [^{125}I]-α-BgTx (Figure 5.15) is in good agreement with a previous report (Hildebrand *et al.*, 1979). The comparable distributions of [^{125}I]-α-BgTx and [^{3}H]-MLA are compatible with both ligands labelling the same nAChR or, alternatively, the ligands labelling distinct sites that share similar distributions. The greatest concentration of binding sites occurs for both toxins at the leading edge of the medulla in the optic lobes, with additional optic lobe sites in the lobula (Figure 5.15). The protocerebrum also contain highly localised sites for both toxins in the corpora pedunculata (mushroom bodies) as previously noted for α-BgTx by Hildebrand *et al.* (1979). This distribution of [^{3}H]-MLA and [^{125}I]-α-BgTx binding sites is consistent with a particular role for nAChR in sensory processing. This is agreement with recent work by Goldberg *et al.* (1999) demonstrating the expression of functional nAChR in mushroom body Kenyon cells isolated from the honey bee *Apis mellifera*. Autoradiographic analysis of [^{125}I]-α-BgTx and [^{3}H]-MLA binding sites in mouse brain has also shown them to share a homologous distribution (Whiteaker *et al.*, 1999).

Specific binding of [^{125}I]-α-BgTx in a region located in a non-neuronal area close to the tapetum suggests that insect nAChR may be involved in cellular activities other than neurotransmission. This observation is consistent with that by Hermsen *et al.* (1998) demonstrating that expression of putative α subunits of nAChR in the migratory locust *L. migratoria*, occurs in the retina of the compound eyes. Participation of nAChR in roles other than neurotransmission have been proposed in vertebrates (Grando *et al.*, 1995).

Displacement studies in *M. persicae* showed that, with the exception of MLA, the tested ligands best fitted a biphasic displacement with high and low affinity components. This pharmacological profile is unlike that determined previously for [^{3}H]-IMI binding in *M. persicae* (Chapter 3), *M. domestica* (Lui and Casida, 1993), or whitefly *Bemisia tabaci* (Chao *et al.*, 1997). It also differs from that of [^{125}I]-α-BgTx in *M. sexta* (Chapter 2), *M. persicae* (Chapter 2) or *A. mellifera* (Tomizawa *et al.*, 1995a), and is distinct from that determined for [^{3}H]-EPI in *P. americana* (Orr *et al.*, 1997) or *M. persicae* (Chapter 4). Thus the high affinity binding site labelled in *M. persicae* by [^{3}H]-MLA has a unique pharmacological profile distinct from that of any previously investigated radioligand.

This study of saturable [^{3}H]-MLA binding complements the previous examinations of [^{125}I]-α-BgTx, [^{3}H]-IMI and [^{3}H]-EPI in Chapters 2 to 4 to *M. persicae* membranes, allowing some comparisons to be drawn (Table 5.3).

Ligand	High affinity K_d (nM)	High affinity B_{max} (fmol/mg)	Low affinity K_d (nM)	Low affinity B_{max} (fmol/mg)	Summed B_{max} values
[^{3}H]-MLA	0.95	1290			1290
[^{125}I]-α-BgTx[1]	1.18	167	33.7	640	807
[^{3}H]-IMI[2]	0.14	284	12.6	883	1167
[^{3}H]-EPI[3]	0.89	344	18.4	904	1248

Table 5.3. Comparison of saturable binding of [^{3}H]-MLA, [^{125}I]-α-BgTx, [^{3}H]-IMI and [^{3}H]-EPI in *M. persicae* membranes providing K_d and B_{max} values taken from Chapters 2, 3, and 4 respectively.

In general, each of these ligands appears to interact with a similar number of binding sites, if both high and low affinity binding components are taken into consideration. They differ, however, in that [^{3}H]-MLA binding appears to be well described by binding to a single high affinity site, whereas the other three nicotinic radioligands appear to differentiate between high and low affinity components. The total number of high plus low affinity binding sites is remarkably similar for [^{3}H]-MLA, [^{3}H]-IMI and

[^{3}H]-EPI. We speculate that the slightly lower B_{max} value for [^{125}I]-α-BgTx may be an underestimate due to this ligand's very slow association kinetics. The most economic hypothesis to explain these results is that [^{3}H]-MLA is able to interact with equal affinity with all of the sites labelled by the other radioligands.

In support of this view, displacement of [^{3}H]-MLA by α-BgTx, IMI, EPI, (-)nicotine and ACh was characterised in each case by low Hill values when fitted to a single site, and displacement data for all these ligands were better described by a biphasic displacement model consistent with high and low affinity components. α-BgTx, IMI, and EPI were each able to displace 10-20% of [^{3}H]-MLA with high affinity, with K_i values which approximate to their own respective high affinity dissociation constants, K_d, determined previously using the individual labelled ligands (Table 3). The lower affinity displacement of [^{3}H]-MLA by α-BgTx, IMI, and EPI did not match the K_d values for these ligands determined in saturation studies; this could reflect the existence of cooperativity between binding sites. Further evidence for cooperativity is provided by isotopic dissociation studies using either α-BgTx or MLA to initiate dissociation of [^{3}H]-α-BgTx from *M. persicae* membranes. The markedly different dissociation rates obtained with these two ligands suggests that allosteric interactions between at least two binding sites on the same aphid nAChR can occur (see Chapter 2). This would be consistent with the absence of any obvious differences in the distribution of [^{3}H]-MLA and [^{125}I]-α-BgTx binding sites in *M. sexta*, as judged by autoradiography.

Previous evidence from binding studies of nicotinic ligands in invertebrate nervous systems has indicated a rather uniform pharmacology (Gundelfinger, 1992; Lui and Casida, 1993). This relatively simple picture does not reflect the multiplicity of nAChR subunit genes now shown to exist in insects and other invertebrates. Recently, genes encoding six α and one non-α putative nAChR subunits have been cloned from *M. persicae*, providing a plausible genetic basis for multiple subunit combinations giving rise to different receptor subtypes and heterogeneous ligand binding (Huang *et al.*,

1998; Huang *et al.,* 1999). Thus the heterogeneity of binding sites in *M. persicae*, could be due to genetically distinct α-subunits or different non-α subunits adjacent to identical α subunits influencing the pharmacology of binding (Papke and Heinemann, 1991; Harvey *et al.,* 1996). Alternatively, different conformational states of the same receptor could influence ligand affinity (Prince and Sine, 1998). Further light will be shed on the origin of heterogeneity by purification of native nAChR and determination of their subunit composition, or successful heterologous expression of cloned insect nAChR subunits in defined mixtures.

In summary, [^{3}H]-MLA demonstrates specific binding to an apparently single binding component present in high density in a number of invertebrates. The kinetic properties of [^{3}H]-MLA binding are more favourable for ligand binding studies than those of α-BgTx, and [^{3}H]-MLA proved an excellent candidate ligand for autoradiography. Because [^{3}H]-MLA was unable to resolve binding sites which were differentiated in insects by other nicotinic radioligands, it appears able to detect all known insect nAChR subtypes. This makes [^{3}H]-MLA an invaluable tool for defining the total nAChR population in invertebrates, and for investigating the heterogeneous binding behaviour of other ligands. [^{3}H]-MLA may therefore be particularly useful in screening for novel agents with nicotinic actions.

Figures 5.1-5.3. Saturable binding of [^{3}H]-MLA to *M. persicae* membranes. Membranes were incubated with of [^{3}H]-MLA (0.05-30nM) for 180 minutes at room temperature. Non-specific binding was determined in the presence of 1µM unlabelled MLA. **Figure 5.1.** Saturation isotherm showing specific binding (●)calculated as the difference between total and non-specific binding (◆). Scatchard (**Figure 5.2**) and Hill plot (**Figure 5.3**) of [^{3}H]-MLA binding to *M. persicae* membranes consistent with a single binding component. Data shown are the mean±SEM from 4 separate experiments, each with triplicate determinations of total and non-specific binding.

Figure 5.1

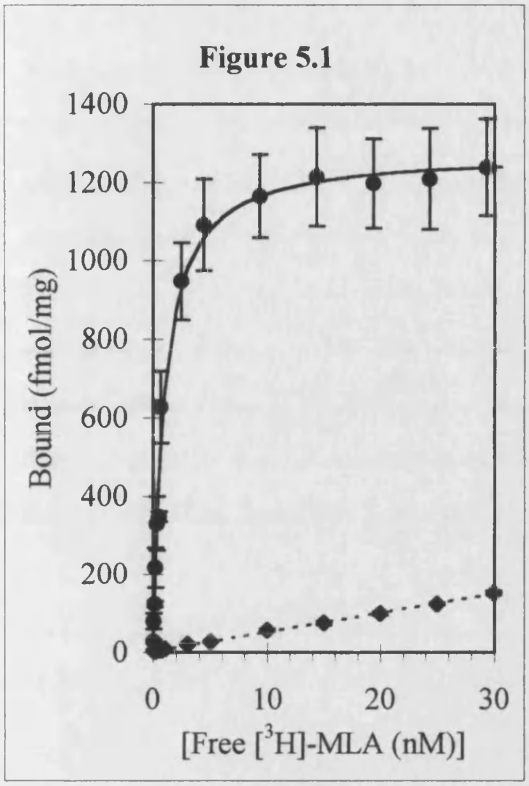

Figure 5.2

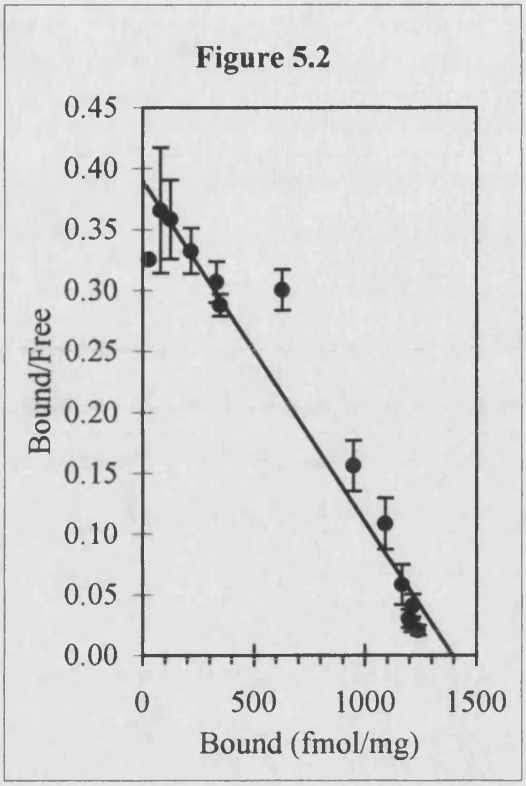

Figure 5.3

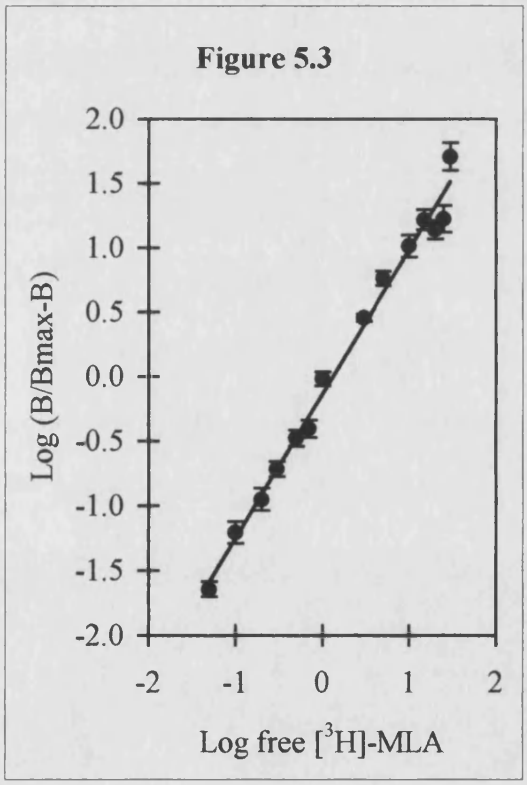

Figures 5.4-5.11. [^{3}H]-MLA Saturation binding in homogenates of *L. vulgaris* (Figures 5.4-5.5), *L. sericata* (Figures 5.6-5.7), *M. sexta* (Figures 5.8-5.9), and *H. virescens* (Figures 5.10-5.11). Symbols denote total binding(◆), specific binding (●), and non-specific binding (▲). Membranes were incubated for 3 hours with a range of [^{3}H]-MLA concentrations (0.1-30nM) and bound and free radioligand separated using vacuum filtration with a cell harvester. A concentration of 1μM unlabelled MLA was used to determine non-specific binding. The Hill plot is inset in the Scatchard plot and the x-axis represents Log_{10} free [^{3}H]-IMI concentration, and the y-axis portrays the Log_{10} (Bound/B_{max}-Bound). Data shown is from a single experiment.

Figure 5.4 - *L. vulgaris*

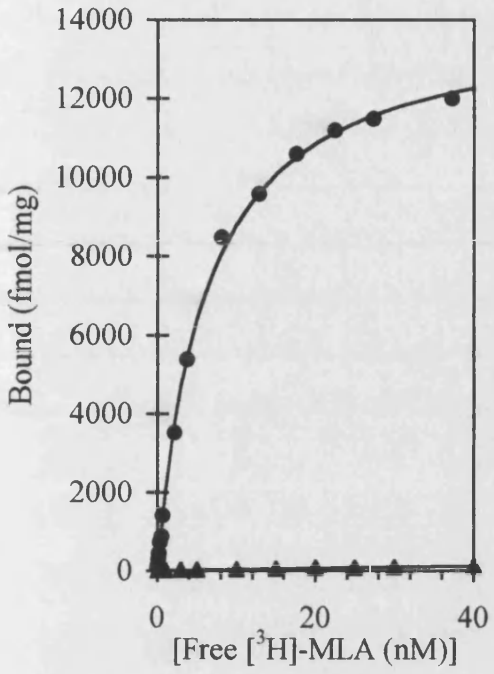

Figure 5.5

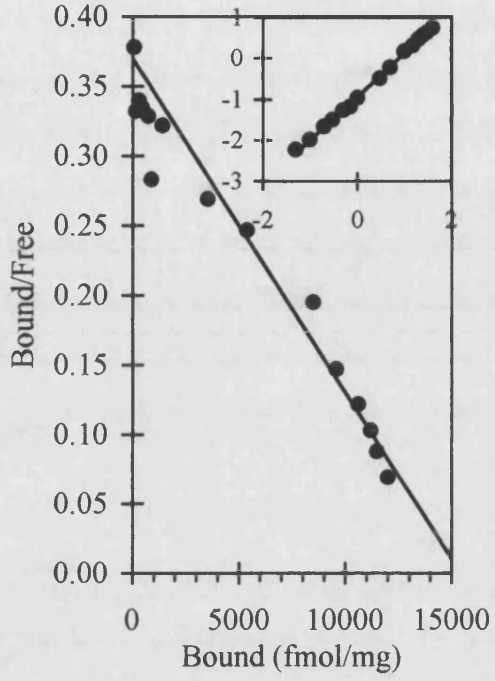

Figure 5.6 - *L. sericata*

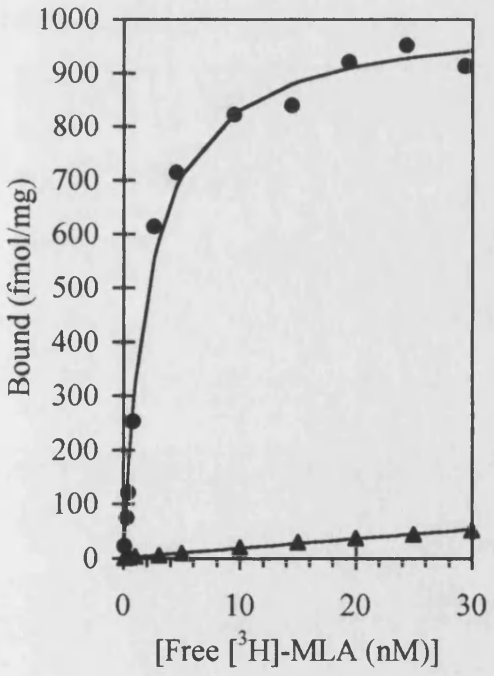

Figure 5.7

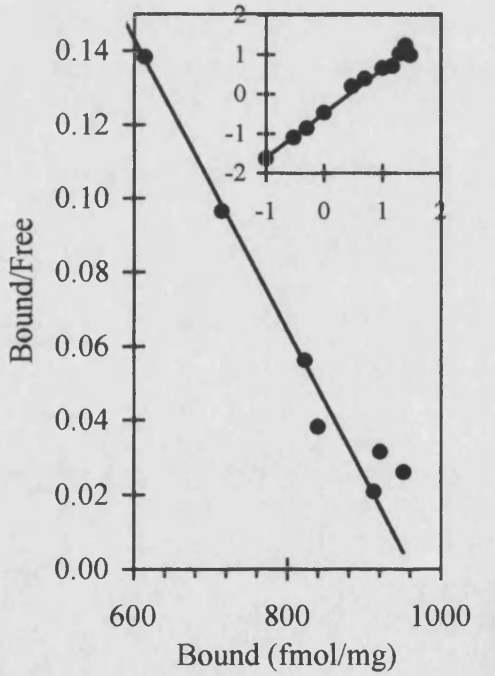

Figure 5.8 - *M. sexta*

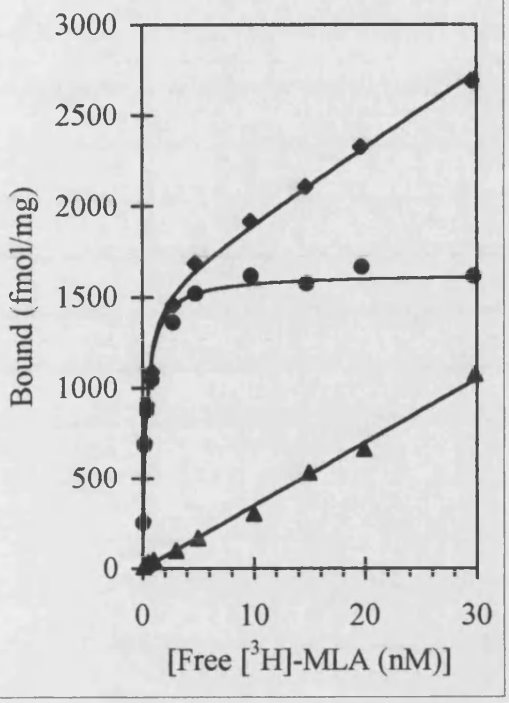

Figure 5.9

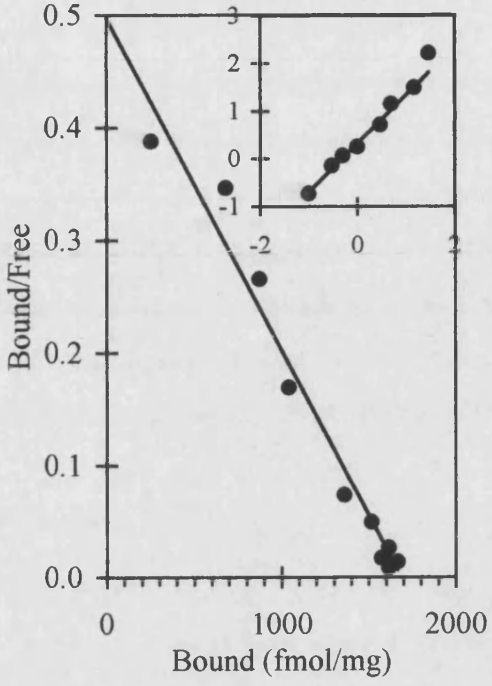

Figure 5.10 - *H. virescens*

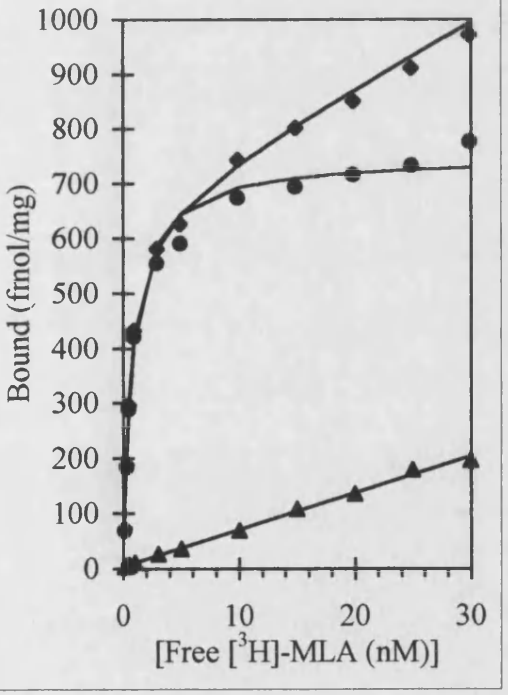

Figure 5.11

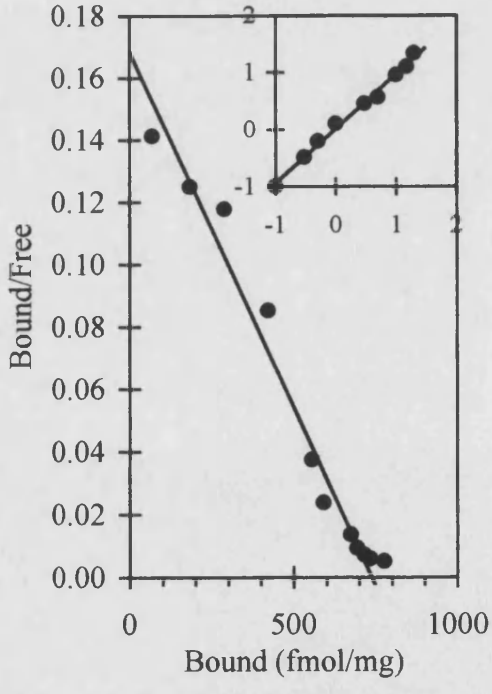

Figure 5.12-5.13. Kinetic analysis of [^{3}H]-MLA binding to *M. persicae* membranes. **Figure 5.12.** Association kinetics. Membranes were incubated with 1nM [^{3}H]-MLA at 22°C before bound ligand was separated by filtration. Data are the mean ± SEM of three independent experiments and are fitted to a two-site model. ***Inset,*** linear transformation of the [^{3}H]-MLA binding kinetics shown in Figure 5.4. **Figure 5.13.** Isotopic dissociation of [^{3}H]-MLA. [^{3}H]-MLA (0.5nM) was allowed to equilibrate for 3 hours with membranes before dissociation was initiated by addition of 1µM MLA. Remaining bound ligand at the specified times was determined by rapid filtration. ***Inset,*** first-order kinetic plot of the dissociation of [^{3}H]-MLA from its binding site. Data are the mean ± SEM of three independent experiments.

Figure 5.12

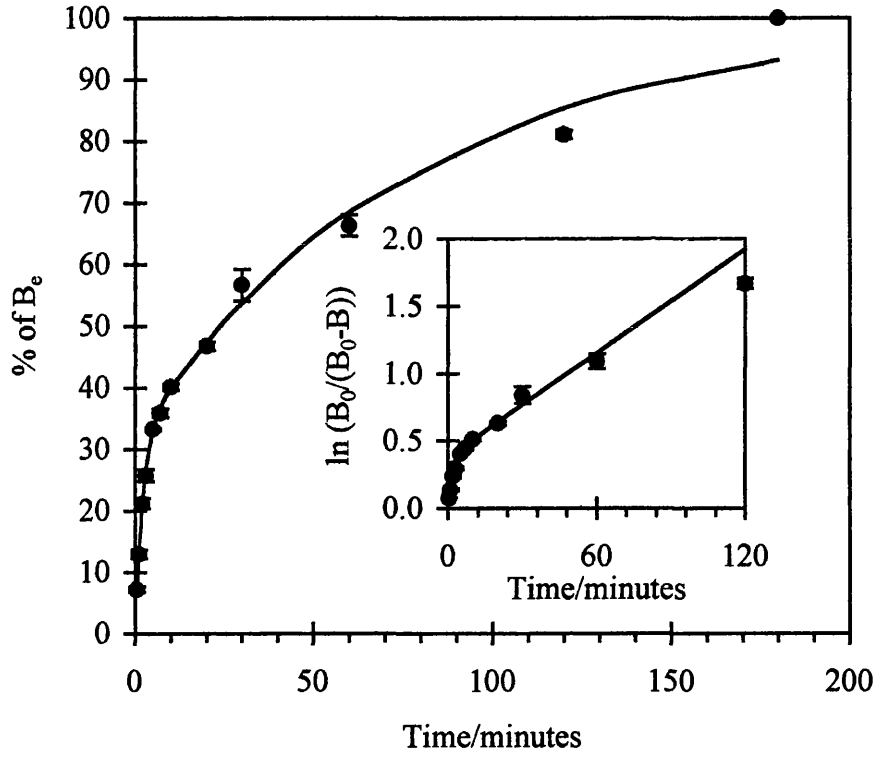

Figure 5.13

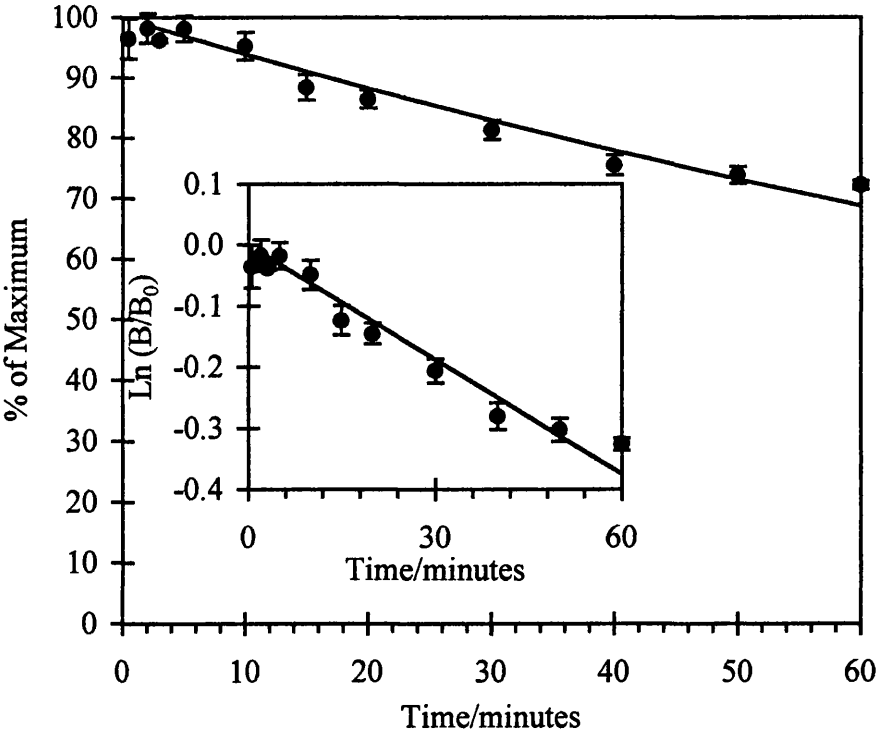

Figure 5.14. Displacement of [^{3}H]-MLA binding to *M. persicae* membranes by nicotinic ligands. Membranes were incubated with MLA (●), IMI (×), α-BgTx (▲), (±)EPI (◆), (-)nicotine (□) and ACh (○) for 30 minutes and further incubated with 0.5nM [^{3}H]-MLA for 120 minutes at room temperature. Bound radioligand was harvested using filtration. Non-specific binding was determined in the presence of 1μM unlabelled MLA. Data points represent the means of at least 3 independent experiments, each conducted in triplicate. Error bars are omitted for clarity, SEM were typically <10% of mean. Data for MLA were fitted to the Hill Equation with a single site and all other ligands were fitted to a two site additive model (see section 2.2.9 Data calculation).

Figure 5.14

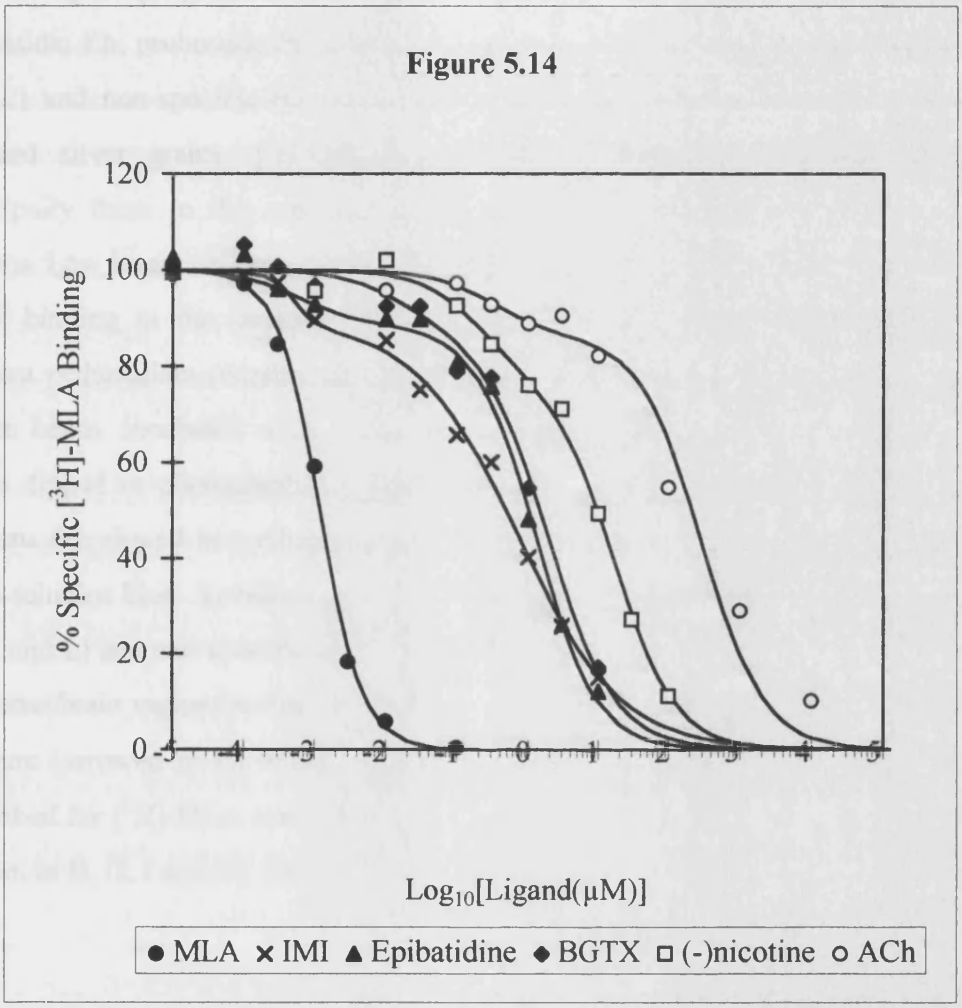
120
100
80
60
40
20
0
% Specific [3H]-MLA Binding
-5
-4
-3
-2
-1
0
1
2
3
4
5
Log10[Ligand(μM)]
● MLA × IMI ▲ Epibatidine ◆ BGTX □ (-)nicotine ○ ACh

Figure 5.15. Autoradiographic localisation of [^{3}H]-MLA and [^{125}I]-α-BgTx binding in the brain of *Manduca sexta*. (A) Partly dissected *M. sexta* head showing location and top view of brain. Pb, proboscis; Pr, protocerebrum; Ol, optic lobes. (B) Dissected brain (front view) showing regions; histological sections were cut in the plane of the dotted line. Ol, optic lobes; Om, Ommatidia of compound eye; Pr, protocerebrum; Seg, subesophageal ganglion. (C) 0.1% Toluidine blue stained section (20μM). Om, ommatida; Pb, proboscis; Pr, protocerebrum; Ol, optic lobe. Localisation of total (D and E) and non-specific (G and H) [^{3}H]-MLA binding sites in the optic lobes as reduced silver grains. [^{3}H]-MLA sites are concentrated in the neuropil areas, principally those in the medulla (Md), lobula (Lb), and lobula plate (Lbp) brain regions. Low levels are present in the lamina (Lm). (F) Total and (I) non-specific [^{3}H]-MLA binding in the protocerebrum demonstrating strong specific binding in the corpora pedunculata (mushroom bodies) (Cp). 20μM sections were cut from whole frozen heads, incubated with 1nM [^{3}H]-MLA, post-fixed in 2% glutaraldehyde and slides dipped in photographic emulsion. Slides were developed after 6 months and sections dehydrated in a ethanol and xylene series before mounting and staining with 0.1% toludine blue. Localisation of [^{125}I]-α-BgTx sites in the optic lobe showing total (J, K and L) and non-specific binding (M, N and O). Specific binding was observed in the same brain regions as for [^{3}H]-MLA, with the addition of a region adjacent to the tapetum (arrowed in L) which bound [^{125}I]-α-BgTx but not [^{3}H]-MLA. Method as described for [^{3}H]-MLA but with a 10 day exposure. Scale bar = 1mm in A, B and C, 250μm in D, G, J and M, 100μm in E, F, H, I, K, L, N and O.

Figure 5.15

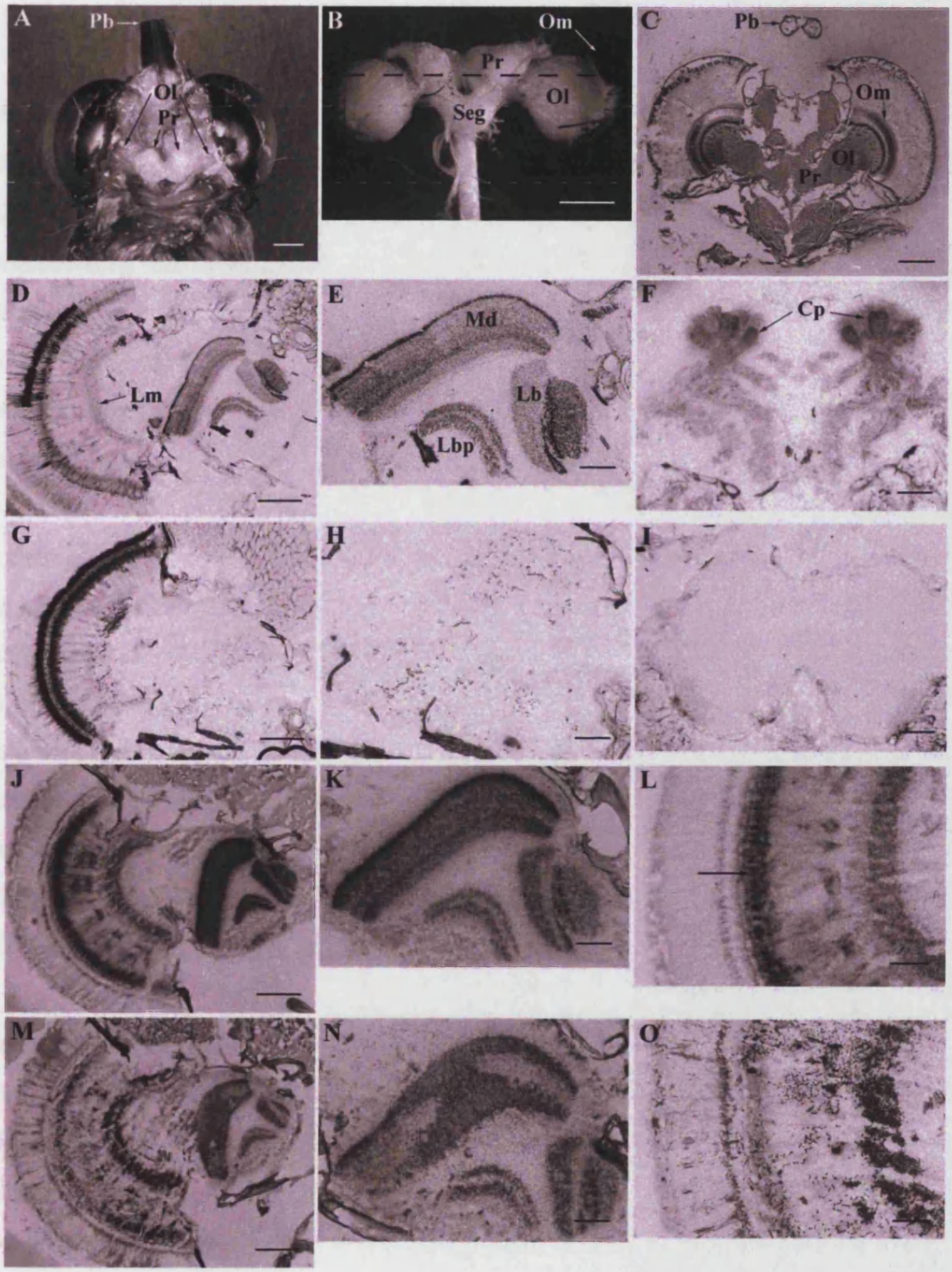

Chapter 6
Quantification of imidacloprid systemic uptake and biological effects on the aphid *Myzus persicae*

6.1 Introduction

The lethal symptoms brought about by IMI in aphids are typical of those produced by a neurotoxin and include tremoring and discoordinated movement (Leicht, 1993). The sublethal effects of IMI toxicology in *M. persicae* were investigated by Nauen (1995) demonstrating that at low leaf systemic doses (e.g. 0.001ppm) IMI induces antifeedant behaviour. This was associated with a decrease in honey dew, nymph production and weight loss and an increase in probing. The behaviour modifying effects of low systemic doses were seen to be reversible when aphids were allowed to feed on untreated leaves.

A sibling species of *M. persicae* the tobacco aphid *Myzus nicotianae* (Blackman) was the subject of investigation of Nauen *et al.* (1996) and Devine *et al.* (1996) since this aphid feeds on tobacco and is therefore likely to be exposed to its alkaloids. The tobacco feeding aphid is differentiated by the electrophoretic mobility of the enzyme glutamate oxaloacetate transaminase (Blackman and Spence, 1992). Earlier studies by Guthrie *et al.* (1962) had proposed that *M. nicotianae* avoids exposure to the nicotine containing xylem by instead feeding from the phloem. However it is also possible this insect is tolerant to nicotine, a trait which could provide cross resistance to the chloronicotinyl insecticides.

Devine *et al.* (1996) studied the susceptibility to nicotine of *M. nicotianae* (isolated from Greek peach), comparing it with a susceptible strain of *M. persicae* (US1L, originating from Rothamsted experimental station). *M. nicotianae* showed a 5-fold resistance factor (i.e. reduction in susceptibility) to both nicotine (fumigation bioassay) and IMI (dip bioassay). Furthermore, although IMI at sublethal concentrations decreased both nymph production and nymph viability, these effects were significantly

less marked in *M. nicotianae* than in *M. persicae* (Devine *et al.*, 1996). A Japanese strain of *M. persicae* also exhibited 4 to 7-fold resistance to IMI depending on the bioassay employed (Nauen *et al.*, 1996). However these resistance factors are relatively small compared to those encountered with carbamate insecticides which in the case of the Japanese *M. persicae* clone were >385-fold compared to the susceptible strain US1L.

The choice of bioassay method is particularly important when a behavioural resistance mechanism is involved. Nauen and Elbert (1997) investigated a French field-collected strain of *M. nicotianae* which exhibited a greater than 50-fold apparent resistance to IMI in oral ingestion bioassays. However dip bioassays have demonstrated that the 'true' tolerance was less than 10-fold and the increased hardiness of the French strain is probably mostly due to its ability to survive a longer starvation period than the susceptible strain. Potential biochemical mechanisms of increased IMI tolerance in *M. nicotianae* were investigated by Nauen *et al.* (1998a), who concluded that oxidative detoxification, hydrolytic metabolism and the involvement of endosymbiotic bacteria were not involved.

The involvement of IMI metabolites in the toxicology of the cotton aphid *Aphis gossypii* and the peach potato aphid *M. persicae* was investigated by Nauen *et al.* (1998b). This study revealed that after foliar or seed treatment application, IMI was more or less completely metabolised within the plant, the extent of conversion depending on the plant species and the sampling time. This metabolic conversion does not however detoxify the insecticide as far as aphids are concerned. Nauen *et al.* (1998b) tested a number of IMI metabolites previously described by Klein (1994) and Anon (1994) (Figure 6.1) against both *A. gossypii* and *M. persicae* in contact and oral bioassays.

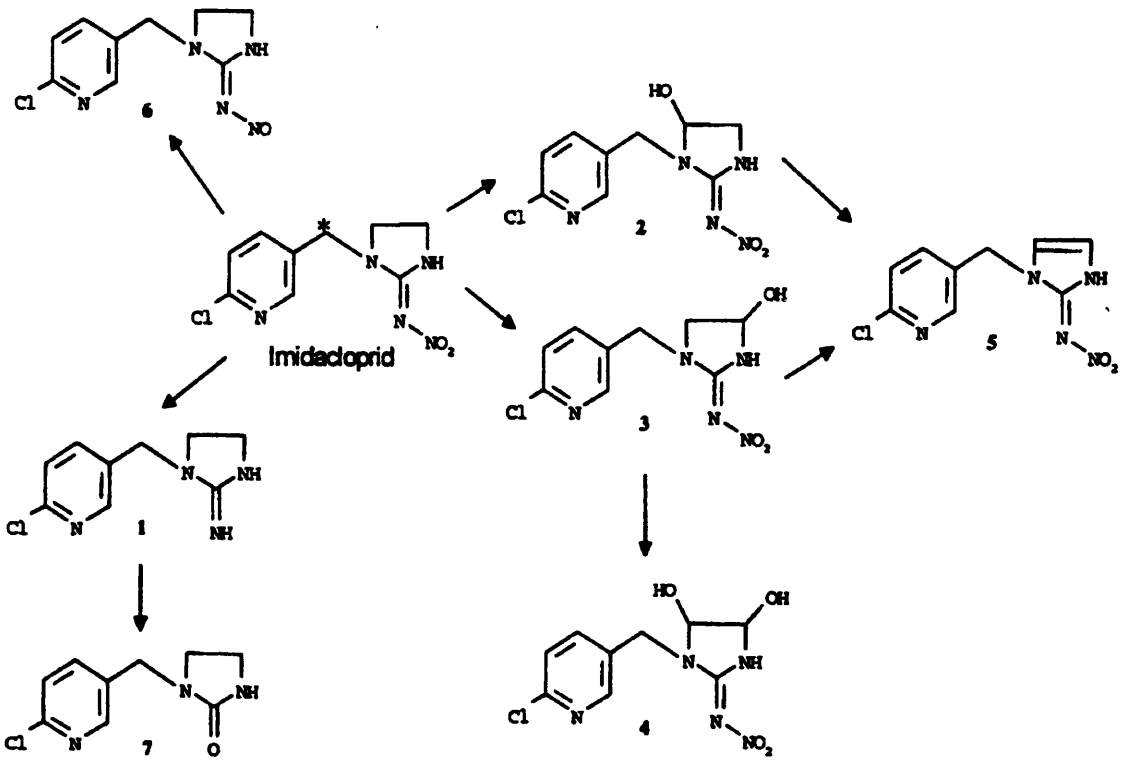

Figure 6.1. Degradation of IMI, metabolites are referred by number in the text. Reproduced from Nauen *et al.* (1998b). * position of tritium

Of these IMI metabolites **5** (an imidazoline derivative) and **6** (a nitroso derivative) demonstrated a higher potency to the aphid *M. persicae* after oral ingestion compared to the parent molecule. The toxicity of **5** was confirmed in displacement studies of [^{3}H]-IMI in radioligand binding experiments, in which **5** proved to be a better displacer than IMI itself. It was concluded that despite the extensive metabolism of IMI in the host plant this insecticide still gives good control of insects by working in concert with its metabolites.

The present study investigates the biological effects and systemic up take of [^{3}H]-IMI to quantify the sub-lethal and lethal internal concentrations in R1 *Myzus persicae* and to assess differences between plant and insect metabolism of [^{3}H]-IMI.

6.2 Methods and Materials

6.2.1 Chemicals

[^{3}H]-IMI (30Ci/mmol, radiochemical purity > 95%) and unlabelled IMI were supplied by Zeneca Agrochemicals. Concentrations of IMI are expressed in terms of ppm in order to allow direct comparisons with previous work.

6.2.2 Aphids

Adult apterous peach potato aphids *M. persicae* were reared under a 16:8 hour light:dark lighting regime on mature chinese cabbage plants (*Brassica pekinensis*). A susceptible strain (405D) originating from Rothamsted Experimental Station was used. This strain has moderate levels of esterases, and may be classified as an 'R1 strain' according to the system of Devonshire (1989).

6.2.3 Systemic uptake of [^{3}H]-IMI

The first true leaves of three week old Chinese cabbage plants were excised, these typically having a surface area of 6-9cm^2. To estimate leaf size the fresh weight of each leaf was recorded. The leaf petiole was immersed in 1500µl [^{3}H]-IMI solutions at concentrations of 0.1, 0.01 and 0.001ppm for 24 hours in order to treat the leaves systemically. The amount of [^{3}H]-IMI solution taken up by the leaf during this period was measured by weighing the eppendorf tube before and after 24 hours. Leaf discs (30mm diameter) were then cut from the centre of the leaf and mounted onto agar (15g/l) wetted with 50µl distilled water in a vented 5cm diameter Petri dish. A 5cm filter paper (Whatman no. 1) was added to the lid to collect honeydew and reduce humidity, and was changed every 24 hours. Ten adult R1 *M. persicae* from culture were added to each leaf disc with a wetted paint brush.

The Petri dishes were inverted and stored in an incubator at 20°C with a photoperiod of 16 light : 8 dark. Every 24 hours an assessment was made of the number of live and dead insects, and after 72 hours each adult was individually added to 5ml of scintillant and left for 24 hours before counting at 43% efficiency. In addition all of the filter papers from the treatment dishes and the leaf disc were counted at the end of the experiment. The number of nymphs produced was recorded, as were the numbers of live and dead insects.

6.2.4 Aphid weights

In order to estimate an internal concentration of [^{3}H]-IMI the average weight of an adult aphid needed to be ascertained. 20 Adult *M. persicae* were weighed on a Mettler UMT2 micro balance to an accuracy of 0.001mg.

6.2.5 Leaf and aphid metabolism of [^{3}H]-IMI

Separation of radioactive compounds used a 20x20 cm silica gel 60 TLC plate with fluorescent indicator (Macherey-Nagel) to investigate metabolism of [^{3}H]-IMI by the leaf and aphids. Aphids were allowed to feed on a leaf disc systemically treated with 0.1ppm [^{3}H]-IMI until death ensued as described previously. Aphid (~100 individuals) and leaf (1 cm^2) material was then homogenised in acetone (100µl) and spotted with capillary tubing onto a TLC plate which was run in dichloromethane and methanol (95:5). The plate was developed for 40 min, until the solvent front was ~2cm from the plate top. Assessment of the purity and chromatographic mobility of the parent [^{3}H]-IMI radiolabelled compound (5µl of 33µM stock) was made by comparison with unlabelled IMI (25µl of 2mg/ml).

6.2.6 Phosphor imaging of the TLC plate

Techniques and methods of phosphor imaging were based on those described by Hamaoka (1990). The TLC plate was exposed for 1 week to a tritium sensitive plate (Bas-TR2040) and radioactivity measured using a Fujifilm Bas1500 phosphor imager and data analysed using Raytest TINA v2.09g software.

6.2.7 Statistical testing

In order to test if there was significant variation between leaf weights and solution uptake between treatments an F probability distribution test was used.

6.3 Results

6.3.1 Systemic uptake of [^{3}H]-IMI

Leaf weight demonstrated no significant differences between treatments and ranged between 0.25 and 0.30g ($F=0.1$; $P>0.1$) (Figure 6.2). This indicates that leaf size did not vary significantly within or between experiments. The uptake of solutions was more variable but showed no obvious trends ($F=1.4$; $P>0.1$) (Figure 6.3). Levels of radioactivity in the leaf disc after the experiment demonstrate a good dose response with an approximate 10-fold difference in counts between 0.1, 0.01 and 0.001ppm treatments as expected (Figure 6.4). The control leaf had background counts <10cpm.

6.3.2 Biological effects of [^{3}H]-IMI

The biological effect of IMI on *M. persicae* can be characterised as either irreversible symptoms such as tremoring and paralysis and those that are reversible such as a decrease in honey dew and nymph production connected with the antifeedant response. Adult mortality was positively correlated with [^{3}H]-IMI concentration and time (Figure 6.5). After 72 hours 100% of adults were dead at a concentration of 0.1ppm, ~50% at 0.01ppm and ~30% at 0.001 with control mortality <10%. The number of nymphs produced after 72 hours was correlated negatively with an increasing [^{3}H]-IMI dose (Figure 6.6) and nymph mortality was correlated positively with dose (Figure 6.7). Honey dew production is an indication of aphid feeding. Thus collection of the filter papers every 24 hours and subsequent counting of radioactivity provided a measurement of the uptake of IMI, and indirectly, of feeding (Figure 6.8). The greatest amount of radioactivity in honey dew was produced by aphids given 0.1ppm IMI. However the amount remained high only for the first 24 hours. By 72 hours the amount of radioactivity excreted had dropped to <10% of that at 24 hours due to the cessation of feeding and subsequent demise of the aphids. A similar, but less pronounced, decrease in honeydew radioactivity at a treatment concentration of 0.01ppm. At

0.001ppm the amount of honey dew produced was not markedly different at 24, 48 or 72 hours indicating that the level of feeding was relatively constant. The amount of honey dew produced could not be compared to the control but a previous study by Nauen (1995) demonstrated that there was a marked reduction in honey dew production by aphids treated with IMI concentrations greater than 0.001ppm.

6.3.3 Internal aphid [^{3}H]-IMI concentrations

Uptake of radioactivity from the tritiated insecticide by adult aphids is shown in Figure 6.9. Data for each concentration is split into that for live and dead insects. At a concentration of 0.1ppm all adult aphids were killed and an internal concentration of ~85cpm was reported. Live and dead aphids were obtained from 0.01 and 0.001ppm. For each dose, these insects contained approximately the same amounts of labelled materials regardless of whether they were alive or dead. However the insects on 0.01ppm contained 2.5-4 fold more radioactivity than those on 0.001ppm. The control aphids contained only background levels of radioactivity. The mean weight of a sample of twenty adult R1 *M. persicae* taken from culture was 0.53±0.2mg. The assumption is made that aphids have a specific gravity of 1 and have a volume of 0.53µl. Thus the cpm per aphid (minus the background radiation) can be converted to an internal molar concentration, Table 6.1.

Treatment	Live (nM)	Dead (nM)
0.1ppm	-	5.1
0.01ppm	2.2	2.2
0.001ppm	0.5	0.8

Table 6.1. Internal concentrations of [^{3}H]-IMI in adult *M. persicae* after systemic uptake for 72 hours.

6.3.4 Leaf and aphid metabolism of [^{3}H]-IMI

The phosphor image of the TLC plate is shown in figure 6.10 and the corresponding traces in figures 6.11-6.13. TLC plate analysis demonstrates that the purity of the [^{3}H]-IMI was 95%. After 120 hours, systemic uptake of [^{3}H]-IMI into the leaf revealed four major tritiated compounds. After 72 hours 5 major peaks could be resolved in the aphid, table 6.2.

Peak	[^{3}H]-IMI	Leaf	Aphid	RF value
1	0.3	6.0	15.3	0.03
2			13.2	0.12
3	0.6			0.24
4	0.1			0.37
5	2.0	35.6	26.3	0.72
6		5.3		0.81
7 (IMI)	**93.3**	**13.7**	**10.7**	**0.83**
8	2.9			0.90
9			4.4	0.96

Table 6.2. Assessment of purity and metabolism of [^{3}H]-IMI in leaf and aphid material determined by TCL separation and subsequent analysis by phosphor imaging. Figures are % of total.

That peak corresponding to the parent [^{3}H]-IMI (peak 7) represented 14% and 11% of the total signal in the leaf and aphid respectively (Figure 6.10, Table 6.2). The remainder in the leaf could be visualised as 3 major metabolite products with a low background level of other metabolites. The background level of metabolites in the aphid was similar to that found in the leaf. However the number of major metabolites included those found in the leaf but with the inclusion of a unique product (peak 2 of Table 6.2). The identity of the metabolites was not investigated further.

6.4 Discussion

This study is in agreement with previous investigations into the lethal and sublethal symptoms produced by IMI in *M. persicae* (Nauen, 1995). The irreversible biological effects of tremoring, paralysis and death are associated with an internal concentration of IMI and its metabolites of approximately 5nM. The reversible symptoms of decreased honey dew and nymph production are linked to antifeedant effects which can be correlated with internal concentrations of [^{3}H]-IMI <1nM. Intermediate concentrations (estimated at 2.2nM here) killed only some insects, and not others.

However, TLC plate analysis of the metabolism of [^{3}H]-IMI demonstrates that the parent [^{3}H]-IMI molecule is subject to substantial metabolic breakdown in the leaf before uptake by the aphid which is in agreement with previous investigations (Klein, 1994 and Anon, 1994). Further breakdown in the aphid is apparent by the appearance of a unique metabolite. In the aphid, parent [^{3}H]-IMI accounts for only about 10% of tritiated compounds. Therefore the internal concentrations of [^{3}H]-IMI in table 6.1 are over estimates and concentrations 10-fold less would be more legitimate. The nature of the [^{3}H]-IMI metabolites was not resolved in this study and their role in IMI toxicology can not be appraised. However it is possible that these breakdown products might also contribute to poisoning, and thus in part IMI would be acting as a pro-insecticide. Nauen *et al.* (1998b) has shown that IMI metabolites have a role to play in IMI toxicology. However, a correlation between the potencies of the IMI metabolites and the relative amounts produced in this study was not possible. Further work to identify the relative amounts of each IMI metabolite in leaf tissue would help to resolve the role they play in toxicology.

Similar findings to this study have resulted from investigation into the metabolism of pyrethroid [^{14}C]-cyfluthrin by the larva of *Spodoptera litoralis* (Lagadic *et al.*, 1994). Excretion was an important detoxifying mechanism and 32 hours after a topical application ~50% of the [^{14}C] was recovered in the faeces. In the present investigation,

excretion of tritiated compounds was also observed, although the relative amounts of [^{3}H]-IMI metabolites that contributed to this was not resolved. Lagadic *et al.* (1994) separated [^{14}C]-cyfluthrin metabolites by TLC and reported 5 metabolites to be present both internally in larvae and in faecal extracts, a similar number to that reported here. Interestingly, only very small amounts of parent [^{14}C]-cyfluthrin were present 24 hours after application. Although the present study and that of Lagadic *et al.* (1994) both reach the same conclusion that significant metabolism occurs, the route of this metabolism appears different. The majority of the metabolism of [^{3}H]-IMI occurs in the leaf prior to aphid feeding, whereas the caterpillar performs its own breakdown, presumably by the cytochrome P450 system. A further point to consider is the rate of metabolism since the tritiated compounds in the aphid were detected after a 24 hour exposure in the leaf (during systemic uptake) followed by 72 hours in the aphid. Thus the dose responsible for aphid death may have been higher than that detected after 72 hours with further metabolism occurring after the onset of the irreversible symptoms.

From binding studies with [^{3}H]-IMI (see Chapter 3), the parent [^{3}H]-IMI has been demonstrated to interact with high affinity at the putative aphid nAChR. Saturable binding of [^{3}H]-IMI in aphid homogenates demonstrated multiple binding sites with the high affinity site having a K_d of 0.15nM. This work reported in this chapter suggests that a 0.1ppm systemic dose would lead to an internal IMI concentration in the aphid of approximately 5nM. Therefore assuming a equal concentration throughout the aphid, the internal IMI concentration from a 0.1ppm systemic dose would represent a saturating amount of IMI at the high affinity binding site.

However, sublethal concentrations of IMI are well known to affect the aphid, disturbing feeding behaviour and adversely affecting nymph production. At sublethal concentrations of 0.001ppm the internal concentrations of [^{3}H]-IMI are very low (<1nM) which may indicate that high affinity IMI binding sites are important in generating the effects of IMI. The sublethal actions of IMI are exemplified by an antifeedant response without any obvious loss of coordination. At these low

concentrations, a subset of high affinity IMI binding sites is likely to play a role. We suggest that these receptors may be linked with the feeding regulation area of the aphid CNS.

In summary, extensive metabolism of systemically administered IMI occurs in both the plant and in the aphid. There is evidence of the presence of a unique metabolite in aphids. Previous investigations have demonstrated that despite near complete breakdown of IMI, toxicology can also be attributed to its metabolites. The internal aphid concentrations of IMI and its metabolites that are responsible for the sublethal effects are sub-nanomolar (ca. 0.5nM); those which bring about aphid death are an order of magnitude higher (ca. 5nM). These experiments provide further evidence for the existence within aphids of very high affinity binding interactions between IMI and its target sites.

Figure 6.2. Mean weights (g) of excised Chinese cabbage leaves demonstrating no marked difference in weight between treatments and control. Bars represent the SEM.

Figure 6.3. Average systemic uptake (µl) of [^{3}H]-IMI solutions and distilled water controls into Chinese cabbage leaves after 24 hours. Bars represent the SEM.

Figure 6.2

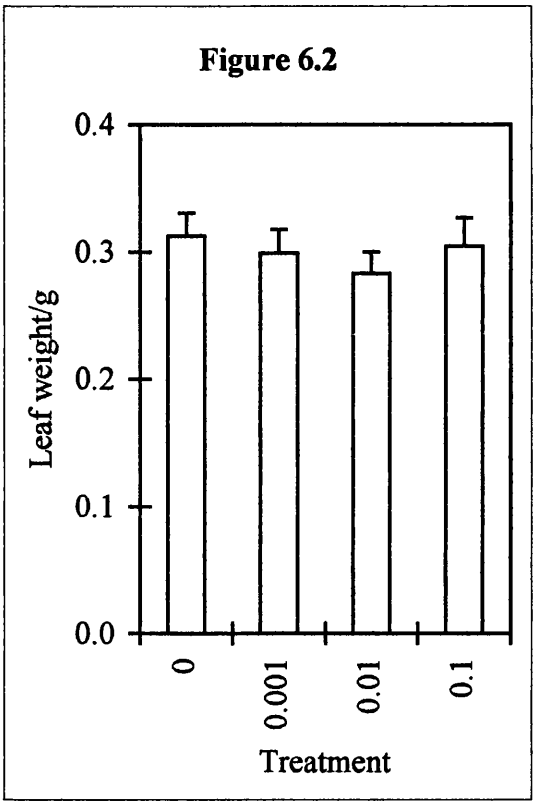

Figure 6.3

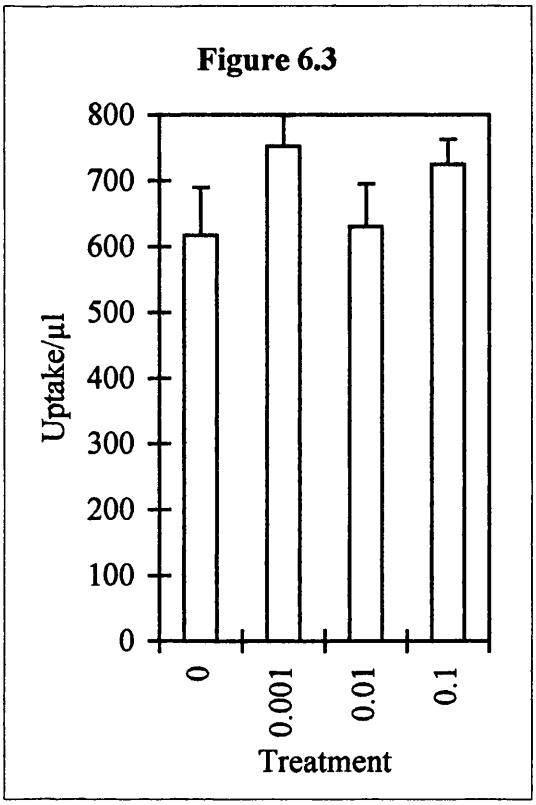

Figure 6.4. Quantification of radioactivity in leaf discs after 96 hours. Leaves were added to 5ml scintillent and counted at 43% efficiency. Bars represent the SEM.

Figure 6.5. Adult *M. persicae* mortality after exposure to [^{3}H]-IMI systemically treated and control leaves after 24, 48 and 72 hours. Bars represent the SEM.

Figure 6.6. Nymph production after 72 hours for [^{3}H]-IMI treatments and control. Bars represent the SEM.

Figure 6.4

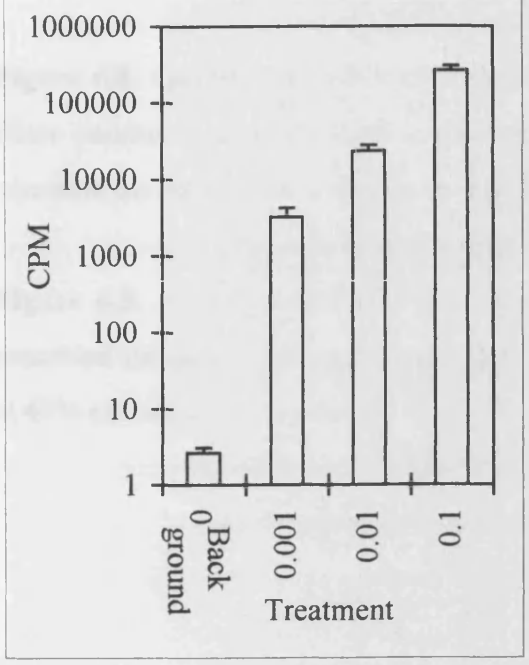

Figure 6.5

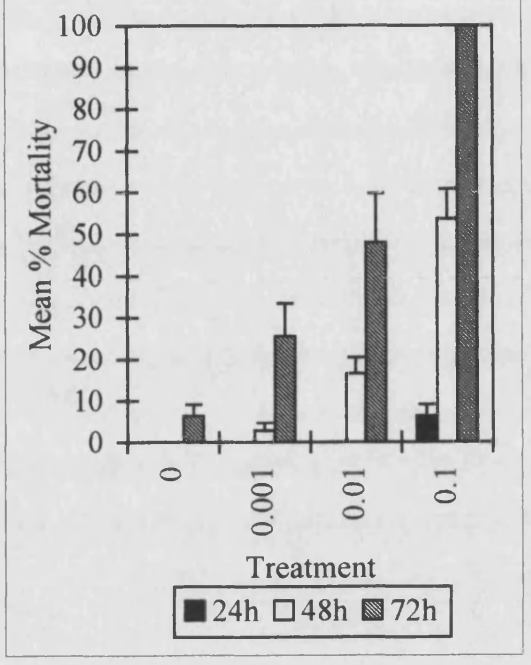

Figure 6.6

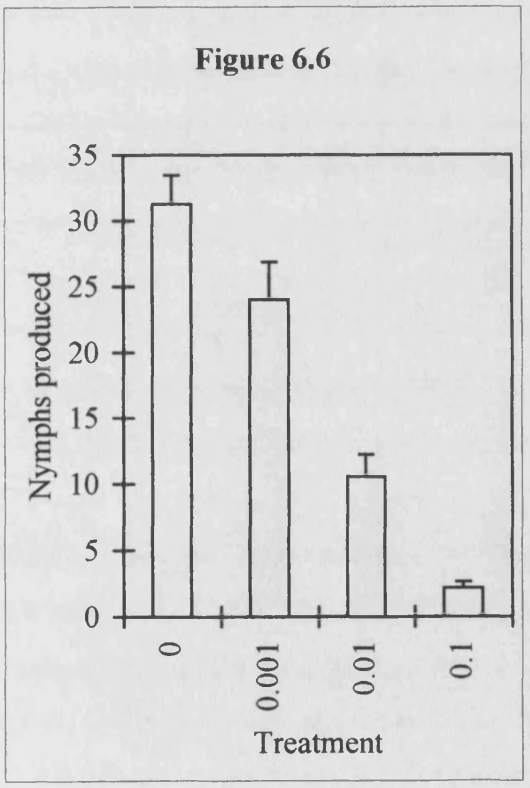

Figure 6.7. Mean mortality of nymphs produced after 72 hours for [^{3}H]-IMI treatments and control. Bars represent the SEM.

Figure 6.8. Quantification of radioactivity in filter papers after 24, 48 and 72 hours. Filter papers were added to 5ml scintillent and counted at 43% efficiency. Bars represent the SEM.

Figure 6.9. Amounts of tritiated material per adult aphid after 72 hours. Data are presented for dead and live insects. Aphids were added to 5ml scintillent and counted at 43% efficiency. Bars represent the SEM.

Figure 6.7

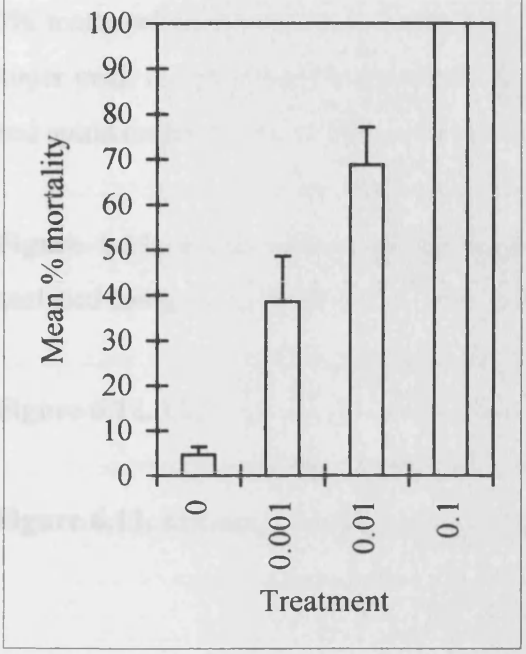

Figure 6.8

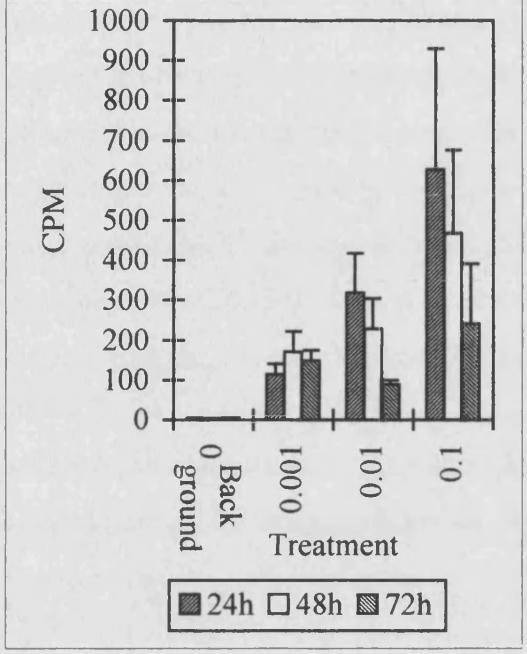

Figure 6.9

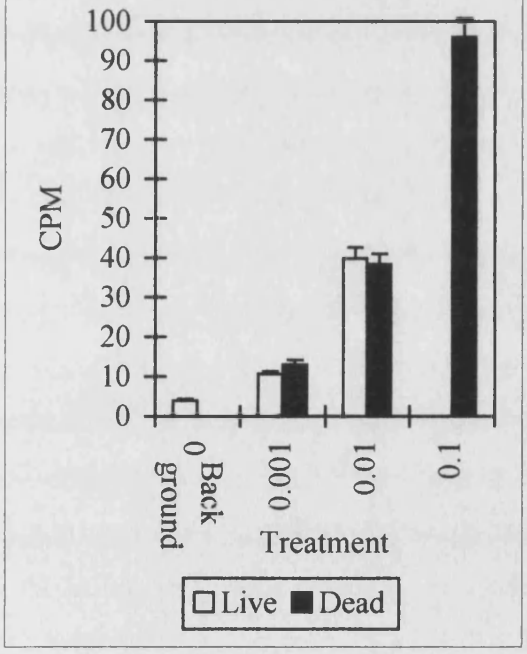

Figure 6.10. Phosphor image of TLC plate used to check the purity of [^{3}H]-IMI and to investigate its metabolism in the leaf and aphid. Samples were run in a solvent mix of 5% methanol and 95% dichloromethane. The unlabelled IMI had the same RF as the major peak in the [^{3}H]-IMI parent lane (1). Lanes 2 and 3 are metabolism by the leaf and aphid respectively.

Figure 6.11. Purity assessment of the parent [^{3}H]-IMI. The phosphor image was analysed using Raytest TINA v2.09g software.

Figure 6.12. Metabolism of [^{3}H]-IMI in the leaf disc.

Figure 6.13. Metabolism of [^{3}H]-IMI by the aphid.

Figure 6.10

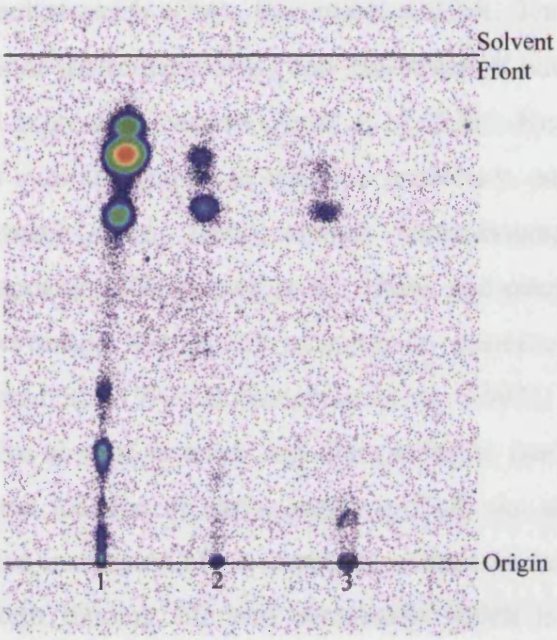

Figure 6.11

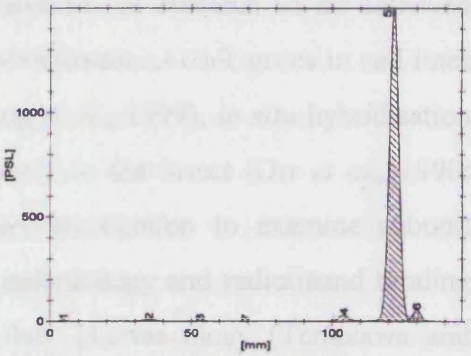

Figure 6.12

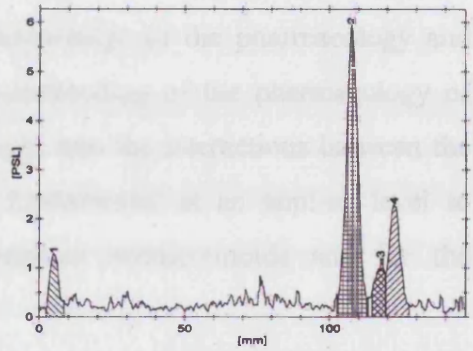

Figure 6.13

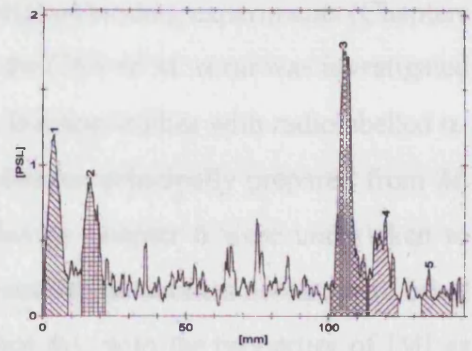

Chapter 7

Overall conclusions

7.1 Introduction

The introduction of nitromethylene (Schröder and Flattum, 1984) and the subsequent superior neonicotinoid insecticides (Elbert *et al.,* 1991) have been the catalyst for the recent research efforts into insect nAChR. The avenues of research so far followed include molecular cloning and expression of putative insect nAChR genes in cell lines and expression systems (Amar *et al.,* 1995; Huang *et al.,* 1999), *in situ* hybridisation and autoradiography to visualise expression patterns in the insect (Orr *et al.,* 1990; Hermsen *et al.,* 1998), affinity chromatography purification to examine subunit composition (Tomizawa *et al.,* 1996), and electrophysiology and radioligand binding experiments with native receptors to examine their pharmacology (Tomizawa and Yamamoto, 1992; Buckingham *et al.,* 1997). The present study complements this active area of research and contributes to our knowledge of the pharmacology and spatial location of native insect nAChR. An understanding of the pharmacology of native insect nAChR is important to gain an insight into the interactions between the protein binding site and insecticide which is fundamental at an applied level to ascertain the potential for cross resistance between neonicotinoids and for the screening of new insecticides.

The pharmacological investigation relied on radioligand binding experiments (Chapters 2-5), while the distribution of putative nAChR in the CNS of *M. sexta* was investigated through autoradiographic techniques (Chapter 5). Binding studies with radiolabelled α-BgTx, IMI, EPI and MLA employed insect membranes, principally prepared from *M. persicae*, using standard methods. Feeding studies in Chapter 6 were undertaken to establish the internal aphid concentrations of IMI and its metabolites necessary to bring about symptoms of IMI toxicology, and to correlate this with the properties of IMI as investigated by [^{3}H]-IMI binding studies reported in Chapter 3.

7.2 Radioligand binding studies

7.2.1 Nicotine tolerant insects

The initial stimulus to the present research came from the need to understand better the genetic and biochemical barriers of tolerance and/or resistance to neonicotinoid insecticides. One approach to this is to investigate the nicotine insensitivity of insects that are specialist tobacco feeders, and which are thus naturally selected to be tolerant of nicotine.

Radioligand binding studies on *Manduca sexta* and *Myzus nicotianae* revealed no differences in [^{125}I]-α-BgTx or [^{3}H]-IMI pharmacology when compared to nicotine sensitive insects (Chapter 2). Saturable binding of [^{125}I]-α-BgTx in membranes of larval and adult *M. sexta* demonstrated a single high affinity binding site with a dissociation constant similar to that seen in nicotine sensitive insects such as *Drosophila melanogaster* (Chapter 2). Although B_{max} values were much lower in larval membranes of *M. sexta* compared to those of the adult (which could in theory provide partial tolerance to nicotine), this reflects the lower purity of the starting material from larvae; adult membranes were produced from isolated brains whereas larvae were used whole and in effect the receptor protein was diluted by body proteins giving underestimates of receptor concentrations in the larval CNS. Displacement of [^{125}I]-α-BgTx by (-)nicotine in larval and adult *M. sexta* membranes did not suggest any difference in affinity when compared to other nicotine sensitive insects.

A further potential resistance strategy of tobacco feeding insects like *M. sexta* would be to avoid having nAChR that are sensitive to nicotine. Investigations of [^{3}H]-EPI binding in *M. persicae* revealed that at this high affinity binding site (-)nicotine was a much more potent displacing ligand than it was at the [^{125}I]-α-BgTx binding site (Chapter 4). A high affinity [^{3}H]-EPI binding site was not detected in *M. sexta*, which at first suggests that this specialist tobacco feeder may have evolved to avoid nicotine

poisoning by losing high affinity sites for nicotine (Chapter 4). However this potentially adaptive trait was not confined to *M. sexta* and specific binding of [^{3}H]-EPI could not be detected in other nicotine sensitive insects such as *D. melanogaster*. Instead the absence of detectable [^{3}H]-EPI binding for some insects may reflect heterogeneity of nAChR that exists between insects of different Orders.

One of the original aims of this work was to investigate IMI resistance in strains isolated from the field or in the laboratory. In the event, such strains only became available late in the course of my studentship. However, I was able to compare saturable binding of [^{3}H]-IMI in a field collected clone of the tobacco aphid *M. nicotianae* to that seen in R1 *M. persicae* and field collected strains, in order to appraise any alteration in affinity or density of binding sites (Chapter 3). In laboratory experiments *M. nicotianae* exhibited a 5-fold resistance to nicotine compared to *M. persicae*, and a similar cross resistance factor to IMI (Devine *et al.*, 1996). Therefore the intrinsic resistance to nicotine demonstrated by *M. nicotianae* could provide a mechanism of resistance to the chloronicotinyl insecticides. However, this study found no detectable differences in affinities, relative densities or ratios of receptors between aphid clones.

In summary, the presence of an altered nAChR in tobacco feeding insects could not be detected and thus tolerance to nicotine must be through other biochemical and physical barriers or behavioural mechanisms. These tolerance mechanisms have been well studied in *M. sexta* and include nicotine metabolism, nicotine excretion and an effective blood-brain barrier to prevent binding of nicotine in the CNS. These mechanisms could also be the basis of tolerance towards the chloronicotinyl insecticides in *M. nicotianae*.

7.2.2 Saturation studies in aphids reveal binding site heterogeneity

Comparative saturation studies using different radioligands to dissect the multiplicity of insect nAChR are sparse. This study of *M. persicae* membranes is unprecedented in the number of radioligands employed, and the comparative nature of the work has allowed novel conclusions to be drawn (Chapter 5). Saturation studies using *M. persicae* membranes have demonstrated that nicotinic ligands appear to interact with a heterogeneous population of receptors. [^{125}I]-α-BgTx, [^{3}H]-EPI, and [^{3}H]-IMI all labelled two binding components of differing affinities in an approximate ratio of 1:3. In each case the sum of the high and low affinity B_{max} values approximated the B_{max} value of the single site labelled by [^{3}H]-MLA. [^{3}H]-MLA is a novel radioligand which is believed to be highly selective for particular vertebrate nAChR subtypes (Davis *et al.,* 1999), but in insects it appears to be unable to distinguish between different components within a heterogeneous population of nicotinic ligand binding sites (Chapter 5).

7.2.3 Evidence for allosteric interactions between binding sites on the same nAChR

Dissociation experiments were used to investigate cooperativity between binding sites on the same nAChR. An increase in isotopic dissociation rate of [^{3}H]-α-BgTx when MLA was used to initiate dissociation instead of either α-BgTx, EPI or IMI is consistent with an allosteric interaction brought about by binding of MLA at a site other than that of the high affinity [^{3}H]-α-BgTx binding site (Chapter 2). One interpretation of this result is that at least the majority of aphid nAChR have two different ligand binding sites at each nicotinic receptor, which can interact allosterically with each other. This finding suggests the presence of more than one α subunit with its associated ligand binding site per nAChR.

Subunit composition of insect nAChR

Vertebrate muscle and neuronal nAChR are known to assemble with a heteromeric stoichometry of 2 α and 3 non-α or homomerically with 5 α subunits (McGehee and Role, 1995). There is at present little or no information about the subunit composition of any invertebrate receptor. Investigation of *D. melanogaster* nAChR in functional expression systems suggests that the assembly of functional receptors requires the input of multiple subunit types and thus insect nAChR may be heteromeric (Bertrand *et al.*, 1994). Moreover Schloß *et al.* (1991) found that the *D. melanogaster* subunits ALS and ARD co-assembled *in vivo*. The ratios of high and low affinity sites in *M. persicae* for [^{125}I]-α-BgTx, [^{3}H]-EPI, and [^{3}H]-IMI compared to the B_{max} value of [^{3}H]-MLA could be interpreted as evidence of the stoichometry in native aphid nAChR (Chapters 2-5). Two models are considered here. The aphid saturation data could be interpreted as either 2 populations of nAChR in which there are two α subunits per receptor (Figure 7.1) or a homomeric receptor (Figure 7.2), assuming a stoichimetry equivalent to that postulated for vertebrates (Anand *et al.*, 1991; Cooper *et al.*, 1991).

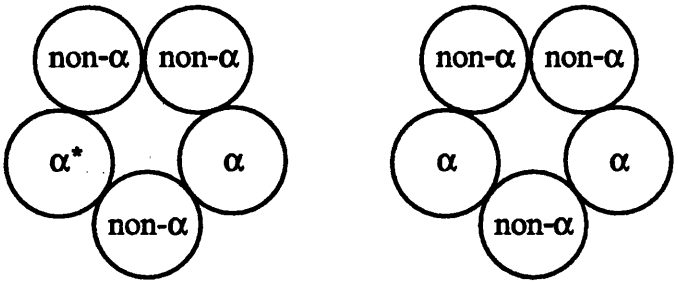

Figure 7.1. *Model 1 of aphid nAChR having 2 populations of receptors. [^{125}I]-α-BgTx, [^{3}H]-EPI, and [^{3}H]-IMI bind to a single alpha (*) with high affinity and to the other 3 with low affinity. The high affinity sites for α-BgTx, EPI and IMI are not necessarily the same α subunit (see text below). [^{3}H]-MLA is unable to distinguish between two kinds of α subunits and can bind to all 4 with equal affinity. The binding heterogeneity exhibited by the alpha subunit towards [^{125}I]-α-BgTx, [^{3}H]-EPI, and [^{3}H]-IMI could be due to differences in the genetic origin of the α subunits and/or the influencing effects of the adjacent non-α subunit.*

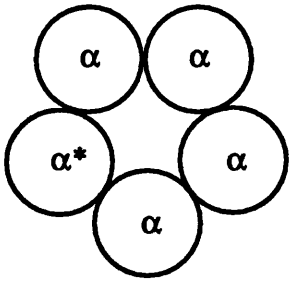

Figure 7.2. *Model 2 of the aphid nAChR shows a homomeric nAChR. The ratios of high and low affinity sites demonstrated by [^{125}I]-α-BgTx, [^{3}H]-EPI, and [^{3}H]-IMI have enough variability to represent a ratio of 1:4 which could be interpreted as a receptor having a complement of 5 α subunits. As in the previous model, the high affinity binding site (*) for [^{125}I]-α-BgTx, [^{3}H]-EPI, and [^{3}H]-IMI could have a different genetic origin from the other α subunits or the different affinities of this receptor subunit for ligand could arise from cooperative interactions. Also as previously mentioned, the high affinity binding sites for α-BgTx and IMI are probably not identical. [^{3}H]-MLA cannot pharmacologically distinguish between α subunits and binds to each with equal affinity.*

Evidence for a degree of heterogeneity at least equal to that postulated in models 1 and 2 at the genomic level comes from the cloning of genes for putative α subunit genes from *M. persicae* (Huang *et al.,* 1998; Huang *et al.,* 1999) which have revealed the presence of at least 6 different α and 1 non-α subunits. Therefore ample genetic heterogeneity exists to justify each of the 2 models in figures 7.1 and 7.2. The finding of multiple insect genes for nAChR subunits is not confined to *M. persicae* and sufficient genomic heterogeneity is also known to be present in *M. sexta* (Eastlake *et al.,* 1997; Eastham *et al.,* 1998), *L. migratoria* (Hermsen *et al.,* 1998) and *D. melanogaster* (reviewed in Gundelfinger (1992)). Moreover the inability so far to express any functional heteromeric insect nAChR could reflect their native subunit complexity (Lansdell *et al.,* 1997) which was confirmed with affinity purification (Tomizawa *et al.,* 1996). Further complementary work of *in vitro* expression and subsequent pharmacological characterisation together with purification and sequencing of native receptors is required to appraise the extent of multiplicity of aphid nAChR.

Displacement studies resolve distinct pharmacological populations of receptors

The question of whether the high affinity binding sites for [^{125}I]-α-BgTx, [^{3}H]-EPI, and [^{3}H]-IMI are the same is of interest. Pharmacological evidence suggests that [^{125}I]-α-BgTx is displaced with low potency by IMI (K_i=800nM) and with greater potency by EPI (K_i=25nM) whilst [^{3}H]-IMI is displaced well by EPI (K_i=5nM) and slightly less so by α-BgTx (K_i=14nM). [^{3}H]-EPI is displaced very well by IMI (K_i=0.5nM) and slightly less avidly by α-BgTx (K_i=5nM). Since the order of potency in displacement experiments differs for each labelled ligand, there is room to suggest that they may be binding to different sites. One simple hypothesis which could be drawn from the data is that EPI and IMI share a common site whereas α-BgTx labels a different site. Displacement studies suggest that MLA is a potent ligand at sites labelled with high affinity by [^{125}I]-α-BgTx, [^{3}H]-EPI, and [^{3}H]-IMI. Biphasic displacement curves obtained when [^{3}H]-MLA is displaced by α-BgTx, EPI, and IMI are likely to be due to displacement of [^{3}H]-MLA from at least 2 distinct binding sites, for which the

displacing ligands have different affinities, but which are indistinguishable by [^{3}H]-MLA (Chapter 5). Therefore MLA appears to label the α-BgTx and the IMI/EPI sites with high affinity. This simple model for the high affinity binding sites in *M. persicae* is shown in Figure 7.3.

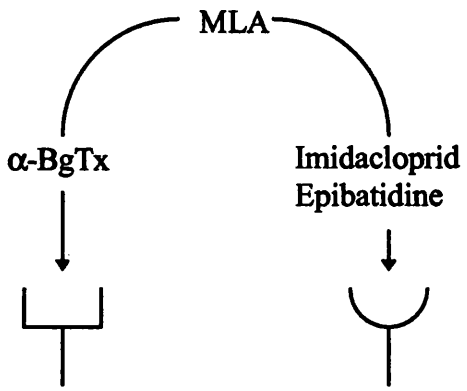

Figure 7.3. *Proposed simple model of high affinity binding of α-BgTx, MLA, imidacloprid and epibatidine in membranes of M. persicae.*

However caution must be exercised in evaluating this model, since true equilibrium conditions were not met in the binding experiments. This is particularly true for α-BgTx which was found to have very slow on and off rates under the conditions used here (Chapter 2). Furthermore the interaction between nAChR and its ligands is an allosteric one, and the receptor protein is capable of many conformational states which can influence the affinity of ligand binding (Prince and Sine, 1998; Changeux and Edelstein, 1998).

The possible non-identity of the α-BgTx and IMI sites in the insect membranes is perhaps not surprising, because IMI is in fact highly selective for insect nAChR. Studies by Liu and Casida (1993) demonstrated no specific high affinity binding of [^{3}H]-IMI in vertebrate brain (human, dog, mouse, chicken, electric eel), while others (Tomizawa *et al.,* 1995a; Eastham *et al.,* 1998) have shown that IMI is a poor

displacer of specifically bound α-BgTx at putative insect nAChR. This was confirmed in the present study (Chapter 2). Interestingly, molluscan neuronal tissue also does not have nAChR that bind IMI but which do bind α-BgTx (Chapters 2 and 5; Kato and Tettrie, 1974). Thus the site specificity of α-BgTx and IMI may be different.

7.2.6 Specificity of IMI binding to hemipteran insect nAChR

A comparison of [^{3}H]-IMI saturable binding in a panel of insects revealed that only the hemipteran membrane preparations contained multiple sites (Chapter 3). Moreover the affinity of the high affinity [^{3}H]-IMI site when compared to that in non-hemipteran insects was at least an order of magnitude higher. Chapter 6 examined the systemic uptake of [^{3}H]-IMI by aphids with the aim of determining internal lethal and sublethal concentrations. The extent of IMI metabolism that occurs in both the leaf and aphid made the determination of the exact concentration of [^{3}H]-IMI difficult to ascertain. Unchanged IMI accounted for only ~10% of the total recoverable tritium signal. According to Nauen *et al.* (1998b), however, the metabolites found in leaves are at least as potent as the parent compound. It is evident that the concentrations to bring about symptomology and mortality were very low in the nM range. Taken together, the [^{3}H]-IMI saturation binding and the quantification of internal [^{3}H]-IMI concentrations in aphids may help explain why IMI is particularly useful for the control of sucking pests.

7.3 Autoradiographic localisation of insect nAChR in the CNS

Head sections of *M. sexta* were used to localise nAChR in the CNS (Chapter 5). This work was undertaken first to confirm that [^{3}H]-MLA and [^{125}I]-α-BgTx were binding to areas of neural connections (and thus probably labelling putative nAChR), and second to examine spatial distributions of each ligand to identify any regions of nAChR with differing pharmacologies. Autoradiographic analysis of the distribution of [^{3}H]-MLA and [^{125}I]-α-BgTx binding sites in *M. sexta* shows discrete labelling of

neuropil areas of the optic and antennal lobes consistent with the expected location of putative nAChR determined previously using [^{125}I]-α-BgTx (Hildebrand *et al.*, 1979; Orr *et al.*, 1990; Goldberg *et al.*, 1999). Specific [^{125}I]-α-BgTx binding was also present in an area located external to the lamina and adjacent to the tapetum, a reflective tracheal structure at the base of the retina; a high level of non-specific binding unfortunately made determination of specific [^{3}H]-MLA binding difficult to assess in this brain region. The potential participation of nAChR in non-neuronal functions has been described in insects by Hermsen *et al.* (1998) and in vertebrates by Grando *et al.* (1995). This may be an interesting area for future research in insect neurobiology.

7.4 Overall Summary

The recent introduction of insecticides which target the insect nAChR has renewed interest in the pharmacology of these receptors. This study of putative insect nAChR has revealed considerable pharmacological heterogeneity consistent with multiple binding sites which may be present on the same receptor. Cloning of insect nAChR genes and cDNAs is revealing a growing portfolio of α and non-α subunit genes which differ in sequence homologies between insect Orders. The present study detected marked differences in numbers, affinities and pharmacologies of putative insect nAChR binding sites investigated with a range of nicotinic ligands which mirrors the heterogeneity that has been revealed at the genomic level. This information will be important at an applied level to help our future understanding of the interaction of neonicotinoid insecticides with the insect nAChR.

Appendix 1 - Structures
Neonicotinoid insecticides

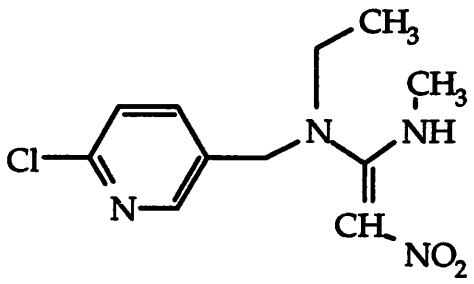

Nitenpyram

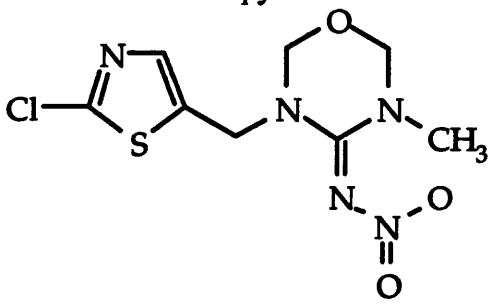

Thiamethoxam

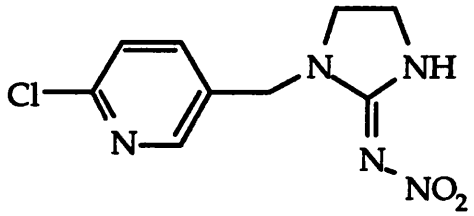

Imidacloprid (IMI)

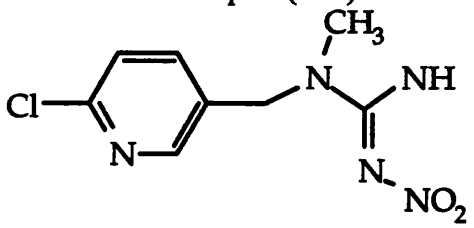

acetamiprid

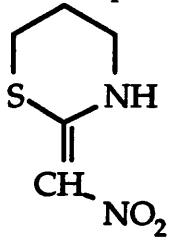

Nithiazin

Appendix 1 - Structures

Nicotinic ligands

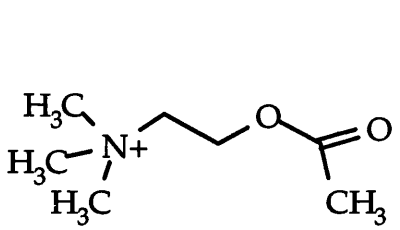

Acetylcholine (ACh)

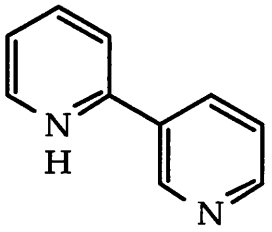

Anabasine

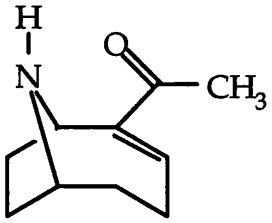

Anatoxin a

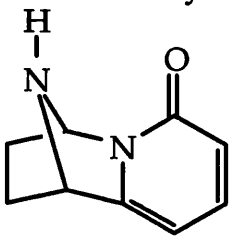

Cytisine

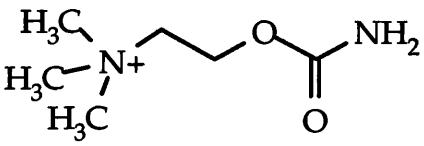

Carbachol

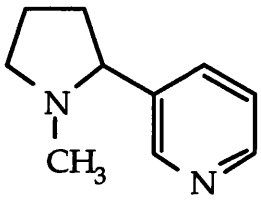

Nicotine

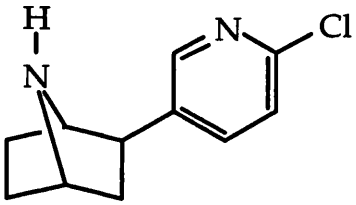

Epibatidine (EPI)

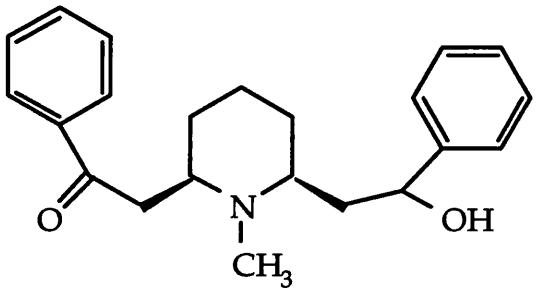

Lobeline

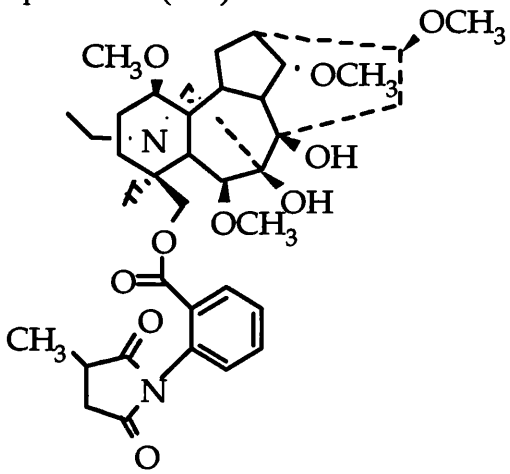

Methyllycaconitine (MLA)

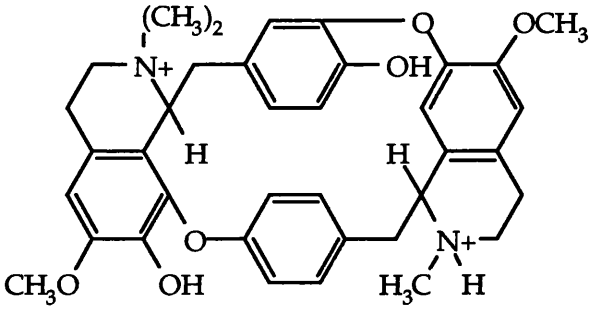

d-tubocurarine

Appendix 1 - Structures

Channel blockers

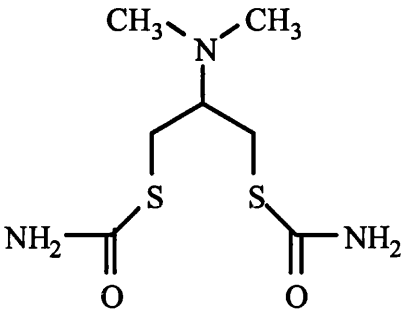

Cartap

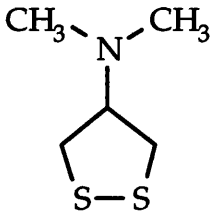

Nereistoxin

Appendix 1 - Structures

Muscarinic ligands

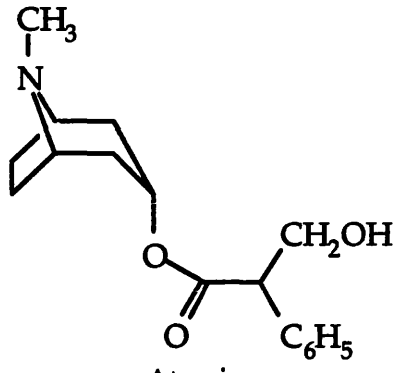

Atropine

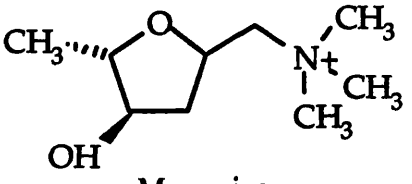

Muscarine

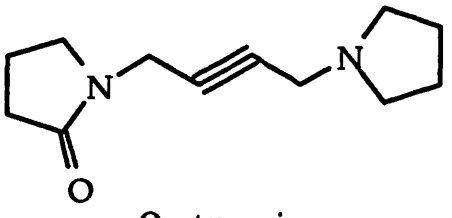

Oxotremorine

Appendix 1 - Structures

Acetylcholine esterase inhibitors

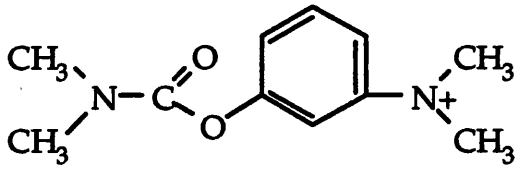

Neostigmine

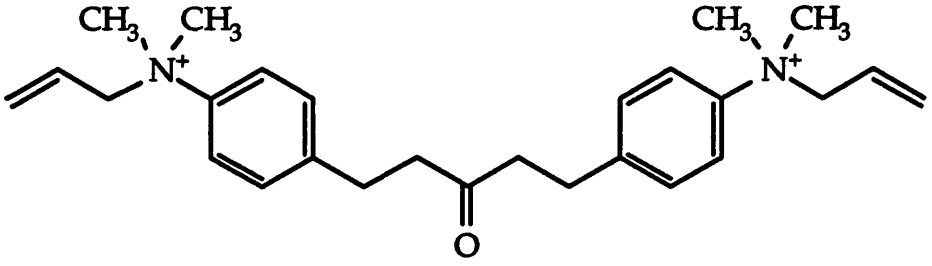

BW284c51 (1,5 bis(4 allyl dimethylammoniumphenyl)pentan3one)

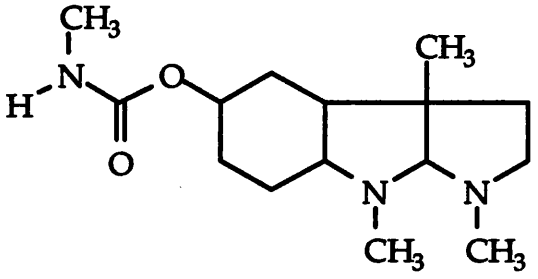

Physostigmine

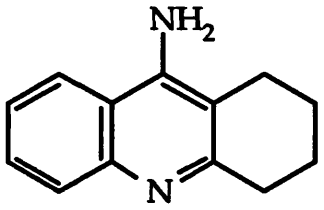

THA (9 amino 1,2,3,4 tetrahydroacridine hydrochloride)

Appendix 1 - Structures

Neurotransmitters

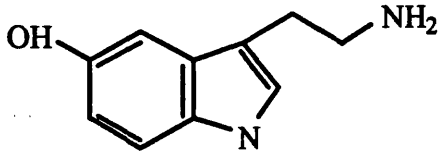

5-hydroxytripamine ($5HT_3$)

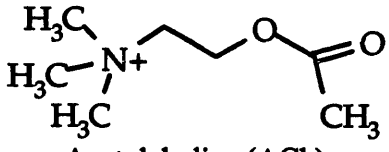

Acetylcholine (ACh)

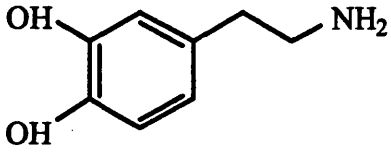

Dopamine

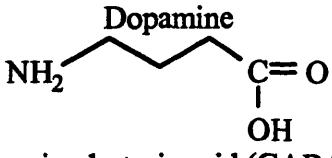

γ-amino butyric acid (GABA)

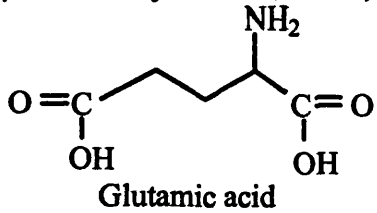

Glutamic acid

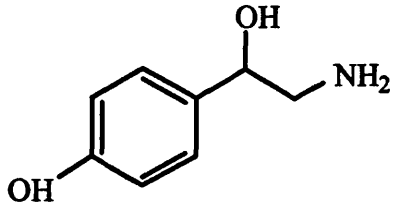

Octopamine

References

Abbink, J. (1991) The biochemistry of imidacloprid. *Pflanzenschutz Nachrichten Bayer.* **44:** 183-195.

Albert, J. L. and Lingle, C. J. (1993) Activation of nicotinic acetylcholine receptors on cultured *Drosophila* and other insect neurones. *J. Physiol.* **463:** 605-630.

Albuquerque, E. X., Maelicke. A. and Pereira, E. F. R. (1991) Single channel currents activated by physostigmine (phy) in hippocampal neurons are blocked by benzoquinonium (bzq) but not by methyllycaconitine (MLA). *Neurosci. Abstr.* **17:** 233-15.

Amar, M., Thomas, P., Wonnacott, S. and Lunt, G. G. (1995) A nicotinic acetylcholine receptor subunit from insect brain forms a non-desensitising homo-oligomeric nicotinic acetylcholine receptor when expressed in *Xenopus* oocytes. *Neurosci. Lett.* **199:** 107-110.

Anand, R., Conroy, W. G., Schoepfer, R., Whiting, P. and Lindstrom, J. (1991) Neuronal nicotinic acetylcholine receptors expressed in *Xenopus* oocytes have a pentameric quaternary structure. *J. Biol. Chem.* **266:** 11192-11198.

Anand, R., Peng, X. and Lindstrom, J. (1993) Homomeric and native α7 acetylcholine receptors exhibit remarkably similar but non-identical pharmacological properties, suggesting that the native receptor is a heteromeric protein complex. *FEBS Lett.* **327:** 241-246.

Anon (1994) Metabolism. *Nihon Noyaku Gakkaishi (J. Pestic. Sci.) Special issue.* **19:** 301-306.

Badio, B. and Daly, J. W. (1994) Epibatidine, a potent analgesic and nicotinic agonist. *Mol. Pharmacol.* **45:** 563-569.

Bai, D., Lummis, S. C. R., Leicht, W., Breer, H. and Sattelle, D. (1991) Actions of imidacloprid and a related nitromethylene on cholinergic receptors of an identified insect motor neurone. *Pestic. Sci.* **33:** 197-204.

Battersby, M. K. and Hall, S. G. (1985) Lobeline, a potent *O*-acetylcholine antagonist at cockroach nicotinic receptors, may be able to distinguish between nicotinic receptor sub-types in insects. *Pestic. Sci.* **16:** 429-431.

Baumann, A., Jonas, P. and Gundelfinger, E. D. (1990) Sequence of Dα2, a novel α-like subunit of *Drosophila* nicotinic acetylcholine receptors. *Nuc. Acids Res.* **18:** 3640.

Bell, R. A. and Joachim, F. G. (1976) Techniques for rearing laboratory colonies of tobacco hornworms and pink bollworms. *Ann. Entomol. Soc. America* **69:** 365-373.

Benson, J. A. (1989) Insect nicotinic acetylcholine receptors as targets for insecticides. In: *Progress and Prospects in Insect Control, BCPC Monograph No. 43* (McFarlane, N. R., ed) Farnham, UK: British Crops Protection Council. 59-70.

Benson, J. A. (1992) Electrophysiological pharmacology of the nicotinic and muscarinic cholinergic responses of isolated neuronal somata from locust thoracic ganglia. *J. exp. Biol.* **170:** 203-233.

Bertrand, D., Ballivet, M., Gomez, M., Bertrand, S., Phannavong, B. and Gundelfinger, E. D. (1994) Physiological properties of neuronal nicotinic receptors reconstituted from the vertebrate β2 subunit and *Drosophila* α subunits. *Eur. J. Neurosci.* **6:** 869-875.

Blackman, R. L. and Spence, J. M. (1992) Electrophoretic distinction between the peach-potato aphid, Myzus persicae, and the tobacco aphid, M. nicotianae (Homoptera: Aphididae). *Bulletin of Entomological Research.* **82:** 161-165.

Blagbrough, I. S., Coates, P. A., Hardick, D. J., Lewis, T., Rowan, M. G., Wonnacott, S., and Potter, B. V. L. (1994) Acylation of lycoctonine: semi-synthesis of inuline, delsemine analogues and methyllycaconitine. *Tetrahedron Lett.* **35:** 8705-8708.

Bossy, B., Ballivet, M. and Spierer, P. (1988) Conservation of neural nicotinic acetylcholine receptors from *Drosophila* to vertebrate central nervous systems. *EMBO J.* **7:** 611-618.

Boucias, D. G., Stokes, C., Storey, G. and Pendland, J. C. (1996) The effects of imidacloprid on the termite *Reticulitermes flavipes* and its interaction with the mycopathogen *Beauveria bassiana. Pflanzenschutz-Nachrichten Bayer.* **49:** 103-144.

Boulter, J., Connolly, J., Deneris, E., Goldman, D., Heinemann, S. and Patrick, J. (1987) Functional expression of two neuronal nicotinic acetylcholine receptors from cDNA clones identifies a gene family. *Proc. Natl. Acad. Sci. USA* **84:** 7763-7767.

Boulter, J., O'Shea-Greenfield, A., Duvoisin, R. M., Connolly, J. G., Wada, E., Jensen, A., Gardner, P. D., Ballivet, M., Deneris, E. S., McKinnon, D., Heinemann, S. and Patrick, J. (1990) α3, α5, and β4: Three members of the rat neuronal nicotinic acetylcholine receptor-related gene family form a gene cluster. *J. Biol. Chem.* **265:** 4472-4482.

Bowen, W. P., and Jerman, J. C. (1995) Nonlinear regression using spreadsheets. *Trends Pharmac. Sci.* **16:** 413-416.

Boyd, G. A. (1955) Autoradiography in Biology and Medicine. Academic Press. New York.

Bradford, M. M. (1976) A rapid sensitive method for the quantitation of microgram quantities of protein utilising the principle of protein dye binding, *Anal. Biochem.* **72:** 248-254.

Brake A.J., Wagenbach M.J. and Julius D. (1994) New structural motif for ligand-gated ion channels defined by an ionotropic ATP receptor. *Nature* **371:** 519-523.

Brattsten, L. B, Holyoke, C. W., Leeper, J. R. and Raffa, K. F. (1986) Insecticide resistance : Challenge to pest management and basic research. *Science.* **231:** 1255-1260.

Breer, H. (1981) Properties of putative nicotinic and muscarinic cholinergic receptors in the central nervous system of *Locusta migratoria. Neurochem. Int.* **3:** 43-52.

Breer, H., Kleene, R. and Hinz, G. (1985) Molecular forms and subunit structure of the acetylcholine receptor in the central nervous system of insects. *J. Neurosci.* **5:** 3386-3392.

Breer, H. and Sattelle, D. B. (1987) Molecular properties and functions of insect acetylcholine receptors. *J. Insect Physiol.* **33:** 771-790.

Bruns, R. F., Lawson-Wendling, K. and Pugsley, T. A. (1983) A rapid filtration assay for soluble receptors using polyethylenimine-treated filters. *Anal. Biochem.* **132:** 74-81.

Buckingham, S. D., Balk, M. L., Lummis, S. C. R., Jewess, P. and Sattelle, D. B. (1995) Actions of nitromethylenes on an α-bungarotoxin-sensitive neuronal nicotinic acetylcholine-receptor. *Neuropharmac.* **34:** 591-597.

Buckingham, S. D., Lapied, B., Le Corronc, H., Grolleau, F. and Sattelle, D. B. (1997) Imidacloprid actions on insect neuronal acetylcholine receptors, *J. exp. Biol.* **200:** 2685-2692.

Burrows, M. (1996) The neurobiology of an insect brain. Oxford University Press.

Bylund, D. B. and Yamamura, H. I. (1990) Methods for receptor binding. In: *Methods in neurotransmitter receptor analysis.* (Yamamura H.I., Enna S.J. and Kuhar M.J. eds) Raven Press, New York. 1-35.

Cachelin, A. B. and Jaggi, R. (1991) Beta subunits determine the time course of desensitization in rat alpha-3 neuronal nicotinic acetylcholine receptors. *Pfluegers Arch.* **419 (6):** 579-582.

Casida, J. E. and Quistad, G. B. (1998) Goldern age of insecticide research: Past, Present, or Future? *Annu. Rev. Entomol.* **43:** 1-16.

Cattell, K. J., Harris, R. and Donnellan, J. F. (1980) Characterisation of α-bungarotoxin binding to homogenates of housefly brain. In: *Neurotox '79: Insect Neurobiology and Pesticide Action* (Rickett, F. E., Bovier, J., Elliott, M., Ford, M. G., Graham-Bryce, I. J. and Sharp, D. H. eds) Society of the Chemical Industry, London 209-212.

Changeux, J-P., Kasai, M. and Lee, C-Y. (1970) Use of a snake venom toxin to characterise the cholinergic receptor protein. *Proc. Natl. Acad. Sci.* **67 (3):** 1241-1247.

Changeux, J-P., Devillers-Thiéry, A. and Chemouilli, P. (1984) Acetylcholine receptor: An allosteric protein. *Science* **225:** 1335-1345.

Changeux, J.P. (1993) Chemical signaling in the brain. *Scientific American.* **268 (5):** 30-37.

Changeux, J. P. and Edelstein, S. J. (1998) Allosteric receptors after 30 years. *Neuron* **21:** 959-980.

Chao, S. L. and Casida, J. E. (1997) Interaction of imidacloprid metabolites and analogs with the nicotinic acetylcholine receptor of mouse brain in relation to toxicity. *Pest. Biochem. Physiol.* **58:** 77-88.

Chao, S. L., Dennehy, T. J. and Casida, J. E., (1997) Whitefly (Hemiptera: Aleyrodidae) binding site for imidacloprid and related insecticides: a putative nicotinic acetylcholine receptor, *J. Econ. Ent.* **90:** 879-882.

Cheng, Y-C. and Prusoff, W. H. (1973) Relationship between the inhibition constant (K_i) and the concentration of inhibitor which causes 50 per cent inhibition (I_{50}) of an enzymatic reaction. *Biochem. Pharmacol.* **22:** 3099-3108.

Cheung, H., Clarke, B. S. and Beadle, D. J. (1992) A patch clamp study of the action of a nitromethylene heterocycle insecticide on cockroach neurons growing *in vitro*. *Pestic. Sci.* **34:** 187-193.

Clarke, P. B. S. and Reuben, M. (1996) Release of [^{3}H]noradrenaline from rat hippocampal synaptosomes by nicotine: mediation by different nicotinic receptor subtypes from striatal [^{3}H]dopamine release. *Brit. J. Pharmacol.* **117:** 595-606.

Coates, P. A., Blagbrough, I. S., Lewis, T., Potter, B. V. L., and Rowan, M. G. (1995) An HPLC assay for the norditerpenoid alkaloid methyllycaconitine, a potent nicotinic acetylcholine receptor antagonist. *J. Pharm. Biomed. Anal.* **13:** 1541-1544.

Cockcroft, V. B., Osguthorpe, D. J., Barnard, E. A. and Lunt, G. G. (1990) Modeling of agonist binding to the ligand-gated ion channel superfamily of receptors. *PROTEINS: Structure, Function, and Genetics* **8:** 386-397.

Cohen, J. B., Sharp, S. D. and Liu, W. S. (1991) Structure of the agonist-binding site of the nicotinic acetylcholine receptor tritiated acetylcholine mustard identifies residues in the cation-binding subsite. *J. Biol. Chem.* **266 (34):** 23354-23364.

Conroy, W. G., Vernallis, A. B. and Berg, D. K. (1992) The α5 gene product assembles with multiple acetylcholine receptor subunits to form distinctive receptor subtypes in brain. *Neuron* **9:** 679-691.

Conroy, W. G. and Berg, D. K. (1995) Neurons can maintain multiple classes of nicotinic acetylcholine receptors distinguished by different subunit compositions. *J. Biol. Chem.* **270:** 4424 4431.

Conti-Tronconi, B. M., Dunn, S. M. J., Barnard, E. A., Dolly, J. O., Lai, F. A., Ray, N. and Raftery, M. A. (1985) Brain and muscle nicotinic acetylcholine receptors are different but homologous proteins. *Proc. Natl. Acad. Sci. USA* **82:** 5208-5212.

Conti-Tronconi, B. M., Tang, F., Walgrave, S. and Gallagher, W. (1990) Nonequivalence of α-bungarotoxin binding sites in the native nicotinic receptor molecule. *Biochemistry.* **29:** 1046-1054.

Cooper, E., Couturier, S. and Ballivet, M. (1991) Pentameric structure and subunit stoichiometry of a neuronal nicotinic acetylcholine receptor. *Nature* **350:** 235-238.

Couturier, S., Bertrand, D., Matter, J-M., Hernandez, M-C., Bertrand, S., Millar, N., Valera, S., Barkas, T. and Ballivet, M. (1990a) A neuronal nicotinic acetylcholine receptor subunit (α7) is developmentally regulated and forms a homo-oligomeric channel blocked by α-btx. *Neuron* **5:** 847-856.

Couturier, S., Erkman, L., Valera, S., Rungger, D., Bertrand, S., Boulter, J., Ballivet, M. and Bertrand, D. (1990b) α5, α3, and non-α3. Three clustered avian genes encoding neuronal nicotinic acetylcholine receptor related subunits. *J. Biol. Chem.* **265:** 17560-17567.

Davies A. R. L., Hardick D. J., Blagbrough I. S., Potter B. V. L., Wolstenholme A. J. and Wonnacott S. (1999) Characterisation of the binding of [^{3}H]-methyllycaconitine: a new radioligand for labelling α7-type neuronal nicotinic acetylcholine receptors. *Neuropharmacology.* **38:** 679-690.

Deneris, E. S., Boulter, J., Connolly, J., Wada, E., Wada, K., Goldman, D., Swanson, L. W., Patrick, J. and Heinemann, S. (1989) Genes encoding neuronal nicotinic acetylcholine receptors. *Clin. Chem.* **35:** 731-737.

Devillers-Thiéry A., Galzi J-L., Eisele J. L., Bertrand S., Bertrand D. and Changeux J-P. (1993) Functional architecture of the nicotinic acetylcholine receptor: A prototype of ligand-gated ion channels. *J. Membrane Biol.* **136:** 97-112.

Devine, G. J., Harling, Z. K., Scarr, A. W., and Devonshire, A. L. (1996) Lethal and sublethal effects of imidacloprid on nicotine-tolerant *Myzus nicotianae* and *Myzus persicae*. *Pestic. Sci.* **48:** 57-62.

Devonshire, A. L. and Moores, G. D. (1984) Different forms of insensitive acetylcholinesterase in insecticide- resistant house-flies *(Musca domestica)*. *Pestic. Biochem. Physiol.* **21:** 336-340.

Devonshire, A. L. (1989) Insecticide resistance in *Myzus persicae* : From field to gene and back again. *Pestic. Sci.* **26:** 375-382.

Devonshire, A. L. and Field, L. M. (1991) Gene amplification and insecticide resistance. *Annual Review of Entomology.* **36:** 1-23.

Dively, G. P., Follett, P. A., Linduska, J. J. and Roderick, G. K. (1998) Use of imidacloprid-treated row mixtures for colorado potato beetle (Coleoptera: Chrysomelidae) management. *J. Econ. Entomol.* **91 (2):** 376-387.

Dudai, Y. and Amsterdam, A. (1977) Nicotinic receptors in the brain of *Drosophila melanogaster* demonstrated by autoradiography with [^{125}I]α-bungarotoxin. *Brain Res.* **130:** 551-555.

Dudai, Y. (1978) Properties of an α-bungarotoxin-binding cholinergic nicotinic receptor from *Drosophila melanogaster. Biochim. Biophys. Acta* **539:** 505-517.

Eastham, H. M., Lind, R. J., Clarke, B. S., Towner, P., Reynolds, S. E., Wolstenholme, A. J., and Wonnacott, S. (1998) Characterisation of a nicotinic acetylcholine receptor from the insect *Manduca sexta. Eur J. Neurosci.* **10:** 879-889.

Eastlake, J. L., Tearle, A. W., Wonnacott, S., Reynolds, S. E., Lunt G. G. and Wolstenholme, A. J. (1997) Nicotinic acetylcholine receptor subunits from *Manduca sexta. Soc. Neurosci Abstr.* **23:** 157.13.

Elbert, A., Becker, B., Hartwig, J. and Erdelen, C. (1991) Imidacloprid - a new systemic insecticide. *Pflanzenschutz-Nachrichten Bayer.* **44:** 113-136.

Elbert, A., Nauen, R., Cahill, M., Devonshire, A. L., Scarr, A. W., Sone, S. and Steffens, R. (1996) Resistance management with chloronicotinyl insecticides using imidacloprid as an example. *Pflanzenschutz-Nachrichten Bayer.* **49:** 5-54.

Eldefrawi, M. E. (1985) Nicotine. In: *Comprehensive Insect Physiology Biochemistry and Pharmacology* (Kerkut, G. A. and Gilbert, L. I. eds) Pergamon Press, Oxford. **12:** 263-272.

Elgoyhen, A. B., Johnson, D. S., Boulter, J., Vetter, D. E. and Heinemann, S. (1994) α9: An acetylcholine receptor with novel pharmacological properties expressed in rat cochlear hair cells. *Cell* **79:** 705-715.

Evans, H. E. (1984) Insect Biology. Addison-Wesley Publishing Company. London.

Ffrench-Constant, R. H., Rocheleau, T. A., Steichen, J. C. and Chalmers, A. E. (1993) A point mutation in a *Drosophila* GABA receptor confers insecticide resistance. *Nature* **363:** 449-451.

Filbin, M. T., Lunt, G. G. and Donnellan, J. F. (1983) Partial purification and characterisation of an acetylcholine receptor with nicotinic properties from the supraoesophageal ganglion of the locust *(Schistocerca gregaria). Eur. J. Biochem.* **132:** 151-156.

Galper, J. B., Klein, W. and Catterall, W. A. (1977) Muscarinic acetylcholine receptors in developing chick heart, *J. Biol. Chem.* **252:** 8692-8699.

Galzi, J-L., Bertrand, D., Devillers-Thiéry, A., Revah, F., Bertrand, S. and Changeux J-P. (1991) Functional significance of aromatic amino acids from three peptide loops of the α7 neuronal nicotinic receptor site investigated by site-directed mutagenesis. *FEBS Lett.* **294:** 198-202.

Georghiou, G. P. (1990) Overview of insecticide resistance. In: *Managing resistance to agrochemicals from fundamental research to practical strategies.* (Green, M. B., LeBaron, H. M. and Moberg, W. K. eds) Washington DC, American Chemical Society. 18-41.

Goldberg, F., Grünewald, B., Rosenboom, H., and Menzel, R. (1999) Nicotinic acetylcholine currents of cultured Kenyon cells from the mushroom bodies of honey bee *Apis mellifera. J. Physiol.* **514:** 759-768.

Goodman, C. S. and Spitzer, N. C. (1979) Embryonic development of identified neurones: differentiation from neuroblast to neurone. *Nature* **280:** 208-214.

Gotti, C., Ogando, A. E., Hanke, W., Schlue, R., Moretti, M. and Clementi, F. (1991) Purification and characterization of an α-bungarotoxin receptor that forms a functional nicotinic channel. *Proc. Natl. Acad. Sci. USA* **88:** 3258-3262.

Gotti, C., Hanke, W., Maury, K., Moretti, M., Ballivet, M., Clementi, F. and Bertrand, D. (1994) Pharmacology and biophysical properties of α7 and α7-α8 α-bungarotoxin receptor subtypes immunopurified from the chick optic lobe. *Eur. J. Neurosci.* **6:** 1281-1291.

Gould, R. J., Ginsberg, B. H. and Spector, A. A (1981) Effects of octyl β-glucoside on insulin binding to solubilized membrane receptors. *Biochemistry* **20:** 6776-6781.

Grafius, J. G. and Bishop, B. A. (1996) Resistance to imidacloprid in Colorado potato beetles from Michigan. *Resistant Pest Management.* **8:** 21-25.

Grando, S. A., Horton, R. M., Pereira, E. F. R., George, P. M., Diethelm-Okita, B. M., Albuquerque, E. X., and Conti-Fine, B. M. (1995) A nicotinic acetylcholine-receptor regulating cell-adhesion and motility is expressed in human keratinocytes. *J. Invest. Dermatol.* **105:** 774-781.

Green, W. G. and Wanamaker, C. P. (1998) Formation of the nicotinic acetylcholine receptor binding sites. *J. Neurosci.* **18:** 5555-5564.

Gundelfinger, E. D. (1992) How complex is the nicotinic receptor system of insects? *TINS* **15:** 206-211.

Gundelfinger, E. D. and Hess, N. (1992) Nicotinic acetylcholine receptors of the central nervous system of *Drosophila. Biochim. Biophys. Acta* **1137:** 299-308.

Gurthrie, F. E., Campbell, W. V. and Baron, R. L. (1962) Feeding sites of the green peach aphid with respect to its adaption to tobacco. *Ann. Entomol. Soc. Am.* **55:** 42-46.

Hall, L. M., Von Borstel, R. W., Osmond, B. C., Hoeltzli, S. D. and Hudson, T. H. (1978) Genetic variants in an acetylcholine receptor from *Drosophila melanogaster. FEBS Letts.* **95:** 243-246.

Hall, L. M. (1980) Biochemical and genetic analysis of an a-bungarotoxin-binding receptor from *Drosophila melanogaster.* In: *Receptors for Neurotransmitters, Hormones and Pheromones in Insects.* (Sattelle, D. B., Hall, L. M. and Hildebrand, J. G. eds) Elsevier/North-Holland Biomedical Press, Amsterdam. 111-124.

Hamaoka, T. (1990) Autoradiography of new era replacing traditional X-ray film. *Cell Technology.* **9:** 456-462.

Hanke, W. and Breer, H. (1986) Channel properties of an insect neuronal acetylcholine receptor protein reconstituted in planar lipid bilayers. *Nature* **321:** 171-174.

Hardick, D. J., Blagbrough, I. S., and Potter, B. V. L. (1996) Isotopic enrichment by asymmetric deuteriation. An investigation of the synthesis of deuteriated (S)-(-)-methylsuccinic acids from itaconic acid. *J. Amer. Chem. Soc.*, **118:** 5897-5903.

Harris, R., Cattell, K. J. and Donnellan, J. F. (1979) Identification of a putative nicotinic acetylcholine receptor in fractions from housefly brain. *Biochem. Soc. Trans.* **7:** 136-138.

Harrow, 1 .D., David, J. A. and Sattelle, D. B. (1982) Acetylcholine receptors of identified insect neurons. In: *Neuropharmacology of insects, Ciba Foundation Symposium 88* (Evered, D., O'Connor, M. and Whelan, J. eds) Pitman, London. 12-31.

Harvey, S. C., Maddox, F. N. and Luetje, C. W. (1996) Multiple determinants of dihydro-β-erythroidine sensitivity on rat neuronal nicotinic receptor a subunits. *J. Neurochem.* **67:** 1953-1959.

Hermans-Borgmeyer, 1., Zopf, D., Ryseck, R-P., Hovemann, B., Betz, H. and Gundelfinger, E. D. (1986) Primary structure of a developmentally regulated nicotinic acetylcholine receptor protein from *Drosophila. EMBO J.* **5:** 1503-1508.

Hermsen, B., Heiermann, R. and Maelicke, A. (1991) Cloning and expression of ganglionic nAChR genes from *Locusta migratoria. Biol. Chem. Hoppe Seyler* **372:** 891.

Hermsen, B., Stetzer, E., Thees, R., Heiermann, R., Schrattenholz, A., Ebbinghaus, U., Kretschmer, A., Methfessel, C., Reinhardt, R., and Maelicke, A. (1998) Neuronal nicotinic receptors in the locust *Locusta migratoria. J. Biol. Chem.* **273:** 18394-18404.

Hess, G. P. and Andrews, J. P. (1977) Functional acetyl choline receptor electroplax membrane micro sacs vesicles purification and characterization. *Proc. Natl. Acad. Sci. USA* **74 (2):** 482-486.

Hildebrand, J. G., Hall, L. M. and Osmond, B. C. (1979) Distribution of binding sites for ^{125}I-labeled α-bungarotoxin in normal and deafferented antennal lobes of *Manduca sexta. Proc. natl. Acad. Sci. USA.* **76:** 499-503.

Hjelmeland, L. M. and Chrambach, A. (1984) Solubilization of functional membrane-bound receptors. In: *Membranes, Detergents, and receptor solubilization* (Liss, A. R. ed), New York. 35-46.

Hoffman, P. W., Ravindran, A. and Huganir, R. L. (1994) Role of phosphorylation in desensitisation of acetylcholine receptors expressed in *Xenopus* oocytes. *J. Neurosci.* **14:** 4185-4195.

Hopfield, J. F., Tank, D. W., Greengard, P. and Huganir, R. L. (1988) Functional modulation of the nicotinic acetylcholine receptor by tyrosine phosphorylation. *Nature* **336:** 677-776.

Hosie, A. M., Aronstein, K., Sattelle, D. B. and ffrench-Constant, R H. (1997) Molecular biology of insect neuronal GABA receptors. *TINS.* **20:** 578-583.

Huang, Y., Williamson, M. S., Devonshire, A. L., Windass, J. D., Lansdell, S. J., and Millar, N. S. (1998) Molecular characterization of nicotinic acetylcholine receptor genes from the homopteran insects, *Myzus persicae* and *Bemisia tabaci. Neurotox '98 proceedings.*

Huang, Y., Williamson, M. S., Devonshire, A. L., Windass, J. D., Lansdell, S. J., and Millar, N. S. (1999) Molecular characterization and imidacloprid selectivity of nicotinic acetylcholine receptor subunits from the peach-potato aphid *Myzus persicae. J. Neurochem.* **73** (in press).

Hucho, F., Tsetlin, V. I. and Machold, J. (1996) The emerging three-dimensional structure of a receptor: The nicotinic acetylcholine receptor. *Eur. J. Biochem.* **239 (3):** 539-557.

Huesing, J. E. and Jones, D. (1987) A new form of antibiosis in *Nicotiana. Phytochemistry* **26 (5):** 1381-1384.

Huganir, R. L., Delcour, A. H., Greengard, P. and Hess, G. P. (1986) Phosphorylation of the nicotinic acetylcholine receptor regulates its rate of desensitization. *Nature* **321:** 774-776.

Hulme, E. C. and Birdsall, N. J. M. (1992) Strategy and tactics in receptor-binding studies, in *Receptor-ligand interactions: A practical approach* (Hulme, E. C. ed) IRL Press, New York. 64-176.

Jacobs, D. E., Hutchinson, M. J. and Krieger, K. J. (1997) Duration of activity of imidacloprid, a novel adulticide for flea control, against *Ctenocephalides felis* on cats. *Veterinary Record.* **140:** 259-260.

Jennings, K. R., Brown, D. G., and Wright Jr, D. P. (1986) Methyllycaconitine, a naturally occurring insecticide with a high affinity for the insect cholinergic receptor. *Experimenta* **42:** 611-613.

Jiminez, F. and Rudloff, E. (1980) Analysis of the solubilised nicotinic acetylcholine receptor of *Drosophila melanogaster. FEBS Lett.* **113:** 183-188.

Jonas, P., Baumann, A., Merz, B. and Gundelfinger, E. D. (1990) Structure and developmental expression of the Dα2 gene encoding a novel nicotinic acetylcholine receptor protein of *Drosophila melanogaster. FEBS Lett.* **269:** 264-268.

Jones, S. W., Sudershan, P. and O'Brien, R. D. (1981) α-Bungarotoxin binding in house fly heads and *Torpedo electroplax. J. Neurochem.* **36:** 447-453.

Kagabu, S. and Medej, S. (1995) Stability comparison of imidacloprid and related compounds under simulated sunlight, hydrolysis conditions, and to oxygen. *Bioscience, Biotechnology and Biochemistry.* **59 (6):** 980-985.

Kao, P. N., Dwork, A. J., Kaldany, R-R. J., Silver, M. L., Wideman, J., Stein, S. and Karlin, A. (1984) Identification of the α subunit half-cystine specifically labeled by an affinity reagent for the acetylcholine receptor binding site. *J. Biol. Chem.* **259:** 11662-11665.

Kao, P. N. and Karlin, A. (1986) Acetylcholine receptor binding site contains a disulfide cross-link between adjacent half-cystinyl residues. *J. Biol. Chem.* **261:** 8085-8088.

Kato, G. and Tattrie, B. (1974) Solubilization of the acetylcholine receptor protein from *Loligo opalescens* without detergents. *FEBS Letts.* **48 (1):** 26-31.

Kemp, G., Bentley, L., McNamee, M. G. and Morley, B. J. (1985) Purification and characterization of the α-bungarotoxin binding protein from rat brain. *Brain Res.* **347:** 274-283.

Klein, O. (1994) Metabolism of imidacloprid in plants. *Book of abstracts IUPAC congress.* **Volume 1.** Washington DC, 2B-157.

Koppenhofer, A. M. and Kaya, H. K. (1998) Synergism of imidacloprid and an entomopathogenic nematode: a novel approach to white grub (Coleoptera: Scarabaeidae) control in turfgrass. *J. Econ. Entomol.* **91 (3):** 618-623.

Kubalek, E., Ralston, S., Lindstrom, J. and Unwin, N. (1987) Location of subunits within the acetylcholine receptor by electron image analysis of tubular crystals from *torpedo-marmorata. J. Cell Biol.* **105 (1):** 9-18.

Lagadic, L., Weile, M., Leicht, W., Salt, D. W., Greenwood, R. and Ford, M. G. (1994) Pharmacokinetics of cyfluthrin in *Spodoptera littoralis* (Boisd.). II. Effects of lindane pretreatment on the toxicity and *in vivo* metabolism of cyfluthrin in susceptible larvae. *Pestic. Biochem. Physiol.* **48:** 173-184.

Lane, N. J., Le B. Skaer, H. and Swales, L. S. (1977) Intercellular junctions in the central nervous system of insects. *J. Cell Sci.* **26:** 175-199.

Lansdell, S. J., Schmitt, B., Betz, H., Sattelle, D. B. and Millar, N. S. (1997) Temperature-sensitive expression of *Drosophila* neuronal nicotinic acetylcholine receptors. *J. Neurochem.* **68:** 1812-1819.

Latli, B. and Casida, J. E. (1992) [^{3}H]Imidacloprid: Synthesis of a candidate radioligand for the nicotinic acetylcholine-receptor. *J. Labelled Compd. Radiopharm.* **31:** 609-613.

Leech, C. A., Jewess, P., Marshall, J. and Sattelle, D. B. (1991) Nitromethylene actions on *in situ* and expressed insect nicotinic acetylcholine-receptors. *FEBS Lett.* **290:** 90-94.

Lees, G., Beadle, D. J. and Botham, R. P. (1983) Cholinergic receptors on cultured neurones from the central nervous system of embryonic cockroaches. *Brain Res.* **288:** 49-59.

Leitch, B., Watkins, B. L. and Burrows, M. (1993) Distribution of acetylcholine receptors in the central nervous system of adult locusts. *J. Comp. Neurol.* **334:** 47-58.

Leicht, W. (1993) Imidacloprid - A chloronicotinyl insecticide. *Pesticide Outlook.* **4:** 17-21.

Leicht, W. (1996) Imidacloprid - a chloronicotinyl insecticide: biological activity and agricultural significance. *Pflanzenschutz Nachrichten Bayer.* **49:** 71-84.

Le Novere, N. and Changeux, J-P. (1995) Molecular evolution of the nicotinic acetylcholine receptor: An example of multigene family in excitable cells. *J. Mol. Evol.* **40:** 155-172.

Lindstrom, J., Merlie, J. and Yogeeswaran, G. (1979) Biochemical properties of acetylcholine receptor subunits from *Torpedo californica. Biochemistry* **18:** 4465-4470.

Lindstrom, J., Anand, R., Peng, X., Gerzanich, V., Wang, F. and Li, Y. (1995) Neuronal nicotinic receptor subtypes. *Ann. N. Y. Acad. Sci.*, **757:** 100-116.

Lippiello, P. M., Sears, S. B. and Fernandes, K. G. (1987) Kinetics and mechanism of L-[^{3}H]nicotine binding to putative high affinity receptor sites in rat brain. *Mol. Pharmacol.* **31:** 392-400.

Liu, M. Y., Lanford, J. and Casida, J. E. (1993) Relevance of [3H]imidacloprid binding sites in house fly head acetylcholine receptors to insecticidal activity of 2-nitromethylene- and 2-nitroamino-imidazolidines. *Pestic. Biochem. Physiol.* **46:** 200-206.

Liu, M. Y. and Casida, J. E. (1993) High affinity binding of [^{3}H]-Imidacloprid in the insect acetylcholine receptor. *Pestic. Biochem. Physiol.* **46:** 40-46.

Liu, M. Y., Latli, B. and Casida, J. E. (1994) Nitromethyleneimidazolidine radioligand ([^{3}H]-NMI) - high-affinity and cooperative binding for house-fly acetylcholine-receptor. *Pestic. Biochem. Physiol.* **50:** 171-182.

Liu, M., Latli, B. and Casida, J. E (1995) Imidacloprid binding site in *Musca* nicotinic acetylcholine receptor: interactions with physostigmine and a variety of nicotinic agonists with chloropyridyl and chlorothiazolyl substituents, *Pestic. Biochem. Physiol.* **52:** 170-181.

Luetje, C. W. and Patrick, J. (1991) Both the α- and β-subunits contribute to the agonist sensitivity of neuronal nicotinic acetylcholine receptors. *J. Neurosci.* **11:** 837-845.

Lukas, R. J., Morimoto, H., Hanley, M. R. and Bennett, E. L. (1981) Radiolabeled α-bungarotoxin derivatives: kinetic interaction with nicotinic acetylcholine receptors. *Biochem.* **20:** 7373-7376.

Lummis, S. C. R. and Sattelle, D. B. (1985) Binding of N-[propionyl-^{3}H]propionylated α-bungarotoxin and L-[benzilic-4,4'-3H]quinuclidinyl benzilate to CNS extracts of the cockroach *Periplaneta americana. Comp. Biochem. Physiol.* **80C:** 75-83.

MacAllan, D. R. E., Lunt, G. G., Wonnacott, S., Swanson, K. L., Rapoport, H. and Albuquerque, E. X. (1988) Methyllycaconitine and (+)-anatoxin-a differentiate between nicotinic receptors in vertebrate and invertebrate nervous systems. *FEBS Lett.* **226:** 357-363.

Maddrell, S. H. P. and Gardiner, B. O. C. (1976) Excretion of alkaloids by malpighian tubules of insects. *J. exp. Biol.* **64:** 267-281.

Mansou, N. A., Pessah, l. N. and Eldefrawi, A. T. (1980) Binding of [^{125}I]α-bungarotoxin and reversible cholinergic ligands to proteins in housefly brains. In: *Neurotox '79: Insect Neurobiology and Pesticide Action* (Rickett F.E., Bovier J., Eliott M., Ford M.G., Graham-Bryce I.J. and Sharp D.H. eds) Society of Chemical Industry, London. 201-207.

Marks, M. J., Stitzel, J. A., Romm, E., Wehner, J. M. and Collins, A. C. (1986) Nicotinic binding sites in rat and mouse brain: Comparison of acetylcholine, nicotine and α-bungarotoxin. *Mol. Pharmacol.* **30:** 427-436.

Marshall, J., David, J. A., Darlison, M. G., Barnard, E. A. and Sattelle, D. B. (1988) Pharmacology, cloning and expression of insect nicotinic acetylcholine receptors. In: *Nicotinic acetylcholine receptors in the nervous system.* (Clementi, F., Gotti, C. and Sher, E. eds) Springer-Verlag, Berlin. Nato ASI series H **25:** 257-281.

Marshall, J., Buckingham, S. D., Shingai, R., Lunt, G. G., Goosey, M. W., Darlison, M. G., Sattelle, D. B. and Barnard, E. A. (1990) Sequence and functional expression of a single α subunit of an insect nicotinic acetylcholine receptor. *EMBO J.* **9:** 4391-4398.

Martinez-Torres, D., Chandre, F., Williamson, M. S., Darriet, F., Berge, J. B., Devonshire, A. L., Guillet, P., Pasteur, N. and Pauron, D. (1998) Molecular characterization of pyrethroid knockdown resistance (*kdr*) in the major malaria vector *Anopheles gambiae* s.s. *Insect Mol. Biol.* **7 (2):** 179-184.

Martino-Barrows, A. M. and Kellar, K. J. (1987) [^{3}H]Acetylcholine and [^{3}H]nicotine label the same recognition site in rat brain. *Mol. Pharmacol.* **31:** 169-174.

Matsuda, K., Buckingham, S. D., Freeman, J. C., Squire, M. D., Baylis, H. A. and Sattelle, D. B. (1998) Effects of the α subunit on imidacloprid sensitivity of recombinant nicotinic acetylcholine receptors. *British J. Pharmacol.* **123:** 518-524.

McCarthy, M. P. and Stroud, R. M. (1989) Conformational states of the nicotinic acetylcholine receptor from *Torpedo californica* induced by the binding of agonists, antagonists, and local anesthetics. Equilibrium measurements using tritium-hydrogen exchange. *Biochemistry.* **28 (1):** 40-48.

McGehee, D. S., Heath, M. J. S., Gelber, S., Devay, P. and Role, L. W. (1995) Nicotine enhancement of fast excitatory synaptic transmission in CNS by presynaptic receptors. *Science* **269:** 1692-1696.

McGehee, D. S. and Role, L. W. (1995) Physiological diversity of nicotinic acetylcholine receptors expressed by vertebrate neurons. *Ann. Rev. Physiol.* **57:** 521-546.

Metcalf, R. L. (1989) Insect resistance to insecticides. *Pestic. Sci.*. **26:** 333-358.

Meyer, M. R. and Reddy, G. R. (1985) Muscarinic and nicotinic cholinergic binding sites in the terminal abdominal ganglion of the cricket (*Acheta domesticus*). *J. Neurochem.* **45:** 1101-1112.

Miles, K., Audigier, S. S. M., Greengard, P. and Huganir, R. L. (1994) Autoregulation of phosphorylation of the nicotinic acetylcholine receptor. *J. Neurosci.* **14:** 3271-3279.

Mishina, M., Tobimatsu, T., Imoto, K., Tanaka, K.-i, Fujita, Y., Fukuda, K., Kurasaki, M., Takahashi, H., Morimoto, Y., Hirose, T., Inayama, S., Takahashi, T., Kuno, M. and Numa, S. (1985) Location of functional regions of acetylcholine receptor α-subunit by site-directed mutagenesis. *Nature* **313:** 364-369.

Morris, C. E. (1983a) Uptake and metabolism of nicotine by the CNS of a nicotine-resistant insect, the tobacco hornworm *(Manduca sexta). J. Insect Physiol.* **29:** 807-817.

Morris, C. E. (1983b) Efflux of nicotine and its CNS metabolites from the nerve cord of the tobacco hornworm, *Manduca sexta. J. Insect Physiol.* **29:** 953-959.

Morris, C. E. (1983c) Efflux patterns for organic molecules from the CNS of the tobacco hornworm, *Manduca* sexta. *J. Insect Physiol.* **29:** 961-966.

Morris, C. E. (1984) Electrophysiological effects of cholinergic agents on the CNS of a nicotine resistant insect, the tobacco hornworm *(Manduca* sexta). *J. Exp. Zool.* **229:** 361-374.

Morris, C. E. and Harrison, J. B. (1984) Central nervous system features of a nicotine-resistant insect, the tobacco hornworm *Manduca* sexta. *Tissue and Cell* **16:** 601-612.

Mulle, C., Vidal, C., Benoit, P. and Changeux, J-P. (1991) Existence of different subtypes of nicotinic acetylcholine receptors in the rat habenulo-interpeduncular system. *J. Neurosci.* **11:** 2588-2597.

Nagata, K., Iwanaga, Y., Shono, T. and Narahashi, T. (1997) Modulation of the neuronal nicotinic acetylcholine receptor channel by imidacloprid and cartap. *Pestic. Biochem. Physiol.* **59:** 119-128.

Nambi-Aiyar V., Benn M. H., Hanna T., Jacyno J., Roth S. H., and Wilkens J. L. (1979) The principle toxin of *Delphinium brownii* (Rydb.) and its mode of action. *Experimenta* **35:** 1367-1368.

Narahashi, T. (1988) Mechanism of tetrodotoxin and saxitoxin action. In: *Handbook of natural toxins Vol. 3, Marine toxins and venoms.* (Tu, A. T. ed) Marcell Dekker, Inc., New York. Pp 185-210.

Narahashi, T. (1992) Nerve membrane Na+ channels as targets of insecticides. *Trends Pharmacol. Sci.* **13:** 236-241.

Nauen, R. (1995) Behaviour modifying effects of low systemic concentrations of imidaloprid on Myzus persicae with special reference to an antifeeding response. *Pestic. Sci.*. **44:** 145-153.

Nauen, R., Strobel, J., Tietjen, K., Otsu, Y. and Elbert, A. (1996) Aphicidal activity of imidacloprid against a tobacco feeding strain of *Myzus persicae* (Homoptera: Aphididae) from Japan closely related to *Myzus nicotianae* and highly resistant to carbamates and organophosphates. *Bull. Entomol. Res.* **86:** 165-171.

Nauen, R. and Elbert, A. (1997) Apparent tolerance of a field-collected strain of *Myzus nicotianae* to imidacloprid due to strong antifeeding responses. *Pestic. Sci.* **49:** 252-258.

Nauen, R., Hungenberg, H., Tollo, B., Tietjen, K. and Elbert, A. (1998a) Antifeedant effect, biological efficacy and high affinity binding of imidacloprid to acetylcholine receptors in *Myzus persicae* and *Myzus nicotianae*. *Pestic. Sci.* **53 (2):** 133-140.

Nauen, R., Tietjen, K., Wagner, K. and Elbert, A. (1998b) Efficacy of plant metabolites of imidacloprid against *Myzus persicae* and *Aphis gossypii* (Homoptera: Aphididae). *Pestic. Sci.* **52:** 53-57.

Nauen, R, Ebbinghaus, U. and Tietjen, K. (1999) Ligands of the nicotinic acetylcholine receptor as insecticides. *Pestic. Sci.* **55:** 608-610.

Nørby, J. G., Ottolenghi, P. and Jensen, J. (1980) Scatchard Plot: Common misinterpretation of binidng experiments. *Analytical Biochem.* **102:** 318-320.

Norman, R. I., Mehraban, F., Barnard, E. A. and Dolly, J. O. (1982) Nicotinic acetylcholine receptor from chick optic lobe. *Proc. Natl. Acad. Sci. USA* **79:** 1321-1325.

Ohana, B. and Gershoni, J. M. (1990) Comparison of the toxin binding sites of the nicotinic acetylcholine receptor from *Drosophila* to human. *Biochemistry* **29:** 6409-6415.

Okazawa, A., Akamatsu, M., Ohoka, A., Nishiwaki, H., Cho, W., Nakagawa, Y., Nishimura, K. and Ueno, T. (1998) Prediction of the binding mode of imidacloprid and related compounds to house-fly head acetylcholine receptors using three-dimensional QSAR analysis. *Pectic. Sci.* **54:** 134-144.

Ong, D. E. and Brady, R. N. (1974) Isolation of cholinergic receptor protein(s) from *Torpedo nobiliana* by affinity chromatography. *Biochemistry.* **13 (14):** 2822-2827.

Orr, G. L., Orr, N. and Hollingworth, R. M. (1990) Localization and pharmacological characterization of nicotinic-cholinergic binding sites in cockroach brain using α- and neuronal bungarotoxin. *Insect Biochem.* **20:** 557-566.

Orr, N., Shaffner,, A. J. and Watson, G. B. (1997) Pharmacological characterization of an epibatidine binding site in the nerve cord of *Periplaneta americana. Pestic. Biochem. Physiol.* **58:** 183-192.

Ortells M. O. and Lunt G. G. (1995) Evolutionary history of the ligand-gated ion channel superfamily of receptors. *TINS* **18:** 121-127.

Osborne, C. S., Cattell, K. J. and Donnellan, J. F. (1982) Affinity labelling of a putative nicotinic acetylcholine receptor from *Musca domestica. Biochem. Soc. Trans.* **10:** 372.

Papke, R. L., Boulter, J., Patrick, J. and Heinemann, S. (1989) Single-channel currents of rat neuronal nicotinic acetylcholine receptors expressed in *Xenopus* oocytes. *Neuron* **3:** 589-596.

Papke, R. L. and Heinemann, S. (1991) The role of the β4-subunit in determining the kinetic properties of rat neuronal nicotinic acetylcholine α3-receptors. *J. Physiol.* **440:** 95-112.

Parr, J. C. and Thurston, R. (1972) Toxicity of nicotine in synthetic diets to larvae of the tobacco hornworm. *Ann. Entomol. Soc. America* **65:** 1185-1188.

Pederson, S. E. and Cohen, J. B. (1990) *d*-Tubocurarine binding sites are located at α-γ and α-δ subunit interfaces of the nicotinic acetylcholine receptor. *Proc. Natl. Acad. Sci. USA* **87:** 2785-2789.

Pedersen, S. E. and Papineni, V. L. (1995) Interaction of *d*-tubocurarine analogs with the *Torpedo* nicotinic acetylcholine receptor. Methylation and stereoisomerization affect site- selective competitive binding and binding to the noncompetitive site. *J. Biol. Chem.* **270 (52):** 31141-31150.

Prince, R. J. and Sine, S. M. (1998) Epibatidine binds with unique site and state selectivity to muscle nicotinic acetylcholine receptors. *J. Biol. Chem.* **273:** 7843-7849.

Raftery, M. A., Hunkapillar, M. W., Strader, C. D. and Hood, L. E. (1980) Acetylcholine receptor: complex of homologous subunits. *Science* **280:** 1454-1457.

Ramirez-Latorre, J., Yu, C. R., Qu, X., Perin, F., Karlin, A. and Role, L. (1996) Functional contributions of α5 subunit to neuronal acetylcholine receptor channels. *Nature* **380:** 347-351.

Rapier, C., Wonnacott, S., Lunt, G. G., and Albuquerque, E. X. (1987) The neurotoxin histrionicotoxin interacts with the putative ion channel of the nicotinic acetylcholine receptors in the central nervous system. *FEBS Lett.* **212 (2):** 292-296.

Restifo, L. L. and White, K. (1990) Molecular and genetic approaches to neurotransmitter and neuromodulator systems in *Drosophila. Adv. Insect Physiol.* **22:** 115-219.

Reynolds, S. E., Yeomans, M. R. and Timmins, W. A. (1986) The feeding behavior of caterpillars *Manduca sexta* on tobacco and on artificial diet. *Physiol. Entomol.* **11 (1):** 39-52.

Rouchard, J., Gustin, F. and Wauters A. (1996) Imidacloprid insecticide soil metabolism in sugar beet field crops. *Bull. Environ. Contam. Toxicol.* **56:** 29-36.

Rudloff, E. (1978) Acetylcholine receptors in the central nervous system of *Drosophila melanogaster. Exp. Cell Res.* **111:** 185-190.

Rudloff, E., Jimenez, F. and Bartels, J. (1980) Purification and properties of the nicotinic acetylcholine receptor of *Drosophila melanogaster.* In: *Receptors for Neurotransmitters, Hormones and Pheromones in Insects.* (Sattelle, D. B., Hall, L. M. and Hildebrand, J. G., eds) Elsevier/North Holland Biomedical Press, Amsterdam. 85-92.

Salgado, V. L., Watson, G. B. and Sheets, J. J. (1997) Studies on the mode of action of spinosad, the active ingredient in Tracer® insect control. *Proc. Beltwide Cotton Conf.* 1082-1086.

Salgado, V. L. (1998a) Studies on the mode of action of spinosad: insect symptoms and physiological correlates. *Pestic. Biochem. Physiol.* **60:** 91-102.

Salgado, V. L. (1998b) Studies on the mode of action of spinosad: the internal effective concentration and the concentration dependence of neural excitation. *Pestic. Biochem. Physiol.* **60:** 103-110.

Sanes, J. R., Prescott, D. J. and Hildebrand, J. G. (1977) Cholinergic neurochemical development of normal and deafferented antennal lobes during metamorphosis of the moth, *Manduca* sexta. *Brain Res.* **119:** 389-402.

Sargent P. B. (1993) The diversity of neuronal nicotinic acetylcholine receptors. *Annu. Rev. Neurosci.* **16:** 403-443.

Satow, Y., Cohen, G. H., Padlan, E. A. and Davies, D. R. (1987) Phosphocholine binding immunoglobulin fab mcpc-603 an x-ray diffraction study at 2.7 angstrom. *J. Mol. Biol.* **190 (4):** 593-604.

Sattelle, D. B. (1980) Acetylcholine receptors of insects. *Adv. Insect Physiol.* **15:** 215-315.

Sattelle, D. B., Harrow, 1. D., Hue, B., Pelhate, M., Gepner, J. 1. and Hall, L. M. (1983) α-Bungarotoxin blocks excitatory synaptic transmission between cercal sensory neurones and giant interneurone 2 of the cockroach, *Penplaneta americana. J. exp. Biol.* **107:** 473-489.

Sattelle, D. B., Harrow, I. D., David, J. A., Pelhate, M., Callec, J. J., Gepner, J. I. and Hall, L. M. (1985) Nereistoxin: actions on a CNS acetylcholine receptor/ion channel in the cockroach *Periplaneta americana. J. Exp. Biol.* **118:** 37-52.

Sattelle, D. B., Buckingham, S. D., Wafford, K. A., Sherby S., Bakry, M., Eldefrawi, A. T., Eldefrawi, M. E. and May, T. E. (1989a) Actions of the insecticide 2-(nitromethylene)tetrahydro-1,3-thiazine on insect and vertebrate nicotinic acetylcholine receptors. *Proc. R. Soc. B.* **237:** 501-514.

Sattelle, D. B., Pinnock, R. D., and Lummis, S. C. R. (1989b) Voltage-independent block of a neuronal nicotinic acetylcholine receptor by N-methyllycaconitine. *J. Exp. Biol.* **142:** 215-224.

Sawruk, E., Hermans-Borgmeyer, 1., Betz, H. and Gundelfinger, E. D. (1988) Characterization of an invertebrate nicotinic acetylcholine receptor gene: the ard gene of *Drosophila melanogaster. FEBS Lett.* **235:** 40-46.

Sawruk, E., Schloß, P., Betz, H. and Schmitt, B. (1990a) Heterogeneity of *Drosophila* nicotinic acetylcholine receptors: SAD, a novel developmentally regulated α-subunit. *EMBO J.* **9:** 2671-2677.

Sawruk, E., Udri, C., Betz, H. and Schmitt, B. (1990b) SBD, a novel structural subunit of the *Drosophila* nicotinic acetylcholine receptor, shares its genomic localization with two α-subunits. *FEBS Lett.* **273:** 177-181.

Schloß, P., Hermans-Borgmeyer, 1., Betz, H. and Gundelfinger, E. D. (1988) Neuronal acetylcholine receptors in *Drosophila:* the ARD protein is a component of a high-affinity α-bungarotoxin binding complex. *EMBO J.* **7:** 2889-2894.

Schloß, P., Betz, H., Schröder, C. and Gundelfinger, E. D. (1991) Neuronal nicotinic acetylcholine receptors in *Drosophila:* Antibodies against an α-like and a non-α-subunit recognize the same high-amnity a-bungarotoxin binding complex. *J. Neurochem.* **57:** 1556-1562.

Schmidt-Glenewinkel, T., Venkatesh, T. R. and Hall, L. M. (1981) Purification and subunit composition of a putative acetylcholine receptor from *Drosophila melanogaster. Soc. Neurosci. Abs.* **7:** 703.

Schmidt-Nielsen, B. K., Gepner, J. L., Teng, N. N. H. and Hall, L. M. (1977) Characterization of an α-bungarotoxin binding component from *Drosophila melanogaster*. *J. Neurochem.* **29:** 1013-1029.

Schoepfer, R., Whiting, P., Esch, F., Blacher, R., Shimasaki, S. and Lindstrom J. (1988) cDNA clones coding for the structural subunit of a chicken brain nicotinic acetylcholine receptor. *Neuron* **1:** 241-248.

Schoepfer R., Conroy W. G., Whiting P., Gore M. and Lindstrom J. (1990) Brain α-bungarotoxin binding protein cDNAs and MAbs reveal subtypes of this branch of the ligand-gated ion channel gene superfamily. *Neuron* **5:** 35-48.

Schrattenholz, A., Godovac-Zimmermann, J., Schafer, H-J. and Albuquerque, E. X. (1993) Photoaffinity labeling of *Torpedo* acetylcholine receptor by physostigmine. *Eur. J. Biochem.* **216:** 671 -677.

Schröder, M. E. and Flattum, R. F. (1984) The mode of action and neurotoxic properties of the nitromethylene heterocycle insecticides. *Pestic. Biochem. Physiol.* **22:** 148-160.

Schulz, R., Sawruk, E., Mulhardt, C., Bertrand, S., Baumann, A., Phannavong, B., Betz, H., Bertrand, D., Gundelfiner, E. D. and Schmitt, B. (1998) Dα3, a new functional α subunit of nicotinic acetylcholine receptors from *Drosophila*. *J. Neurochem.* **71:** 853-862.

Schuster, R., Phannavong, B., Schröder, C. and Gundelfinger, E. D. (1993) Immunohistochemical localization of a ligand-binding and a structural subunit of nicotinic acetylcholine receptors in the central nervous system of *Drosophila melanogaster*. *J. Comp. Neurol.* **335:** 149-162.

Self, L. S., Guthrie, F. E. and Hodgson, E. (1964) Adaptation of tobacco hornworms to the ingestion of nicotine. *J. Insect Physiol.* **10:** 907-914.

Senn, R., Hofer, D., Hoppe, T., Angst, M., Wyss, P., Wyss, P., Brandl, F., Maienfisch, P., Zang, L. and White, S. (1998) CGA 293'343: a novel broad-spectrum insecticide supporting sustainable agriculture worldwide. *Proceedings of BCPC.* **1:** 27-36.

Sgard, F., Obosi, L. A., King, L. A. and Windass, J. D. (1993) ALS and SAD-like nicotinic acetylcholine receptor subunit genes are widely distributed in insects. *Insect Mol. Biol.* **2:** 215-223.

Sgard, F., Fraser, S. P., Katkowska, M. J., Djamgoz, M. B. A., Dunbar, S. J. and Windass, J. D. (1998) Cloning and functional characterisation of two novel nicotinic acetylcholine receptor α subunits from the insect pest *Myzus persicae*. *J. Neurochem.* **71:** 903-912.

Shaw, K. P., Aracava, Y., Akaike, A., Daly, J. W., Rikett, D. L. and Albuquerque, E. X. (1985) The reversible cholinesterase inhibitor physostigmine has channel-blocking and agonist effects on the acetylcholine receptor-ion channel complex. *Mol. Pharmacol.* **28:** 527-538.

Shirai, Y., Hosie, A. M., Buckingham, S. D., Holyoke Jr, C. W., Baylis, H. A. and Sattelle, D. B. (1995) Actions of picrotoxinin analogues on an expressed, homo-oligomeric GABA receptor of *Drosophila melanogaster. Neurosci. Letts.* **189:** 1-4.

Shiu, R. P. and Friesen, H. G. (1974) Solubilization and purification of a prolactin receptor from the rabbit mammary gland, *J. Biol. Chem.* **249:** 7902-7911.

Snyder, M. J., Walding, J. K. and Feyereisen, R. (1994) Metabolic fate of the allelochemical nicotine in the tobacco hornworm *Manduca* sexta. *Insect Biochem. Molec. Biol.* **24:** 837-846.

Soloway, S. B., Henry, A. C., Kollmeyer, W. D., Padgett, W. M., Powell, J. E., Roman, S. A., Tieman, C. H., Corey, R. A. and Horne, C. A. (1979) Nitromethylene insecticides. In: *Advances in Pesticide Science Part 2* (Geissbühler, H., Brooks, G. T., Kearney, P. C., eds) Pergamon Press. 206-227.

Sone, S., Hattori, Y., Tsuboi, S. and Otsu, Y. (1995) Difference in susceptibility to imidacloprid of the populations of the small brown planthopper, *Laodelphax striatellus* Fallen, from various localities in Japan. *J. Pestic. Sci.* **20:** 541-543.

Sone, S., Tsuboi, S-I., Otsu, Y. and Shono, T. (1997) Mechanisms of low susceptibility to imidacloprid in a laboratory strain of the small brown planthopper, *Laodelphax striatellus* Fallén. *J. Pestic. Sci.* **22:** 236-237.

Stroud, R. M., McCarthy, M. P. and Shuster, M. (1990) Nicotinic acetylcholine receptor superfamily of ligand-gated ion channels. *Biochemistry* **29:** 11009-11023.

Sullivan, J. P., Decker, M. W., Brioni, J. D., Donnelly-Roberts, D., Anderson, D. J., Bannon, A. W., Kang, C-H., Adams, P., Piattoni-Kaplan, M., Buckley, M. J., Gopalakrishnan, M., Williams, M. and Arneric, S. P. (1994) (±)-Epibatidine elicits a diversity of *in vitro* and *in vivo* effects mediated by nicotinic acetylcholine receptors. *J. Phammacol. Exp. Ther.* **271:** 624-631.

Sussman, J. L., Harel, M., Frolow, F., Oefner, C., Goldman, A., Toker, L. and Silman, 1. (1991) Atomic structure of acetylcholinesterase from *Torpedo califomica:* A prototypic acetylcholine-binding protein. *Science* **253:** 872-879.

Swope, S. L., Moss, S. J., Blackstone, C. D. and Huganir, R. L. (1992) Phosphorylation of ligand-gated ion channels: a possible mode of synaptic plasticity. *FASEB J.* **6:** 2514-2523.

Tano, T., Pereira, E. F. R., Maelicke, A and Albuquerque, E. X. (1992) Definition of a novel agonist binding site on nicotinic acetylcholine receptors (nAChR). *Neurosci. Abstr.* **18:** 337-6.

Tietjen, K., Nauen, R. and Ebbinghaus, U. (1998) Pharmacological characterisation of imidacloprid receptors. *IUPAC Abstr.* **4B:** 014.

Tomizawa, M. and Yamamoto, L. (1992) Binding of nicotinoids and related compounds to the insect nicotinic acetylcholine receptor. *J. Pestic. Sci.* **17:** 213-236.

Tomizawa, M. and Yamamoto, L. (1993) Structure-Activity relationships of nicotinoids and imidacloprid analogs. *J. Pestic. Sci.* **18:** 91-98.

Tomizawa, M., Otsuka, H., Miyamoto, T., Eldefrawi, M. E. and Yamamoto, 1. (1995a) Pharmacological characteristics of insect nicotinic acetylcholine receptor with its ion channel and the comparison of the effect of nicotinoids and neonicotinoids. *J. Pestic. Sci.* **20:** 57-64.

Tomizawa, M., Otsuka, H., Miyamoto, T. and Yamamoto, I. (1995b) Pharmacological effects of imidacloprid and its related compounds on the nicotinic acetylcholine receptor with its ion channel from the *Torpedo* electric organ. *J. Pestic. Sci.* **20:** 49-56.

Tomizawa, M., Latli, B. and Casida, J. E. (1996) Novel neonicotinoid-agarose affinity column for *Drosophila* and *Musca* nicotinic acetylcholine-receptors, *J. Neurochem.* **67:** 1669-1676.

Trimmer, B. A. and Weeks, J. C. (1989) Effects of nicotinic and muscarinic agents on an identified motoneurone and its direct afferent inputs in larval *Manduca sexta. J. exp. Biol.* **144:** 303-337.

Usherwood, P. N. R. (1980) Neuromuscular transmitter receptors of insect muscles. In: *Receptors for Neurotransmitters, Hormones and Pheromones in Insects* (Sattelle, D. B., Hall, L. M. and Hildebrand, J. G., eds), Elsevier/North Holland, Amsterdam. 141-153.

Unwin N. (1993) Nicotinic acetylcholine receptor at 9 Å resolution, *J. Mol. Biol.* **229:** 1101-1124.

Unwin, N. (1998) The nicotinic acetylcholine receptor of the Torpedo electric ray. *J. Structural Biol.* **121 (2):** 181-190.

Vernallis, A. B., Conroy, W. G. and Berg, D. K. (1993) Neurons assemble acetylcholine receptors with as many as three kinds of subunits while maintaining subunit segregation among receptor subtypes. *Neuron* **10:** 451-464.

Wada, K., Ballivet, M., Boulter, J., Connolly, J., Wada, E., Deneris, E. S., Swanson, L. W., Heinemann, S. and Patrick, J. (1988) Functional expression of a new pharmacological subtype of brain nicotinic acetylcholine receptor. *Science* **240:** 330-334.

Wadsworth, S. C., Rosenthal, L. S., Kammermeyer, K. L., Potter, M. B. and Nelson, D. J. (1988) Expression of a *Drosophila melanogaster* acetylcholine receptor-related gene in the central nervous system. *Mol. Cell. Biol.* **8:** 778-785.

Ward, J. M., Cockcroft, V. B., Lunt, G. G., Smillie, F. S., and Wonnacott, S. (1990) Methyllycaconitine: a selective probe for neuronal α-bungarotoxin binding sites. *FEBS Lett.* **270:** 45-48.

Watkins, B. L., Leitch, B., Burrows, M. and Knowles, B. H. (1995) Localization of a nicotinic acetylcholine receptor-like antigen in the thoracic nervous system of embryonic locusts, *Schistocerca gregaria. J. Comp. Neurol.* **351:** 134-144.

Wess, J., Gdula, D. and Brann, M. R. (1991) Site-directed mutagenesis of the m3 muscarinic receptor identification of a series of threonine and tyrosine residues involved in agonist but not antagonist binding. *EMBO J.* **10 (12):** 3729-3734.

West, L. K. and Huang, L. (1982) Acetyl choline receptor mediated sodium ion efflux after rapid hypo osmotic loading of radio tracer. *Arch. Biochem. Biophys.* **215 (2):** 508-513.

Whiteaker, P., Davies, A., Marks, M., Hardick, D., Blagbrough, I., Potter, B., Wolstenholme, A. J., Collins, A. and Wonnacott, S. (1999) An autoragiographic study of the distribution of binding sites for the novel α7-selective nicotinic radioligand [^{3}H]methyllycaconitine in the mouse brain. *Eur. J. Neurosci.* **11,** 2689-2696.

Whiting, P., Esch, F., Shimasaki, S. and Lindstrom, J. (1987b) Neuronal nicotinic acetylcholine receptor ,β-subunit is coded for by the cDNA clone α4. *FEBS Lett.* **219:** 459-463.

Whiting, P. and Lindstrom, J. M. (1986) Purification and characterization of a nicotinic acetylcholine receptor from chick brain. *Biochemistry* **25:** 2082-2093.

Whiting, P. and Lindstrom, J. (1987a) Affinity labelling of neuronal acetylcholine receptors localizes acetylcholine binding sites to their β-subunits. *FEBS Lett.* **213:** 55-60.

Whiting, P. and Lindstrom, J. (1987b) Purification and characterization of a nicotinic acetylcholine receptor from rat brain. *Proc. Natl. Acad. Sci. USA* **84:** 595-599.

Whiting, P., Liu, R., Morley, B. J. and Lindstrom, J. M. (1987) Structurally different neuronal nicotinic acetylcholine receptor subtypes purified and characterized using monoclonal antibodies. *J. Neurosci.* **7:** 4005-4016.

Whiting, P. J., Schoepfer, R., Conroy, W. G., Gore, M. J., Keyser, K. T., Shimasaki, S., Esch, F. and Lindstrom, J. M. (1991) Expression of nicotinic acetylcholine receptor subtypes in brain and retina. *Mol. Brain Res.* **10:** 61-70.

Wonnacott, S., Albuquerque, E. X., and Bertrand, D. (1993) Methyllycaconitine: a new probe that discriminates between nicotinic acetylcholine receptor subclasses. *Methods in Neurosci.* **12:** 263-275.

Wonnacott, S. (1997) Presynaptic nicotinic acetylcholine receptors. *TINS* **20:** 92-98.

Yamamoto, I., Yabuta, G., Tomizawa, M., Saito, T., Miyamoto, T. and Kagabu, S. (1995) Molecular mechanism for selective toxicity of nicotinoids and neonicotinoids. *J. Pesticide Sci.* **20:** 33-40.

Yamamoto, I., Tomizawa, M., Saito, T., Miyamoto, T., Walcott, E. C. and Sumikawa, K. (1998) Structural factors contributing to insecticidal and selective actions of neonicotinoids. *Arch. Insect Biochem. Physiol.* **37:** 24-32.

Yum, L., Wolf, K. M., and Chiappinelli, V. A. (1996) Nicotinic acetylcholine receptors in separate brain regions exhibit different affinities for methyllycaconitine. *Neurosci.* **72:** 545-555.

Zhang, H-G., ffrench-Constant, R. H. and Jackson, M. B. (1994) A unique amino acid of the *Drosophila* GABA receptor with influence on drug sensitivity by two mechanisms. *J. Physiol.* **479:** 66-75.

Zhao, G., Liu W., Brown J. M. and Knowles, C. O. (1995) Insecticide resistance in field and laboratory strains of western flower thrips (Thysanoptera: Thripidae) *J. Econ. Entomol.* **88 (5):** 1164-1170.

Zhimou, W. and Scott, J. G. (1997) Cross-resistance to imidacloprid in strains of german cockroach (*Blattella germanica*) and house fly (*Musca domestica*). *Pestic. Sci.* **49:** 367-371.

Zlotkin, E. (1999) The insect voltage-gated sodium channel as target of insecticides. *Annu. Rev. Entomol.* **44:** 429-455.

Zwart, R., Oortgiesen, M. and Vijverberg, H. P. M. (1992) The nitromethylene heterocycle 1-(pyridin-3-yl-methyl)-2-nitromethylene -imidazolidine distinguishes mammalian from insect nicotinic receptor subtypes. *Eur. J. Pharmac. env. Toxic. Pharmac.* **228:** 165-169.

Zwart, R., Oortgiesen, M. and Vijverberg, H. P. M. (1994) Nitromethylene heterocycles: selective agonists of nicotinic receptors on locust neurones compared to mouse NE-115 and BC3H1 cells. *Pestic. Biochem. Physiol.* **48:** 202-213.